Dynamique hydro-sédimentaire en milieu portuaire : application au port de plaisance de La Rochelle

Jean-Rémy Huguet

LA ROCHELLE UNIVERSITÉ

ÉCOLE DOCTORALE
Euclide

Laboratoire LIENSs

THÈSE

Présentée par:

Jean-Rémy HUGUET

Soutenue le 04 décembre 2019
Pour l'obtention du grade de Docteur de La Rochelle Université

Discipline: Terre, enveloppes fluides

Dynamique hydro-sédimentaire en milieu portuaire: application au port de plaisance de La Rochelle

JURY:

Jaak MONBALIU	Professeur, Katholieke Universiteit Leuven / *rapporteur*
Catherine VILLARET	Ingénieure de recherche, East Point Geo / *rapporteur*
Isabelle BRENON	Maître de conférences, La Rochelle Université / *directrice de thèse*
Xavier BERTIN	Directeur de recherche, La Rochelle Université / *examinateur*
Pierre LE HIR	Cadre de recherche, IFREMER / *examinateur*
Aldo SOTTOLICHIO	Maître de conférences, Université de Bordeaux / *examinateur*
Damien SOUS	Maître de conférences, Université de Toulon / *Invité*
Adeline THOMASSIN	Ingénieure, Port de plaisance de La Rochelle / *Invitée*
Régis WALTHER	Ingénieur de recherche, Artelia / *Invité*

Avant-propos

Contexte

Cette thèse a été réalisée sous la direction d'Isabelle Brenon au laboratoire LIENSs (UMR, CNRS 7266 Littoral ENvironnement et Sociétés), au sein de l'équipe DPL (Dynamique Physique du Littoral).

La bourse de thèse provient d'une allocation de la Région Nouvelle-Aquitaine et du Port de Plaisance de la Rochelle.

Ce travail de recherche est en lien direct avec le projet DYPOMAR (Dynamiques portuaires, Milieux urbains et environnement MARitime) dans le cadre de la gestion des environnements intra et extra portuaires.

La grande majorité des sorties terrain dédiées au projet de thèse ont pu être réalisées grâce à l'appui technique de Thibault Coulombier, Ingénieur d'Etude au LIENSs, et de toute l'équipe du port de plaisance de La Rochelle, en particulier Adeline Thomassin.

Une collaboration avec Vincent Hamani, doctorant LIENSs de l'équipe AMARE (Réponse des Animaux MARins à la variabilité Environnementale) a également été entreprise afin de mener à bien l'installation et au maintien d'équipements optiques (ALTUS, UVP).

Ce travail a bénéficié de la contribution d'étudiants en stage :

- Pierric Contal, en Master 1 SPE, La Rochelle Université. Durée : 3 mois. "Caractérisation de la repartition des apports sédimentaires du Port des Minimes par traitement de données bathymétriques"
- Antoine Mérigot en Master 1 Géographie, La Rochelle Université. Durée : 3 mois. Originellement sous la direction d'Adeline Thomassin au département Dragage de la régie du port de plaisance de La Rochelle, mais qui a dévié sur une étude historique des aménagements du port des Minimes.

Valorisation scientifique

Quatre chapitres de cette thèse font actuellement l'objet de quatre publications scientifiques en premier auteur: deux publiées (Chapitres IV,VI), une soumise et en review (Chapitre VII) et une en cours de finalisation (Chapitre V). Les Chapitres I à III sont écrits de manière continue en français et les chapitres de résultats sont écrits en anglais sous format article. Les travaux présentés au cours de ce manuscrit ont aussi été présentés lors de conférences nationales et internationales.

Publications en premier auteur:

- **Huguet, J. R.,** Brenon, I., & Coulombier, T. (2020a). Influence of Floating Structures on Tide-and Wind-Driven Hydrodynamics of a Highly Populated Marina. *Journal of Waterway, Port, Coastal, and Ocean Engineering*, *146*(2), 05019004.
- **Huguet, J. R.,** Brenon, I., & Coulombier, T. (2019). Characterisation of the Water Renewal in a Macro-Tidal Marina Using Several Transport Timescales. *Water*, *11*(10), 2050.

Publication under review:

- **Huguet, J. R.,** Brenon, I., & Coulombier, T. (2020b). Sediment Dynamics and Siltation Management in a Highly Populated Marina. *Ocean and Coastal Management*.

Conférences:

- **Huguet, J. R.,** Brenon, I., & Coulombier, T. Hydrodynamic and siltation management in a highly populated marina (La Rochelle, south-west France). *Proceedings of Coastal Management 2019, La Rochelle, 24-26 September 2019.*
- **Huguet, J. R.,** Brenon, I., & Coulombier, T. (2018). L'influence des pontons dans la courantologie du port de plaisance de La Rochelle. *15th National Days « Génie Côtier – Génie Civil ». La Rochelle, France, 29-31 May 2018. pp 67-76.*
- **Huguet, J. R.,** Brenon, I., & Coulombier, T. Impact of pontoons on water circulation and turbulence in La Rochelle marina (France). *24th Biennial CERF Conference, Providence, USA, 5-9 November 2017.*

Remerciements

A l'heure où j'écris ces lignes, c'est le calme après la tempête. Ici, je vais en profiter pour parler avec le cœur, et pour faire à la fois un bilan de ces trois années de doctorat mais aussi sur mon parcours et sur toutes les personnes que j'ai rencontrées jusqu'à la fin de ma thèse.

J'aimerai remercier tout d'abord la vie, ou Dieu, ou je ne sais qui, pour me permettre chaque jour d'expérimenter de nouvelles expériences, sensations, et partager ça avec le maximum de gens possible. La vie parfois c'est dur, parfois c'est bien, mais au moins on la vit. Ensuite, je remercie toutes les personnes que j'ai croisées, qu'elles m'aient fait du mal ou du bien, elles m'ont toutes apporté quelque chose, que ce soit une gastro, ou un kinder bueno. Plus spécifiquement je tenais à remercier, ma conseillère d'orientation qui m'a conseillé en terminale de partir dans l'enfer de la prépa. Après ça, les différents combats scolaires que j'ai dû mener c'était de la poudre de perlimpinpin. Je tenais à remercier Anne Petrenko et Andrea Doglioli, chercheurs au MIO, dont les cours, l'énergie et la pédagogie m'auront vraiment donné le goût de la recherche et de l'océanographie. Je me rappelle aussi, des moments passionnants passés à écouter Pierre Le Hir ou encore Xavier Carton à l'UBO de Brest. Je remercie d'ailleurs mes camarades de promotion dont le nombre était inversement proportionnel à la cohésion et au dynamisme affiché. Les années à Brest, c'était vraiment sympa. (Du rhum des vagues, de la mer nom de dieu…) Muchas gracias Marta Marcos pour ta gentillesse et ta disponibilité au cours de mon (premier) stage de recherche à l'IMEDEA aux Baléares. Merci ensuite à toi Bruno Castelle de m'avoir fait confiance en 2015 pour mon stage de fin d'études sur la morphologie des plages sableuses. Ce sujet vaste, m'a passionné et je ne remercierai jamais assez Vincent Marieu et surtout Benjamin Dubarbier qui m'ont fourni une aide précieuse sur le plan technique. Merci à toi Xavier de m'avoir permis par la suite de mettre un pied à l'étrier dans le monde de la recherche, au LIENSs, puis de m'avoir soutenu pour décrocher cette thèse. Même si j'ai parfois du mal à suivre sur le plan scientifique, nos conversations et nos petites missions à Rivedoux/Côte Sauvage me ravissent toujours autant.

Ensuite, un grand merci au port de plaisance de La Rochelle et à La Région Nouvelle-Aquitaine d'avoir cofinancé cette thèse. Je pense surtout à celles qui sont à l'origine de ce co-financement: Adeline Thomassin et Isabelle Brenon, dont les discussions ont fait naître un sujet de thèse mixte et appliqué. Merci à toute l'équipe du port et à Mr. Moquay pour le soutien technique et logistique ainsi que pour les discussions riches et ouvertes notamment pendant les comités de dragages et autres réunions informelles. C'était un réel plaisir d'observer l'intêret pour mon travail et de voir tous ces différents acteurs travailler en commun pour la durabilité du port, cette micro-cité dans la cité. J'espère avoir répondu aux attentes et être allé plus loin encore, et j'espère surtout que ce travail servira à la fois en

soutien à d'éventuelles prises de décision mais aussi aux nombreuses autres études interdisciplinaires effectuées au sein du port voire ailleurs en France ou dans le Monde. Merci Isabelle de m'avoir laissé l'opportunité de devenir docteur. Merci de m'avoir laissé du temps et de m'avoir permis de consacrer quasi-exclusivement à la recherche sans que je ne me soucie trop du monde réel tels que les papiers, le paiement des salaires, l'administration (Merci Laetitia !) … et surtout merci pour ces goûters et cacahuètes! Tout ce travail n'aurait pu être possible sans toutes les personnes qui ont participé aux mesures de terrain et je pense au personnel du port mais aussi et surtout à Thibault Coulombier, le MacGyver du LIENSs, éternel fan du FC Sochaux, résident permanent du bureau 108 et maillon essentiel de la confrérie café-commérages représentée par Médékic, Little John et moi-même. Médéric lorsque je suis arrivé tu étais un tout jeune freluquet et maintenant tu es marié, père de deux jolis bambins, membre du CS et tu t'es enfin fait JC… Little John, aka mister corse aka Raphaël Savelli le surfeur d'argent du dimanche. On en aura fait/dis des conneries en trois ans bordel mais ce que je vois maintenant en te regardant, c'est qu'on a décidément plus affaire à un élève, mais bien au professeur. Prends soin de Barnabé…

Un grand merci à tous les collègues qui m'ont accueilli ou que j'ai accueillis au LIENSs: Lucille, Gaël, Guillaume, Yann, Alice, Camille, Valentin, Yannick, Juliette, Luuk, Anouk, Cyril, Vincent H., Nicolas, Etienne, Philippe, Marc, Ion, Treden, Laura, Eric C., Micha (Mikhail)... (sorry si j'en oublie !) Les Olienspiades, galettes des rois, pots de départs et autres pauses café en tout genre étaient très appréciables en votre compagnie ! Je tiens tout spécialement à remercier Vincent Le Fouest, Laurence Murillo, Mélanie Becker, Florian Ploquin et Olivier de Viron pour leur aide précieuse pendant les derniers moments de la préparation à ma soutenance. Sans eux, j'aurai réalisé une piètre prestation ! Je n'oublie pas l'aide reçue par Cécilia sur QGIS et le travail graphique impressionnant de Thierry. Au cours de ces années au LIENSs, j'ai aussi passé un temps certain avec les L2 Sciences de la Terre et les M1 Sciences pour l'Environnement que je remercie pour leur attention et leur respect. Je remercie aussi Pierric Contal mon seul et unique vrai stagiaire (ça m'aura vacciné cette courbe de ma raie!) pour la future lettre de recommandation qu'il va me rédiger maintenant qu'il a un vrai boulot, lui ! Vincent Hamani merci pour ton aide sur les manips et sur notre actuelle et future collaboration pour le Hamani & Huguet (ou Huguet & Hamani ?). J'espère que je te le rends assez bien quand je passe des heures sous la flotte pour tes fécès ! Je me dois aussi de remercier toute la communauté telemac-mascaret.org (notamment Pierre-Louis Ligier) avec qui j'ai pu converser par ordinateur interposé et qui m'aura bien aidé face aux nombreux verrous techniques que j'ai pu vivre notamment au début de la thèse. Merci à Météo France, au NCEP et au réseau REFMAR pour la disponibilité de leurs données de vent et de niveaux d'eau que j'ai pu récupérer tout au long de la thèse. Enfin, plus généralement, je tiens à exprimer ma profonde gratitude à ceux qui étaient présents et qui ont participé à la soutenance, un moment que Tabletoute ma vie en mémoire cette journée.

Une multitude d'autres amis et connaissances a jalonné mon parcours jusqu'ici et elles pourraient toutes être citées mais j'ai bien peur que cela prenne trop de place alors sachez que j'ai une pensée pour vous tous. Plus spécifiquement, j'aimerai remercier mes amis d'ailleurs avec, pour commencer, les Marseillais que j'essaie de revoir à chaque fois que je redescends dans le sud. Et

notamment la famille Lagier, Romain, Baptiste et Guillaume, qui ont réussi à survivre là-bas, dans la jungle magnifique mais trop urbaine (pour moi) qu'est Marseille. Mes amies de Lyon, Lolo et Marine je vous souhaite tout le meilleur du monde et j'espère vous revoir encore malgré la distance je vous garde toujours dans mon cœur. Je pense aussi à vous, mes amis de licence et de master, Samos, Hugo, gros Jules, Cocletus c'est toujours un plaisir de vous revoir et de partager nos expériences, j'ai hâte qu'on se refasse des contrées et des baby! Clemstein merci pour tous ces moments passés dans et hors de l'eau, avec toi je me suis vraiment bien marré, j'ai hâte que tu reviennes de Martinique avec Gipsy, ou qu'en tout cas nos chemins se recroisent très très vite (je t'en veux quand même de ne pas avoir fait l'aller-retour pour ma soutenance). Au fait, quand-est-ce qu'on monte notre baraque à frites avec Tutur (et le grosse Bertha)? D'ailleurs toi aussi Tutur, merci pour ta science des vagues, tes petits repas bien cuisinés et tes conseils toujours bien avisés sur la thèse (Martine aussi, un grand merci pour ce houmous de qualité et tout le reste). J'espère pouvoir un jour me souvenir de toutes ces vagues qu'on aura pris ensemble et avec tous mes compagnons de surf de Marseille (si si ça surf !) jusqu'à Brest, en passant par la côte aquitaine et vendéenne : Baptiste (ptit poulet pétoman perfectionniste de la vague et du code), Le Scoul (enlève ta casquette), Brody (Nugget Ball !!), Valère (j'ai toujours espoir que tu viennes me voir avec ton avion… autour de minuit n'attend que toi), Guillaume (à quand une session marin d'eau douce?!), Régis, Brunal, Boilux (sauce aigre douce), Zach… et plus globalement merci à ceux qui ne m'ont jamais taxé ou qui m'ont laissé les taxer sans aboyer avec véhemence Hep Hep Hep ! J'ai aussi une grosse pensée pour tous les collocs qui m'auront supporté pendant mes études, notamment Justine, Céloche, Véroche, Victor, Chloé, Ragnar et Atilla. Votre présence m'aura apporté, ces quelques années, un réconfort certain et des repas divins ! Les rochelais aussi je vous remercie, notamment le Squicky Squip Gang avec qui on passe de super soirées « Cheap and Beauf » : Dévi, Jarro, Ohay, PL, Loann, Roméo, Santi, Quentin, JuL, ClemiX, Popo... Alexia tu as été la première personne que j'ai rencontrée sur LR city beach et je ne l'oublierai pas ! Enfin, petit coup de cœur 2019 pour Zaza même si, elle aussi, n'a pas daigné faire un détour Nouméa-La Rochelle pour la soutenance (revois tes priorités bordel !).

J'aimerai maintenant ouvrir un paragraphe un peu plus personnel et qui me tient à coeur. Papa, merci pour ton aide tu as été un grand soutien toute ma vie, tu m'as poussé à « forger pour devenir forgeron » et malgré toutes les épreuves tu es resté fort et surtout tu es resté présent. Béné, je n'arrêterai jamais de t'embêter tu le sais, merci à toi pour ton premier degré et ta vitalité permanente et encore désolé de t'avoir volé la vedette à ma naissance. Tu rayonnes partout où tu passes et c'est ce que les gens retiennent. Maman, tu n'es plus là depuis longtemps mais j'espère t'avoir fait honneur, comme tu me l'avais demandé et j'espère continuer à te faire honneur le reste de ma vie. Ton bijounet qui t'aime… Mamie, tu es toujours là mais plus trop ici, et j'espère m'occuper aussi bien de toi que tu t'es occupée de moi toute mon enfance, jusqu'à ce que tu rejoignes l'amour de ta vie... Papy, même si tu avais tes humeurs, tu étais l'une des personnes les plus humaine et cultivée que j'ai pu côtoyer dans ma petite vie. Tu étais intéressé par tout et par tout le monde, et si j'ai poursuivi ce doctorat jusqu'au bout c'est aussi pour toi et pour l'importance que tu accordais à mes travaux de recherche. C'est pour cela que je te dédie cette thèse. Toi et mamie vous nous avez apporté, à toute notre famille et à moi, la possibilité de passer des moments inoubliables sur l'île de Ré, entre les fougères et les pins, dans la magnifique demeure de l'éclade. C'est cette proximité forte avec la nature et avec la mer qui m'a donné l'envie de poursuivre

mes études dans ce domaine et qui m'a amené, plus tard, à revenir aux sources, à La Rochelle. D'une certaine manière, cette passion je vous la dois. Ico et Pierre Havard, merci pour tous ces échanges enrichissants, ces repas succulents (et longs !). Vous vivez dans la simplicité, et vous m'en apprenez à chaque fois sur la nature, la cuisine, le véganisme et surtout sur le whisky. Thierry, merci de t'occuper si bien de l'éclade et désolé si pour moi être là-bas rime avec vacances, mais j'essaierai de me lever avant 10 heures la prochaine fois, c'est promis ! Serge, tu étais quelqu'un d'inspirant et de toi je retiens le sourire et l'impulsivité. Je regrette de ne jamais avoir pu te battre au bras de fer mais ce n'est que partie remise là-haut ! Je remercie tout le reste de la famille mes cousins cousines français mais aussi ceux d'Allemagne et d'Argentine que j'espère revoir vite. Je n'oublie pas bien sûr ma famille du côté de Maman, celle qui a l'accent chantant du sud-ouest et qui nous a toujours accueilli chaleureusement en Terre du milieu à Montauban et Mont-de-Marsan. Merci à vous Claire, Tonton, Tatie et Fabienne pour votre disponibilité et votre accueil toujours au top, vous avez été là quand nous en avions besoin. J'ai aussi rencontré d'autres familles pendant mon parcours, à Guiclan, à l'Aiguillon-sur-mer mais aussi à Sète et je les remercie de m'avoir toujours accueilli chaleureusement…

Enfin, Manon, merci d'avoir été là pendant tous ces moments, tous ces hauts et tous ces bas. Tu connais toutes mes imperfections et surtout mon discours de soutenance par cœur. Tu fais partie de la famille maintenant et tu resteras à jamais gravée dans mon cœur. J'espère te soutenir aussi bien pour la suite que tu m'as soutenu pendant ce long périple. Une pensée aussi pour mon chat Pascal, qui m'aura mis des bâtons dans les roues jusqu'au bout, ce folcochon.

A vous tous qui lisez des lignes, je vous souhaite le bonheur le plus complet, mais surtout, une bonne lecture and j'espère que vous likez le franglish !

Table des matières

Chapitre I

Introduction

Sur Terre, la population humaine qui était estimée à 6 milliards en 1999 (*U.S. Census Bureau 2009*), a déjà dépassé les 7,7 milliards d'individus aujourd'hui. Alors qu'il aura fallu attendre le XIVe siècle pour atteindre un milliard d'êtres humains, il se pourrait que nous soyons près de 12 milliards sur Terre d'ici 2100 (*Samir & Lutz, 2017*). Cette explosion démographique a considérablement augmenté l'utilisation des zones côtières au cours des dernières décennies et cette tendance devrait se poursuivre, à l'avenir, avec la croissance de la population mondiale et le développement des zones urbaines près des côtes. La plupart des grandes agglomérations sont déjà situées près des zones côtières (*Timmerman & White, 1997; Brown et al., 2014; Von Glasow et al., 2013*) et plus de 75 % de la population mondiale devrait vivre à moins de 100 *km* des côtes d'ici 2025 (*EEA, 2006*). Le développement socio-économique de ces métropoles, voire mégalopoles, repose sur le bon fonctionnement de leurs infrastructures côtières (Figure I.1). Celles-ci peuvent être déployées pour la défense côtière, en soutien aux activités littorales telles que la pêche, le tourisme et la navigation, mais aussi pour répondre à des besoins industriels ou d'énergie (*Airoldi & Beck 2007*). L'artificialisation est particulièrement marquée dans les ports où de nombreux aménagements (cale, jetée, quais, moles, pontons…) sont mis en place pour faciliter l'accueil des bateaux et navires. Les espaces portuaires assurent depuis longtemps des fonctions vitales pour la société, comme la pêche ou la défense militaire, mais ils se sont récemment complexifiés et organisés sur des espaces d'échelles multiples aux enjeux économiques certains. A l'ère de la mondialisation ils sont devenus des interfaces majeures par où transite plus de 80 % du commerce mondial, et ils accompagnent aussi, activement, l'essor des pratiques récréatives nautiques de ces dernières décennies. Afin de mieux comprendre leur rôle et leur place dans le monde actuel, nous allons retracer les lignes principales de leur histoire.

Figure I.1. *Illustration de différentes typologies d'ouvrages présents sur le littoral maritime dans le monde. On distingue les ouvrages liés à la défense côtière des ouvrages liés aux activités littorales. Dans l'ordre de haut en bas et de gauche à droite: Marseille, France; Palavas-Les-Flots, France; La digue Houtrib entre Enkhuizen et Lelystad, Pays-Bas; Shanghaï, Chine; Marina du Moulin Blanc à Brest, France; Toulon, France; Le pont le plus long du monde à Hong Kong, Chine; Camargue, France; Ronce-les-Bains dans l'estuaire de la Gironde, France; Saint-Nazaire, France; Pont Danyang-Kushan, Chine; La jetée d'Huntington Beach, Etats-Unis; L'usine marémotrice de l'estuaire de la Rance, France; Aménagement d'une route littorale à La Réunion, France; Plage du solarium à Monaco. (Images obtenues via Google Image. Sources respectives: Guy Quéral; eid-med.org; vesselfinder.com; wpblink.com; brestaim-events.com; defense.gouv.fr; flickr.com; aires-marines.fr; nantes.port.fr; linternaute.com; surfcityusa.com; usinenouvelle.com; regionreunion.com; plages.tv).*

I.1. Les ports dans le monde et dans l'histoire

I.1.1. Histoire des ports

Les ports ont toujours été porteurs d'imaginaires multiples, source d'inspiration autant qu'objet de fascination, ils sont intrinsèquement reliés à la navigation maritime et à la sensation de liberté qu'elle procure. Si les sources ne sont pas définitives dans le domaine, la navigation maritime serait bien antérieure au Néolithique, tandis que la présence de ports en tant qu'abri pour les bateaux, n'est avérée que depuis 4500 ans, en Egypte (*Gould, 2011; Strasser et al., 2011*). Les Egyptiens, mais aussi les Mésopotamiens furent parmi les premières civilisations occidentales à utiliser les routes fluviales et maritimes, ce qui a joué un rôle déterminant dans le développement de leurs sociétés. Les ports entretenaient la prospérité de leur activité commerciale et maritime en assurant une interface entre la terre et la mer et en servant d'intermédiaire pour le transfert et le stockage des marchandises. Alors qu'au début de l'Antiquité on se servait de baies naturelles abritées pour échouer radeaux et pirogues, les infrastructures portuaires se sont diversifiées en passant du premier môle Phénicien, daté du XIIe siècle avant Jésus-Christ, jusqu'aux grandes constructions offshore de la période romaine, rendues possible par la découverte du béton hydraulique (*Oleson et al., 2004; Goiran et al., 2010*). De nombreux ports furent construits pendant cette période notamment en Méditerranée, considérée comme l'un des berceaux de l'ancienne technologie maritime, avec Phocée, Carthage ou encore Byzance. Suite au déclin de l'Empire Romain et aux destructions liées aux Grandes Invasions eurasiennes, l'activité maritime du monde occidental a brutalement freiné (*Berling, 2015*).

C'est au Moyen-Âge qu'un essor nouveau de la navigation se dessine, faisant de cette période un âge d'or des ports (*Tranchant, 2005*). La découverte de certaines techniques, telle que la boussole au XIIIe siècle, et l'utilisation de la voile unique comme mode de propulsion, vont donner un essor nouveau à la navigation. Ce n'est qu'au cours du XVe siècle que la plupart des ports français bénéficièrent de véritables travaux d'aménagements pour remplacer les installations primitives (*Tranchant, 2010*). Ensuite, au XIX^{e} siècle, la révolution industrielle et la naissance de la propulsion motorisée à vapeur vont modifier l'apparence des ports. Les progrès techniques permettront d'améliorer et d'augmenter les constructions et les ports vont se spécialiser entre ports de commerce, ports de pêche et ports militaires. Cette transformation continue au XXe siècle où l'accroissement des échanges par voie maritime augmente la segmentation des ports de commerce en sous-ensemble de terminaux spécialisés afin de répondre à l'augmentation en taille et en nombre de navires marchands. C'est après la Seconde Guerre mondiale que survient l'avènement des pétroliers et des vraquiers puis celui de la conteneurisation, procédé qui va révolutionner la manutention portuaire et rendre possible le développement de la mondialisation (*Frémont, 2019*). Les ports de commerce sont depuis, devenus des interfaces majeures du transport de marchandise, au cœur de la chaîne logistique d'approvisionnement des territoires. Durant les vingt dernières années la folle croissance des marchés maritimes et le mouvement perpétuel de l'évolution des navires et des acteurs ont radicalement modifié le tissu portuaire. Aujourd'hui, l'Asie orientale et la zone Pacifique polarisent l'activité commerciale maritime en opérant plus des deux tiers des manutentions portuaires mondiales.

I.1.2. Le cas particulier des ports de plaisance

Les dernier-nés des ports, en tant qu'entités uniques, sont les ports de plaisances. Répartis majoritairement dans les pays occidentaux, ces ports n'ont pas suivi le même schéma de développement que les ports de commerce. Les processus ayant conduit à leur apparition, puis à leur évolution, sont plus complexes. La plaisance est relative à la navigation lorsqu'elle est pratiquée pour le loisir et pour le sport. Même si la rupture entre travail et loisir n'a jamais été évidente, il n'est pas exclu que la navigation de plaisance ait été pratiquée déjà dans l'Antiquité sur les rives du Nil et de la Méditerranée (*Charles, 1980*). Le témoignage le plus ancien est celui d'une fresque grecque découverte à Santorin, représentant une fête nautique de voiliers (*Le Carrer, 2003*) mais son origine moderne est aristocratique (*Daryl, 1890*). Cette pratique s'est principalement développée en Hollande et en Angleterre à partir du XVIIe siècle, sous l'appellation « yatching », initiée par les familles royales avant d'être reprise par la bourgeoisie. Le développement de cette plaisance élitiste entraîna la création de yacht-club et l'essor des régates de la Manche à la mer du Nord, au milieu du XIXe siècle, puis plus tard, jusqu'en Méditerranée (*Daryl, 1890*). La concentration de yachts a rapidement incité la Hollande à mettre en service des bassins permettant le stationnement des navires, mais des structures spécifiques comparables ne seront visibles ailleurs, qu'à partir du milieu du XIXe siècle. En France, ces « ports à yacht » se développent rapidement dans l'aire d'influence des grandes villes mais surtout dans les secteurs à forte tradition maritime tels que la Bretagne (*Sonnic, 2005*). L'apparition des moteurs fin XIXe, puis l'introduction du polyester dans la construction des bateaux dans les années 40, favoriseront grandement l'essor de la plaisance. Après-guerre, comme beaucoup d'autres industries, celle de la navigation de plaisance va exploser tout d'abord aux Etats-Unis puis à la fin des années 50, en Europe Occidentale.

En France, à partir des années 60, l'engouement suscité par les victoires des grands navigateurs tels qu'Éric Tabarly, ainsi que la popularisation de la voile légère, vont désacraliser le nautisme et le rendre accessible à un plus grand nombre: c'est le début de la plaisance moderne. L'essor des loisirs et du tourisme, la hausse du niveau de vie et les politiques d'aménagement littoral, vont créer un contexte favorable au développement de véritables infrastructures portuaires conçues pour la plaisance moderne (*Sonnic, 2005*). Libéré des contraintes liées aux ports de commerce et de pêche, ces ports modernes vont pouvoir s'adapter totalement aux nombreuses pratiques du monde de la plaisance. En 1965, le premier port dédié uniquement aux activités de plaisance est mis en place à Cannes (*Bernard, 2000*). Cela marquera le début d'une période d'intense construction qui atteindra son paroxysme dans les années 70 (*Bernard, 1999*). Cette frénésie d'urbanisation fut freinée et partiellement réglementée par l'Etat dans les années 80, à une époque où les règles d'urbanisme et de protection de l'environnement sont devenues plus contraignantes (*Bétourné & Valcke, 2015*).

Depuis les années 90, la diminution progressive de la création de structures portuaires lourdes profite à la reconversion des ports traditionnels, anciennement voués à d'autres activités, aux nombreux projets d'extension de structures déjà présentes, et à la multiplication de zones de mouillages (*Bétourné & Valcke, 2015*). De simples abris naturels, à éléments structurants du littoral, les ports de plaisance sont devenus au cours du temps des ouvrages complexes dont la hiérarchisation n'est pas chose évidente (*Sonnic, 2010*). Entre ports artificiels ou en site naturel, ports fluviaux ou maritimes, ports mouillages ou d'échouages, ports mixtes ou voués à la plaisance, une grande diversité de structures et de fonctions caractérise les ports de plaisance modernes. Les diverses infrastructures doivent s'adapter aux conditions

naturelles du rivage ainsi qu'aux besoins des plaisanciers en mer (digues, môles, enrochements, corps morts, pontons, catways, pieux…) comme sur terre (zone de carénage, cales de mise à l'eau, sanitaires, parking, structures d'accueil et de commerce).

En chiffres aujourd'hui dans le monde, on compte 25 750 ports de plaisance et près de 33 millions de bateaux sont immatriculés (*ICOMIA, 2018*). On observe une suprématie occidentale dans ce secteur, avec une forte densité d'équipements nautiques sur les littoraux des Etats-Unis, de l'Europe mais aussi du Canada, de l'Australie, de la Nouvelle-Zélande ou encore de l'arc Antillais. La France métropolitaine dispose du plus important espace nautique d'Europe avec 5 500 km de côtes. Si on prend compte ses départements et régions d'outre-mer, elle arrive à la seconde place mondiale avec près de 20 000 km de côtes (*Cerema, 2018*). Le littoral français accueille 40% de l'économie liée au tourisme, le principal moteur économique du pays (*UNWTO, 2015*). C'est près de 4 millions de plaisanciers réguliers et 1 million d'immatriculations de bateaux de plaisance qui ont été recensés en 2017 (*ICOMIA, 2018*). De plus, la France est le premier constructeur naval de plaisance en Europe, et le second dans le monde après les Etats-Unis. Les ports de plaisance constituent donc un enjeu stratégique d'aménagement et de développement économique et territorial, d'autant que le secteur de la plaisance et du nautisme bénéficie actuellement d'une activité très forte (*DGITM, 2018*).

La Méditerranée domine en termes d'aménagements et de capacité d'accueil, alors que la façade Manche-Atlantique présente une répartition plus hétérogène, concentrée sur le sud de la Bretagne, le bassin d'Arcachon et les Pertuis Charentais. En 2018 on compte en métropole près de 473 installations portuaires maritimes et 556 installations portuaires ou haltes nautiques en eaux intérieures. La capacité d'accueil pour les bateaux de plaisance tourne seulement autour des 500 000 places, ce qui génère des délais d'attente particulièrement longs depuis les années 90. Pour pallier à ce problème, de nombreux ports maritimes sont en voie de développement (30 % des ports maritimes en 2015 selon *DAM, 2015*), mais depuis l'application de la loi littoral en 1986 ces procédures sont ralenties. Certaines réponses technologiques ont été apportées au travers des pontons mobiles Mobi-Deck (*McKinley, 2012*), ou encore du concept BlueRing (*Abessolo, 2015*) mais les ports à sec demeurent aujourd'hui une vraie alternative pour les plaisanciers (Figure I.2, Port à sec du Cap d'Adge). Aujourd'hui, les ports de plaisance se caractérisent par une très grande diversité de lieux d'implantation mais aussi de degré d'équipement et d'infrastructures. La Figure I.2 présente les principaux types de ports rencontrés en France, d'après les typologies établies par *Retière (2003)* et *Bernard (2005)*.

Figure I.2. *Typologie non-exhaustive des différents ports de plaisance visibles en France, d'après les classifications de Dorothée Retière (2003) et Nicolas Bernard (2005). (Images obtenues via Google Image. Sources respectives de haut en bas et de gauche à droite: tourisme-fouesnant.fr; kercabellecmerquel.com; nautisme.lefigaro.fr; france3-regions.francetvinfo.fr; matthieucolin.com; bateaux.com; matthieucolin.com; bateaux.com; marinaworld.co.uk; leportasecducap.com).*

I.2. La Rochelle, Ville-Port

La Rochelle est située sur la façade atlantique française, nichée au fond de la partie Nord du Pertuis d'Antioche où elle se retrouve abritée du grand large par les îles de Ré et d'Oléron. (Figure I.3). Sa configuration géographique privilégiée lui a permis de développer de nombreux espaces portuaires, crées à des époques différentes, pour des besoins différents (Figure I.3). Cette ville-port, qui fut d'abord considérée comme grand port de pêche et de commerce, est devenue aujourd'hui une capitale de la plaisance (*Dussier, 2015*). Le compte-rendu historique qui va suivre permettra de retracer la dynamique portuaire contrastée de La Rochelle et les nombreux problèmes rencontrés pour assurer la pérennité de l'économie rochelaise par la voie maritime.

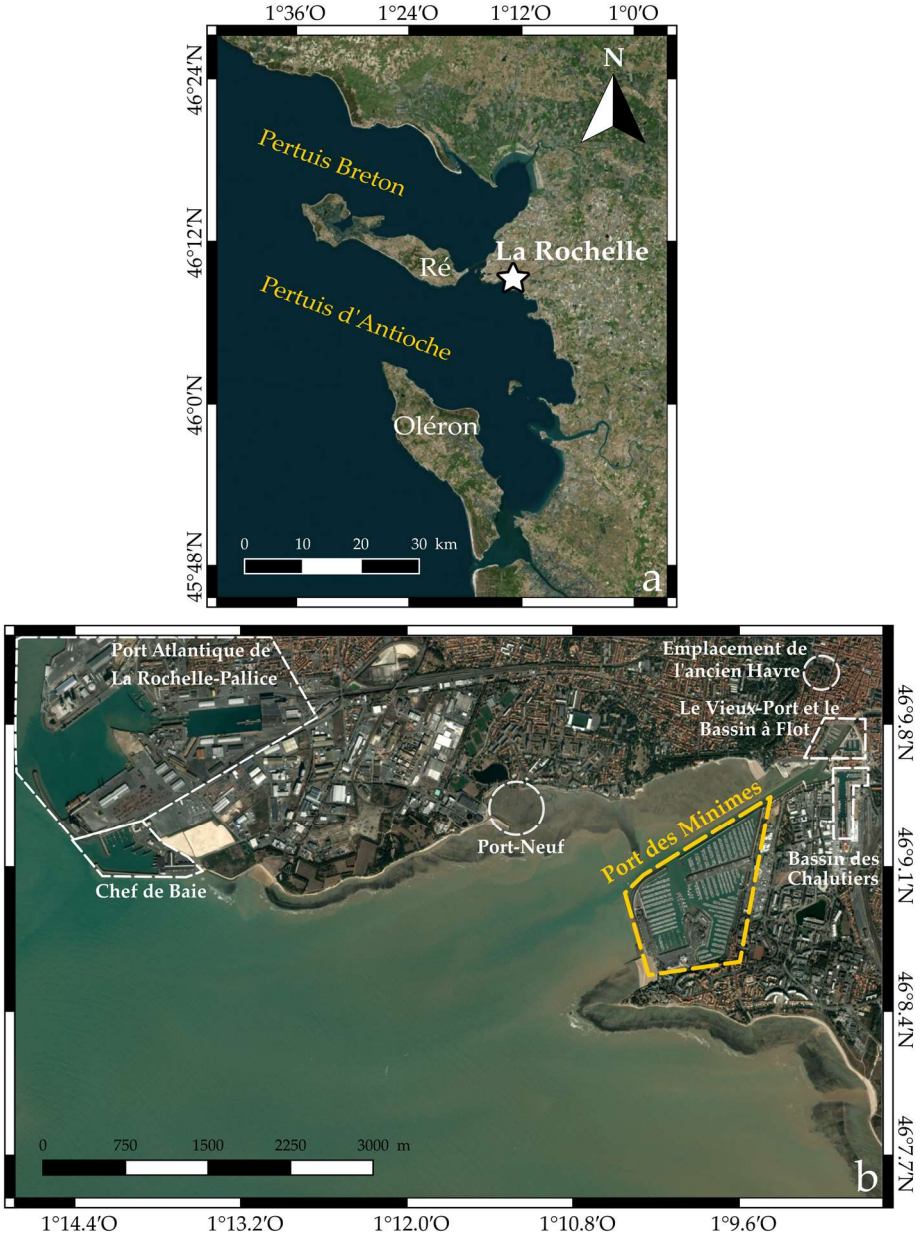

Figure I.3. *Image satellite des Pertuis Charentais (a) ainsi que les différents aménagements portuaires de La Rochelle (b).*

I.2.1. L'histoire portuaire de La Rochelle

Il est difficile d'assigner une date, même approximative, aux origines de La Rochelle. Des fouilles effectuées durant l'aménagement du quartier des Minimes ont permis d'identifier un vaste domaine agricole de l'époque gallo-romaine, vraisemblablement exploité du Ier au IVe siècle et délaissé par la suite (*Dussier, 2015*). Mais il est généralement admis que c'est aux environs du IXe siècle que de modestes habitants vinrent établir leurs cabanes dans cette région déserte et marécageuse, délaissée par la vie urbaine antique au profit de la métropole gallo-romaine Saintes qui s'établissait plus au loin à l'intérieur des terres, au bord de la Charente (*Dion, 1956*). Au XIIe siècle, cette petite bourgade de pêcheurs était une possession des barons de Châtelaillon et ne comptait qu'un modeste port de pêche édifié au niveau de l'actuelle place de Verdun (*Gouriou, 2012*) (Figure I.3). En 1130, après avoir désobéi au duc d'Aquitaine et Comte du Poitou, Guillaume X, Châtelaillon est détruite et La Rochelle lui succède alors en tant que capitale de l'Aunis (*Dion, 1956*). Guillaume X lui octroie de nombreux privilèges et débute alors un formidable essor pour cette ville qui va devenir, dès le XIIIe siècle, une ville noble et connue dans le monde entier (*Arcère, 1756*). Alternativement française et anglaise, La Rochelle aura notamment bénéficié de régimes fiscaux avantageux en matière de taxes et d'impôts ce qui lui a permis de devenir au fil des années un véritable carrefour commercial (*De Beaucé & Thurninger, 1885*). Ses privilèges mais aussi son exceptionnel emplacement naturel sur la façade atlantique lui permettront de connaitre une prospérité croissante et de devenir, en Europe, une place importante de négoce maritime face à Nantes et Bordeaux, alors confinées au fond de leur estuaire. Afin de répondre à une flotte toujours plus grandissante de navires de commerce, les Rochelais construisirent un nouveau havre en 1222, ébauche de l'actuel Vieux-Port, cumulant la fonction de port de pêche et de commerce (Figure I.3). Grâce à ce nouveau port, la ville s'enrichit en participant activement aux échanges avec l'Europe du Nord, notamment dans le commerce du vin et du sel. A partir du XVIe siècle, de nouvelles perspectives s'ouvrent, avec l'annonce des grandes expéditions transatlantiques et La Rochelle devient alors premier port d'embarquement à destination de l'Amérique française dès le XVIIe siècle.

Devenue progressivement le bastion, puis la capitale du protestantisme, La Rochelle va s'attirer les foudres du roi de France Louis XIII qui charge le cardinal de Richelieu de soumettre la ville en 1627. Celui-ci décida de faire tomber La Rochelle par la famine en assiégeant la ville rebelle côté terre avec treize forts entourant la ville, et côté mer avec une digue empêchant toute sortie du port. Large de 18 m à sa base et de 8 m à son sommet, elle culminait à près de 2 m au-dessus des plus hautes mers (Figure I.4). Elle était composée de centaines de tonnes de pierres et de kilomètres d'énormes pieux mais aussi d'épaves de bateaux coulés pour l'occasion (*De Beaucé & Thurninger, 1885*). Après avoir perdu les trois quarts de ses habitants au cours du siège, La Rochelle capitula le 30 octobre 1628, et perdit tous ses privilèges ainsi que ses fortifications, côté terre (*Faucherre et al., 1996*). La digue, communément appelée digue de Richelieu ne put ni n'être conservée ni détruite et elle resta donc abandonnée face aux assauts de la mer. Ses vestiges sont d'ailleurs encore bien visibles dans la baie de La Rochelle et rappellent le tragique épisode de ce grand siège. Les soubassements de la digue formaient inexorablement un piège à vase qui asphyxiait le port. Toutefois, conscient de l'importance de cette ville, le royaume permit à La Rochelle de garder une porte ouverte vers la mer. Le chenal d'accès au havre fut entretenu afin de permettre la navigation et de grands travaux de rétablissements du havre furent entrepris entre 1670 et 1672 sous le royaume de Louis XIV. Ce

nouveau port, qui enrichit la ville en participant activement aux échanges avec l'Europe du nord et le nouveau monde, demeure jusqu'au XIXe siècle la seule infrastructure portuaire de La Rochelle.

Figure I.4. *Plan du Grand siège de La Rochelle et de la digue érigée dans la baie.*
(Source: Masse, Claude. Recueil des plans de La Rochelle, Éditions Rupella, 1979, feuille 10)

La Rochelle redevint rapidement prospère et dès le XVIIIe siècle, un des premiers ports du royaume (*Couneau, 1904*). A la fois port de pêche et de commerce, ses échanges avec les pays du Nord et l'Amérique sont réduits pendant la révolution française et les guerres de l'empire qui signent le déclin du grand commerce maritime rochelais. Les multiples usages du havre et son envasement chronique vont entraîner la municipalité à réaliser une extension du Vieux-Port en 1808 sous l'empire de Napoléon 1er. Depuis bien longtemps, les marées et les envasements successifs entravaient l'accès des gros navires obligés de mouiller plus au large du côté de Chef de Baie (Figure I.3b). La construction de ce bassin à flot intérieur, fermé par une écluse le délimitant du Vieux-Port (Figure I.3b), donna un peu d'air à La Rochelle mais il devint vite insuffisant pour accueillir les navires de commerce. Durant le Second Empire, l'augmentation du trafic maritime, l'essor de la pêche et l'arrivée du chemin de fer vont obliger la ville à réaliser d'importants travaux pour aménager le Vieux-Port. Dès 1862, elle initie la construction d'un deuxième bassin: le bassin extérieur à flot, dit bassin des Chalutiers en 1922 après avoir été agrandi (Figure I.3b). Ce bassin spécialisé sera rapidement rempli d'une flotte hauturière, et jouera pleinement sa fonction de port de commerce jusqu'en 1891, date à laquelle le port de La Pallice sera inauguré (Figure I.3b). Ce port en eau profonde, situé à 5 km à l'ouest du centre historique redonnera un nouveau souffle à la vie maritime en assurant l'accueil des navires à fort tonnage qui étaient depuis longtemps obligés de mouiller du côté de Chef de Baie à cause de l'envasement récurrent de la baie. (*Bouquet de la Grye & Hatt, 1876*). Une bonne partie du trafic maritime commercial quitte le bassin des Chalutiers pour les nouvelles installations, mais certains trafics et activités de pêche subsistent. Le port de front de mer de La Pallice joua principalement un rôle militaire au cours des deux guerres mondiales successives du XXe siècle, mais les nombreux aménagements d'après-guerre ont permis de

développer son activité commerciale. De l'autre côté, dans le havre et le bassin à flot c'est une cohabitation entre pêcheurs et plaisanciers qui se met petit à petit en place. Celle-ci se terminera en 1970 suite à la création d'un espace portuaire de grande envergure dédié à la plaisance: le port des Minimes. En 1994, toutes les activités de pêche sont transférées à Chef de Baie (Figure I.3b), port ultra-moderne situé près du port de la Pallice délaissant le havre, le bassin à flot intérieur et le bassin des Chalutiers aux activités de plaisance.

La Rochelle possède des atouts naturels maritimes qui lui ont permis de développer des activités portuaires multiples afin d'assurer sa croissance économique et urbaine. Elle concilie encore aujourd'hui le commerce, la pêche et la plaisance au travers de nombreuses infrastructures portuaires spécialisées (Figure I.3b). Son port de pêche, à Chef de Baie, est classé 27ème au niveau national et son port de commerce, le port Atlantique de La Rochelle situé à la Pallice, est le 6ème grand port maritime français. Enfin, le port de plaisance, qui regroupe le Port des Minimes, la zone de mouillage de Port-Neuf, le Vieux-Port, le Bassin à Yatch (ancien bassin à flot), et le bassin des Chalutiers (Figure I.3b), est considéré comme l'un des plus grands ports de plaisance mondiaux et le plus grand port de la façade Atlantique.

I.2.2. L'aménagement du port de plaisance des Minimes

Sans se substituer aux autres activités portuaires, les services dédiés à la plaisance ont permis d'atténuer les difficultés croissantes de la pêche à La Rochelle et de modérer le déclin du grand commerce maritime qui eut ses heures de gloire du XVIe au XVIIIe siècle. Au lendemain de la 2nde guerre mondiale, la société des régates rochelaises (SRR), l'un des plus anciens clubs de voile en France, insuffle une dynamique sans pareille à La Rochelle, qui devient très vite le centre français de la voile (*Dussier, 2011*). A la fin des années 50, plusieurs chantiers navals rochelais s'étaient déjà diversifiés, voire reconvertis, vers la plaisance et au moment où ce type de navigation prenait un essor considérable, la municipalité prit conscience du potentiel économique de cette activité. Des aménagements réservés uniquement à la pratique de la plaisance furent développés au sein des bassins préexistants dès 1964 mais ils apparurent vite insuffisants. En 1971, la ville décida donc de construire un grand port réservé uniquement à cette activité au sud de la ville, à la pointe des Minimes, en bordure de vastes espaces inoccupés. Un port de plaisance moins gigantesque et luxueux que prévu sera finalement aménagé au cours des deux décennies suivantes (*Dussier, 2011*).

La Figure I.5 retrace les différentes étapes de construction et d'aménagement du port de plaisance des Minimes. Les photos datant de 1958 et 1972 permettent de mettre en avant l'aspect originel du bassin, avant son utilisation pour abriter des bateaux. Avant la construction du port, des vasières bordaient le chenal de navigation et recouvraient certainement toute la baie avant que l'Homme y laisse son empreinte. En 1972, trois ans après le début du chantier, l'érection de la digue du Lazaret et de la digue de Bout Blanc est achevée. Une première souille est draguée pour accueillir les premiers bateaux au nord de la digue Lazaret et en 1973, les dragages se poursuivront le long de cette digue jusqu'au fond du port. En 1974, la construction d'une digue-épi marque le début de la construction du môle central et les aménagements du Lazaret porteront la capacité d'accueil à 1000 places dès 1975. L'année 1976 marque le début de l'aménagement du bassin du Bout Blanc qui va se poursuivre durant deux ans puis en 1978 le bassin Marillac est creusé à sec par dévasage et déroctage. A la fin des années 70, le nouveau port à flot est entièrement creusé et prêt à accueillir des bateaux de toute la France mais la marie décide d'aménager les pontons en fonction des besoins. C'est

seulement en 1992 que les aménagements se terminent et dès 1999 la capacité totale du port est atteinte (Figure I.5). Dans les années 2000, les délais d'attente pour obtenir une place à flot dans les ports de plaisance français, sont très longs (jusqu'à 5 à 12 ans en fonction des dimensions du bateaux). Le conseil municipal décide alors de créer une extension à cette époque et une étude d'impact est menée en 2006, afin de décider du site d'implantation possible. Cet agrandissement est entrepris en 2011 et s'achève en 2014: une partie de la digue du Lazaret est d'abord démontée, puis déplacée, de manière à permettre l'implantation de trois pontons supplémentaires; le nouveau bassin des Tamaris est creusé au nord de la digue du Bout Blanc puis délimité par la nouvelle digue du Nouveau monde. Cette digue est elle-même rattaché au trait de côte via la passerelle Nelson Mandela. L'extension du port a permis de réduire les délais d'attente en assurant une capacité d'accueil de près de 4 500 places à flot ce qui constitue la moitié de la capacité totale des infrastructures portuaires de plaisance en Charente-Maritime. La Rochelle, ville-port tournée vers l'océan depuis sa création, est aujourd'hui la capitale de la plaisance en Charente-Maritime et l'un des principaux centres nautiques en France (*Dussier, 2015*).

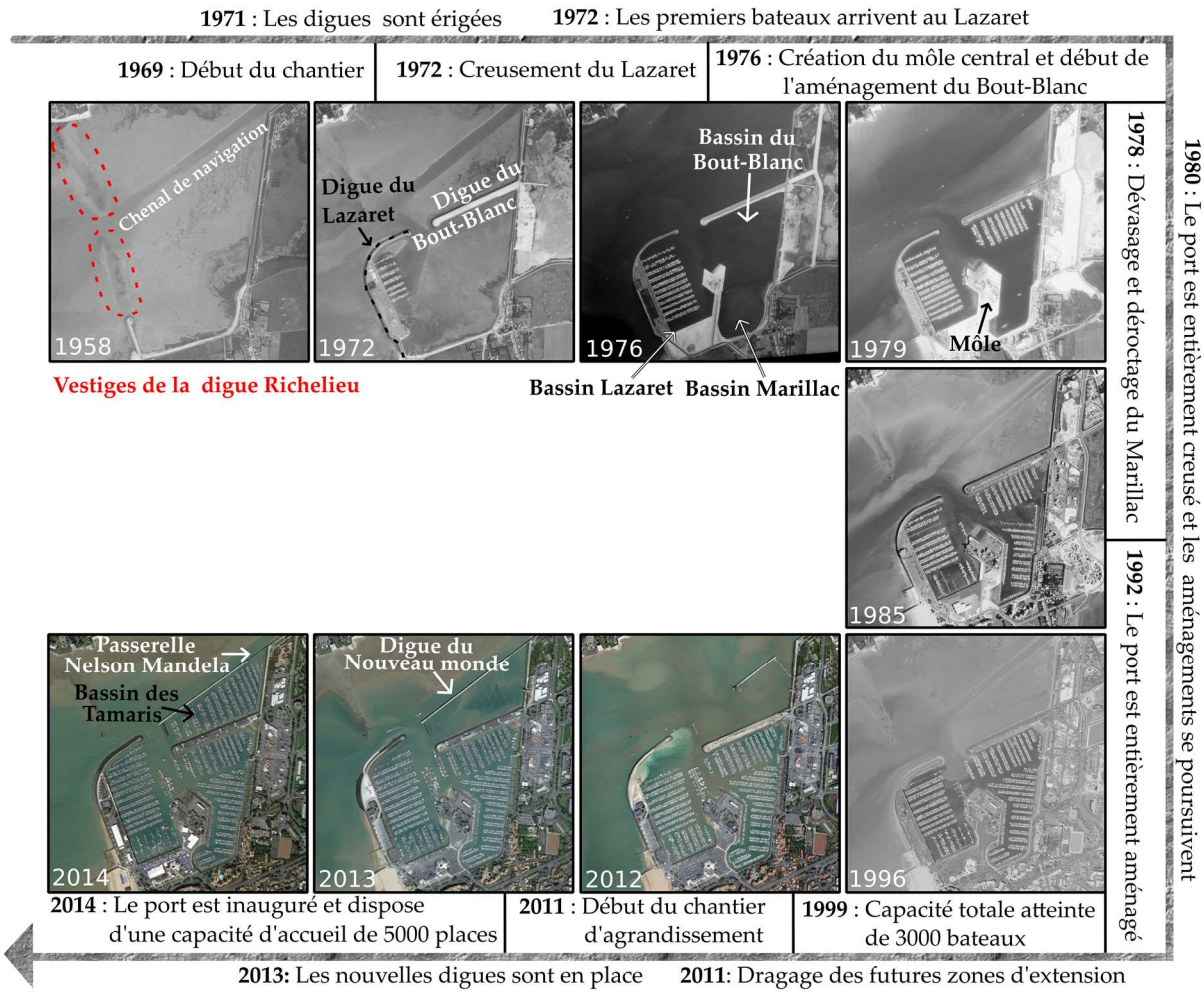

Figure I.5. *Evolution de la baie de La Rochelle au cours de la construction du port des Minimes et de son extension. (Sources: IGN de 1958 à 1996 et Google Earth de 2012 à 2014)*

I.2.3. Une lutte historique contre l'envasement

Malgré son histoire mouvementée, La Rochelle a su profiter de son principal atout pour prospérer: une position géographique unique sur la façade atlantique. Pourtant, au travers des différents écrits sur l'histoire de La Rochelle, il apparaît que sa lutte contre l'envasement, principale objet de cette thèse, ne date pas d'hier. Nous retraçons ici cette lutte inexorable contre cet ennemi insidieux, qui fut parfois un frein au trafic maritime et au développement de la ville. Protégée par les brises lames naturels que constituent Ré et Oléron, la baie de La Rochelle fut, depuis toujours, un refuge idéal aux navigateurs (*Chasse-marée, 1991*). Le premier havre utilisé par les pêcheurs s'envasait rapidement malgré les efforts, dérisoires, des riverains, qui entretenaient et curaient les quais attenant à leurs habitations avec des pelles et des paniers. C'est pourquoi, dès le XIIIe siècle, l'envasement progressif et l'augmentation de la taille des navires conduisent rapidement à aménager un bassin portuaire au niveau de l'actuel vieux port, au fond de la baie. Ce nouveau havre connait un régime hydrodynamique calme et est donc sujet à un dépôt lent et constant de vases (*Bouquet de la Grye & Hatt, 1876).* L'utilisation de systèmes d'écluses de chasse des ruisseaux débouchant sur le havre permettront de diminuer l'envasement en créant un fort courant à leur ouverture. Un éperon de pierre sera aussi aménagé le long de l'entrée Est du bassin et 2500 lignes de pieux seront plantées près de la tour de la lanterne afin de diminuer l'apport de galets bloquant l'accès au havre.

Ces aménagements ne seront pas tous fructueux et l'envasement suscitera encore des inquiétudes à l'époque, mais c'est réellement à partir du Grand Siège de La Rochelle, en 1627, que l'envasement sera très fortement accentué par les vestiges de la digue qui ne laissaient, à l'entrée de la baie, qu'un étroit goulet. Le royaume de France entreprit l'entretien du chenal d'accès au havre d'échouage, néanmoins un siècle plus tard, près de 2 m d'envasement furent constatés ce qui devenait préoccupant pour la survie du port. Au XVIIIe siècle les travaux successifs sont insuffisants et l'envasement, à la fois du havre, et du chenal, demande de décharger et charger les plus gros navires au large du port. A cette époque, les cure-moles sont les premières machines à curer, mues par la force humaine, et utilisés en combinaison avec des marie-salope à voile. Ces techniques ne permettront pas d'assurer un accès constant au port et les échouages et les accidents de navigation seront légion. Il faudra attendre les progrès de la révolution industrielle et l'invention des dragues à vapeur pour que soit enfin maitrisé l'adversaire (*Chasse-marée, 1991*). Les révolutions technologiques du XIXe siècle, et surtout l'apparition de la machine à vapeur, vont accompagner l'évolution des engins de dragage. C'est en 1867 que La Rochelle se dote de sa première drague à vapeur mais c'est réellement la drague à vapeur « D6 » qui marquera les esprits, dès son arrivée en 1956. Cette drague stationnaire à godets aidera notamment à débarrasser le port de La Rochelle des nombreuses épaves qui l'encombrent. Sa carrière s'achève en 1987 lorsqu'elle est remplacée par des dragues aspiratrices plus modernes, aux capacités de stockage et de rendement plus élevées.

Aujourd'hui comme dans le passé, les différentes infrastructures portuaires de La Rochelle subissent un envasement naturel toujours aussi prononcé qui nécessite un entretien par les dragues quasi-constant. C'est près de 10 % du budget annuel total du port de plaisance de La Rochelle qui est consacré au dragage, actuellement. En moyenne, 200 000 m^3 de sédiments cohésifs sont dragués dans l'enceinte du port chaque année. Les opérations de dragage s'étalent sur huit mois consécutifs, et concernent un tiers de la surface du port par an.

Le chenal de navigation, au nord de la digue du Nouveau monde, (Figure I.5) est dragué chaque année jusqu'à la profondeur cible de -1 *m* sous le zéro hydrographique. Le bassin des Tamaris doit être dragué tous les trois ans pour atteindre entre -2 et -3m. Enfin, le reste du port est dragué entre -1 et -2 *m* en fonction de l'envasement observé lors de la dernière campagne. Le chenal de navigation est dragué par la Cap d'Aunis (Figure I.6b), une drague aspiratrice à marche ouvrante. Les différents bassins du port sont dragués par Avalis II (Figure I.6a), une drague suceuse stationnaire reliée à un tuyau d'aspiration qui relargue directement les boues de dragage à l'extérieur du port via une canalisation. En complément de ces dragues hydrauliques, le rotodévaseur Mer d'Antioche (Figure I.6c) est aussi utilisé pour remettre en suspension les vases les moins accessibles, en bordure de quais.

Figure I.6. *Photographies des trois principaux navires permettant de lutter contre l'envasement dans le port des Minimes et son chenal de navigation. (a) La drague suceuse stationnaire « Avalis II » (b) La drague aspiratrice « Cap d'Aunis » (c) Le rotodévaseur « Mer d'Antioche ». (Source: Antoine Mérigot)*

I.3. Positionnement des travaux et objectifs de thèse

Comme toute région abritée, les ports font office de bassins de décantation pour les vases en suspensions, apportées par l'effet conjoint des courants et de la houle. Cet envasement naturel n'est pas nouveau et existe depuis l'apparition des tous premiers ports (*Noli & Franco, 2009; Marriner & Morhange 2007; Galili et al., 2010; Raban, 1995*). Les conditions d'envasement d'un port dépendent du régime hydro-sédimentaire présent à l'extérieur du bassin, mais aussi de sa configuration d'entrée. Une grande variété de ports sont présents à travers le monde et les taux d'envasement peuvent varier drastiquement en fonction des environnements. Certains, comme à Emden et Burnsbuttel (Allemagne), subissent plus de 2 m d'envasement annuel (*Nasner, 1992; Nasner, 1997*). Si l'envasement est aujourd'hui un problème que la plupart des ports doivent gérer, il est intéressant d'observer la relative absence de prise en compte de ce risque dans la création des ports. L'aménagement côtier s'est souvent effectué sans tenir compte des caractéristiques du milieu et de leur évolution naturelle (*Paskoff, 2010*). D'une manière générale à travers le monde et l'histoire, le choix d'implantation des structures portuaires a davantage reposé sur des critères économiques terrestres et sociaux voire politiques, liés au développement du territoire, que sur des données océanographiques et climatiques (*Béthourné & Valcke, 2015*).

Bien que les technologies aient évoluées, les méthodes pour lutter contre l'envasement naturel n'ont pas changé et le moyen le plus direct et le plus efficace pour se débarrasser du surplus de vase reste encore le dragage. Cette technique d'excavation ancienne était déjà utilisée sur les rives du Tigre et de l'Euphrate (*Herbich, 1975*) ainsi que dans les ports antiques du Levant (*Marriner & Morhange, 2006; Marriner et al., 2014*). Le dragage a traversé les âges et les révolutions technologiques, en s'adaptant à la demande tout en accroissant son rendement, mais le concept reste toujours le même: on cure la vase là où elle s'est installée et accumulée afin d'éviter d'entraver la navigation et les activités portuaires. Aujourd'hui, c'est la méthode la plus fréquemment utilisée dans le milieu portuaire (*Montgomery, 1984; Batuca and Jordaan, 2000; Bianchini et al., 2019*) et on estime, dans le monde, que des dizaines de milliards de tonnes de sédiment sont dragués chaque année (*EPA, 1989*). A titre indicatif, en 2011, c'est près de 58 millions de m^3 qui furent dragués en France pour l'entretien et les travaux des voies navigables et bassins portuaires (*El Fadili & Messager, 2015*). Les sept grands ports maritimes de métropole se partagent 86% de ces volumes mais ce sont principalement les ports en estuaire (Bordeaux, Rouen et Nantes) qui nécessitent le plus de besoin.

La plupart du temps, aucune stratégie n'est préalablement définie et la seule indication est de curer les fonds qui ne sont plus compatibles avec la navigation. Bien qu'efficace sur le court terme, cette méthode dite de « réaction » ne s'attaque pas à la source d'envasement en tant que tel et ne garantit donc pas une diminution, ou un contrôle de l'envasement, sur le long terme. Le manque de connaissance de l'environnement local et des processus physiques amenant au dépôt des vases dans le milieu, conduit souvent les gestionnaires des ports à utiliser de manière automatique et récurrente cet indispensable travail de Sisyphe qu'est le dragage. De nombreux ports semblent s'accommoder de ces opérations encombrantes et chronophages, si bien qu'elles font désormais partie du quotidien portuaire, au même titre que les activités liées à la plaisance, au commerce ou encore à la pêche. Alors que les plus grands ports ne lésinent pas sur les moyens pour conserver des profondeurs compatibles avec la

navigation, les ports de plus petites tailles doivent se serrer la ceinture pour allouer une grande partie de leur budget à cette problématique. A titre d'exemple, aux Pays-Bas, c'est près de 500 millions d'euros qui sont dépensés annuellement pour le dragage des ports de plaisance (*Ommen & Schaap 1995*). Même si elles sont onéreuses, les opérations de dragage restent fiables, ce qui explique leur récurrence et leur expansion dans le paysage portuaire. C'est pourquoi, ces méthodes apparaissent difficiles à remplacer, ce qui explique le manque d'appétence pour d'autres technologies qui pourraient nécessiter moins d'entretien sur le long terme. Le dragage peut aussi interférer avec les activités nautiques et impliquent parfois d'interdire l'accès d'une partie ou de la totalité du port.

Cependant, le dragage génère des impacts environnementaux à différentes échelles. Les écosystèmes marins peuvent être significativement perturbés (*Sabol & Shafer, 2005 ; Rehitha et al., 2017*), en particulier les communautés benthiques, particulièrement présentes dans les vases, et dont la structure trophique, la biomasse mais aussi la diversité peuvent être gravement affectées par les activités de dragage (*Newell et al., 1998 ; Gulbin et al., 2003*). Dans certains cas, cela peut même favoriser l'établissement et le développement d'espèces non-indigènes au détriment d'espèces déjà installées (*Oricchio et al., 2019*). Qu'il soit réalisé de manière mécanique ou hydraulique, le dragage contribue aussi, nettement, à la remise en suspension de sédiment dans la colonne d'eau, ce qui augmente par conséquent la turbidité ambiante (*Van Maren et al., 2015*). Cela peut avoir des effets adverses sur les écosystèmes, en diminuant la pénétration de la lumière dans l'eau (*Onuf, 1994; Short & Wyllie-Echeverria 1996; Becker et al., 2015*), mais aussi sur la qualité globale de l'eau, en libérant des particules polluées directement dans le milieu (*Cearreta et al., 2004; Turekian et al., 2010*). Dans les milieux portuaires, les polluants tels que les métaux lourds, pesticides et hydrocarbures stagnent et se concentrent tout particulièrement sur les sédiments. La prise de conscience environnementale assez récente de l'impact du dragage a conduit à une législation internationale plus restrictive depuis une vingtaine d'années. Les opérations portuaires doivent maintenant s'inscrire dans une gestion intégrée et concertée de la mer et du littoral, prenant en compte l'ensemble des activités humaines, la préservation de l'environnement et la valorisation des ressources dans une perspective de développement durable (*Béthourné Nathalie & Valcke, 2015*). Depuis 1990 en France, le groupe GEODE (Groupe d'Etudes et d'Observation sur le Dragage et l'Environnement) produit un guide technique des bonnes pratiques en matière de dragage portuaire et permet de statuer sur le devenir des sédiments (rejet en mer, remblais, stockage à terre, traitement…). Même si c'est la méthode la plus utilisée à ce jour pour régler les problèmes d'envasement récurrents, le dragage, et la gestion des sédiments qui en découle, présentent donc des contraintes techniques, économiques et environnementales. A l'heure où des stratégies durables et contrôlées pour la conception, la réalisation et l'aménagement des ports devient un enjeu important (*Kavakeb et al., 2015; Acciaro et al., 2014 ; Di Vaio & Varriale, 2018*), la lutte contre l'envasement doit être plus proactive. Néanmoins, le développement et la mise à l'essai d'alternatives potentielles (*Parchure & Teeter, 2003; Salman et al., 2004 ; Winterwep, 2005*) sont souvent entravés par un certain nombre d'obstacles, non seulement technologiques, mais principalement liés aux risques perçus par l'investissement élevé et l'incertitude des coûts d'exploitation.

A La Rochelle, l'envasement oblige à procéder au curage d'entretien du port des Minimes huit mois par an, avant que la saison estivale ne démarre. Depuis l'extension de son site principal en 2014 (Figure I.5), la régie du port de plaisance nécessite encore plus de moyens

pour draguer le port. Un des objectifs était donc d'apporter des éléments de réponse pour optimiser les stratégies de dragage déjà mises en place par le port, en limitant le coût mais aussi le temps associé à ces opérations. Pour répondre à cette question, la compréhension de la dynamique hydro-sédimentaire du système était nécessaire. D'où vient principalement la vase ? Comment se répartit-elle dans le port ? Quel est l'impact des structures et des aménagements sur le dépôt ? Quels sont les principaux contributeurs de cet envasement ? Toutes ces questions restaient sans réponse avant ce travail, même si de nombreuses études avaient déjà été réalisées dans le port. La cellule CREOCEAN avait en-effet pris en charge l'étude des conditions naturelles en vue de l'extension du port des Minimes (*CREOCEAN 2004, 2008, 2005, 2010*) et elle avait aussi réalisé une étude de dispersion des sédiments clapés afin de procéder au renouvellement de la demande d'autorisation de dragage (*CREOCEAN, 2012*). S'ajoutent à cela, des mesures régulières de la qualité de l'eau et du sédiment et de nombreuses études environnementales. Sans se substituer aux études passées, cette thèse permet donc d'approfondir en détail les processus physiques et sédimentaires inhérents à cet espace ultra-anthropisé, dans le but d'optimiser l'une de ses activités les plus chronophage, onéreuse et encombrante: le dragage.

Originellement tourné vers le secteur de l'ingénierie civile, le développement des ports a progressivement dévié vers de nouvelles disciplines. Depuis le milieu des années 90, la recherche a explosé dans ce secteur en consacrant un nombre croissant d'articles (Figure I.7) spécifiques aux domaine économique, politique et de gestion (*Parola and Musso, 2007; Woo et al., 2010 ; Woo et al., 2011*). La thématique de l'envasement, souvent restreinte au cadre privé, ne concerne qu'une légère proportion des publications et il ne semble pas y avoir de tendance vers un accroissement (Figure I.6b). La recherche portuaire est encore un domaine peu cohérent et dans une phase d'émergence, se caractérisant par la présence de plusieurs petites communautés de chercheurs ayant peu d'interactions entre elles (*Pallis et al., 2010*). Au travers des différents enjeux qu'ils représentent, les ports sont devenus des carrefours à partir desquels devrait néanmoins s'organiser la recherche interdisciplinaire. La complexité des transports, des services et aménagements, ainsi que des impacts associés, nécessite une approche plus intégrée de ces environnements (*Heaver, 2006*), contraints à la fois par l'Homme et ses besoins mais aussi et surtout par la Nature. C'est dans cette optique que s'est déroulée cette thèse, qui jongle entre plusieurs thématiques, gravitant toutes autour de la compréhension de la dynamique hydro-sédimentaire, et dont les principaux objectifs sont les suivants:

- Quelle est la dynamique hydro-sédimentaire du port des Minimes ?

- Quelle est la contribution de la marée, du vent et des vagues dans cette dynamique et quels sont les principaux mécanismes physiques mis en jeu ?

- Quelle est l'influence des aménagements portuaires sur cette dynamique ?

- Quel est le renouvellement des masses d'eaux dans le port ?

- Est-il possible de réduire l'envasement, et comment y arriver ?

-Comment optimiser les stratégies de dragage déjà mises en place ?

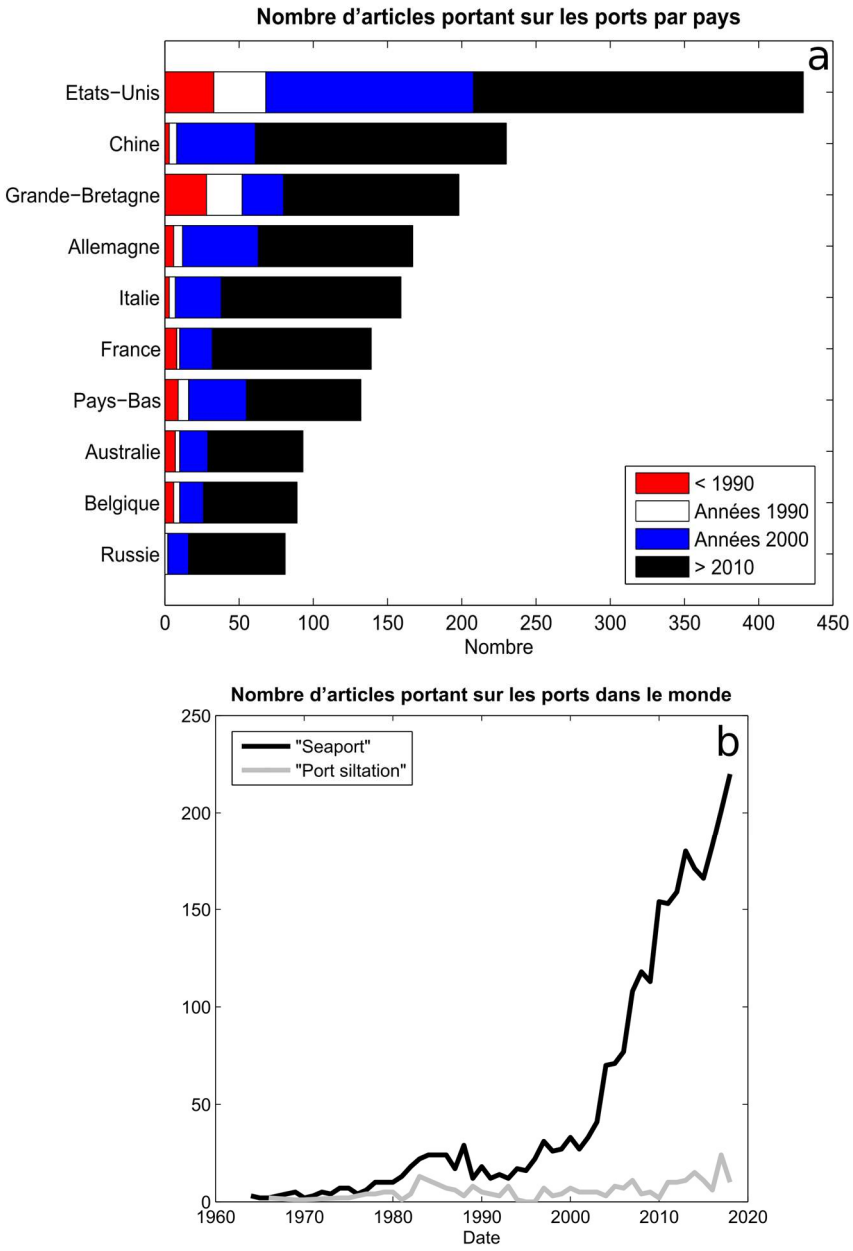

Figure I.7. *Etude bibliographique du nombre et de l'origine des publications relatives à la recherche portuaire dans la base de données SCOPUS. (a) montre le nombre d'articles portant sur les ports, classés par décennie à partir de 1990, pour le top 10 des pays actuels dans le domaine. (b) permet de constater l'évolution du nombre d'articles sur les ports de 1964 à 2018. La courbe noire correspond au nombre de publications trouvées avec le mot-clé « seaport » correspondant à « port maritime » alors que la courbe tiretée en gris correspond au nombre de publications trouvées avec le mot-clef « port siltation » correspondant à « envasement portuaire ». Les résultats de recherche issus de ces deux mot-clefs sont les plus concordants trouvés pour le thème initial recherché.*

I.4. Organisation du Manuscrit

Le manuscrit s'organise de la manière suivante:

Les Chapitres II et III sont alloués respectivement, à la description du site d'étude, puis à la méthodologie utilisée pendant la thèse. Le Chapitre II est découpé en deux parties. Il décrit l'environnement local du site d'étude (les Pertuis Charentais) puis le site d'étude (le Port des Minimes) dans un second temps. Aux descriptions géographiques et géomorphologiques, s'ajouteront des données océanographiques et climatiques. Cette partie nous permettra de comprendre le système hydro-sédimentaire dans lequel le port des Minimes se situe. Dans le Chapitre III, la stratégie employée dans cette thèse est exposée, ainsi que les données et les méthodes utilisées. Cette partie tentera de résumer les efforts fournis en instrumentation et en modélisation mais elle restera assez succincte pour éviter les redondances avec les Chapitres de résultats qui suivront. Les méthodes seront en-effet abordées de manière plus détaillée au sein même des articles.

Les Chapitres IV, V, VI, VII présentent tous les résultats issus des trois ans de travaux de thèse, sous forme d'article. Au moment où j'écris ces lignes, le premier article, correspondant au Chapitre IV, est publié ainsi que le second article, correspondant au Chapitre VI. Le troisième article, correspondant au Chapitre V tout comme le quatrième article constituant le Chapitre VII sont tous les deux écrits et en forme pour être envoyés à des revues scientifiques. Afin de garder une certaine cohérence nous avons respecté le même formalisme que dans le reste du manuscrit mais ces quatre chapitres sont rédigés en anglais. Toutefois, un résumé court et concis sera écrit en français à chaque début de Chapitre afin d'exposer les objectifs et les résultats principaux de l'article. Les parties « site d'étude » sont assez courtes et similaires dans chacun des articles soumis mais nous avons décidé de les conserver dans le corps du texte en estimant que la continuité du manuscrit serait peu affectée.

Le Chapitre IV présente l'impact des aménagements flottants (bateaux, pontons...) sur l'hydrodynamique portuaire. Le Chapitre V décrit, plus en détail, l'effet du vent et de la marée sur la circulation portuaire, en lien avec la géométrie du port. Le Chapitre VI a pour but de caractériser le renouvellement des eaux dans le port, à travers l'étude de plusieurs descripteurs temporels. Le Chapitre VII vise à quantifier l'influence de différentes techniques de lutte contre l'envasement dans le port tout en identifiant l'apport relatif de la marée, du vent et des vagues dans la dynamique sédimentaire du port.

Le Chapitre VIII énoncera ensuite, les conclusions et perspectives découlant de ce travail de thèse. Toutes les thématiques abordées au cours du manuscrit seront discutées et mises en relations afin de faire un bilan de ce travail et de montrer les possibles pistes de recherche. Cette partie sera suivie par les Annexes où seront disponibles les différents tests de sensibilité du modèle ainsi que d'autres résultats.

Chapitre II

Site d'étude

II.1. Les Pertuis Charentais

II.1.1. Contexte Géographique et Géomorphologique

La Rochelle et son port de plaisance sont situés le long de la côte Atlantique française, au niveau de la partie centrale du golfe de Gascogne (Figure II.1). Ils profitent d'une position enclavée au fond de la partie nord du Pertuis d'Antioche, une zone maritime abritée par deux îles principales: Ré et Oléron. Cette zone fait partie d'un plus vaste ensemble, appelé Pertuis Charentais, et dont le domaine littoral s'étend de la côte Aquitaine, rectiligne et sableuse, au sud, aux côtes mixtes sablo-rocheuses et découpées de la Vendée, au nord. La continuité terrestre des Pertuis Charentais correspond à de larges bandes côtières de basse altitude qui abritent en grande partie des marais s'enfonçant jusqu'à plus de 40 km dans les terres. Ces marais sont parcourus par quatre rivières débouchant dans les Pertuis Charentais, du Nord au Sud: le Lay, la Sèvre Niortaise, qui se jettent dans le Pertuis Breton au nord; la Charente et la Seudre qui débouchent dans le Pertuis d'Antioche. Ces ensembles terre-mer correspondent à des segments d'anciennes vallées incisées (*Weber, 2004; Chaumillon & Weber, 2006*). D'après *Barusseau (1973)*, elles ont été creusées dans un socle calcaire d'origine Mésozoïque (de −252.2 à −66.0 Ma) par l'alternance d'épisodes de glaciation et de réchauffement pendant le Quaternaire (depuis -2.58 Ma), avant d'être partiellement comblées par des formations fluviomarines depuis la fin de la transgression flandrienne (*Weber et al., 2004; Chaumillon et al., 2008*). Aujourd'hui, les Pertuis Charentais, longs de 90 km et larges d'environ 40 km, présentent un linéaire côtier de plus de 350 km, renforcé par la présence d'un archipel dense et de nombreuses baies.

Côté mer, les fonds atteignent en moyenne 20 m à l'entrée des Pertuis et faiblissent progressivement aux abords des côtes des îles de Ré et Oléron. Le Pertuis Breton, qui sépare l'île de Ré du continent, présente des profondeurs maximales de 55 m au niveau de la partie orientale des fosses de Chevaraches (Figure II.1). Sa morphologie ressemble à un canal semi-fermé long de 25 km et large de 10 km. Il est relié au Pertuis d'Antioche dans sa partie sud, au

niveau du courreau étroit de la Pallice, séparant l'île de Ré du continent. Le Pertuis d'Antioche, séparant les deux îles, fait 35 km de long pour 15 km de large. Il est constitué d'une fosse de 45 m de profondeur, cernée au nord et au sud par les estrans rocheux des îles de Ré et d'Oléron. Le sud du Pertuis d'Antioche est directement connecté à la baie de Marennes-Oléron, une baie peu profonde. Il est connecté dans sa partie sud au golfe de Gascogne et à l'estuaire de la Gironde via le Pertuis de Maumusson, une ancienne vallée incisée (*Chaumillon and Weber, 2006*) aujourd'hui principalement constituée de sable et dont la profondeur maximale atteint les 15 mètres. La spécificité de la baie de Marennes-Oléron tient à son fort pourcentage en zones intertidales, estimé à près de 58 % alors que les Pertuis Breton et d'Antioche en présentent respectivement 19 % et 13 %. Les caractéristiques géo-morphologiques et hydrologiques de ces trois zones spécifiques des Pertuis sont résumées dans le Tableau II.1 (*Stanisière et al., 2006).*

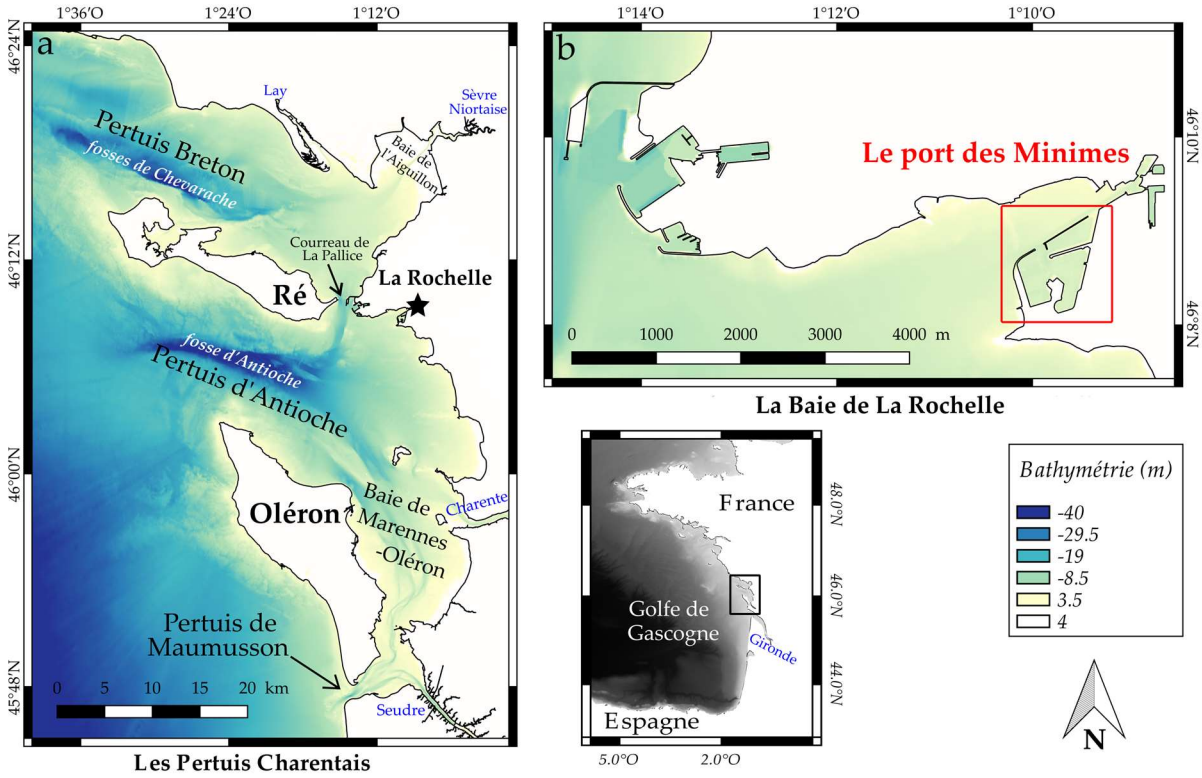

Figure II.1. *Bathymétrie des Pertuis Charentais (a) et de la baie de la Rochelle (b). (Source: SHOM, 2015)*

Tableau II.1. *Caractéristiques morphologiques et hydrologiques des Pertuis Charentais.*

	Pertuis Breton	**Pertuis d'Antioche**	**Baie de Marennes-Oléron**
Profondeur (m)	13.8	19.8	8.6
Surface moyenne (km^2)	425	399	156
Surface intertidale (km^2)	80 (19 %)	51 (13 %)	91 (58 %)
Nombre d'ouvertures	2	3	2
Volume moyen (Mm^3)	4920	5527	805
Volume oscillant (Mm^3)	1650 (34 %)	1560 (28 %)	604 (75 %)
Bassin versant (Nombre fleuves / surface km^2)	2/4074	1/432	2/10842

II.1.2. Contexte hydro-climatique

L'environnement des Pertuis Charentais est considéré mixte, dominé par la marée, les vagues et le vent, mais aussi impacté par les fleuves. Une contextualisation de ces différents agents hydrodynamiques s'impose.

II.1.2.1. Marée

La marée préside à la circulation des masses d'eaux dans les Pertuis Charentais (Nicolle, 2006). Comme dans le reste du golfe de Gascogne, le spectre de marée est dominé par des composantes semi-diurnes. La plus importante est l'onde M2 de période 12 heures 25 et dont l'amplitude, qui atteint 174 *cm* au fond des Pertuis, est fortement amplifiée par l'effet combiné des faibles profondeurs (*Poincaré & Fichot, 1910*) et de la résonance (*Bertin et al., 2012*). L'analyse harmonique du signal de marée, enregistré par le marégraphe de La Rochelle, a permis d'obtenir la structure harmonique de la marée dans la zone (*Bertin et al., 2012; Gouriou, 2012; Nicolle & Karpytchev, 2007*). Le Tableau II.2 présente les amplitudes et phases des composantes harmoniques principales à La Rochelle, issues de la thèse de *Gouriou (2012)* après analyse sur une série temporelle de 60 ans.

Tableau II.2. *Principales composantes harmoniques à La Rochelle ainsi que leurs phases et amplitudes.*

Composantes harmoniques	**Amplitude** (*cm*)	**Phase** (°)
O1	7.3	326
K1	6.2	74
M2	174.6	99
S2	62.9	132
N2	36.2	80
K2	17.9	130
NU2	6.9	83
M4	24.8	11
MS4	10.2	97
MN4	10.8	323

L'analyse spectrale est marquée par une forte contribution des composantes semi-diurnes (M2, S2, N2 et K2) mais les composantes quart-diurnes (M4, MS4 et MN4), des harmoniques résultant d'interactions non linéaires, affichent également des amplitudes non-négligeables. A l'inverse, les ondes diurnes ont une amplitude très faible dans les Pertuis. L'onde M4 atteint une amplitude de 24.8 *cm* à La Pallice, ce qui est quasiment comparable à l'amplitude de N2 et représente une des particularités des Pertuis. L'interaction de cette onde avec M2 est une des causes principales des asymétries de marée dans les environnements semi-diurnes et peu profonds tels que les Pertuis (*Speer & Aubrey, 1985; Ranasinghe & Pattiaratchi, 2000; Toublanc et al., 2015*). La résultante de toutes les composantes harmoniques soumet la région à un marnage moyen de 4 *m* ce qui équivaut à un régime macro-tidal. La plus haute marée astronomique atteint près de 6.75 *m* au-dessus du zéro hydrographique pour un coefficient théorique de 120 et le marnage peut descendre en-dessous de 2 *m* lors des plus faibles périodes de mortes-eaux (*Nicolle, 2006*).

L'onde de marée semi-diurne en provenance de l'océan Atlantique progresse du sud vers le nord dans le golfe de Gascogne. Elle se gonfle à l'entrée des Pertuis, à la rencontre des petits fonds, et se déforme à l'approche des côtes rochelaises, notamment en période de mortes-eaux. Au flot, l'onde de marée pénètre simultanément dans les eaux des deux Pertuis. Les eaux en provenance du Pertuis d'Antioche alimentent la baie de Marennes-Oléron, la baie de la Rochelle ainsi que le courreau de la Pallice et une partie de la baie de l'Aiguillon (Figure II.1). Les courants de marée dans la baie de La Rochelle sont plutôt faibles (0.6 nœuds en vives eaux, alternatifs et réguliers (*CREOCEAN, 2004*). Les eaux venant du Pertuis Breton ne pénètrent pas dans le courreau de la Pallice et n'influencent pas la circulation induite au flot dans le Pertuis d'Antioche, ce qui génère une circulation résiduelle du sud vers le nord au niveau du courreau, mais aussi dans le Pertuis Breton (Figure II.2). L'asymétrie engendrée par la séparation de l'onde de marée autour de l'île d'Oléron est encore plus forte et génère une domination du jusant dans le Pertuis de Maumusson, où les courants de marée peuvent atteindre les 1.8 ms^{-1} en vives-eaux. Les plus forts courants de marée sont de manière générale localisés aux pointes des îles avec des vitesses maximales de 1 à 1.8 ms^{-1} (*Bertin et al., 2005*). Une circulation résiduelle s'établit alors dans le sens nord-sud entre le Pertuis d'Antioche et la baie de Marennes-Oléron (Figure II.2).

Du point de vue hydrologique, la morphologie des différents bassins des Pertuis contribue de manière significative au déplacement des masses d'eaux induit par la marée. Les volumes oscillants tidaux représentent 34 % et 28 % du volume d'eau pour le Pertuis Breton et d'Antioche, respectivement, et 75 % pour la baie de Marennes-Oléron. Dans ces conditions, les temps de renouvellement ont été estimés à 85 jours pour le Pertuis Breton, 104 jours pour le Pertuis d'Antioche et seulement 12 jours pour la baie de Marennes-Oléron (*Stanisière et al., 2006*).

II.1.2.2. Conditions météorologiques

Dans les Pertuis, les vents dominants sont issus de directions nord-ouest à sud-ouest (50% des observations) puis de directions Est à Nord-Est (20 % des vents). L'oscillation nord-atlantique contrôle en grande partie la variabilité interannuelle des régimes de vents dans les Pertuis, ainsi que dans tout le golfe de Gascogne (*Dodet et al., 2010*). La zone géographique est soumise à des variations climatiques saisonnières et on peut identifier deux principaux régimes saisonniers. En hiver, les systèmes dépressionnaires qui ont traversé l'Atlantique sont particulièrement actifs et peuvent générer des vents très violents, de secteur sud-ouest à nord-ouest. Les vents les plus forts de l'année y sont enregistrés avec des vitesses supérieures à 13 ms^{-1} environ 25 % du temps (*Weber, 2004; Allard et al., 2008*). Le centre Météo France de La Rochelle a enregistré au cours de l'ouragan Martin le 27/12/1999, la vitesse record instantanée de vent à 42 ms^{-1}. Le régime estival se démarque du régime hivernal avec une activité dépressionnaire beaucoup plus faible, et des vents de secteur est à nord-est plus présents. A cette période, ce sont des brises thermiques de secteur nord-ouest qui dominent principalement le littoral avec une quasi-absence de vents supérieurs à 13 ms^{-1} (*CREOCEAN, 2004*). D'après *Stanisière et al. (2008)*, le vent est le principal paramètre impliqué dans le renouvellement des masses d'eaux dans les Pertuis Charentais. Même si son effet est nettement moins marqué dans la baie de Marennes-Oléron, sa contribution reste très forte dans les Pertuis Breton et d'Antioche. La Figure II.2 permet de restituer le comportement relatif de la circulation résiduelle dans les Pertuis, sous l'action conjuguée de la marée et de vents d'orientation différente et d'intensité moyenne. Alors que les vents d'est et de sud favorisent

une courantologie orientée du Pertuis d'Antioche vers le Pertuis Breton, les vents de secteur ouest à nord favorisent l'entrée d'eaux océaniques dans le Pertuis Breton et leur évacuation par le Pertuis d'Antioche et la baie de Marennes-Oléron.

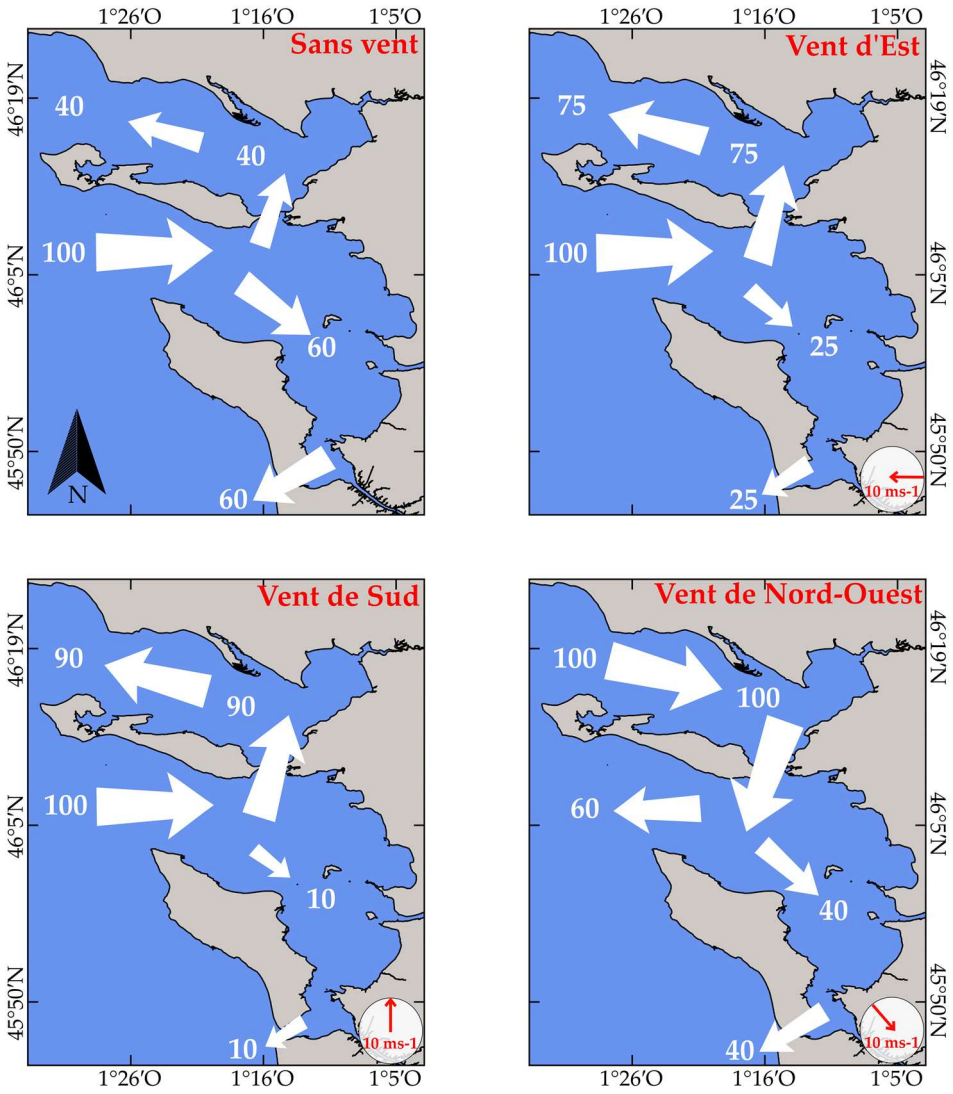

Figure II.2. *Flux résiduels relatifs pour différentes configurations de vent soufflant à 10* ms^{-1}.

II.1.2.3. Climat de houle

Deux types d'agitation sont susceptibles d'être observées au niveau de la baie de La Rochelle: les houles d'origine océanique générées au large des Pertuis et caractérisées par des périodes élevées, et les mers de vent formées par l'action directe des vents locaux. Le climat de houle a été analysé localement par *Bertin et al. (2008)*, à partir de données de vagues entre 1997 et 2008, sur un point au large des Pertuis charentais (46°N - 2.5°O). Il en résulte que 60 % des vagues présentent des hauteurs significatives comprises entre 1 et 2 m, tandis que les vagues de hauteur significative supérieure à 5 m représentent à peu près 3 % des cas. La hauteur significative moyenne annuelle est d'environ 1.5 m. Les périodes de pic comprises entre 8 et 12 s représentent 60 % de la distribution et les périodes de pic supérieures à 15 s ne sont observées que 2 % du temps. Enfin, les directions de vagues prédominantes sont d'origine

ouest à nord-ouest, ce qui représente 60 % du climat de vague et les plus fortes houles proviennent généralement de l'ouest. On observe une variabilité saisonnière du climat de vagues dans le golfe de Gascogne et plus au large, avec des hauteurs significatives de vagues en moyenne plus de deux fois plus importantes en hiver qu'en été. La hauteur significative des vagues peut dépasser 8 m lors des tempêtes hivernales à l'entrée du Pertuis d'Antioche (Bertin et al., 2015). *Dodet et al. (2010)* ont mis en évidence l'influence de l'oscillation nord-atlantique sur la forte variabilité interannuelle du climat de vagues dans l'Atlantique Nord. La Figure II.3 restitue le comportement des vagues modélisé à un point au large d'Oléron (*Chaumillon et al., 2019*). Quelles que soient les conditions de houle au large celles-ci sont très vite atténuées au cours de leur propagation dans les Pertuis. Pendant leur trajet, les houles subissent des phénomènes de réfraction, de diffraction mais aussi de friction au fond qui diminuent et perdent une grande partie de leur amplitude. Le fond des Pertuis, comme la baie de l'Aiguillon ou la baie de la Rochelle, se retrouve donc abrité des houles énergétiques.

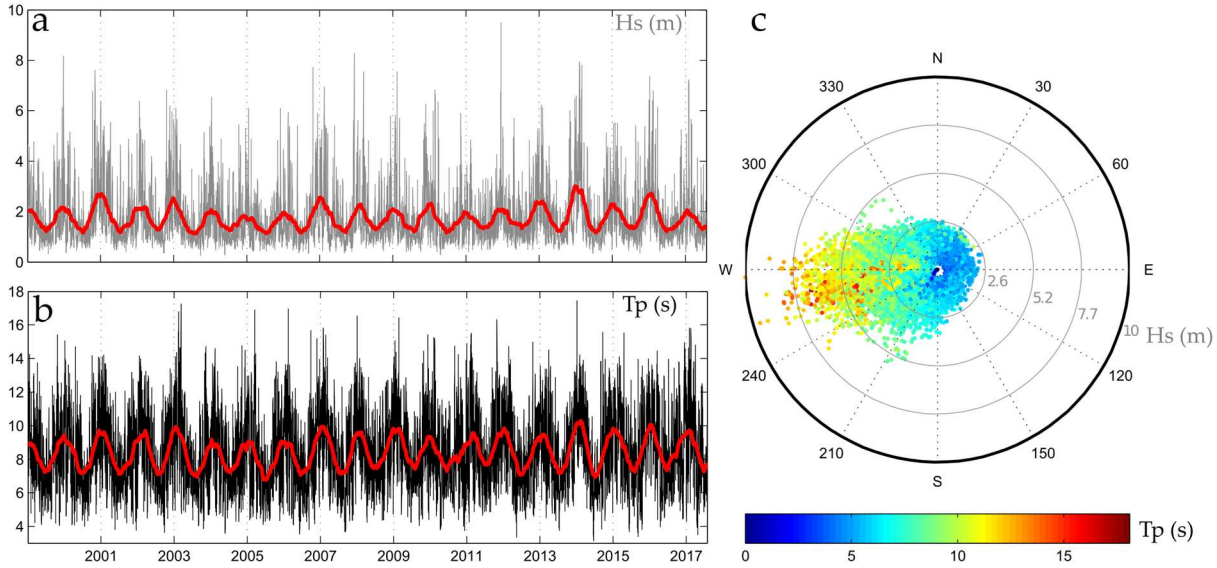

Figure II.3. *Reconstitution du climat de houle par modélisation (WWM) au large de l'île d'Oléron (46°N - 2.5°O) pour la période 1999-2017. (a) Hauteur significative (b) Période pic (c) Scatter wind rose. (Source: Chaumillon et al., 2019)*

II.1.2.4. L'influence fluviatile

En tant que zones côtières, les Pertuis Charentais sont soumis aux apports terrigènes provenant de différents bassins versants, dont la surface est vingt fois plus grande que celle des Pertuis. Ces apports sont drainés, d'une part par les fleuves internes aux Pertuis Charentais: Lay, Sèvre Niortaise, Curé, Charente, Seudre et leurs affluents du nord au sud, et d'autre part, par le fleuve Gironde (Garonne, Dordogne) qui est externe aux Pertuis (Figure II.1). Les caractéristiques de ces fleuves sont résumées dans le Tableau II.3. La Charente est le fleuve interne qui draine la plus grande surface de bassins versants et contribue à hauteur de 60 % aux apports régionaux (*Soletchnik et al., 2014*). Les débits des différents fleuves affichent de fortes variations saisonnières mais les apports moyens d'eau douce aux Pertuis représentent des volumes environ deux ordres de grandeur inférieurs aux volumes engagés

par la marée (*Bertin et al., 2008*). Les fleuves sont donc généralement considérés comme ayant peu d'impact sur l'hydrodynamique des Pertuis. Pendant l'hiver, le débit des fleuves peut influencer la courantologie du Pertuis Breton et de la baie de Marennes-Oléron (*Stanisière et al., 2009; Stanisière et al., 2006*). Dans le Pertuis d'Antioche, seules les propriétés physico-chimiques de l'eau (température, salinité…) sont affectées de manière substantielle.

Tableau II.3. *Caractéristiques des fleuves principaux influençant l'environnement des Pertuis Charentais. Toutes les données sont issues de la base hydrologique (www.hydro.eaufrance.fr/) et récoltées dans Le Moine (2013).*

	Lay	**Sèvre Niortaise**	**Charente**	**Gironde**	
				Dordogne	***Garonne***
Longueur du fleuve (km)	120	158	381	483	647
Surface du bassin versant (km^2)	2 023	3 346	~10 000	24 500	56 000
Débits de crue (m^3s^{-1})	~260	~200	~655/755	~1 500/ 2 000	~4 000/ 5 000
Débits moyens reconstitués (m^3s^{-1})	14	44.4	50	380	650
Charge sédimentaire ($tonnes/an$)	/	/	0.1 x 10^6 *(Tesson, 1973)*	1.2 à 1.5 x 10^6 *(Lesueur et al., 2002)*	

1 *Pour le bassin versant et les débits de la Charente on compte aussi la Boutonne qui est un affluent majeur de la Charente.*

II.1.3. Contexte sédimentaire

II.1.3.1. Lithologie du bassin versant des Pertuis

La Charente-Maritime, principal département bordant les Pertuis, appartient à la partie septentrionale du bassin d'Aquitaine. Elle est majoritairement constituée de terrains sédimentaires du Jurassique (- 201.3 à – 145 Ma) et du Crétacé (145.0 à 66.0 Ma) voire du Tertiaire (- 66 à – 2.58 Ma) affleurant dans la partie sud tandis que sa bordure littorale est composée de vallées fluviales issues en grande partie du Quaternaire. Les roches sédimentaires carbonatées impures correspondent aux formations du Jurassique Supérieur et les calcaires en bleu correspondent aux formations du Crétacé (Figure II.4). Les argiles en violet correspondent à des dépôts issus du Pléistocène (entre -2.58 Ma et -10 000 ans) alors que les vases et les sables (respectivement en marron et en jaune sur la Figure II.4) sont issus de l'Holocène (depuis -10 000 ans) (*Weber et al., 2004*). La mer ayant reculé vers le sud-ouest, on observe donc une chronologie ascendante Nord-Sud, en plus de la chronologie Est-Ouest. Les plaines côtières, ou marais, s'étendant dans le prolongement des Pertuis, vers l'est, sont comblés par des sédiments meubles comprenant tourbe et sables très fins. Ces dépôts d'origine fluvio-marine sont majoritairement argileux (plus de 50 %) et calcaires (autour de 15 %).

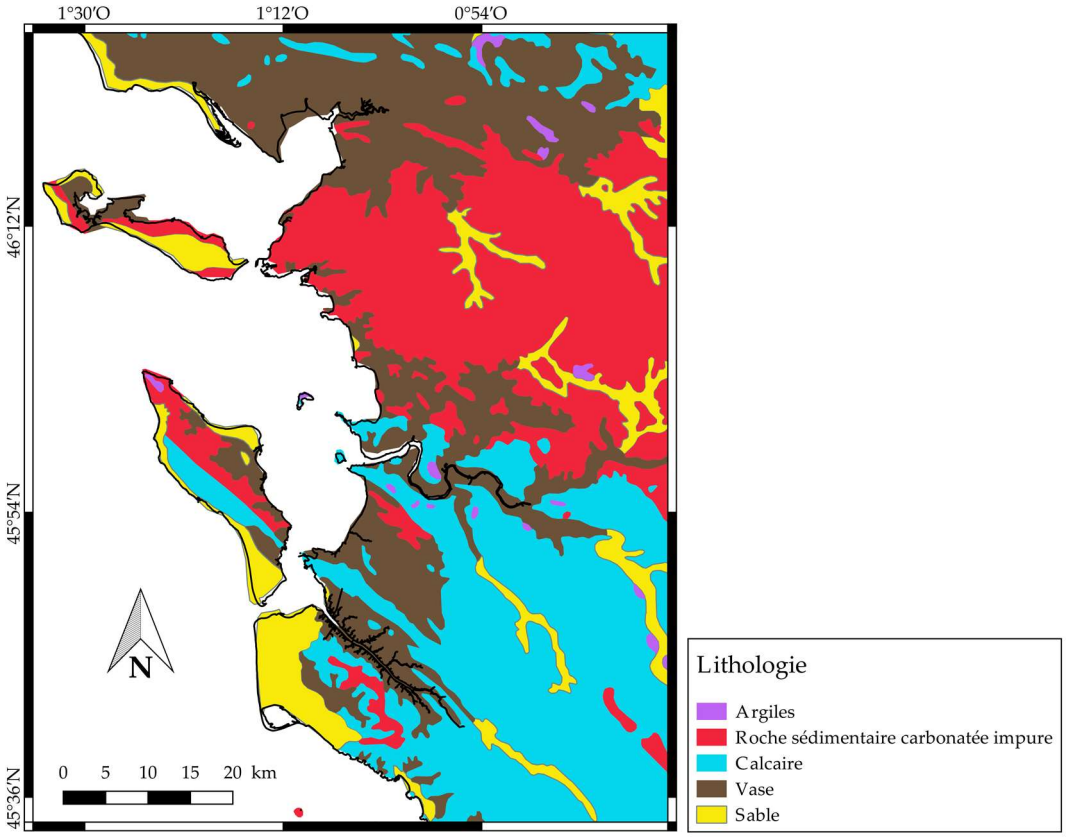

Figure II.4. *Lithologie d'une partie des bassins versants des Pertuis Charentais. (Source: BRGM)*

II.1.3.2. Nature des fonds sédimentaires

On peut distinguer différents faciès sédimentaires dont la représentation peut rapidement devenir une mosaïque à mesure qu'on affine l'échelle, mais globalement on observe trois types d'ensemble sédimentaire dans les fonds marins des Pertuis (Figure II.5): le substratum rocheux qui affleure largement sous la forme de platiers dans la continuité des îles notamment sur leurs flancs Ouest; les fonds sableux qui sont majoritairement situés au large sur le proche plateau continental mais aussi près des rivages insulaires; et les vases (< 63 μm) qui occupent les parties internes et les moins profondes des Pertuis. Les fosses des Pertuis sont généralement composées de vase et localement de sable excepté pour le Pertuis de Maumusson qui affiche essentiellement des sables fins. La partie interne du Pertuis d'Antioche est majoritairement composée de vase dont l'épaisseur varie de 20 à 30 m à mesure que l'on se rapproche de l'embouchure de la Charente. Les plages vendéennes sont caractérisées par des estrans sablo-rocheux dans la partie nord du Pertuis Breton, alors que plus à l'est, la baie de l'Aiguillon affiche de fortes proportions de vase. La baie de Marennes-Oléron est constituée de vases et de sables vaseux au niveau des estrans avec une majorité de sables au niveau des chenaux sud.

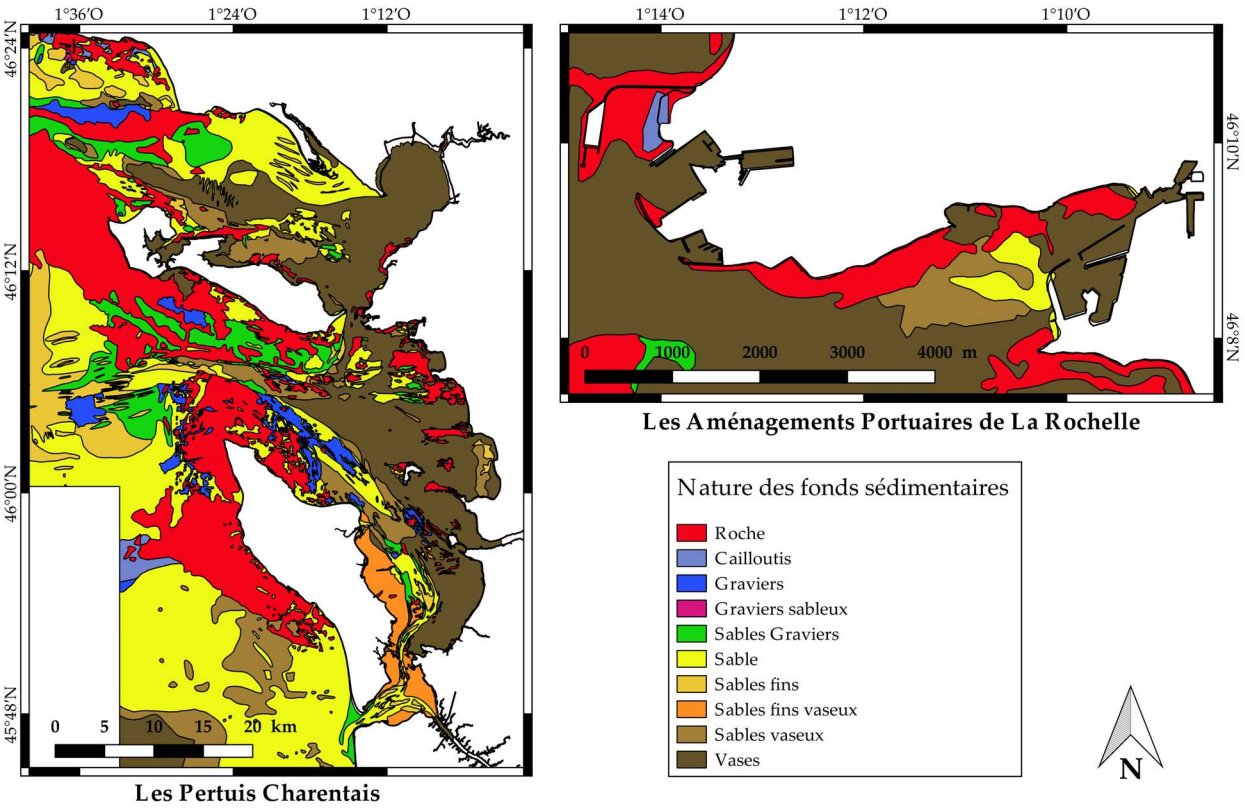

Figure II.5. *Nature des fonds sédimentaires superficiels dans les Pertuis Charentais. L'échelle est de l'ordre de 1:50 000. (SHOM, 2010)*

II.1.3.3. Dynamique sédimentaire

Selon *André (1986)* une dérive Nord-Sud, mise en place durant la transgression flandrienne, aurait construit le prisme sableux du proche plateau Vendéo-Charentais. Guidé par les systèmes dépressionnaires nord-atlantique, le climat de vagues local, principalement d'orientation d'ouest à nord-ouest, engendre un courant de dérive littorale généralement orienté vers le sud (*Weber, 2004; Bertin et al., 2007, 2008; Allard et al., 2008; Chaumillon et Weber, 2006*). Concernant le matériel fin, des estimations ont montré que le gain sédimentaire des Pertuis représentait 500 000 à 600 000 $tonnes/an$ (*LCHF, 1987*). Sur la façade ouest de l'île d'Oléron, les dernières mesures disponibles (*Bertin et al., 2008*) ont toutefois montré que ces quantités étaient 3 à 10 fois moins importantes.

Des travaux antérieurs ont montré que les vases provenaient principalement des panaches turbides de la Gironde déviant par le Nord (*Lesueur, 1992; Boutier et al., 2000; Parra et al., 1998; Lesueur et al., 2002; Kervella, 2009; Strady et al., 2011; Dabrin et al., 2013*) mais aussi des différentes rivières débouchant dans les Pertuis. Les apports dans le Pertuis d'Antioche attribués à la Charente seraient de l'ordre de 0.1×10^6 $tonnes/an$ (*Tesson, 1973*) mais comme l'indique *Le Hir et al. (2010)*, le flux net de matières en suspension à la sortie de la Charente est très mal connu. Il est d'ailleurs encore difficile aujourd'hui d'estimer l'apport sédimentaire de la Charente dans les Pertuis. Les vagues générées lors d'évènements de tempête et les courants de marée de vives-eaux sont considérés comme les principaux moteurs de la remise en suspension et contribuent à un niveau élevé de turbidité à l'échelle de la baie (*Le Hir et al.,*

2010). Ce sont les tempêtes qui génèrent le plus de remise en suspension mais les courants de marée contribuent majoritairement au transport puis au dépôt de ces particules dans les baies. La concentration des matières en suspension peut varier significativement dans les Pertuis en fonction des conditions hydrodynamiques. Dans le courreau de la Pallice les concentrations oscillent entre quelques mgl^{-1} en mortes-eaux sans vent, à plus de 1 gl^{-1} en vives-eaux avec un vent d'ouest établi (*LCHF, 1987*) alors que les taux moyens observés se situent entre 50 et 100 mgl^{-1}.

II.2. Le port des Minimes

Le port des Minimes de La Rochelle est un port de plaisance de 50 ha, divisé en quatre bassins principaux. Le bassin Lazaret est le plus grand (17 ha), suivi de près par le bassin d'extension (15 ha), tandis que les bassins Bout Blanc et Marillac s'étalent respectivement sur 9 et 13 ha. Pour la suite de l'étude, nous avons compartimenté le port en trois sous-bassins afin de l'étudier de la manière la plus compréhensible possible: le bassin Ouest (O) correspondant au Lazaret, le bassin Nord-Est (NE) correspondant au bassin d'extension et le bassin Sud-Est (SE) correspondant à l'ensemble des bassins Bout Blanc et Marillac. L'ensemble portuaire adopte une morphologie assez particulière qui témoigne de la chronologie marquée des différents aménagements mis en place à travers le temps. Les bassins affichent des configurations et des orientations différentes ainsi qu'une couverture spatiale des aménagements flottants (pontons, catways…) assez hétérogène. Les bassins d'Ouest et de Sud-Est sont séparés par un môle central et communiquent de manière continue au niveau ponton capitainerie situé dans le prolongement du chenal d'entrée. Ce chenal est en accès direct avec la baie de la Rochelle via l'entrée principale des Minimes au nord, large de 110 m. Le bassin d'extension est totalement séparé des deux autres et a la spécificité de présenter deux ouvertures. Large de seulement 64 m l'entrée 2 est située au sud-ouest et correspond à une entrée interne reliant le bassin directement avec l'entrée du port tandis que la plus large est située au nord-est (150 m) relie le bassin au chenal de navigation principal de la baie de La Rochelle. Cette dernière est parcourue par une dizaine de pieux soutenant la passerelle Nelson-Mandela, une structure piétonne permettant d'accéder à une promenade le long de la digue des Tamaris. L'accès nautique n'est possible qu'au niveau de l'entrée principale en raison de la faible profondeur de la faible hauteur permise par la passerelle au niveau de la deuxième entrée. Le port comptabilise 4500 places dont 440 pour les visiteurs sur un linéaire de près de 15 km de pontons dont la partie immergée est environ de 25 cm. Les tirants d'eau, longueur et largeur moyens des bateaux du port sont respectivement de 1.18 m, 9.07 m et 3.16 m (Communication Personnelle).

La bathymétrie de la baie de La Rochelle est marquée par un estran vaso-rocheux (Figure II.5b) traversé par un chenal de navigation de 30 m de large de côte théorique -1.3 par rapport au zéro des cartes marines, bordé au sud par le port des Minimes et au nord par une vasière découvrant de 1.5 à 2 m (*CREOCEAN, 2004*). En raison des forts courants qui le traversent, le chenal d'accès le long de la digue nord du bassin Lazaret (Figure II.6) s'auto-entretient jusqu'à l'entrée principale du port. Il affiche des profondeurs comprises entre -2 et -3 m sous le zéro hydrographique et n'a donc pas besoin d'être dragué. La partie ouest du

chenal de navigation, qui longe la digue du Nouveau-monde (Figure 1.5), a néanmoins besoin d'être dragué tous les ans jusqu'à la profondeur cible de -1 *m*. Les bassins Lazaret, Bout Blanc et Marillac sont en général dragués entre -1 et -2 *m* mais c'est le bassin d'extension qui nécessite le plus d'entretien. Celui-ci accueille des bateaux aux tirants d'eau plus élevés et doit donc être dragué pour atteindre des profondeurs de -2 *m* au nord-est du bassin, à -3 *m* au sud-ouest du bassin. L'étude granulométrique des fonds sédimentaire effectuée par la cellule *IDRA (2015)* montre que le port présente une très forte proportion vaseuse avec en général plus de 80 % de fraction limoneuse dans tous ses bassins jusqu'au chenal d'accès (Tableau II.4). Le reste des sédiments correspond à des sables et des argiles, en plus faibles proportions.

Tableau II.4. *Granulométrie des différentes entités du port des Minimes, issue de prélèvements effectués par la cellule IDRA en 2015 aux points notés en Figure II.6.*

	Sables (2 *mm* à 63 *μm*)	**Limons** (63 *μm* à 2 *μm*)	**Argiles** (< 2 *μm*)
Tamaris	4.62	84.77	10.61
Bout Blanc	2.09	87.75	10.16
Marillac	18.52	72.8	8.68
Lazaret	1.78	87.47	10.75
Accès Minimes	12.04	79.2	8.76
Chenal de navigation	7.21	83.76	9.03

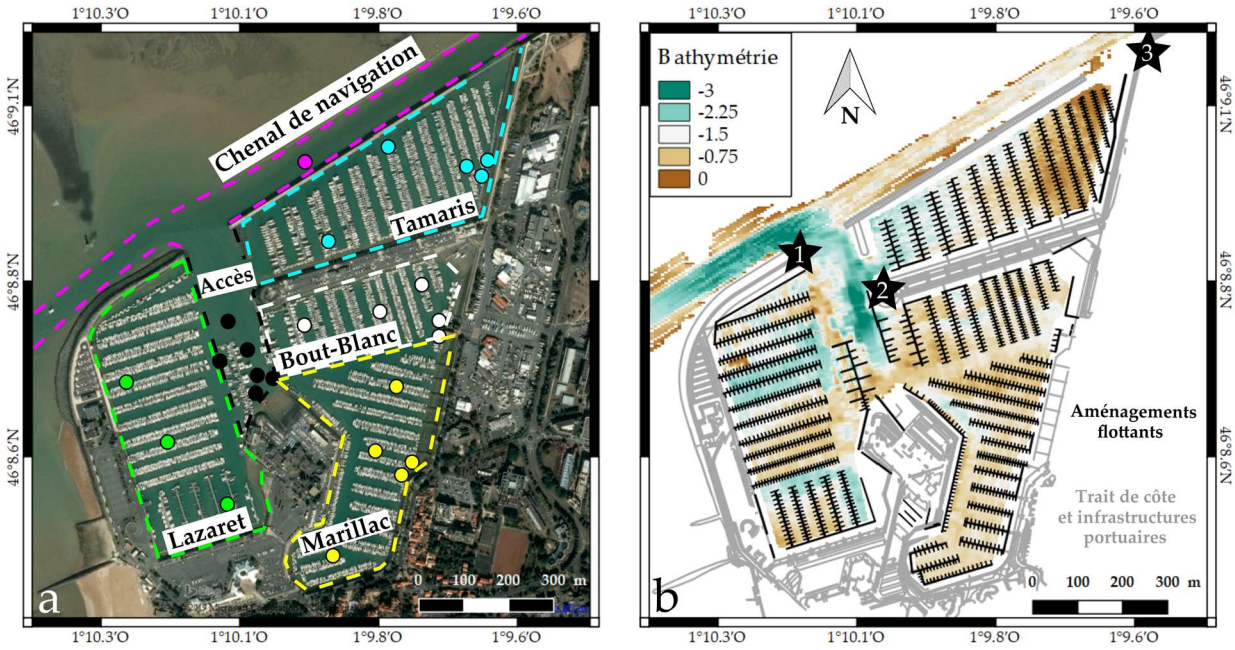

Figure II.6. *Le port de plaisance des Minimes à La Rochelle: Image satellite (a) et Bathymétrie (b). Les trois étoiles noires numérotent les entrées. On peut distinguer à gauche les différents bassins et les cercles correspondent aux endroits où les prélèvements ont été effectués en 2015 pour étudier la granulométrie des fonds (Table II.4).*

Chapitre III

Méthodologie

III.1. Stratégie adoptée

La modélisation numérique connaît un essor grandissant, lié à l'accroissement des moyens de calcul et l'amélioration des méthodes numériques. Très fortement basée sur des approches multi et transdisciplinaires, la modélisation numérique permet d'aborder de manière holistique les sciences de l'environnement. L'usage de modèles déterministes basés sur les équations de la physique permet tout particulièrement de représenter des processus naturels complexes et variés dans le but d'apporter les informations nécessaires à la prise de décision.

Les transferts sédimentaires dans les milieux océaniques semi-fermés sont des phénomènes complexes. Il nous apparaissait donc primordial de recourir à la modélisation comme moyen d'étude privilégié pour mener à bien ce projet de thèse. D'un point de vue méthodologique, le projet consiste en une approche instrumentale *in situ* couplée à une modélisation numérique opérationnelle. De nombreux paramètres y sont mêlés: transport par les différents processus hydrodynamiques (marée, vent, houle…), dépôt/érosion, consolidation sur le fond, bio-interaction (impact des fèces et de la bioturbation) et impact anthropique (bateaux, aménagements…). Les mesures de terrain (capteurs de pression, courantomètres, capteurs de salinité, température, turbidité…) nous ont permis d'appréhender et d'enregistrer le comportement hydro-sédimentaire du port. Dans un second temps, les mesures de terrain nous ont permis d'assurer la calibration et la validation du modèle numérique mis en place. Ce modèle nous a ensuite permis d'identifier et hiérarchiser l'impact des différents processus mis en jeu dans la circulation et l'envasement dans le port des Minimes. Son utilisation a permis de tester et évaluer différents scenarii d'optimisation des stratégies de lutte contre l'envasement. Les deux sections qui vont suivre décrivent les différentes données récoltées puis employées pendant la thèse ainsi que le modèle numérique hydro-sédimentaire choisi.

III.2. Mesures de terrain

Une grande variété de données aux couvertures spatiales et temporelles diverses a été utilisée dans le cadre de cette thèse. La majeure partie de ces données ont été récoltées au cours des trois ans de thèse mais certaines observations de terrain antérieures complètent l'éventail de données. Certaines ont été nécessaires à la paramétrisation du modèle hydro-sédimentaire mis en place (bathymétries, conditions aux limites, trait de côte) alors que d'autres (niveaux d'eau, courants, turbidité, envasement…) ont fourni des éléments de comparaison nécessaires à la validation du modèle. Les données acquises sur le terrain sont résumées dans le Tableau III.1. Les données qui ont seulement présenté un caractère informationnel permettant de contextualiser et caractériser le site d'étude (nature des fonds, granulométrie, lithologie du bassin-versant…) n'y sont pas décrites.

Tableau III.1. *Données utilisées dans le cadre de la thèse.*

Mesure	**Produit/instrument**	**Position**	**Date**	***Organisation***
Bathymétrie	MNT Bathymétrique	Façade Atlantique	2015	*SHOM*
	Bathymétries mono-faisceau	Port des Minimes	2010 à 2018	*Port de plaisance*
Hauteur d'eau	Capteur de pression	3 stations dans les Pertuis	Mars 2017	*SHOM*
		4 stations dans le Port des Minimes	Mars 2017	*La Rochelle Université*
Courantologie	ADCP	3 stations à l'entrée du port	Octobre 2014	*CREOCEAN*
		1 station au bassin Lazaret	Mai 2018	*La Rochelle Université*
	Bouées Dérivantes	2 à l'entrée du port et 3 dans la Baie	Mai à Juin 2017 et Janvier 2019	*La Rochelle Université*
Turbidité	Sonde YSI	1 à l'entrée du port	Mars 2014	*La Rochelle Université*
		1 au bassin des Tamaris et 1 au bassin Marillac	Février à Juin 2019	*La Rochelle Université*
Envasement	Différentiels bathymétriques	Port des Minimes	2010 to 2018	*La Rochelle Université*
	ALTUS	1 au bassin Marillac 1 au bassin des Tamaris	Février à Juin 2019	*La Rochelle Université*

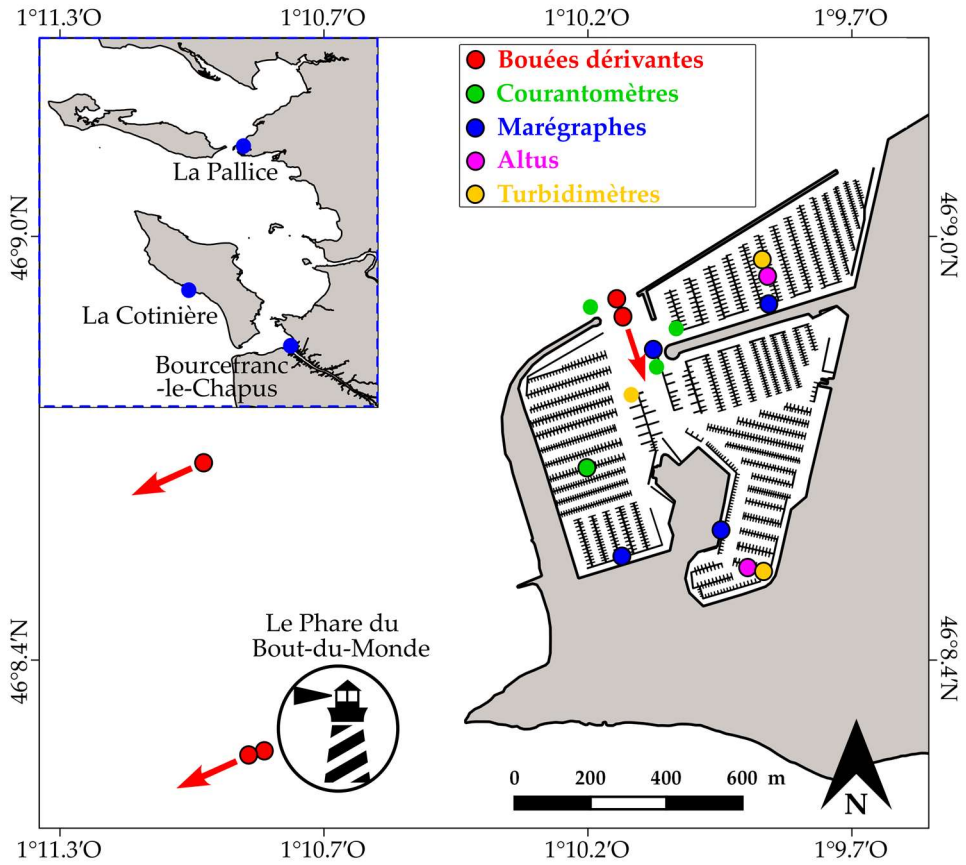

Figure III.1. *Répartition géographique des données in situ utilisées pour calibrer et valider le modèle. Les cercles avec contour correspondent à des données qui ont été récoltées au cours de la thèse contrairement aux cercles sans contour.*

III.2.1. Données bathymétriques

III.2.1.1. MNT bathymétriques des Pertuis

La Figure II.1 présente la bathymétrie des Pertuis Charentais. Celle-ci est issue d'un modèle numérique de terrain (MNT) topo-bathymétrique fourni par la base de données du *SHOM (2015)*. Ce MNT représente une combinaison de données provenant de différentes sources et méthodes (sondeurs mono-faisceau et multifaisceaux, Lidar, levés au plomb…). Il couvre l'ensemble de l'océan Atlantique Nord-Est avec une résolution horizontale de l'ordre de 0.001° (111 m), puis la zone des Pertuis Charentais avec une résolution horizontale moyenne de l'ordre de 0.0002° (22 m). Enfin, la topographie des zones intertidales a été acquise grâce à un levé Lidar réalisé en 2010 suite à la tempête Xynthia, dans le cadre du programme national LITTO3D coordonné par l'IGN et le SHOM.

III.2.1.2. Bathymétries du port

Des bathymétries de contrôle de l'ensemble du port sont effectuées par le service dragage du Département de la Charente Maritime, avant et après les campagnes de dragage du port, à l'aide d'un sondeur mono-faisceau. Le sondeur utilisé est un sondeur bi-fréquence

33/210 *kHz Marimatec E-sea sound 206* installé sur la vedette Babydro et dont la précision peut approcher le centimètre sur la verticale. Le sondeur est couplé à une antenne GPS de type *Leicas GX 1230* qui permet un positionnement au DGPS à une précision métrique sur l'horizontale. Une fois le survey terminé, les fichiers de points (x, y et z) sont nettoyés mais une interpolation est nécessaire pour générer un modèle numérique de terrain (MNT).

Les sondeurs mono-faisceau présentent une limitation certaine: une seule mesure de profondeur est réalisée à la verticale de l'appareil en un seul et unique point. Lors des levés dans le port, la vedette doit circuler entre les pontons et les bateaux amarrés pour acquérir environ une sonde tous les 20 *cm* le long de son axe de propagation. Cette limitation physique rend impossible la réalisation d'une grille régulière de sondes comme on peut le voir sur la Figure III.2, où chaque point représente une sonde du survey réalisé en mai 2016. On retrouve une densité de 1 point tous les 20 *cm* dans la direction du survey mais un écart d'une vingtaine de mètres entre certaines lignes. C'est cette densité très hétérogène de points qui peut poser problème lors du choix de l'interpolation.

C'est pourquoi une évaluation des différentes méthodes d'interpolation a été effectuée dans le cadre d'un stage de Master 1 au printemps 2017. En se basant sur le procédé de différents travaux de recherche (*El-Hattab, 2014*, *Rodriguez, 2014*), nous avons évalué puis comparé trois types d'interpolations: Krigeage, Inverse Distance to a Power (IDP) et Triangulation with Linear Interpolation (TLI). En comparant les MNT visuellement mais aussi statistiquement (Table III.2.) la méthode IDP s'est avérée être la plus précise. Pour produire des MNT du port des Minimes, comme celui présenté en Figure II.9, nous avons donc choisi d'utiliser cette méthode.

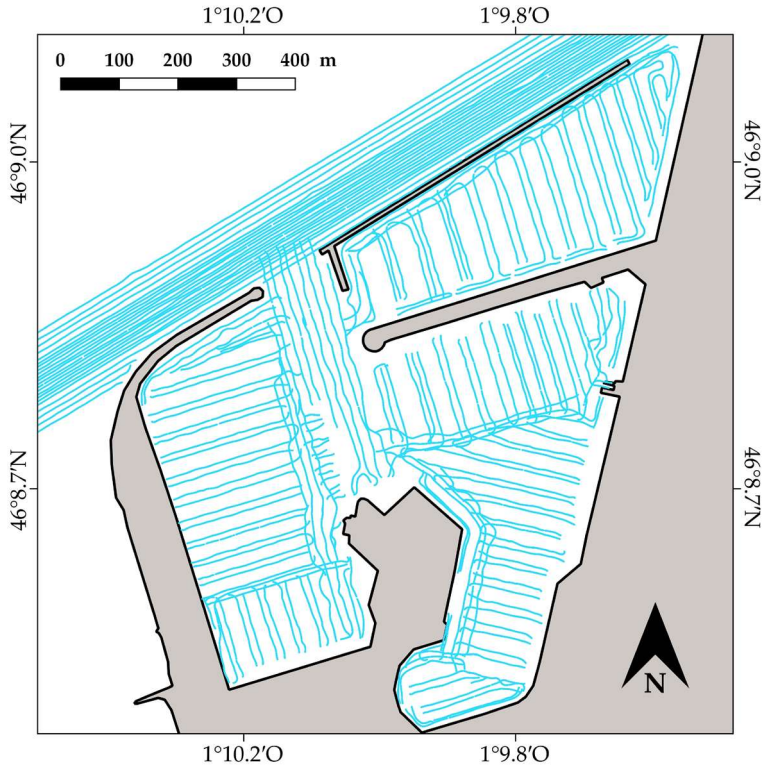

Figure III.2. *Lignes d'un survey bathymétrique réalisé en mai 2016 dans le port des Minimes et son chenal d'accès.*

Tableau III.2. *Comparaison statistique entre les MNT produits par les différentes méthodes d'interpolation et les bathymétries mono-faisceau récoltées. (dz correspond à l'écart entre la donnée acquise et interpolée).*

Méthode d'interpolation	Biais (m)	Moyenne des écarts (m)	Ecart-Type (m)	*RMSE* (m)	Nombre de dz > 10 cm
IDP	2×10^{-4}	0.018	0.029	0.08	2708
TLI	9×10^{-4}	0.021	0.035	0.58	4348
Krigeage	4.5×10^{-4}	0.019	0.029	0.15	2561

III.2.2. Niveaux d'eau

Le modèle numérique a été calibré puis validé à l'aide d'observations des niveaux d'eau dans le port, mais aussi dans le reste des Pertuis. Les observations faites par les marégraphes permanents sont disponibles via le portail du SHOM. Les données de certains marégraphes comme ceux de l'île d'Aix, de l'Aiguillon (Lay) et du Pont du Brault (Sèvre niortaise) n'ont cependant pas été utilisées car elles étaient manquantes ou trop bruitées pendant l'intervalle de temps étudié (du 23/02/17 au 23/03/17). Durant cette période nous avons pu profiter de données continues en 4 points du port et en trois points des Pertuis. Leurs caractéristiques sont exposées dans le Tableau III.3 et sont visibles en Figure III.1 (cercles bleus). Les comparaisons des données au modèle sont présentées dans le Chapitre IV et mettent en avant la bonne reproductivité du modèle, aussi bien en vives-eaux qu'en mortes-eaux avec des conditions météorologiques mixtes.

Tableau III.3*. Caractéristiques des différents marégraphes utilisés pour la validation du modèle.*

	Position	Instrument de mesure	Période couverte	*Organisation*
La Rochelle	Chenal d'Accès	Capteurs de pression RBR TWR 2050	09/01/17 – 23/03/17	*La Rochelle Université*
	Bassin Lazaret	Capteur de pression NKE SP2T	23/02/17-17/05/17	*La Rochelle Université*
	Bassin Marillac	Capteur de pression NKE SP2T	23/02/17-17/05/17	*La Rochelle Université*
	Bassin des Tamaris	Capteur de pression NKE SP2T	23/02/17-17/05/17	*La Rochelle Université*
La Pallice	46° 9' N 1° 13' O	Radar à ondes guidées	1885 – aujourd'hui	*SHOM*
La Cotinière	45° 54' N 1° 19' O	Capteur de pression	2008 – aujourd'hui	*SHOM*
Bourcefranc-le-Chapus	45°51′ N 1°10′ O	Marégraphe radar	1878 – aujourd'hui	*SHOM*

III.2.3. Données Courantologiques

III.2.3.1. Courantométrie ADCP

La courantologie 3D des masses d'eaux portuaires a aussi été enregistrée en différents points du port, pour différentes périodes. Les premiers points de mesure par ADCP ont été réalisés par un bureau d'étude (*CREOCEAN, 2014*), suite à l'extension du port des Minimes. Notre analyse porte sur trois points à l'entrée du port, du bassin des Tamaris côté ouest et du Bout Blanc (Figure III.1). La période d'acquisition s'étale du 3 au 15 octobre 2014, présentant de grandes amplitudes de marée (coefficient 45 à 111) et de vent. Ces données nous ont aussi permis d'identifier et de caractériser les différents régimes hydrodynamiques présents à l'entrée du port. La circulation induite dans les bassins est fonction des courants générés à l'entrée, mais la géométrie complexe des infrastructures et la forte densité en structures flottantes (estimé à plus d'un tiers de la surface totale) peuvent aussi moduler l'hydrodynamique. Afin de mieux comprendre le comportement des masses d'eaux sous l'action des paramètres physiques et anthropiques, nous avons déployé un courantomètre ADCP au milieu du bassin ouest, éloigné de l'entrée principale. L'objectif était aussi de tester la validité du modèle dans des parties plus internes du port. Ces mesures ont été réalisées du 27 avril au 5 mai 2018, pendant des conditions moyennes de vives-eaux et un temps calme. Le courantomètre ADCP *Aquadopp Profiler*, dont les caractéristiques sont décrites dans le Tableau III.4, était fixé en haut d'une structure tripode de manière à être positionné environ 75 cm au-dessus du fond lors de son déploiement (Figure III.3). L'acquisition des vitesses de courants dans la colonne d'eau sus-jacente affichait une précision verticale de 0.008 ms^{-1} et une précision horizontale de 0.003 ms^{-1}. Les données obtenues ont mis en avant l'influence importante des pontons dans l'atténuation des courants. Ces données nous ont par la suite permis de calibrer puis de valider l'influence des aménagements flottants dans la modélisation hydrodynamique du port des Minimes. Toutes ces étapes sont détaillées dans le Chapitre IV.

Tableau III.4. *Caractéristiques des différents mouillages de courantomètres ADCP utilisés pour la validation du modèle.*

Localisation	Type d'ADCP	Discrétisation verticale (cm)	Fréquence d'acquisition	Installation	Période	*Organisation*
Entrée du port côté Lazaret	RDI Workhorse Sentinel	50	600 kHz	Fond	07/10/14 - 15/10/14	*CREOCEAN*
Entrée Ouest des Tamaris	RDI Workhorse Sentinel	50	1200 kHz	Surface	03/10/14 – 14/10/14	*CREOCEAN*
Entrée du Bout Blanc	RDI Workhorse Sentinel	50	1200 kHz	Surface	03/10/14 – 14/10/14	*CREOCEAN*
Bassin du Lazaret	Nortek Aquadopp Profiler	20	2 MHz	Fond	27/04/18 – 02/05/18	*Université*

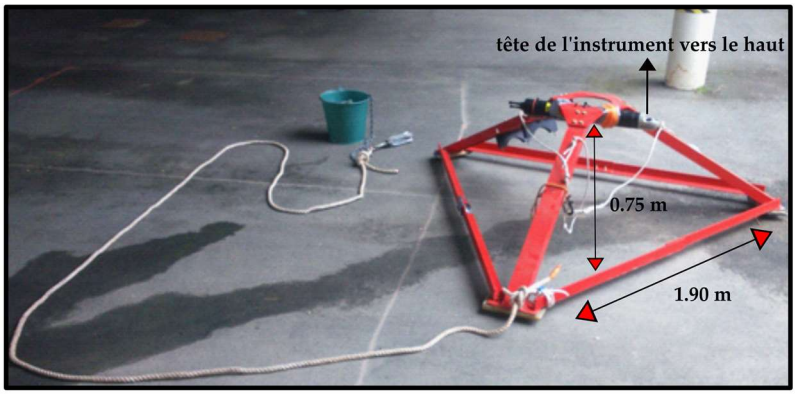

Figure III.3. *L'ADCP Aquadopp Profiler 2 MHz et la structure tripode sur lequel il reposait pendant son acquisition. Collaboration effectuée avec le soutien technique de Thibault Coulombier (IE Université).*

III.2.3.2. Bouées dérivantes

Les données obtenues par courantométrie ADCP ont permis d'étudier les courants de manière eulérienne au niveau de quelques points seulement. Afin de tester et d'améliorer la capacité du modèle à reproduire les courants dans le port et la baie de La Rochelle, nous avons eu recours à l'utilisation de bouées dérivantes à 5 reprises (Tableau III.5). Celles-ci, en suivant les masses d'eaux de surface, et en restituant leur position en temps réel, permettent une description lagrangienne de la circulation. Les bouées sont fabriquées par *Pacific Gyres* et sont composées d'un flotteur en surface d'un diamètre de 0.2 m relié à une voile immergée d'une longueur de 1.2 m (Figure III.4b). Le capteur GPS présent dans le flotteur utilise l'iridium pour envoyer ses positions successives avec une résolution temporelle de 5 minutes. Les voiles guident l'ensemble au gré des courants situés à plus d'1 m sous la surface. Le déploiement de ces bouées a permis d'étudier la circulation des masses d'eaux de surface à différentes échelles temporelles et spatiales (Figure III.4). La validation lagrangienne des modèles numériques est moins couramment utilisée car l'analyse comparative se révèle plus complexe à réaliser et à comprendre. La durée des expérimentations dépend essentiellement des contraintes de récupération des bouées échouées ou coincées par les pontons. Les détails de cette validation sont visibles dans le Chapitre VI de ce manuscrit.

Tableau III.5. *Les différents déploiements de bouées dérivantes effectués au cours de la thèse.*

Date de déploiement	Nombre de bouées utilisées	Nombre de lâchers effectués	Position du lâcher	Durée	Conditions météo-marines
09/05/17	3	5	46°08'54.1"N 1°10'08.0"W	Flot (6 h)	Vives-eaux avec des vents forts
17/05/17	3	5	46°08'54.1"N 1°10'08.0"W	Flot (6 h)	Mortes-eaux sans vent
14/06/17	5	1	46°08'16.2"N 1°10'46.4"W	Jusant (6 h)	Mortes-eaux sans vent
26/06/17	5	1	46°08'15.8"N 1°10'46.6"W	Jusant (6 h)	Vives-eaux sans vent
15/01/19	3	1	46°08'39.2"N 1°10'52.7"W	2 cycles de marée (24 h)	Mortes-eaux avec vent

Figure III.4. *(a) Vue d'ensemble (en Lambert 93) des trajets effectués (en noir) par les bouées dérivantes lors des 5 déploiements décrits dans le Tableau III.5. (b) Structure d'une bouée dérivante Pacific Gyre.*

III.2.3. Données relatives à la sédimentation

III.2.3.1. Différentiels bathymétriques

La production de MNT du port à partir de levés mono-faisceau a aussi permis de réaliser des différentiels bathymétriques entre deux levés successifs et de mesurer, indirectement, l'évolution du fond en fonction du temps. Le premier levé bathymétrique est effectué avant une campagne de dragage du port, en septembre ou octobre, et le second est effectuée après la campagne, au mois de mai ou juin suivant. En réalisant un différentiel entre deux levés successifs, on peut quantifier le taux d'envasement généré pendant la période de dragage en chaque point du port (zone en rouge sur la Figure III.5b). On peut aussi observer des régions du port dont le différentiel bathymétrique est négatif, ce qui témoigne de la présence de souilles crées par les machines de dragage dans les différents bassins du port (les larges zones bleues sur la Figure III.5b). Pendant la période « hivernale » on peut observer des taux d'envasement atteignant jusqu'à 7 *cm* par mois. A l'inverse, la différence entre deux MNT d'une même année permet d'observer l'envasement « estival » (Figure III.5a), plus faible (en moyenne 2 à 4 *cm* par mois) et qui n'est pas impacté par les activités de dragage. Malgré l'usage d'un sondeur mono-faisceau pour mesurer le fond, les MNT et les différentiels bathymétriques obtenus nous ont permis de caractériser le taux de déposition pour une période s'étalant de 2010 à 2017. On observe la présence de certains artefacts coïncidant avec la position des pontons et bateaux. Ces régions ne sont pas sondées et les artefacts résultent donc de cette absence d'information. La marge d'erreur permise par la méthode d'interpolation étant assez conséquente (7 *cm*), ainsi que la présence de bathymétries parfois très incomplètes, nous n'avons pas pu caractériser de manière exhaustive les variations

spatiales et temporelles de l'envasement du port des Minimes. Cependant plus de détails émanant de l'analyse des différentiels post-extension sont fournis dans le Chapitre VII.

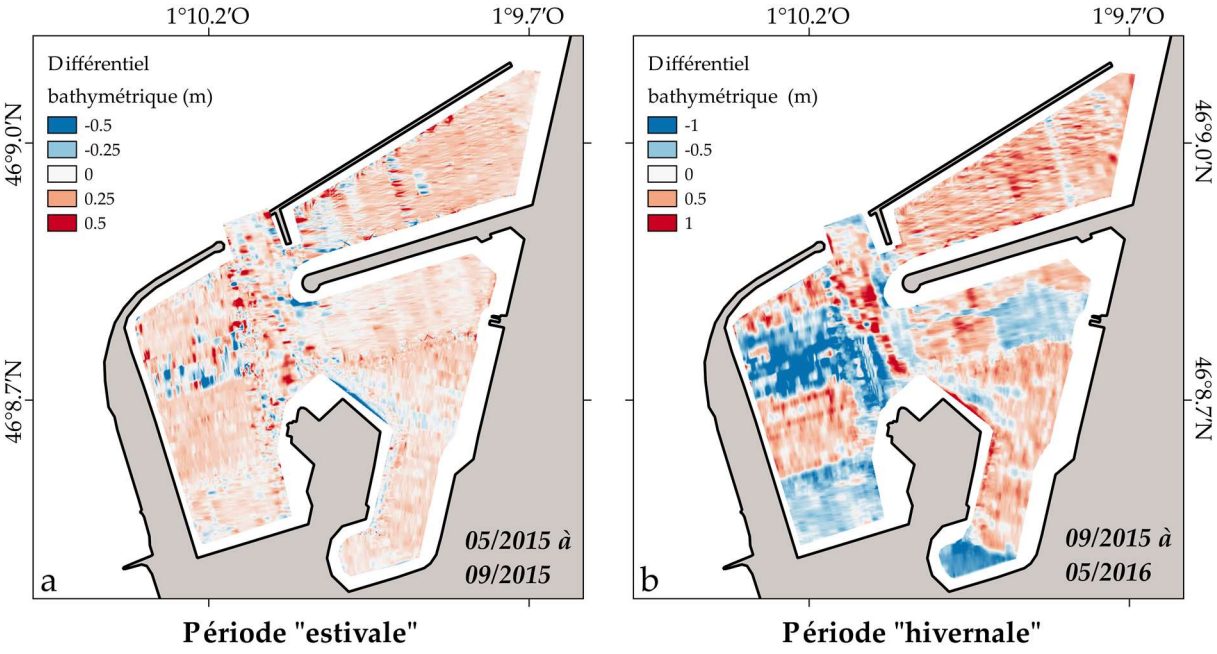

Figure III.5. *Exemple de différentiels bathymétriques pour deux périodes différentes distinctes.*

III.2.3.2. Mesures directes de l'évolution du fond

Afin d'étudier de manière continue l'évolution du fond, nous avons déployé deux altimètres submersibles *ALTUS* (NKE). L'utilisation de l'*ALTUS* a déjà été validée dans un large éventail d'environnements côtiers (*Jestin et al., 1998; Deloffre et al., 2007; Verney et al., 2007; Bassoullet et al., 2010; Ganthy et al., 2013*). Cet appareil permet d'étudier les variations du niveau du fond à une résolution de 0.6 à 2 mm à l'aide d'un transducteur acoustique de 2 MHz couplé à un capteur de pression. Le transducteur est fixé sur un grand trépied en acier inoxydable. Le boitier d'acquisition contient l'enregistreur de données, le capteur de pression et la batterie (Figure III.6a). Du 26 février au 30 avril 2019, deux ALTUS furent positionnés au fond du bassin Marillac et au centre du bassin des Tamaris (cercles jaunes entourés en noir sur la Figure III.1). L'ensemble nous a permis d'obtenir des observations de l'évolution du fond à haute résolution temporelle en deux points très différents du point de vue hydrodynamique mais aussi du point de vue de l'envasement. L'installation a été assurée par un plongeur (Vincent Hamani), afin de stabiliser l'ensemble de la structure à la bonne hauteur et le plus horizontale possible en enfonçant les piquets de la structure tripode dans la vase.

III.2.3.3. Mesures de la turbidité

Parallèlement au déploiement des ALTUS, nous avons attaché une sonde *YSI 6600 V2* sur chacune des structures tripodes afin de mesurer la teneur en suspension à une profondeur constante au fond de l'eau (quasiment au même niveau que le transducteur de l'ALTUS, voir

Figure III.6a). Ces sondes sont équipées d'un capteur de turbidité 1000 NTU préalablement calibré et d'une précision de 0.3 NTU, ainsi que d'autres capteurs (salinité, température) dont les mesures n'ont pas été analysées dans le cadre de cette thèse. Nous avons également bénéficié de mesures de turbidité de fond, obtenues pour la période du 19 avril 2014 au 21 mai 2014 avec la même sonde, mais cette fois-ci à l'entrée du port (cercle jaune sans contour sur la Figure III.1). Ces données avaient été acquises dans le cadre du stage de fin de licence d'Elisa Perrotey à La Rochelle Université, sous la direction d'Isabelle Brenon. L'ensemble des données de turbidité couvre donc trois sites spécifiques du port pour une durée totale de 3 mois. Ces données ont été analysées dans le Chapitre VII, en lien avec les dépôts mesurés par les ALTUS, afin de caractériser l'effet conjoint de la marée, de la houle, du vent et des fleuves dans la dynamique sédimentaire du port des Minimes.

Figure III.6. *(a) Type de structures déployées dans le port afin d'estimer les flux sédimentaires et l'envasement. (b) Manipulation de terrain effectuée en collaboration avec Thibault Coulombier (IE Université) et Vincent Hamani (Doctorant Université et plongeur pour l'occasion).*

III.3. Le système de modélisation mis en place

III.3.1. Description générale du modèle utilisé

Afin d'étudier la circulation des masses d'eaux, les flux sédimentaires et l'évolution du fond, nous avons utilisé le modèle tri-dimensionnel TELEMAC-3D (*Hervouet, 2007*). Nous avions hésité à l'époque avec le modèle MARS-3D mais la flexibilité du maillage non-structuré, nous permettant d'avoir une seule grille pour étudier l'ensemble des processus régionaux et portuaires, nous a convaincu d'utiliser TELEMAC-3D. Le modèle fut originellement introduit pour résoudre les équations en eaux peu profondes mais il est aussi capable de résoudre les équations de Navier-Stokes en mode non-hydrostatique pour modéliser les écoulements à surface libre. Une description détaillée du modèle, de ses paramétrisations ainsi que de l'implémentation des structures flottantes est présente dans le Chapitre IV. Concernant la partie sédimentaire du modèle, nous avons utilisé le module SEDI-3D présent dans TELEMAC-3D. Les détails concernant ce module ainsi que les paramétrisations choisies sont détaillées dans le Chapitre VII.

III.3.2. Implémentation du modèle

L'implémentation du modèle sur le domaine d'étude a nécessité la création d'un maillage triangulaire non-structuré réalisé à l'aide du logiciel SMS. Sa résolution varie de 2 km au large des pertuis (et donc au niveau de la frontière ouverte) à près de 5 m dans le port. Cette définition était obligatoire dans le port pour représenter les structures du port telles que les digues, le mole mais aussi les aménagements flottants tels que les pontons. L'ensemble totalise près de 41 000 nœuds dont la moitié sont définis dans le port. Le maillage est interpolé sur les bathymétries présentées dans la section III.2.1 et correspondent pour la plupart des études proposées à un assemblage de la bathymétrie du SHOM (2015) et d'une bathymétrie pré-dragage effectuée au port des Minimes en octobre 2016 (Figure II.2). L'usage de 8 couches verticales sigma est apparu suffisant en termes de temps de calcul/représentativité des résultats pour reproduire la circulation tridimensionnelle dans le port. Au total c'est plus de 320 000 nœuds qui sont utilisés et le pas de temps optimal est de 5 s. Au-delà, les simulations affichaient de nombreuses instabilités.

Afin de simuler les courants dans les Pertuis et dans le port, le modèle nécessite plusieurs types de données. Tout le long de la frontière maritime ouverte à l'Ouest du domaine (Figure III.7a) le modèle est forcé par 34 composantes harmoniques de la marée (O1, K1, P1, Q1, M2, S2, N2, K2, 2N2, MU2, NU2, L2, T2, M3, M4, MN4, MS4, M6, M8, EPS2, MSF, MSQM, MM, SSA, SA, S4, MKS2, MF, LA2, J1, N4, MTM, R2, et S1) calculées par le modèle de marée FES 2014. Ce modèle produit par Noveltis et le LEGOS, est distribué par Aviso+ avec le soutien du CNES. Ce modèle de marée globale résout des équations barotropes des marées dans une configuration spectrale, sur un maillage haute résolution (1/16°) constitué de près de 2.9 millions de nœuds. Comparé à ses prédécesseurs (FES 2012 et FES 2004), la précision du modèle a été améliorée par l'assimilation optimisée de données altimétriques sur 20 ans (Topex/Poseidon, Jason-1, Jason-2, TPN-J1N, et ERS-1, ERS-2, ENVISAT) et d'un vaste ensemble de données d'observations marégraphiques. Afin d'implémenter la marée au niveau de la frontière ouverte, une interpolation des hauteurs d'eau mais aussi des vitesses de courant de marée, reproduits par FES 2014, a été réalisée au niveau des nœuds de la grille régionale.

Même si l'atlas de marée FES 2014 est assez récent, il a pu être validé et utilisé dans un grand nombre d'études et de domaines océaniques différents (*Melet et al., 2016; Zawadski et al., 2017; Ward et al., 2018; Seifi et al., 2019; Athar et al., 2019*), ce qui a motivé notre démarche.

Le forçage météorologique emploie des données du système de réanalyse climatique CFS V2 (*Saha et al., 2014*), la version améliorée de CFSR (*Saha et al., 2010*) développée par le NCEP (National Center for Environmental Prediction) et opérationnelle depuis Mars 2011. Ce système de prévision nécessite lui aussi une assimilation de données de stations météorologiques au sol. Il est initialisé quatre fois par jour et une grande variété de paramètres sont disponibles jusqu'à une résolution horizontale régulière de 0.2°, et à des pas de temps horaires. Le forçage atmosphérique du modèle développé dans la thèse a nécessité des données de vitesses et directions du vent à 10 m du sol ainsi que de la pression atmosphérique. CFS V2 et son prédécesseur CFSR ont été largement étudiés et utilisés et la qualité des prédictions et des hindcast produits n'est plus à démontrer (*Silva & Mendes, 2013; Silva et al., 2014; Stopa et al., 2016; Liria et al., 2018; Silvestrova et al., 2019*). Enfin, les fleuves ont été implémentés pour la partie sédimentaire du modèle afin d'identifier leur influence sur la dynamique sédimentaire mais leur effet n'a pas encore été étudié et nous n'en parlerons donc pas dans ce manuscrit. Pour la partie hydrodynamique, nous avons choisi de ne pas en tenir compte car ils sont supposés négligeables en comparaison des flux mis en jeu par la marée (*Bertin, 2005*).

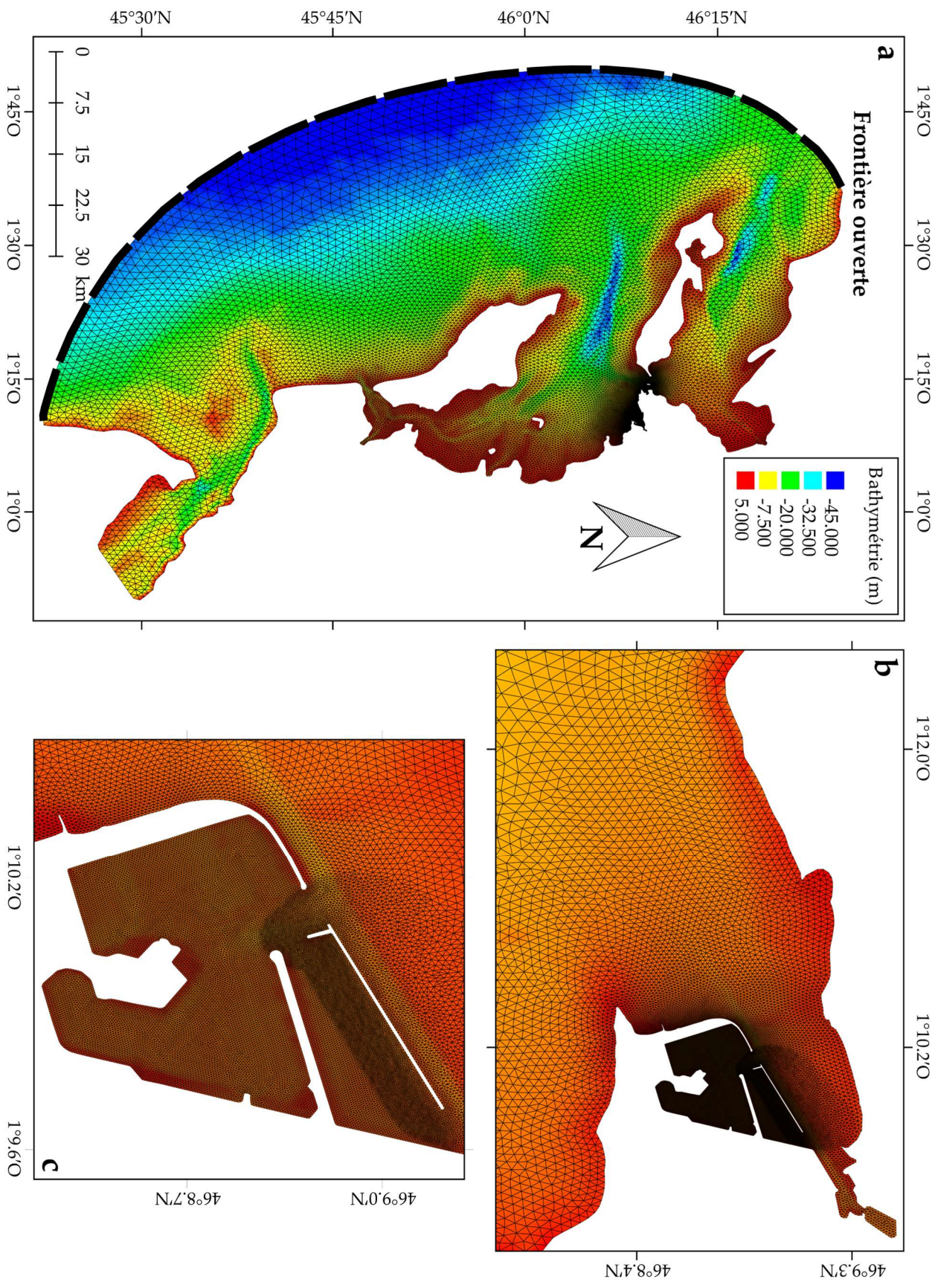

Figure III.7. *Grille non-structurée définie pour étudier la circulation hydro-sédimentaire et l'évolution du fond dans la baie de la Rochelle (b) et son port des Minimes (c). La frontière ouverte est signifiée sur (a) par une ligne tiretée noire.*

Chapitre IV

Influence of Floating Structures on Tide and Wind-Driven Hydrodynamics of a Highly Populated Marina

Jean-Rémy Huguet[1], Isabelle Brenon[2] and Thibault Coulombier[3]

[1] PhD student at UMR 7266 LIENSs, CNRS-La Rochelle Université, 2 rue Olympe de Gouges, 17000 La Rochelle, France (corresponding author). E-mail: jean-remy.huguet@univ-lr.fr
[2] Associate professor at UMR 7266 LIENSs, CNRS-La Rochelle Université, 2 rue Olympe de Gouges, 17000 La Rochelle, France. E-mail: isabelle.brenon@univ-lr.fr
[3] Research engineer at UMR 7266 LIENSs, CNRS-Rochelle Université, 2 rue Olympe de Gouges, 17000 La Rochelle, France. E-mail: thibault.coulombier@univ-lr.fr

Keywords: Hydrodynamics; Marina; Numerical modelling; Floating structures; Residual fluxes.

Ce Chapitre fait l'objet d'une publication dans la revue Journal of Waterway, Port, Coastal and Ocean Engineering.

Résumé

Bien que les pontons ou autres structures du même type aient déjà fait l'objet de nombreuses études dans le cadre de l'ingénierie (agitation, corrosion…), la littérature scientifique est très pauvre voire quasi-inexistante quand il s'agit d'étudier leur effet sur l'hydrodynamique. Depuis son extension en 2014, le port des Minimes de La Rochelle, principal bassin de plaisance de la ville, dispose de plus de 4500 places réparties sur près de 15 km de pontons. La couverture spatiale des pontons et des bateaux amarrés représente plus d'un tiers de la surface totale du port, estimée à 50 ha. Etant donné la faible profondeur moyenne (environ -1 m par rapport au zéro hydrographique pour un niveau d'eau moyen de 3.9 m), il apparaissait évident que l'ensemble de ces structures flottantes agissait de manière non-négligeable sur la circulation et l'envasement.

Notre première contribution dans cette thèse s'est donc attachée à caractériser l'impact que pouvait avoir une forte densité d'aménagements, en surface, sur l'hydrodynamique horizontale et verticale, dans un environnement semi-fermé tel que le port des Minimes. Nous avons bénéficié de plusieurs points de mesure par courantométrie ADCP, réalisés par la cellule CREOCEAN en 2014, mais ceux-ci étaient situés à proximité de l'entrée principale, où les pontons et bateaux sont moins présents. Un courantomètre ADCP a donc été déployé en avril 2018 dans une partie plus interne du port afin de vérifier à la fois la qualité de prédiction du modèle et l'influence que pouvaient avoir les structures flottantes sur les courants. Les observations ont indiqué une stratification beaucoup plus prononcée des vitesses, contrairement aux observations effectuées à l'entrée du port, avec des intensités plus élevées au fond qu'en surface.

En termes de modélisation, TELEMAC-3D a permis de prendre en compte l'effet des structures flottantes en appliquant des pertes de charge aux nœuds correspondants, afin de simuler indirectement la dissipation par frottement générée par leur présence. La calibration des coefficients de frottements par rapport aux mesures observées a permis de valider l'usage d'un modèle hydrodynamique 3D permettant de reproduire les courants liés à la marée et au vent. Dans les bassins, les vitesses modélisées sans l'effet des structures flottantes sont beaucoup plus fortes que les vitesses observées et ne permettent pas de reproduire la stratification présente dans les parties internes du port. L'étude spatiale a montré que les structures flottantes atténuaient de manière significative les vitesses dans les bassins tout en augmentant légèrement les courants au niveau des chenaux d'accès. La circulation générale des courants pendant le flot est la plus affectée. Les aménagements flottants freinent le développement des tourbillons naturellement formés à l'échelle des bassins, sous l'action conjuguée du flot tidal advectif et de la géométrie portuaire. La circulation pendant le jusant, principalement focalisée au niveau de l'entrée, est moins affectée par la présence des pontons et des bateaux. Une dernière étude a mis en avant le faible effet de ces structures flottantes sur les flux résiduels constatés aux entrées du port. D'une manière générale, l'effet de ces structures reste très localisé et ne dépasse pas le champ d'action du port. Ce Chapitre apporte donc un regard nouveau sur l'impact non-négligeable que peuvent avoir des aménagements côtiers flottants dans des espaces semi-fermés de faible profondeur. Enfin, la direction et l'intensité des flux est cependant très sensible aux différents vents dominants mais cet effet sera tout particulièrement détaillé au cours du Chapitre suivant.

Abstract: Harbour siltation is a problem that will exist as long as harbours exist and it is intrinsically linked to their primary function – providing shelter for anchorage and operative conditions for loading/unloading ships. In these semi-enclosed basins, flow characteristics are one of the main factors influencing siltation and water quality. One of the largest recreational ports of Europe, La Rochelle Marina (southwestern France), is not spared by siltation, which requires serious dredging operations during a major part of the year. In this context, a three-dimensional model (TELEMAC-3D) has been used to investigate its hydrodynamics. Using a simplified approach, floating structures were implemented in the model. Comparison with observations has demonstrated the need to consider these structures in our study. They significantly reduce velocity in the inner parts of the marina and concentrate current on access channels. Numerical results also highlight the joint role of the macrotidal regime and wind stress in the movement of water masses and their residual circulation.

IV.1 Introduction

Similar to every area protected from the combined action of waves and marine currents, ports suffer siltation (*Winterwep, 2005*). This siltation depends on environmental parameters, such as the local tidal range and wave climate, meteorological conditions, and river input. Port siltation is also influenced by the planform geometry and basin state of enclosure (*Falconer, 1992; Nece, 1984*). Furthermore, these areas are used extensively, and thus require particular attention in terms of currentology, sediment deposition and water quality.

The increasing concern of planners and designers for hydro-environmental problems relating to semi-enclosed environments fosters development of an operational modelling system. However, they are difficult to model accurately due to their composite geometry (quays, channels, docks, etc.) affecting the circulation of water, both occasionally and permanently. Indeed, docks and boats floating in the port could also play a substantial role, by attenuating surface currents with friction and by decreasing wind action. Many modelling studies have been carried out to investigate environmental and engineering problems at the harbour scale. For instance, *Sanchez-Arcilla et al. (2002)* correlated the capacity to flush to hydrodynamics and *Murphy et al. (2012)* characterised dead zone mixing processes in several marina configurations. In this paper, we focus on the effect of floating structures. Indeed, although some studies have investigated the effect of currents and/or waves on floating docks (*Tajali et al., 2011; Ghadimi et al., 2014*), few have investigated the influence of floating bodies on water circulation (*Bohlin et al., 2016*).

The study site, La Rochelle Marina, located in southwestern France, is currently considered as the largest marina on the European Atlantic coast. Recently, in order to satisfy continued growth of recreational sailing, the marina has been expanded after three years of construction and transformation. The marina is not spared by siltation and has to spend 10% of its total budget to dredge around 200 000 m^3 of cohesive sediment each year. Thus, characterising hydrodynamics and sediment flux is of key importance in this area where annual sediment deposition can overpass 50 cm in some basins (Pers. Com. La Rochelle Marina). This study aims to investigate the influence of floating structures on marina hydrodynamics by three-dimensional numerical simulation. In the next two sections, we describe the area and methods used in the model to perform realistic numerical simulations of

water circulation at several temporal and spatial scales. Numerical results are then compared against *in situ* observations before analysing the influence of floating structures at the marina scale. Their implementation is finally discussed before concluding.

IV.2. Description of the study site

IV.2.1. La Rochelle Marina

The study area is a 50 *ha* recreational port located along the French Atlantic Coast, in the central part of the Bay of Biscay. It is located in the landward part of the Pertuis d'Antioche embayment, corresponding to a drowned river valley segment (*Chaumillon & Weber, 2006*) and characterised by silty to sandy-silty bottoms. This shallow water coastal area, protected from the Atlantic Ocean by the Ré and Oléron islands, is characterised by a 44 m deep trench and many tidal flats (Figure IV.1). Moreover, it is an urban marina with the city of La Rochelle displaying a land area of 2 843 km^2 and a population of 80 000 inhabitants.

Created in 1972, La Rochelle Marina has been the largest marina along the Atlantic coast, since its expansion in 2014. This 900 *m*-long and 820 *m*-wide semi enclosed area is divided into 3 basins totaling 4500 moorings, distributed along 15 km of floating docks. The southeastern (SE) basin is larger, with 22 *ha*, whereas the western (W) and the northeastern (NE) basins, contain 17 and 15 *ha*, respectively. The marina is accessible by a 110 *m* wide main entrance, and the expansion basin has two openings: 150 *m* wide to the northeast and 64 *m* wide to the southeast. To mitigate siltation, the marina requires recurring dredging of its basins, 8 months a year, so that the whole marina is dredged every 3 years.

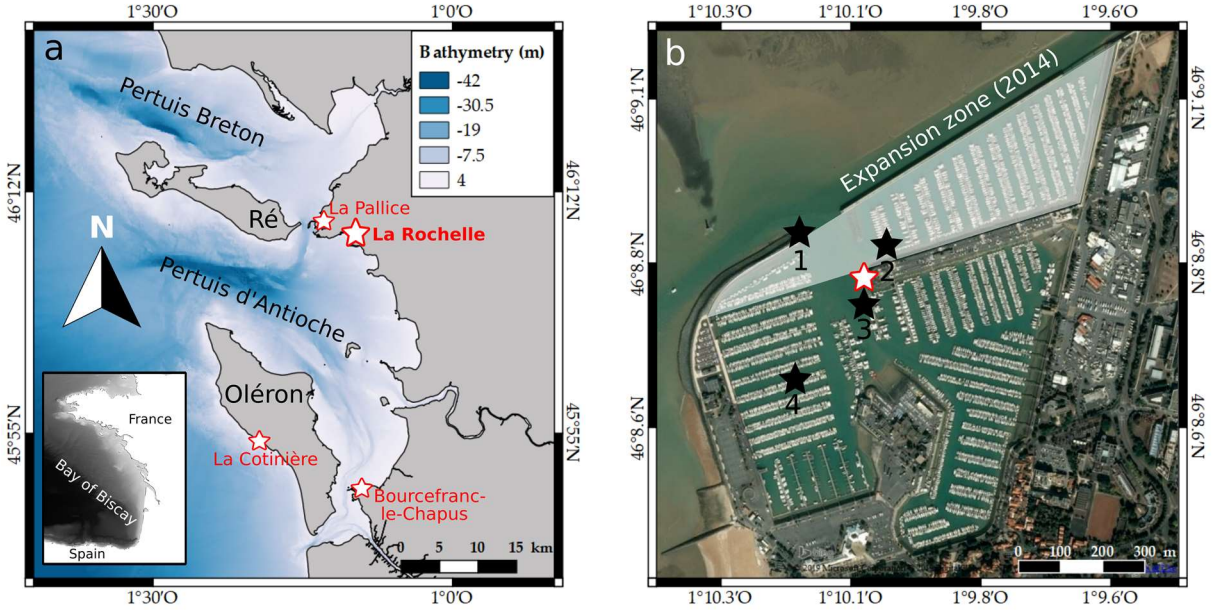

Figure IV.1. *Bathymetric/topographic (a) and Bing satellite image of La Rochelle Marina (b). Altitudes are given with respect to mean-sea-level, and white stars with red borders indicate tide gauges. The shoreline is indicated by straight bold black line in a, and black stars represent ADCP moorings in b.*

IV.2.2. Coastal area hydrodynamics

The coastal area is considered a mixed, wave and tide-dominated estuary (*Chaumillon & Weber, 2006*). The tidal schedule is semidiurnal and the tidal range varies from 2 m during neap tides to more than 6 m during spring tides, where strong tidal currents can locally reach up 2 ms^{-1}. Tides are dominated by M2, and its amplitude grows to more than 1.8 m in the inner part of the estuaries due to resonance and shoaling (*Bertin et al., 2012*). Furthermore, the quarter-diurnal tidal constituents (M4, MS4 and MN4) are strongly amplified shoreward, because of resonance occurring on the Bay of Biscay shelf (*Le Cann, 1990; Toublanc et al., 2015*). The yearly average significant wave height is approximately 1.5 m with periods between 8 and 12 s, whereas wave height can be larger than 8 m during winter storms in front of the Pertuis d'Antioche (*Bertin et al., 2015*). However, refraction, diffraction and bottom friction in the inner part of the estuaries drastically decrease wave energy. Storm waves and strong tidal currents are considered the main drivers of resuspension and contribute to a high level of turbidity at the scale of the bay (*Le Hir et al., 2010*).

IV.3. Numerical modelling

IV.3.1. General description of the modelling system

In this study, we employed the TELEMAC-3D model (*Hervouet, 2007*), part of the open-source hydrodynamic suite of TELEMAC system (*Hervouet, 2000*) adapted to free-surface flow modelling.

TELEMAC-3D is used and validated in a wide range of studies (*Kopmann & Markofsky, 2000; Cornett et al., 2010; Bedri et al., 2011; Villaret et al., 2013*) by solving the following 3D Navier-Stokes equations:

$$div(\vec{U}) = 0 \qquad \text{(IV.1)}$$

$$\begin{aligned}
\frac{\partial U}{\partial t} + \vec{U}.\overrightarrow{grad}(U) &= \frac{-1}{\rho_0}\frac{\partial p}{\partial x} + div\left(\nu_t\,\overrightarrow{grad}(U)\right) + f_x \\
\frac{\partial V}{\partial t} + \vec{U}.\overrightarrow{grad}(V) &= \frac{-1}{\rho_0}\frac{\partial p}{\partial y} + div\left(\nu_t\,\overrightarrow{grad}(V)\right) + f_y \\
\frac{\partial W}{\partial t} + \vec{U}.\overrightarrow{grad}(W) &= \frac{-1}{\rho_0}\frac{\partial p}{\partial z} + div\left(\nu_t\,\overrightarrow{grad}(W)\right) + f_z
\end{aligned} \qquad \text{(IV.2)}$$

where t is the time (s); x, y, and z the sigma-coordinates; U,V,W are the velocity components in the x, y, and z directions (ms^{-1}); ρ_0 is the reference density (kgm^{-3}); p is the pressure term (Nm^{-2}); ν_t is the turbulent diffusion coefficients (m^2s^{-1}) and f_x, f_y, and f_z are the source and sink terms (ms^{-2}).

Turbulence is modelled with k-ε model and the non-hydrostatic mode is used to perform simulations over an unstructured grid (Figure IV.2), from the regional (embayment) to local scale (marina), and at a large range of temporal scales. Mesh is varying in function of the bathymetry and the area of interest, from 2 km offshore to almost 5 m in the whole marina. Bottomstress is computed through the widely used Chézy parameterization (*Van Rijn, 1984; Weltz et al., 1992; Deng et al., 2002; Nicolle and Karpytchev, 2007*). The bottom frictional stress τ is then represented by the quadratic relationship:

$$\tau = \rho \frac{gU^2}{C^2} \qquad \text{(IV. 3)}$$

Where U is the vertically averaged velocity; ρ the water density (kgm^{-3}); g the gravity acceleration (ms^{-2}) and C is the Chézy friction coefficient ($m^{0.5}s^{-1}$). We set spatially variable friction in the model by prescribing different value of Chézy coefficient depending on the bottom nature. Following the methodology in *Nicolle (2006)* concerning the Chézy parametrization in the Pertuis, we used a 100 $m^{0.5}s^{-1}$ coefficient for mud, 80 $m^{0.5}s^{-1}$ for fine sand, 60 $m^{0.5}s^{-1}$ for sand and 45 $m^{0.5}s^{-1}$ for rocky bottoms.
The semi-implicit Galerkin finite element method is used to solve continuity and momentum equations. An Eulerian–Lagrangian treatment of advective terms and a semi-implicit method insures numerical stability, even with large time steps. The treatment of tidal flats ensured the conservation of mass and momentum (*Hervouet et al., 2015; Hervouet et al., 2011*). Finally, wind effects are modelled as a two-dimensional condition at the water surface through the equation:

$$\nu_H \frac{\partial \overrightarrow{U_H}}{\partial \eta} = \frac{\rho_a}{\rho} a_w \vec{w} \|\vec{w}\| \qquad \text{(IV. 4)}$$

Where $\vec{w}$ is the wind velocity 10 m above the water surface (ms^{-1}); $\overrightarrow{U_H}$ is the horizontal velocity of the water surface (ms^{-1}); η is the elevation (m); ρ_a is the air density (kgm^{-3}); and a_w the wind stress coefficient defined by *Flather (1976).*

IV.3.2. Model implementation

The modelled area is 35 km wide and 100 km long and is discretised on a 41 000 nodes unstructured grid, with resolution from 2 km offshore to nearly 5 m inside the marina. In this study, the coordinate system is converted into a topography-following coordinate system via a sigma transformation. A sensitivity analysis has revealed that the use of 8 vertical sigma levels was optimal/sufficient to reproduce three-dimensional circulation in the marina. These sigma levels are treated with the Arbitraty Lagrangian-Eulerian method (*Donea, 1982*), and lead to 320 000 nodes. We use bathymetry from the French Navy (hereafter SHOM) and benefit from a twice per year single beam survey in the marina. Then, the topography of intertidal areas are determined using LiDAR survey, acquired in 2010 (LITTO3D, French National Geographic Institute and SHOM).

Four kinds of boundary conditions are used in the model. Firstly, the coastline, that corresponds to a solid boundary, where the friction governs the relation between velocity and its gradient. The bottom also plays the role of a boundary wall where a spatially variable Chézy friction is imposed. Along, its open boundary, the model is forced by 34 astronomical tidal constituents (O1, K1, P1, Q1, M2, S2, N2, K2, 2N2, MU2, NU2, L2, T2, M3, M4, MN4, MS4, M6, M8, EPS2, MSF, MSQM, MM, SSA, SA, S4, MKS2, MF, LA2, J1, N4, MTM, R2, and S1), obtained by linear interpolation from the global tide model FES2014 (Finite Element Solution - v.2014). Then, the surface boundary of the model is forced with space and time variable sea-level atmospheric pressures and 10 m winds from the CFSR (The Climate Forecast System Reanalysis provided by the National Centre for Environmental Prediction), with spatial and temporal resolution of 0.5° and 1 h. Atmospheric forcing is set over the whole domain with hourly sea-level atmospheric pressure and 10 m wind speed and direction originating from

the Climate Forecast System Reanalysis (CFSR) provided by the National Center for Environmental Prediction (NCEP). The hydrodynamic time step is set to 5 s after a sensitivity analysis. Observations (*CREOCEAN, 2004*) showed that the marina is sheltered enough from ocean waves and is more sensitive to the development of small wind-generated waves, in particular during storms where maximum wave height approach 15 cm. Thus, in the framework of this study, we did not simulate wave propagation.

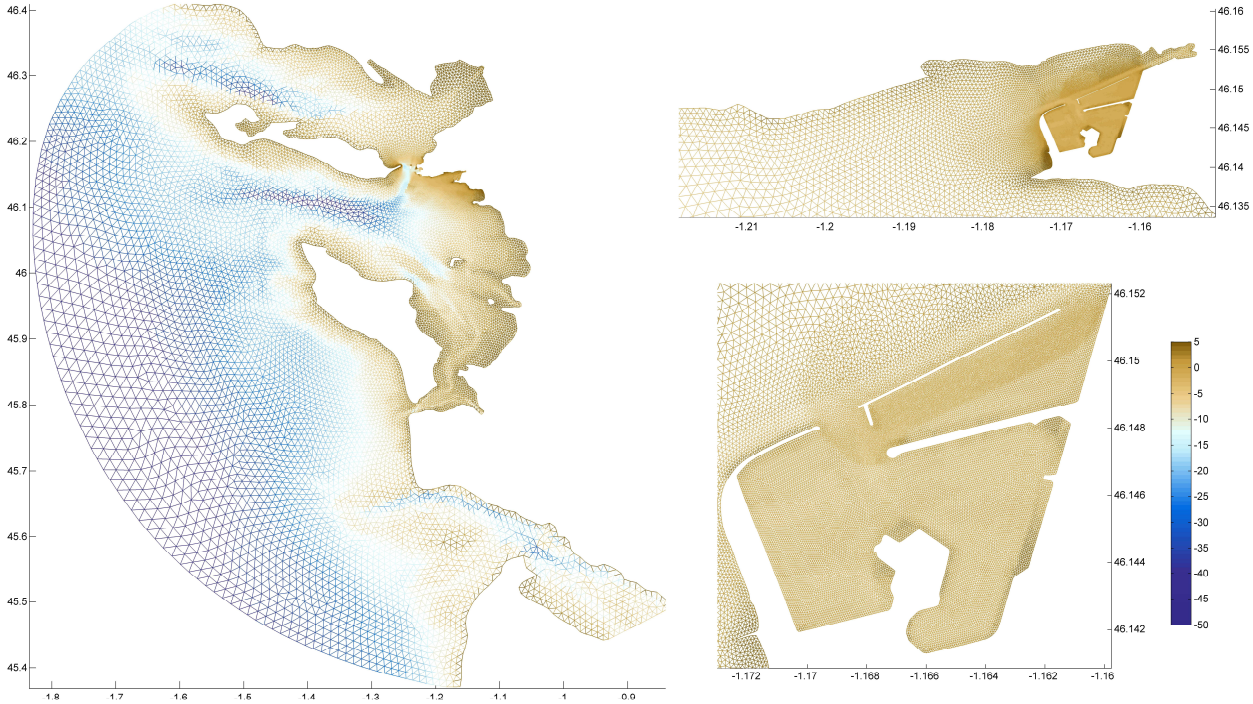

Figure IV.2. *Unstructured grid used in this study, implemented over the Pertuis Charentais embayment. Colors indicate grid bathymetry ranging from 44 to 0 m.*

IV.3.3. Implementation of the floating structures in the model

Field trips involving the deployment of surface drifting buoys inside the marina have shown the complexity of water mass circulation. Steady currents and local eddies were visible at the channel entrance during the deployment; some buoys experienced stagnant conditions ($< 0.001\ ms^{-1}$) while others were moved rapidly in the inner parts of the marina by high intensity currents ($> 0.5\ ms^{-1}$). Small-scale eddies and steady currents were also noticed near floating structures that, combined with the high density of docks and moorings in the marina, could have a significant impact on the velocity field in the inner part of the marina. Indeed, all the floating docks and moored boats represent more than a third of the total surface of this semi-enclosed area. Flows near floating obstacles were studied through numerical modelling and lab experiments (*Drobyshevski, 2004; Tajali et al., 2008*). However, they are poorly understood because of the complexity of three-dimensional unsteady currents and sensitivity to a large number of parameters (*Baker, 1980; Martinuzzi and Tropea, 1993*). To evaluate the effect of floating docks and moorings on the water mass circulation in the inner part of the marina, we conducted a modelling study with the presence of floating structures. Two methods are available with TELEMAC-3D. The first is to locally increase the atmospheric

pressure gradient to lower the free surface and apply surface friction according to the Nikuradse friction law. As it would have been computationally expensive to apply this method, we chose to implement a second method. This method consists of applying local head losses at each involved computational node. The head losses correspond to friction loss terms at the free surface that represent the flow resistance created by a rough surface in contact with the fluid. This method has been implemented in an implicit way as a source term in the three-dimensional momentum equations (2) via the following expressions:

$$\begin{aligned} f_x &= S1U.U \\ f_y &= S1V.V \\ f_w &= S1W.W \end{aligned} \qquad \text{(IV.5)}$$

With f_x, f_y, and f_z the source terms in three directions (ms^{-2}) included in the 3D momentum equations; U, V, and W are the three velocity components (ms^{-1}) and $S1U$, $S1V$, $S1W$ the intermediate terms (s^{-1}) defined by:

$$\begin{aligned} S1U &= C.\|U\| \\ S1V &= C.\|V\| \\ S1W &= C.\|W\| \end{aligned} \qquad \text{(IV.6)}$$

With C the coefficient corresponding to a friction coefficient (m^{-1}).

The nodes involved in the model correspond to the position of floating docks and boats, whose draught varies between 0.5 m and 2 m with a mean value of 1.18 m for the whole marina. We independently integrated the two kinds of structures in the model. A third of the marina surface nodes were affected by this implementation. In term of CPU time, simulations with floating structures requires about one-quarter higher CPU time than basic simulations. Using forty cores of a supercomputer, it approximately leads to a total of 20 h to simulate 15 days with 8 sigma layers.

This method is relatively sensitive to mesh resolution, which has been considered in our numerical simulations. A sensitivity analysis was performed to calibrate C in agreement with field observations. The calibration of C was performed with one measurement point (visible in validation section). The best C coefficient was found to be 0.6 $m^{-1}$for mooring boats and 0.5 m^{-1} for floating docks. During the calibration process, a large number of C coefficient was tested, ranging from 0.1 to 2 $m^{-1}$and the modelled results were found consistent with the observations for a C coefficient ranging from 0.3 to 0.8 m^{-1}.

IV.4. Validation

IV.4.1. Water levels

The model was calibrated and validated using water level measurements taken offshore and inside the marina (the white stars with red borders in Figure IV.1). La Pallice data (radar) were collected through the REFMAR portal (data.shom.fr/), and water levels in the marina (pressure sensors) were acquired in March 2017. The comparison between numerical results and 10-minute continuous time series measurements (Figure IV.3) shows a Root Mean Squared Error (*RMSE*) of 0.18 m for La Pallice with 0.17 m average for the four stations in La

Rochelle Marina (Table IV.1). Globally, water levels are very well reproduced by the model at the five stations with errors about 3 - 4 %, once normalised by the mean local tidal range. Offshore, at the other stations (Figure IV.1), water levels are also well reproduced with the same level of error (Table IV.1). It is also important to note that there are few differences in the water level signal between simulations with and without floating structures.

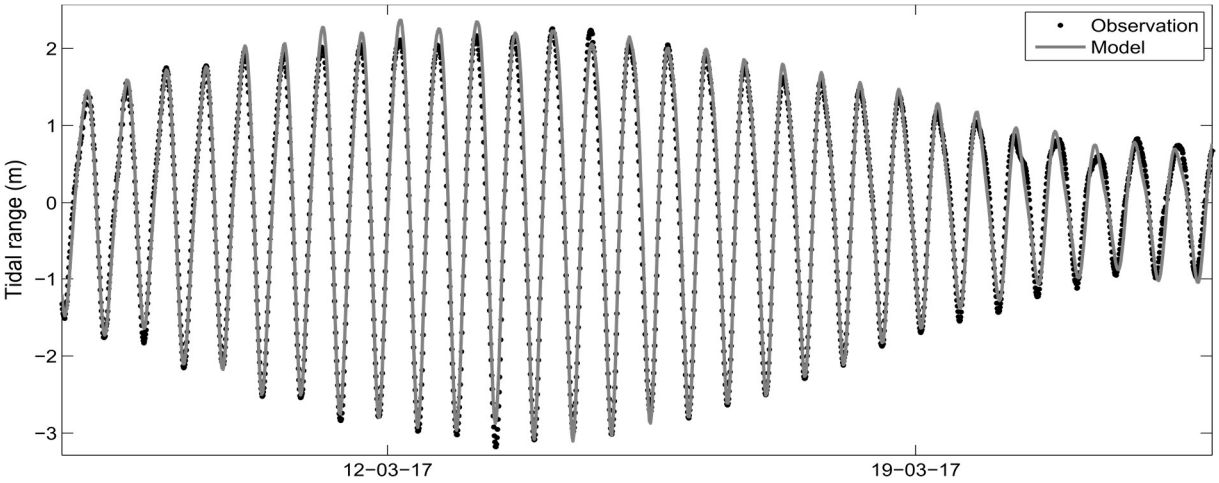

Figure IV.3. *Comparison of marina entrance water levels between modelled results (gray line) and observations (black circles) for 15 days including neap and spring tides.*

Table IV.1. *Metrics between numerical results and measurements. (RMSE = Root Mean-Squared Error). Measurements were taken at the several tide gauges corresponding to white stars bordered in red in Figure IV.1. Metrics for La Rochelle Marina are averaged for comparison between numerical results and data from the four tide gauges deployed in the marina.*

Location	RMSE (m)	Maximum Errors (m)	Bias (m)
La Rochelle Marina	0.17	0.25	0.08
La Pallice	0.18	0.30	0.13
La Cotinière	0.19	0.31	0.17
Bourcefranc-le-Chapus	0.19	0.31	0.11

IV.4.2. Current in the channel entrance

Three ADCP current-meters were deployed in 2014 by the CREOCEAN engineering company, after the marina expansion (black stars 1, 2, 3 in Figure IV.1). In this section, we display vertical profiles of current at the marina entrance (black star 1 in Figure IV.1) obtained during spring tides where the mean tidal range was approximately 6 m. Observations revealed a strong distortion of the tide at the entrance, with a strong tidal flood that is not compensated, in terms of intensity, during ebb; during spring tides, current can overpass 1.5 ms^{-1} at the beginning of flood tide and reach 0.8 ms^{-1} at the end of ebb tide. Figure IV.4 displays the comparison between numerical results obtained with floating structures and the observations. Surface velocity was observed 0.5 m below the free surface and bottom velocity was observed 1.5 m above the bottom. The model faithfully reproduces this behaviour, with a very good reproduction of the peak flow of the ebb and flood tides. Moreover, speeds are relatively in phase, from the bottom to the surface and the main directions (north at flood and south at ebb)

are well reproduced. Table IV.2 summarises the differences between numerical results and *in situ* observations of current both in terms of intensity and direction. RMSE is approximately 0.07 $ms^{-1}$and 51.3° for intensity and direction, respectively. The model underestimates velocity by less than 2 %, mainly due to underestimating peak flows. For a simulation without floating structures, the current behaviour is similar, with a slight intensity decrease during peak flows (approximately 0.05 ms^{-1}).

Table IV.2. *Metrics between depth-averaged numerical results and ADCP measurements of velocity. (FS = floating structures). ADCP measurements were acquired during three spring tide days in October 2014 (ADCP 1, 2 and 3), and in May 2018 (ADCP 4).*

Meter	**Intensity (ms^{-1})**			**Direction (degrees)**	
	RMSE	Maximum Errors	Bias	*RMSE*	Bias
ADCP 1	0.072	0.16	0.032	51.3	20.1
ADCP 2	0.065	0.12	0.028	46.1	11.2
ADCP 3	0.069	0.17	0.034	62.3	24.8
ADCP 4 (without FS)	0.064	0.10	0.091	129.7	-68.4
ADCP 4 (with FS)	0.012	0.02	0.005	75.8	-12.5

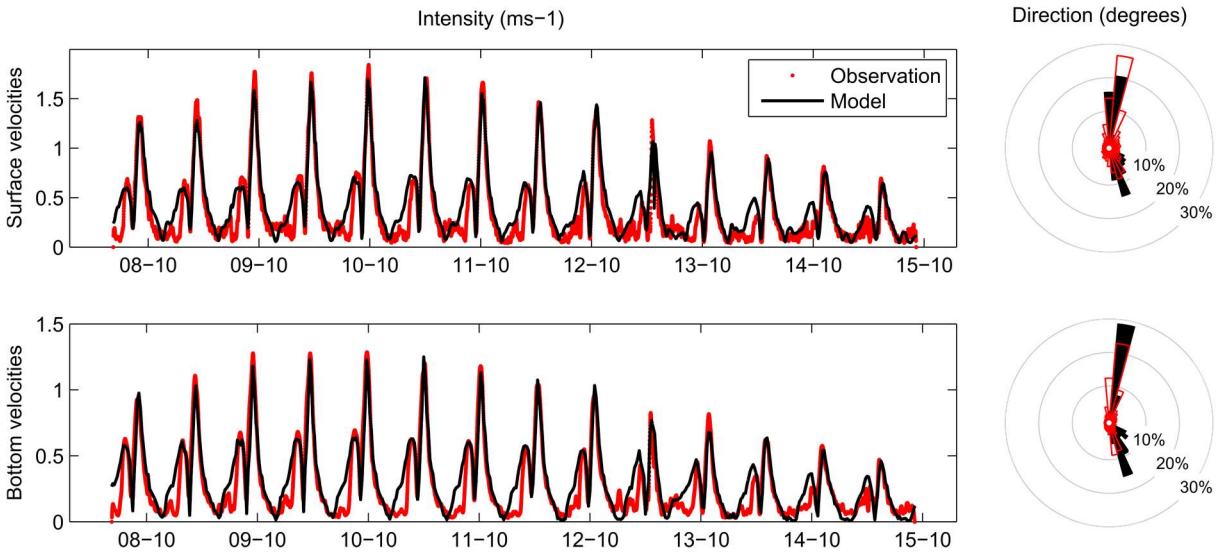

Figure IV.4. *Comparison of velocity at the marina entrance between numerical results (black line) and observations (red dots) for one week of spring tides in October 2014 (mean tidal range = 6 m).*

IV.4.3. Currents in the vicinity of the marina

To better understand the dynamics of the marina, an up-looking ADCP current-profiler (*Aquadopp Profiler*, 2 Mhz, 20 cm cells) was deployed just below floating docks (black star 4 in Figure IV.1). Data acquisition displayed vertical accuracy of approximately 0.008 $ms^{-1}$and horizontal accuracy of approximately 0.003 ms^{-1}**.** The aim of this instrumentation was not only to understand how currents are modified by the presence of floating docks but also to calibrate and compare our modelling system in the inner parts of the marina. The 5-day measurement occurred from April to May 2018, with a relatively important tidal range (4 to

5 m) and calm weather (mean wind speed approximately 5 ms^{-1}). Figure IV.5 shows the comparison between simulated and measured velocity for one day. Measured velocity displays the maximum current during the flood 2 h after low tide but, contrary to the channel entrance, the water column is stratified. Indeed, the velocity is stronger at the bottom (Figure IV.5a). Then, floating structures appear to have a role in the attenuation of surface velocity. A preliminary calibration of the friction loss coefficient has been carried out to fit the model results to measurements in the inner part of the marina. The corresponding results for the period of acquisition are shown in Figure IV.5b, and the simulations without floating structures are shown at the bottom (Figure IV.5c). The simulation without floating structures overestimates the velocity by a factor of two during peak flow. No stratification is found in the water column. In terms of current intensity, current seems quasi-homogeneous as at the channel entrance (Figure IV.4). The simulation with floating structures, better reproduces the measured velocity order of magnitude of approximately 0.07 ms^{-1} during peak flow. Moreover, the stratification is well represented and fits the measurements. There is still some bias compared to reality: the attenuation along the vertical axis is not strong enough and the ebb tide is slightly overestimated. This behaviour is displayed in Figure IV.6 where a comparison is provided in term of intensity and directions. Directions are more dispersed and less channeled than in the channel entrance (Fig 4) and their reproduction is slightly worse with a 75.8° *RMSE* and -12.5° bias. However, the main directions are conserved with the model with FS contrary to the model without FS.

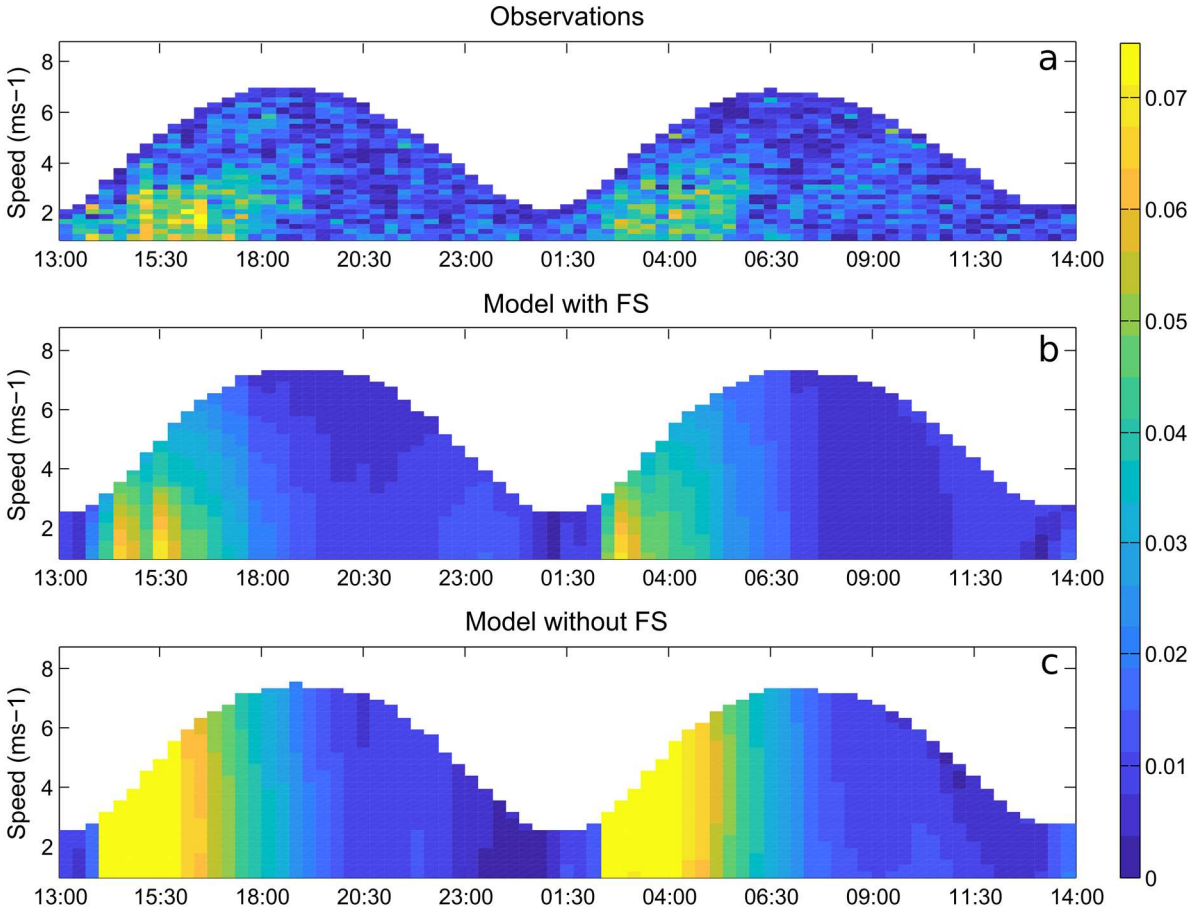

Figure IV.5. *Comparison of velocity intensity (ms^{-1}) computed with floating structures (b), without floating structures (c) and acquired with ADCP (a) in the inner part of the western marina basin for one day in May 2018 (mean tidal range = 4 m). FS corresponds to floating structures.*

Comparison of surface velocity (Figure IV.6), observed 0.5 m below the free surface, confirms the overestimation by the simulation without floating structures. Between measurements and numerical results, a 0.064 ms^{-1} *RMSE* is reached, with maximum error of approximately 0.10 ms^{-1}. With floating structures in the simulation, the peak flow occurred in phase with measurements, and accurately fit the magnitude of intensity**.** The *RMSE* is much better, with 0.012 ms^{-1} accuracy for a maximum error approximately 0.025 ms^{-1} and an average overestimation of 0.5 %.

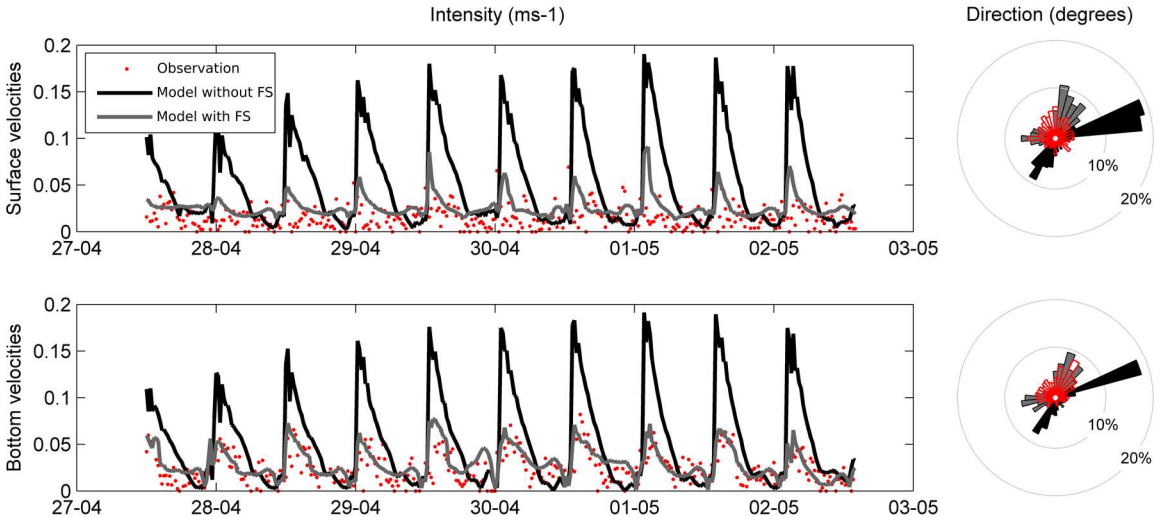

Figure IV.6. *Comparison of velocity computed with floating structures (gray line), without floating structures (black line) and acquired with ADCP (red) inside the marina for three days in May 2018 (mean tidal range = 4 m). FS corresponds to floating structures.*

IV.5. Results

IV.5.1. Tidal circulation in the marina

Hydrodynamic simulations were performed under tidal and meteorological forcings. Even if wind forcing can influence velocity fields, considering the relatively shallow depths of the water column, numerical modelling suggests a major impact for tide on the currents. Then, contrary to the Bilbao (*Grifoll et al., 2009*) and Genoa ports (*Cutroneo et al., 2017*), density-driven circulation is considered nonexistent in La Rochelle marina. Indeed, there is no freshwater influence except during occasional heavy rainfall. Therefore, in this section, the modelled results are analysed assuming that the tide is the main factor controlling the water circulation pattern.

The main circulation patterns are shown in Figure IV.7. The depth-averaged velocity displayed was computed for a spring tide (tidal range = 6 m), with and without the implementation of floating structures in the model. The maximum velocity in the marina is located in the channel entrance at the end of the ebb and beginning of the flood, when the section is the lowest. The behaviour of water bodies during flood and ebb is very different. A strong flood enters the marina by the main entrance with maximum amplitude up to 1.7 ms^{-1}, 1 h after low tide, whereas the ebb is two times lower in intensity and mainly focused on the

channel entrance. At the end of ebb tide the current is rapidly reversed by the flood at the channel entrance. The opposition between these two flows leads to complex current in terms of direction and intensity. Current presents a large range of intensity substantially influenced by basin geometry. For instance, the W basin displays stagnant water with velocity lower than 0.01 ms^{-1}, reaching only 0.05 ms^{-1} at peak flow. During neap tide, where the tidal range is approximately 2 m, the velocity decreases by a factor of two, but the same trend remains in the marina. The main changes occur during ebb with weak eddy reduction and lower water flux compared with spring tide.

At the entrance sections, there is an asymmetry in term of flood-ebb duration, which is inverse function of the tidal range. At the main entrance (section 1), during spring tides there is a 5 h 30 min – 6 h 40 min ratio against a 4 h 30 min – 7 h 20 min ratio during neap tides but fluxes at the entrances are globally enhanced during flood. The tidal asymmetry of the offshore area explains this asymmetry of flux between flood and ebb tide, as discussed earlier (*Guo et al., 2018*). The asymmetry can also result from signal distortion generated by the system geometry (quays, entrances sections) and bathymetry (*Nece & Richey 1972; Sztano & De Boer, 1995*).

IV.5.2. Impact of floating structures on marina tidal circulation

The main difference between the simulation with and without the floating structures concerns the flood. With FS, there is a faster velocity decrease and faster divide of the entering flood into two directions. Furthermore, the addition of floating structures reduces the development of eddies at the scale of each sub-basin (Figures IV.7a-7b). Once the stream enters the W and SE basins, we observe a strong decrease in eddy intensity in surface layers and a very strong reduction in the size and intensity of the eddies. During the ebb, water circulation is slightly noticeable in the inner part of the marina. Consequently, the impact of floating structures in the model is weak. Indeed, the main currents are located along the channel entrance, which appears to be slightly impacted by the presence of floating structures. During flood and ebb tide the maximum velocity along the channel entrance is slightly accentuated by floating structures (Table IV.3). The southern part of the W and SE basins are the most impacted by the attenuation of velocity, displaying large stagnant water areas (Figures IV.7g-7h) where intensity is lower than 0.01 ms^{-1} except during the flood where intensity can reach 0.05 ms^{-1}.

Quantitatively, Table IV.3 reveals the impact of the implementation of floating structures on the velocity field of the marina. The effect is more significant during spring tides when currents are stronger. From neap to spring tides, in the W basin, velocity intensity was reduced from 8 % to 28 %, respectively. In the SE basin, the velocity was reduced from 3 % to 15 %, respectively, and in the NE basin, the main reductions were 10 % and 65 %, respectively. However, the velocity decrease in the inner parts of the marina is compensated by velocity acceleration in other locations. The relatively higher velocity during ebb supports this assertion with the presence of floating bodies (Table IV.3). The effect of floating structures increases towards the inner parts of basins. Their presence attenuates currents at the surface that consequently reduce the currentology of the inner parts of the marina.

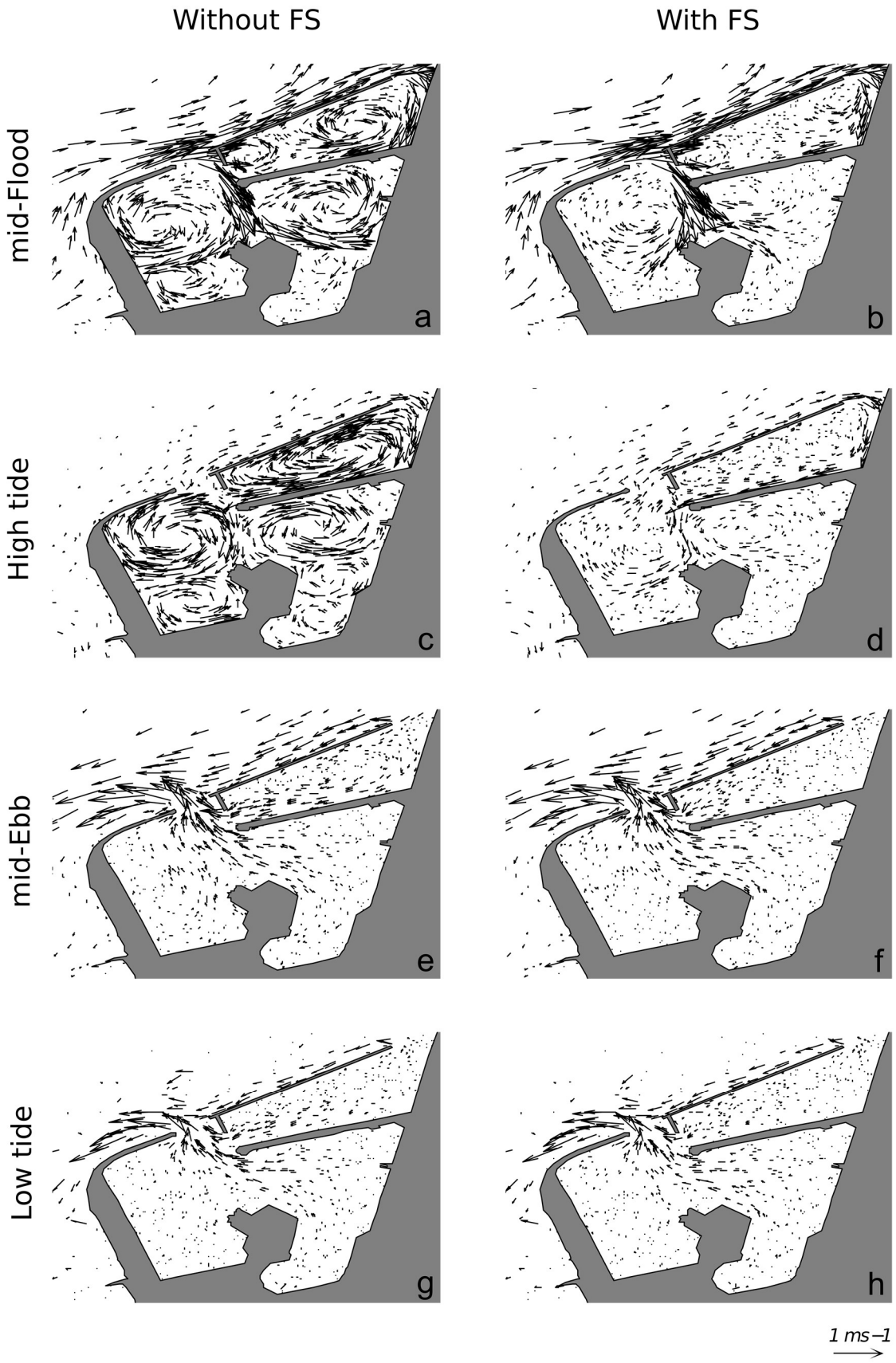

Figure IV.7. *Depth-averaged velocity field (ms^{-1}) for simulations with (right) and without (left) floating structures. a and b correspond to flood. c and d correspond to high tide. e and f correspond to ebb. g and h correspond to low tide.*

Table IV.3. *Depth averaged velocity computed in the marina for spring and neap tides (W = western basin; SE = southeastern basin; NE = northeastern basin; CE = channel entrance). Each entry corresponds to mean velocity, maximum velocity during ebb, and maximum velocity during flood, with (and without) floating structures.*

Location	Spring tides (ms^{-1})	Neap tides (ms^{-1})
W	0.50 (0.76) – 0.81 (0.80) – 1.17 (1.50)	0.12 (0.14) – 0.15 (0.11) – 0.27 (0.34)
SE	0.61 (0.74) – 0.94 (0.81) – 1.45 (1.59)	0.13 (0.14) – 0.23 (0.23) – 0.37 (0.43)
NE	0.25 (0.73) – 0.39 (1.01) – 0.73 (1.56)	0.07 (0.08) – 0.09 (0.10) – 0.38 (0.45)
CE	0.90 (0.89) – 1.19 (1.16) – 1.68 (1.68)	0.23 (0.23) – 0.19 (0.17) – 0.59 (0.58)
Total Marina	0.56 (0.75) – 1.19 (1.16) – 1.68 (1.68)	0.14 (0.18) – 0.23 (0.23) – 0.59 (0.58)

IV.5.3. Residual fluxes at the marina entrances under the action of tides and wind

The wind regime in the area, and more globally in the whole Bay of Biscay, experiences a significant interannual variability (*Dodet et al., 2010*), which is partly controlled by the North-Atlantic Oscillation. The weakest winds, lower than 4 ms^{-1}, occur 58 % of the time, moderate winds, from 4 to 8 ms^{-1}, occur 29 % of the time and the strongest, from 8 to 16 ms^{-1}, occur 12 % of the time. Summer presents weak low-pressure system activity resulting in weak winds mostly originating northeasterly while the littoral is mainly dominated by thermic breezes from the north-west. During autumn, low-pressure systems cross the Atlantic Ocean, creating more energetic winds from south-west to west. These low-pressure systems are most active during winter, and they can potentially cross the French Atlantic coast where strong winds are often observed. These systems result in the predominance of four winds over the area of study: northwestern (22 % occurrence), western (21 % occurrence), northeastern (19 % occurrence) and southern (14 % occurrence) winds.

To understand the role of the wind in the area, twelve specific cases were studied, corresponding to six atmospheric conditions (one without wind, four with an average 7.5 ms^{-1} wind from several directions, one with a strong 15 ms^{-1} wind from the west) linked with 2 tidal conditions (spring and neap tides). Residual flux (RF) was computed over five tidal cycles, at three different sections for every case. The first case corresponds to a situation with only tides; the four following are simulations of combined tide and wind forcing related to the four dominant area winds. These five cases were simulated for a spring tide with 6 m tidal range and a neap tide with 2 m tidal range, from 2nd to 4th February 2016 and from the 9th to 11th February 2016, respectively. Three sections were defined in this study to compare residual flux (Figure IV.8).

This study shows that the total RF in the marina is a general inflow mainly governed by section 3. For neap and spring tides, the configuration is the same with an offshore RF at section 1 and 2 and an onshore RF at section 3. The only difference is that RF are significantly higher during spring tides. The presence of a west wind enhances the westward residual circulation established from section 3 to section 1. This residual dynamic is also conserved, but with less intensity, when the wind is northwest. With a northeast wind, this residual circulation is completely reversed and oriented from section 1 to section 3. RF for simulations with a southern wind is not presented in Figure IV.8 because it is relatively unchanged

compared with no-wind simulations. Depending on its direction, the wind has an anisotropic effect, which can be significant in particular during neap tides. Finally, it is important to notice that the absence of floating structures in the model does not noticeably affect the RF at the sections.

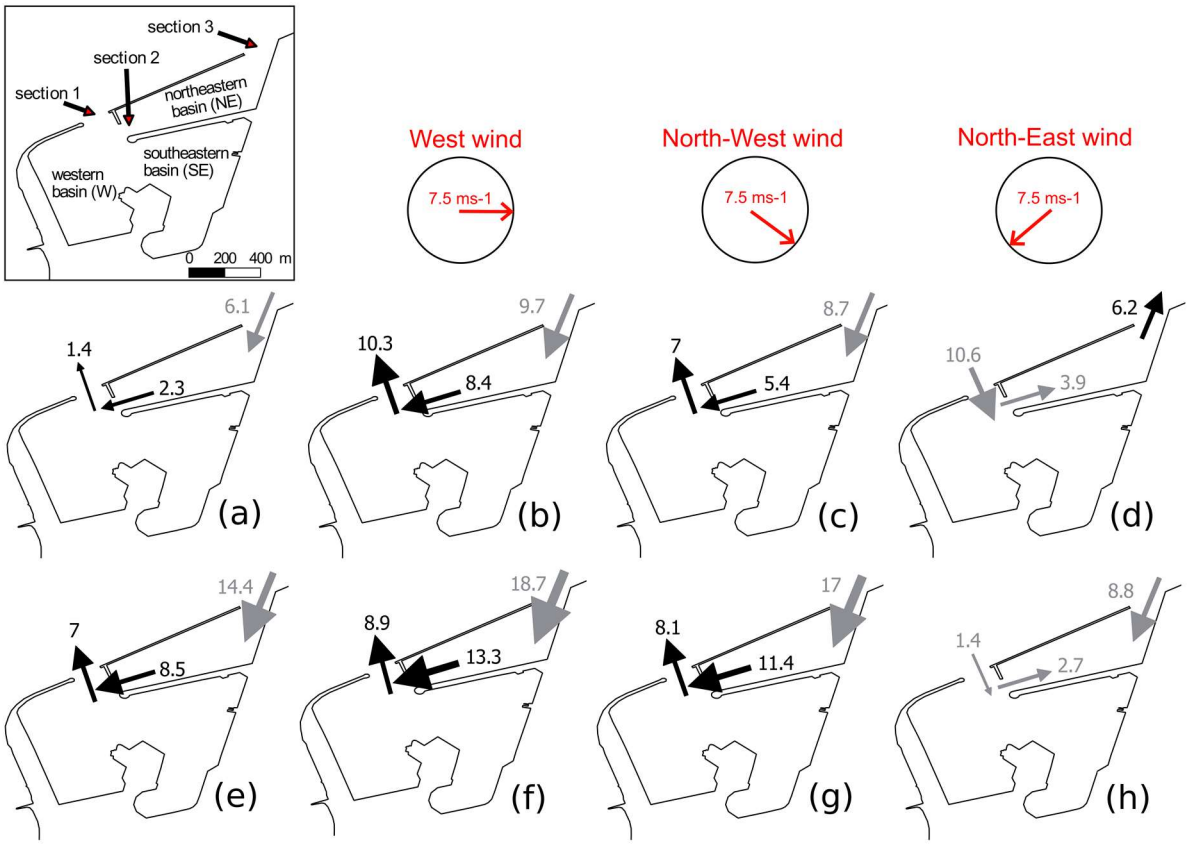

Figure IV.8. *Residual fluxes (m^3s^{-1}) at the entrances defined in the top figure for several conditions of wind and tides. a, b, c, d correspond to neap tide conditions and e, f, g, h correspond to spring tide conditions. a-e represent the situation without wind and b-f, c- g, and d-h, correspond to simulations with 7.5 ms^{-1} west, northwest, and northeast winds.*

IV.5.4. Assessment of the main drivers of circulation

To more accurately investigate the influence of the water circulation-driving mechanisms, velocity depth average was computed with numerical modelling and analysed for the 12 specific cases. The mean differences between states without and with wind stress, regardless of direction, range from 0.02 ms^{-1} to 0.01 ms^{-1} with maximum difference of approximately 0.70 ms^{-1} during the maximum flood/ebb tide. Table IV.4 reveals the mean velocity averaged over 5 tidal cycles for several wind directions. Large differences appear according to wind directions but, globally, wind decelerates water mass dynamics during spring tides and accelerates them during neap tides. For spring tides, only a 7.5 ms^{-1} south wind is able to increase the water circulation whereas other winds decrease circulation (up to 25 % for an NE wind). During neap tides, the west, northwest and south winds increase velocity up to 34 %, whereas the northeast wind only increases it by 14 %. The behaviour of water masses is consistent, first with the direction of tidal propagation in the bay for a northeast wind and

second with the direction of channel entrance for a south wind. More generally, average winds have a significant influence on velocity mainly during neap tides. Strong events as 15 ms^{-1} west winds that occur frequently during winter in the area, can overpass the tidal forcing by increasing the neap tides velocity by more than 50 %. Finally, the results show that the significant influence of the wind follow the same trend with and without floating structures (Table IV.4). However, while their effect is similar during spring tides (a decrease of the mean velocity), the wind and the floating structures display an antagonistic effect during neap tides by increasing and decreasing the velocity, respectively.

Table IV.4. *Depth averaged velocity for several configurations of tides and wind (WW = west wind; NW = north-west wind; NEW = north-east wind; SW = south wind). Each entry corresponds to the total mean marina velocity computed over 5 tidal cycles for 6 specific cases with (and without) floating structures: without wind, with strong 15 ms^{-1} WW (typical storm wind during winter), and four with a 7.5 ms^{-1} wind.*

Wind configuration	**Spring tides (ms^{-1})**	**Neap tides (ms^{-1})**
No wind	0.56 (0.75)	0.14 (0.18)
WW (15 ms^{-1})	0.50 (0.70)	0.29 (0.42)
WW (7.5 ms^{-1})	0.49 (0.65)	0.18 (0.22)
NWW (7.5 ms^{-1})	0.44 (0.60)	0.20 (0.22)
NEW (7.5 ms^{-1})	0.42 (0.56)	0.16 (0.19)
SW (7.5 ms^{-1})	0.57 (0.64)	0.21 (0.25)

IV.6. Discussion

IV.6.1. Relevance of considering floating structures in the model

Structures such as floating docks and breakwaters are often encountered in the modelling domain, but their effect is often neglected. This effect can be very complex to incorporate in some applications. *Tsay and Liu (1983)* and *Li et al. (2005)* proposed an approach to approximate the effect of floating structures in a 2D elliptic harbour wave model. However, a simplified approach has permitted us to simulate their effect on hydrodynamics. Indeed, comparison with observations has shown the necessity to implement floating structures in order to better fit the reality. Even if floating structures have not a real effect on residual flux, a strong influence of floating structures has been identified. The main impact is the drastic reduction of microscale eddy structures in the inner part of the marina (Figure IV.7B). The velocity intensity has decreased by more than 30 % in the whole marina whereas the NE basin displays a maximum attenuation of 65 % (Table IV.3). This reduction is compensated by a slight velocity increase in the channel entrance during peak flood and ebb flows. These significant differences between the model with and without floating structures raised questions about the resuspension and siltation of the marina. Therefore, it appears relevant that a highly populated port should consider the effect of floating docks and boat moorings in any hydro sedimentary modelling study.

Further research needs to be carried out to characterise the influence of floating structures on wind stress. Indeed, the effect of wind is decreased by floating structures and that could

have a significant impact on water agitation and hydrodynamics in the marina. The results show that the influence of wind, in terms of velocity intensity, is weaker with the presence of floating structures. The floating structures naturally decrease the wind effect by "protecting" the surface. As both the influence of wind and implementation of floating structures in the model mainly concerns the surface layers, our methodology also considers the wind decrease effect on the marina.

It is also important to consider some limitations of this study. First, we do not explicitly represent floating bodies as obstacles in the flow field. We considered floating structures only in the momentum equation while in reality they also affect the depth-integrated continuity equation. This simplification could result in an underprediction of current velocity between floating structures, as there is no contraction of the hydraulic section. Then, we do not consider the motion and dynamic forces of the floating structures. In our methodology, we do not model these effects, but we are trying to estimate the global effect of floating bodies at the scale of the entire marina. It is also important to note that our method is sensitive to the number of vertical sigma layers used in the study as well as the number of layers involved in the representation of floating structures.

IV.6.2. Impact of floating structures on eddy generation

Even with the implementation of floating structures, transient small-scale eddies are generated in the inner part of the marina from the flood beginning until the ebb (Figures IV.7a-7b-7c-7d). This behaviour is the result of tidally driven flow separation at the channel entrance that ensures eddy development behind the quays. It is a well-known phenomenon that has been easily reproduced by barotropic numerical models (*Pingree and Maddock, 1977; Imasato, 1983; Signell and Geyer, 1991*). These are considered topographic eddies (*Babu et al., 2005; Vethamony et al., 2005*). The geometry of the marina leads to a considerable difference in terms of eddy structure intensity between flood and ebb tide. Whereas ebb tide is characterised by the absence of eddies, the flood time displays eddies of basin size. Depending on tidal and wind forcing, the number and size varies from between 2 and 3 eddies in the W basin, to 3 to 5 in the SE basin and 1 to 3 in the NE basin (Figure IV.7). The number and size are dependent on hydrodynamic conditions, the geometry of the marina and its bathymetry (presenting strong lateral gradients due to recurring dredging). Nevertheless, the presence of floating structures substantially reduces their action and intensity by concentrating flow at the channel access. Although the natural generation of eddies during the flood is conserved, their presence leads to a channeling of the flow that also has an impact on residual circulation.

IV.6.3. The role of residual circulation in particle residence time

According to *Babu et al. (2005)* tide-topography interaction is the main mechanism generating residual eddies because topographic variations in the eddy region slow tidal wave propagation, inducing a phase shift. In La Rochelle Marina, residual flow computed from the averaging of depth-averaged currents over 5 tidal cycles presents microscale eddies. In terms of size and location, these eddies correspond to the topographic eddies created by tide-topography interaction during the flood discussed earlier. Their intensity is weaker, and it can reach a maximum of 0.2 ms^{-1} intensity in the NE basin, during spring tides.

Our results show that the presence of both average 7.5 ms^{-1} wind and floating structures is sufficient to significantly affect the shape and intensity of residual eddies. Whereas wind stretches the tide-induced eddies in its direction of propagation, the floating structures focus the residual flow on the channel entrances. The wind and floating structures alter the residual circulation of the marina differently; although the former modifies the RFs substantially at the entrance section, the latter reorganises residual flow without really modifying RFs.

Vethamony et al. (2005) suggested the contribution of residual eddies to the net transport of material from the system and their potential role in the transport of pollutants. Although *Wolanski & King (1990)* presented enhancement by eddies by flushing process, long term-transport is altered by the presence of residual eddies, reducing the flushing rate (*Babu et al., 2005*). Thus, questions are raised about particle residence time and more generally about water quality. Floating structures could influence significantly the residence time of particles or discharged material in the marina. To address this question, further research is conducted to characterise water mass exchanges under the influence of wind and tide forcings, with the presence of floating structures.

IV.7. Conclusion

This paper presents the influence of floating structures on the hydrodynamics of a highly populated marina. Assessment of the main driving mechanisms, tide and wind forcings, has been conducted and an original implementation of floating structures was conducted and discussed. *In situ* velocity measurements have shown model overestimation without floating structures in the inner parts of the marina. Conversely, the implementation of floating bodies has permitted one to fit observations and highlight their strong influence on the attenuation of current. This reduction in intensity is mainly compensated by a slight increase in the access channels during peak flow. Furthermore, the residual circulation is also impacted by their presence; the residual eddies naturally formed in the marina by tide-topography interaction are strongly attenuated. As tidally induced eddies play an important role in the dispersion of matter (*Yanagi, 1974*), they could decrease this dispersion as well as the resuspension. Thus, questions are raised about water quality, siltation and more extensively, dredging maintenance strategy.

Even if the area is under the influence of a macrotidal regime, the role of wind is also undeniable; although significant during spring tides, its influence can be dominant during neap tides, approaching 50 % in terms of mean velocity. Wind also affects the residual circulation, by modifying the size and form of eddies and by reversing the RFs. To assess the relative importance of the different processes a study is being conducted. Its objective is to characterise particle residence time under tidal and wind forcing with the presence of floating structures.

Chapitre V

Numerical Modelling of Water Fluxes in La Rochelle Marina (France): Sensitivity to Physical Forcing and Role of the Design

Jean-Rémy Huguet[1], Isabelle Brenon[2] and Thibault Coulombier[3]

[1] PhD student at UMR 7266 LIENSs, CNRS-La Rochelle Université, 2 rue Olympe de Gouges, 17000 La Rochelle, France (corresponding author). E-mail: jean-remy.huguet@univ-lr.fr
[2] Associate professor at UMR 7266 LIENSs, CNRS-La Rochelle Université, 2 rue Olympe de Gouges, 17000 La Rochelle, France. E-mail: isabelle.brenon@univ-lr.fr
[3] Research engineer at UMR 7266 LIENSs, CNRS- La Rochelle Université, 2 rue Olympe de Gouges, 17000 La Rochelle, France. E-mail: thibault.coulombier@univ-lr.fr

Keywords: Marina; Multiple-entrance geometry; Macro-tidal regime; Wind influence; Residual fluxes; Volume transport;

Ce Chapitre sera soumis sous forme d'article.

Résumé

Dans la continuité du Chapitre 4, ce volet décrit l'hydrodynamique au sein du port des Minimes et sa modulation sous l'influence de la marée, des vents dominants et de la configuration spécifique du port et de la baie de La Rochelle. Le Chapitre précédent s'est attaché à caractériser l'influence des structures flottantes sur l'hydrodynamique, mais cette dernière a été abordée de manière succincte. Pourtant, celle-ci est complexe et variable en fonction des conditions océanographiques et climatiques. C'est d'ailleurs cette complexité qui a principalement motivé l'élaboration de ce Chapitre. L'influence conjointe de la configuration spatiale et des facteurs environnementaux, sur l'hydrodynamique, a déjà fait l'objet de nombreuses études dans les bassins-semi-fermés naturels. Cependant, ce type d'analyse n'a rarement, voire jamais, été appliqué aux bassins artificiels tels que les ports, à notre connaissance. Au vu de l'intérêt grandissant porté à ces espaces et à leur développement il nous est apparu important d'explorer le port des Minimes en tant que système dynamique à part entière. Un fort accent a donc été porté sur les flux générés aux différentes sections d'entrées du port ainsi que sur la circulation résiduelle induite. La dynamique des masses d'eaux assez complexe nous a conduit à utiliser divers outils et méthodes afin de caractériser de manière intégrée les différents mécanismes, tidaux et non tidaux, impliqués.

L'asymétrie de marée, déjà présente dans la baie, est accentuée dans le port, principalement au niveau des entrées. Elle se traduit par un déphasage important des courants. Les volumes engagés diffèrent de manière significative en fonction des conditions de marée et de vent. Pendant les périodes de vives-eaux, seuls les vents forts sont capables de modifier le sens du transport tidal résiduel, alors qu'en mortes-eaux, l'effet d'un vent moyen peut s'avérer déterminant. La direction du vent est un facteur clé: les vents d'ouest génèrent un transport résiduel entrant dans la baie et sortant dans le port alors que pour les vents de nord-est c'est le contraire. Ce résultat met en avant le rôle important que joue le système port-baie dans la résultante du transport résiduel à l'échelle locale. La présence et la configuration des trois entrées permet au port d'être interconnecté avec la baie, ce qui, à la faveur des vents dominants, peut générer une circulation résiduelle tourbillonnaire impliquant spatialement la partie nord du port et la baie sus-jacente. Cette circulation est fonction de l'intensité et de la direction du vent. Ce Chapitre établit donc les principaux mécanismes engagés dans la dynamique résiduelle et instantanée du port et de la baie, et issus de l'interaction de la marée, et du vent avec la géométrie locale. La saisonnalité marquée du régime des vents dans la zone peut impliquer non seulement des différences notables sur l'hydrodynamique portuaire mais aussi sur les flux sédimentaires qui s'y déroulent.

Abstract: In the present paper we investigate the exchange processes and the resulting residual circulation in a multiple-entrance and highly populated marina, located at the south-west of France. Both the influence of the macro-tidal regime and the local wind forcing were studied with the use of a 3D-numerical model (TELEMAC-3D). Several tidally-averaged or related quantities were computed in order to characterise the fluxes and the volume transported through each entrance and particular attention was given to the spatial residual circulation in the marina and its adjacent sea. Particle and tracer tracking studies were also performed in order to quantify the exchange processes occurring in the marina and between the marina and its adjacent sea. Results highlight the role of the marina geometry in the development of tidal current asymmetries. The resulting tidal asymmetry generates a net residual inflow through the marina. Average and strong winds are responsible for a significant variability of the volume transported through the entrances which impact the long-term residual transport. The response of the circulation to wind action is highly anisotropic depending on wind direction but the exchanges and volumes involved are generally increased. Large-scale structures can develop in the bay by interacting with the marina via the entrances. Finally, both the physical setup of the interconnected system bay-marina and the wind can substantially modify the tidal asymmetry, which influences the transport and accumulation of sediments in the marina.

V.1. Introduction

The use of coastal areas has increased significantly in recent decades, and this trend is expected to continue in the future with the growth of the world population and the development of urban areas near the coastline (*Small et al., 2003*). The main cities are located in the coastal zone (*Brown et al., 2013; Von Glasow et al., 2013*) and their socio-economic development is based on the well-being of major coastal infrastructures such as waterways and ports. Encouraged by a flourishing leisure and tourism activity, recreational boating has experienced unprecedented growth since the last few decades. This rising popularity requires infrastructures that can host an ever-increasing number of boats. As the number of suitable natural sites is becoming increasingly rare, the expansion, maintenance and improvement of the existing ports is essential. (*Bizzarri et al., 2011; Saz-Salazar et al., 2012; Fan et al., 2012; Valadez-Rocha & Ortiz-Lozano, 2013*). However, expanding port areas has become more complicated due to the rising awareness about the related degradation of water quality and the ecosystems and coastal processes modifications. (*Di Franco et al., 2011; Patterson & Hardy, 2008; Rivero et al., 2013*). To ensure the sustainable development of these areas research interest in the field of port management has grown since the mid-1990s. (*Pallis et al., 2010; Woo et al., 2011*). The results obtained are considered as integrated tools for decision-making in the management of ports. Understanding the hydro and morphodynamic processes in port environments is a very challenging issue due to their complexity. They are driven by many physical factors such as tide, wind, waves, and water density gradients. (*Falconer et al., 1991*) but the structural features such as planform geometry, water depth and bottom slope also influence these mechanisms (*Nece, 1984; Falconer et al., 1991*).

Over the last decades, new methods and techniques have been developed to provide a more synthetic understanding of the coastal environment hydrodynamics (*Zimmerman, 1976; Takeoka, 1984; Oliviera & Baptista,1997; Monsen et al., 2002; Deleersnijder & Delhez, 2007*). The use of these synthetic quantities derived from measurements or simulations, such as residual

flows, oscillating volumes or renewal times, allows to easily summarise the mixing and exchange processes occurring in a semi-enclosed system. In tidal environments, the time-varying residual circulation is defined as the instantaneous circulation obtained after averaging over an entire tide. It is controlled by several mechanisms operating over a wide range of spatial scales. At intermediate scales (of order $100\,m$–$10\,km$) flood-ebb tidal asymmetry driven by the tide-topography interaction (*Aubrey and Speer, 1985; Zimmerman, 1976; Wang et al., 2009*), can contribute to a complex residual flow. In many tide-dominated coastal areas, an asymmetry between flood and ebb tide is observed (*Aubrey and Speer, 1985; Blanton et al., 2002; Toublanc et al., 2015*). On a larger scale the wind stress was found to be of primary importance in the subtidal residual flow as it was pointed out by several studies (*Heaps and Jones, 1977; Geyer, 1997*). The cumulative effect of the resulting residual circulation allows describing the long-term transport of water and sediment particles that influence not only the water quality but also the morphological evolution of the system (*Prandtle, 2004; Dronkers, 1998*). Characterising the spatial structure and the time variation of this circulation is of importance for port management in particular with regard to the siltation issue.

Furthermore, in semi-enclosed systems with narrow entrances, the geometry and the configuration of entrances significantly control the dynamic processes inside the system as evidenced by *Stommel & Farmer (1952)*. The presence of multiple openings particularly complexifies the currents pattern which has been extensively studied in natural coastal systems (*Salles, 2005; Duran-Matute & Gekerma, 2015; Li, 2013; Liu & Aubrey, 1993*). However, the detailed interpretation of these processes in artificial multiple-entrance/inlet systems, such as waterways and ports, are often set apart in favour of environmental and engineering studies. In this work, we investigate the variability of exchange processes into a multiple-entrance marina located at La Rochelle, in the south-west of France. The influence of typical weather-marine forcings and the geometrical configuration of the system will be analysed in order to characterise their level of implication in the circulation. Several approaches were employed with the use of an operational 3D hydrodynamic model (*Huguet et al., 2019b*). Tidally-related quantities such as velocities, fluxes and oscillatory volumes were examined in relation with the residual circulation, and the modulation of the sea-level. The use of tracer and particles-methods help us understanding exchange flows processes from the bay to the inner parts of the marina. The chapter is structured as follows. In section 2 the study site and the numerical implementation of the simulations are described. Section 3 gives insight into the exchange processes occurring through the entrance while Section 4 provides a spatial vision of the influence of the several forcings studied. Finally, discussion and conclusions are highlights in section 6.

V.2. Materials and Methods

V.2.1. Study Site

V.2.1.1. Geographic location

La Rochelle Marina is located in the northern landward part of the Pertuis d'Antioche embayment, situated along the French Atlantic Coast, in the central part of the Bay of Biscay. This shallow water coastal area is protected from the Atlantic Ocean by Ré and Oléron islands,

and connected to the Pertuis Breton embayment through a narrow inlet (Figure V.1). The area is considered as a mixed, wave and tide-dominated estuary (*Chaumillon & Weber, 2006*) with shallow silty to sandy-silty bottoms and the presence of many tidal flats (*SHOM*, 2015). Since its expansion in 2014, La Rochelle marina has been considered as the biggest marina on the European Atlantic coast. This 900 m long and 820 m wide semi-enclosed system is divided in 3 basins totalling 4500 moorings, distributed along 15 km of floating docks. The southeastern (SE) basin is the bigger, with 22 ha, while the western (W) and the northeastern (NE) basin, present respectively 17 and 15 ha (Figure V.1). The marina is accessible by a 110 m wide main entrance, while the extension basin (W) presents two entrances: 150 m wide to the northeast and a 64 m wide to the southeast. The marina is not spared by siltation and has to spend 10 per cent of its total budget to dredge around 200 000 m^3 of cohesive sediment each year. The annual sediment deposition can overpass 50 cm in some of its basins, which requires recurring dredging, eight months per year. To reduce the cost and procedures associated with dredging, port managers have been willing in recent years to better understand the internal dynamics of the port and the sediment inputs to the system.

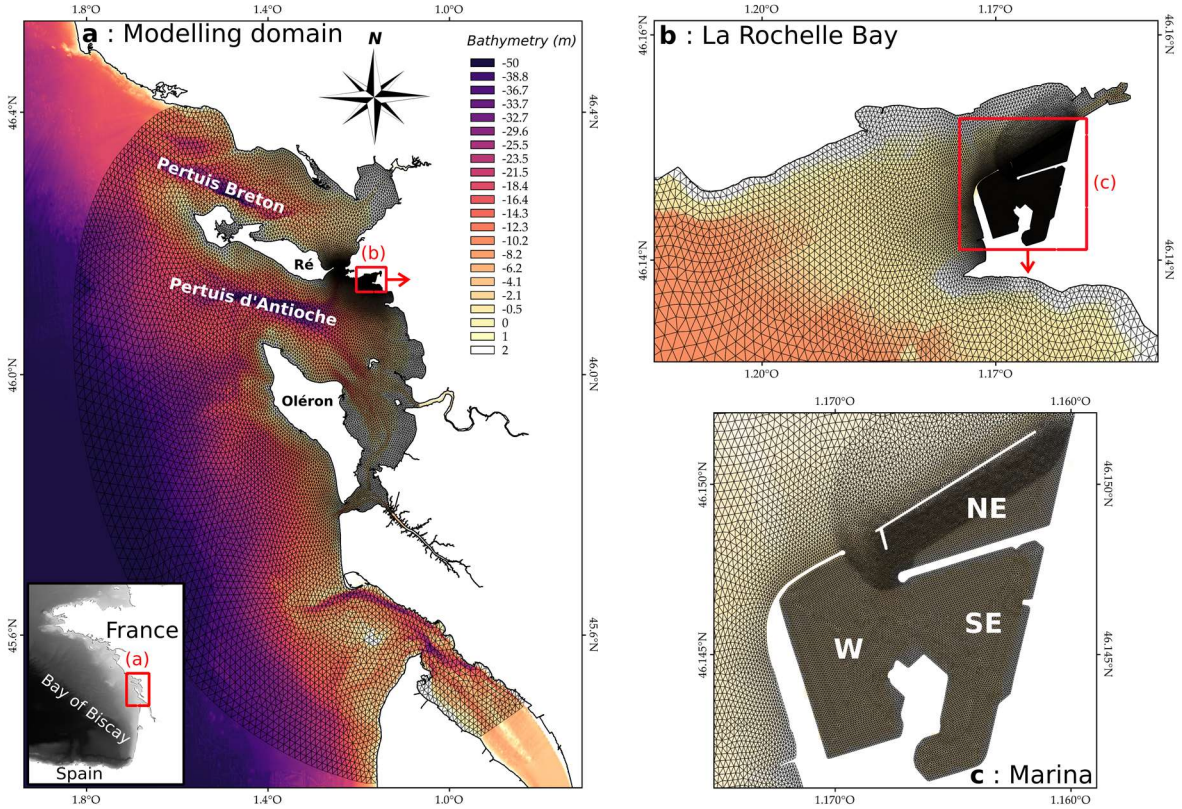

Figure V.1. *Bathymetry/topography map of the modelling domain with the surimposed 41 000 nodes horizontal unstructured grid in black line. (a) represents the regional domain, (b) provides an overview of the La Rochelle bay and (c) shows the La Rochelle marina. Altitudes are given with respect to mean-sea-level and the shoreline is indicated by a straight bold black line.*

V.2.1.2. Oceanographic and meteorological conditions

The tidal regime is semidiurnal and tidal range varies from 2 m during neap tides to more than 6 m during spring tides. In the embayments, tidal flows are two orders of magnitude

higher than freshwater inflows (*Bertin et al., 2005*). Tides are dominated by M2, which amplitude grows to more than 1.8 m in the inner part of the embayment due to resonance and shoaling (*Bertin et al., 2012*), and the quarter-diurnal tidal constituents (M4, MS4 and MN4) are also strongly amplified shoreward (*Le Cann, 1990*). The yearly average significant wave height is approximately 1.5 m offshore the islands, with periods between 8 s and 12 s but wave energy is drastically reduced in the inner part of the estuaries by refraction, diffraction and bottom friction. The study area is subjected to wide inter and intra-annual seasonal climate variations with a strong activity of west and north-west winds during the winter period and a weak activity with thermic breezes dominance in summer. A wind analysis available in *Huguet et al. (2019b)* reveals the predominance of four winds over the area: north-western, western, north-eastern and southern.

V.2.2. Numerical modelling and setup of the simulations

V.2.2.1. Computation of tidally averaged quantities

In order to compute current velocities and water levels, the three-dimensional numerical simulations were performed using TELEMAC-3D model with a resolution from 2 km offshore to 5 m within the marina and 8 vertical sigma layers. Equations and parametrizations used are described in details in *Huguet et al. (2019a)*. The open boundaries, located far enough (50 km) from the marina, were forced with realistic boundary conditions of tidal elevation and wind forcing. The model performance was already assessed in previous studies, in term of water levels within the marina but also at offshore stations, and current velocities in the marina and the bay of La Rochelle (*Huguet et al. 2019a, 2019b*). The floating docks and moorings boats were implemented in the model by adding head losses at the surface.

For this study, ten specific scenarios (Table V.1) were investigated, corresponding to 5 atmospheric conditions (one without wind, three with an averaged 7.5 ms^{-1} wind from several directions and one with 15 ms^{-1} west wind typical of winter events) linked with 2 tidal conditions (spring tides with 6 m mean tidal range and neap tides with 2 m mean tidal range). Results for north-west wind simulations were not presented here because their effect onto the circulation was found similar to the effect found with west wind simulations. For each scenario, current velocities and water levels were extracted in the modelling domain during five tidal cycles of neap and spring tides. They correspond realistic tidal conditions that occurred from the 2nd to 4th February 2016 and from the 9th to 11th February 2016, respectively. From the spatial information of these parameters, we produced maps of tidally averaged sea level and residual circulation in the whole marina. Fluxes and oscillatory volumes were computed through each entrance by integrating the instantaneous transport over five tidal cycles through the three sections delineated in Figure V.2a. The identification of the tidal period was crucial because of the strong tidal asymmetry occurring at each entrance in the function of meteorological and tidal conditions. Finally, the strong tidal regime in the area, the shallowness of the system and the absence of fluvial influence partly explain the absence of stratification in the water column. In the present paper, results were depth-averaged in order to clarify the analysis.

Table V.1. *Summary of the ten scenarios analysed in this study.*

Condtions		Scenarios									
		a	b	c	d	e	f	g	h	i	j
Tides	Neap	●	●	●	●	●					
	Spring						●	●	●	●	●
Wind	West 7.5 ms^{-1}		●					●			
	West 15 ms^{-1}			●					●		
	North-East 7.5 ms^{-1}				●					●	
	South 7.5 ms^{-1}					●					●

V.2.1.2. Tracer and particles-tracking simulations

TELEMAC-3D provides the opportunity to release and track the transport of passive tracers and drifters in the water column. The methods are detailed in *Huguet et al. (2019b)* where tracers and drifters were used to investigate the spatial variability of the renewal in the marina. Here, the objective was to provide additional and complementary insight into the exchange processes intra-marina (Figure V.2b) and inter-marina its adjacent sea (Figure V.2a). These approaches differ from the traditional computation of tidally averaged quantities and offer an original way to show the influence of wind. The first study aims to represent the catchment variability of the entrances through the release of drifters in the La Rochelle bay (Figure V.2a). A very large number of particles, corresponding to water parcels, is necessary to capture the diffusive processes generated by the small-scale turbulence (*Spivakovskaya et al., 2007*). During one flood tide, 60 particles were released every 5 minutes, which led to several 4320 drifters used for each simulation. Their release both at the surface and bottom layers, along a line located upstream of the marina entrances and the model returned their location in the water column during the simulation period. Along this line, the bathymetry is variable (it is indirectly visible in Figure V.2). We have therefore differentiated the drifters according to their origin: zone a corresponds to intertidal areas that are not covered 25 % of the time during spring tides; zone b corresponds to intertidal areas that are uncovered 95 % of the time during spring tides, and zone c corresponds to the navigation channel (Figure V.2a). It is important to note that during spring tides, a major part of the bay is exposed at low tide where currents are channelled along the northern edges of the marina. We then detected the passage of particles through the different entrances during the post-treatment.

The objective of the second study was to characterise the variability of the intra-basins exchanges. We released a passive tracer from the two entrances directly connected to the open sea. Over one flood tide, the tracer was released continuously at five source points evenly spaced along the sections S1 and S3 (Figure V.2b) both at the surface and the bottom layers. Contrary to the previous particle-tracking method, we extracted the tracer concentration at each grid cell for the whole marina to compute the relative concentration contained in each of the nine boxes defined for the study (Figure V.2b). These boxes were defined by considering the local geometry and the hydrodynamics. For the two studies (Figure V.2), we worked with the same weather-marine conditions than previously but the duration of the simulations was shorter (one tidal cycle). For each scenario, we repeated the operation on five different cycles (corresponding to realistic tidal conditions that occurred from the 2nd to 4th February 2016 for neap tides and from the 9th to 11th February 2016 for spring tides).

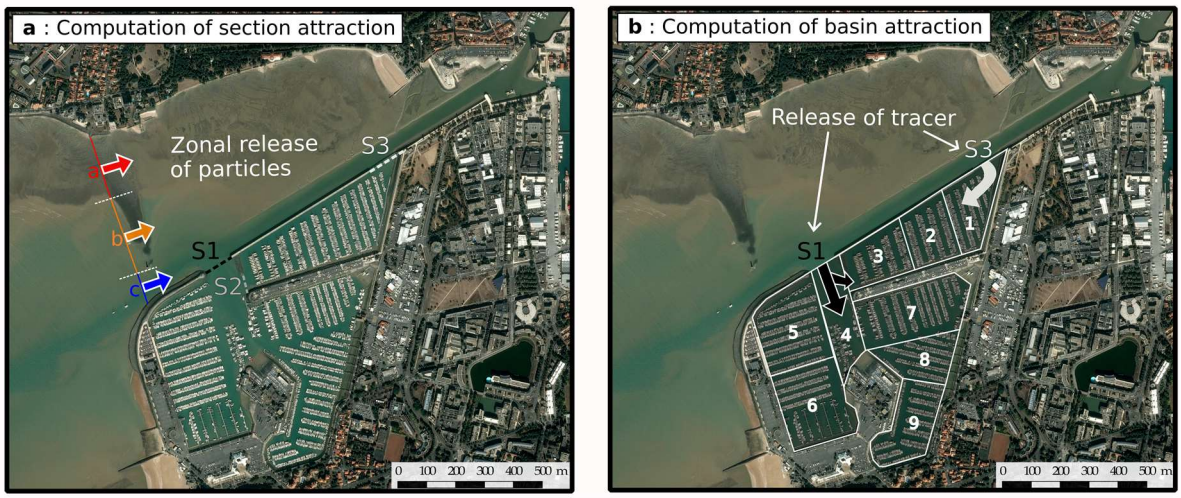

***Figure V.2**. Satellite maps of the study zone and illustration of the methodology employed for both the study of the entrance catchment (a) and the study of the basin catchment (b) under typical weather-marine conditions. The numbers in (b) labelled the boxes studied in the computation of basin attraction.*

V.3. Assessment of the exchange processes at the entrances

V.3.1. Influence of the wind on water fluxes

Velocities computed by numerical simulations were extracted and averaged along with each section (Figure V.3). Flood and ebb current velocities were distinguished in details because their duration strongly varied depending on the entrance and the weather-marine conditions. During spring tides, current velocities are always higher during flood than during ebb. The largest and lowest velocities are generally found along sections 1 and 3, respectively. During neap tides, the flood-ebb asymmetry and the entrance asymmetry are conserved, but the presence of wind globally alters their behaviour. The wind can modify significantly the duration and the intensity of flood and ebb currents along each entrance. At average intensity, the wind direction exerts an anisotropic effect on the velocities. The south wind is the less impacting wind while north-east and west generate an antagonist effect. West wind increases the intensity of currents and decreases flood currents in section 1 and 2, while it globally increases section 3 currents. This behaviour is accentuating for strong 15 ms^{-1} that almost double the current intensity. Conversely, during a 7.5 ms^{-1} north-east wind, currents in section 3 are globally hindered while flood currents in section 1 and 2 are enhanced. Here, only the intensity of currents was investigated, but the impact of the wind on the flood and ebb currents duration will be analysed in the next section.

The computation of fluxes at the entrances section is a good proxy for the assessment of physical mechanisms that drives the circulation through the marina (Figure V.4). The tide generates an asymmetry of fluxes in terms of duration and intensity. This is particularly increased during neap tides when the asymmetry is more developed. At the main entrance (section 1) it globally results in a 5 h – 7 h 30 of the flood-ebb ratio, which is homogenised during spring tides (6 h – 6 h 15). When the tide reverses, an equilibrium state, represented by slack water, is reached between the marina and its adjacent sea. Here, there are significant tidal

phase lags and temporal variations of the flood, ebb and slack water durations depending on the entrances. The reverse of fluxes always comes first at the intermediary entrance (section 2) and always comes last in the north-eastern entrance (section 3). More generally, slack water is longer in section 3 than in the other two sections. During neap tides, an ebb-flood transition occurs 10 min and 1 h 20 min later for section 1 and 3, and these delays reach up 1 h and 3 h 30 min during the flood-ebb transition. The tidal phase lags are globally reduced by a factor 2 for spring tides, but they also play an important role in the modulation of tidal durations. The research for slack water moments was crucial in the determination of flood and ebb periods at the scale of each entrance.

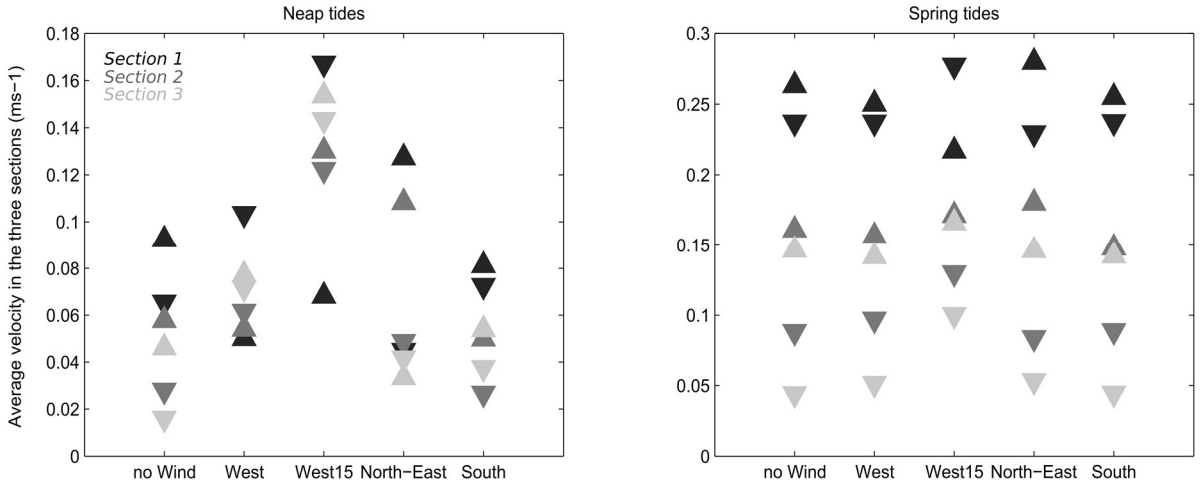

Figure V.3. *Ebb (downward triangles) and flood (upward triangles) averaged velocities obtained along each section. Each plot corresponds to tidal conditions (spring tides at right and neap tides at left) where the weather conditions are (without wind, with a 7.5 ms^{-1} west wind, a 15 ms^{-1} west wind, a 7.5 ms^{-1} northeast wind and 7.5 ms^{-1} south wind) and columns represent the tidal regime.*

The wind globally increased their intensity, but their duration and tidal phase lag were highly variable depending on the entrances and the wind direction. The effect of average winds does not appear significant during spring tides. With a south wind, the shape of time-varying fluxes is almost unchanged except slightly relative homogenisation of the intensities. North-east wind accentuates the duration and intensity of flood-oriented fluxes for section 1 and 2, to the detriment of ebb-oriented fluxes. However, it hinders the development of flood-oriented fluxes through section 3 where the intensity and duration of ebb-oriented fluxes are increased. To the opposite, west wind fosters outflows in section 1 and 2 and inflows mainly in section 3. It also causes ebb-flood reverse to arrives early in section 3 and 2 while flood-ebb reverse arrives later on which creates a quasi-constant inflow circulation at these places. This effect intensifies for a strong 15 ms^{-1} west wind and leads to a quasi-permanent circulation from section 3 to 2 that alters the pattern flow in section 1. This wind also alters significantly the tidal regime in the marina during spring tides.

The response of the circulation to the wind is anisotropic according to the wind direction and intensity. Depending on the direction, it can drive a significant circulation in the northern part of the marina. The section 3 is the most sensitive to the wind action and its connectivity with section 2 highly modified the tidal flows in the NE basin and to a lesser

extent at the section 1. Slack water momentum are reorganised, particularly for section 3 where opposite currents can occur more frequently. Despite the macro-tidal influence of the area, the marina circulation seems highly-dependent to the wind action. In such tidally-dominated multiple-entrance systems, a detailed characterisation of the several mechanisms driving the net circulation is necessary.

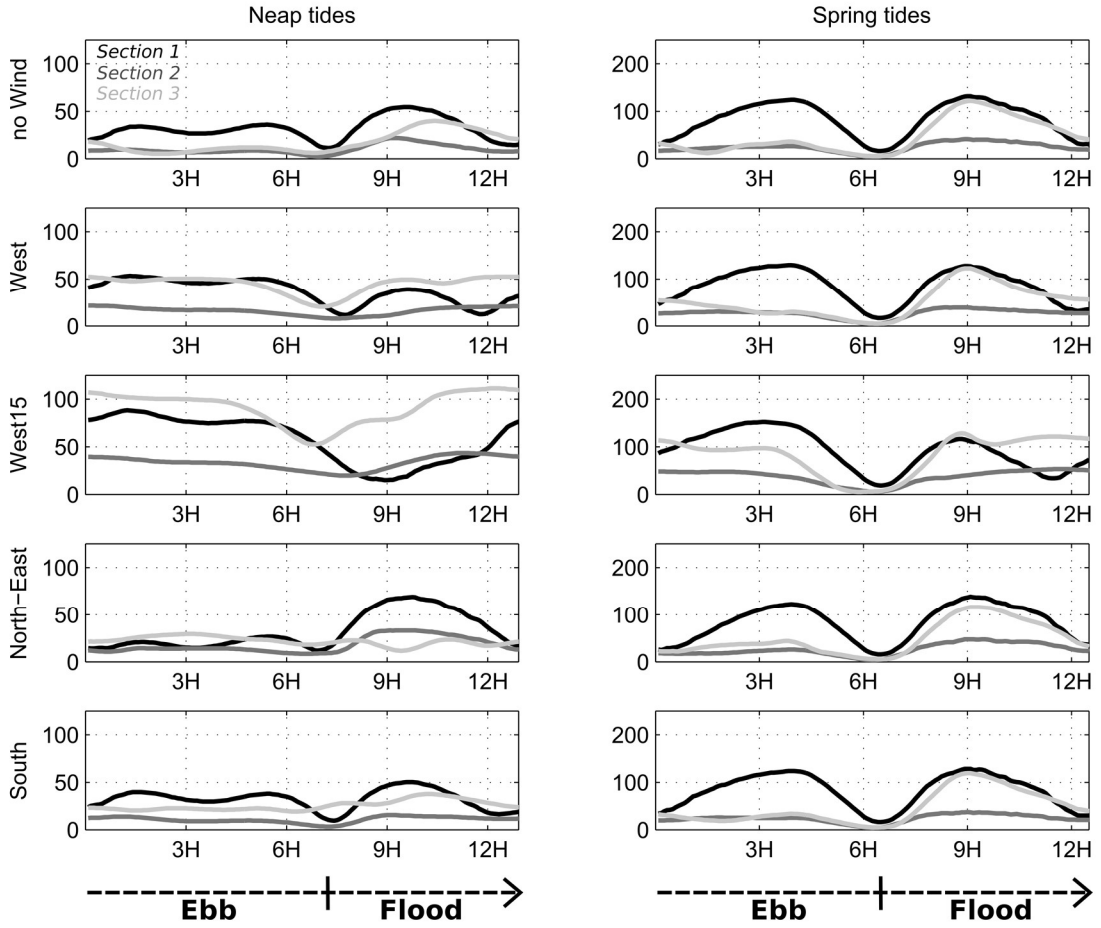

Figure V.4. *Typical water fluxes (m^3s^{-1}) through each section during one tidal cycle. Rows characterise wind conditions defined in Table V.1.*

V.3.3. Tidally-averaged volume transport

To investigate more in details the exchange processes in the marina, we integrated the instantaneous transport passing through the three sections over five tidal cycles. In Figure V.5, inflow, outflow and residual volumes are displayed for every weather-marine conditions and Table V. 2 presents the residual fluxes. A major part of the total volume is transported through section 1, and the spring tide carries three times more material on average. There is a general residual inflow entering the marina, and it accentuates with the tidal range. It results in a significant residual inflow activity driven via section 3, which is not compensated by the slight residual outflow activity in sections 1 and 2. The presence of wind drives more volume during neap tides, but during spring tides only 15 ms^{-1} west wind can substantially increase water transport through the marina. Spring tides are not spared by the effect of average winds and cumulated and residual volumes can be substantially modified (Figure V.5). Every average situation combined, the larger inflows are generated by north-east wind in sections 1 and 2

and by the west wind in section 3. To the opposite, large outflows are generated by west wind in sections 1 and 2 and by the north-east wind in section 3. The larger residual transport occurs during neap tides, and they are caused by the west wind. The most important residual inflow and outflow are situated in sections 3 and 1, respectively. Strong west winds drastically enhance the total and residual transport during neap tides, by more than doubled the total and residual volume transported by the tide in the whole marina. Every wind direction is able to substantially modify the residual transport during neap tides (Figure V.5a). West accentuates the residual circulation through the entrances while south globally decreases it. However, they can reverse the total residual flow generated by the tide. To the opposite, north-east wind totally reverses the residual circulation inside the marina, but it enhances the total residual inflow established by the tide. Their effect is less significant during spring tides (Figure V.5b) even if they can reverse or enhance the residual transport at the scale of the entrance (Table V. 2).

Figure V.5 and Table V.2 demonstrate the importance of wind forcing in such complex and shallow coastal systems, in particular for strong winds. Moreover, several entrances show different patterns. Globally, entrances 1 and 3 always generate a residual outflow and inflow, respectively, except with a north-east wind. However, the most impacting wind in terms of volume transported is from the west. These two quasi-opposite wind directions (west and north-east) force largest outflows and inflows, respectively. Average winds are sufficient to reverse the residual transport through the entrances by involving the same order of magnitude of volumes than those with the tide. Our results show that the total residual transport in the marina can be significantly modified in function of the meteorological conditions, and not necessarily with strong winds. Such finding is important because residual volumes are used as a good proxy for the long-term exchanges between a coastal area and the adjacent open sea.

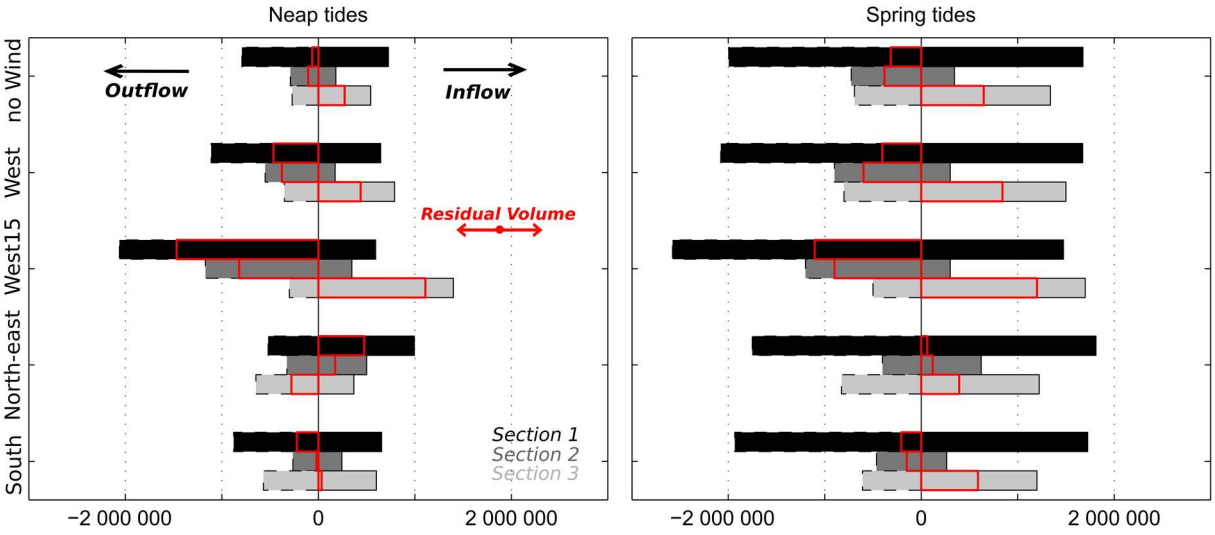

Figure V.5. *Inflow, outflow and residual volume transport (m^3) through each section for one tidal cycle. Each plot corresponds to a specific tidal condition (spring tides at right and neap tides at left). On the y-axis, every wind condition is represented (without wind, with a 7.5 ms^{-1} west wind, a 15 ms^{-1} west wind, a 7.5 ms^{-1} northeast wind and 7.5 ms^{-1} south wind). The X-axis represents the volume of water in m^3.*

Table V.2. *Residual fluxes (m^3s^{-1}) at each section for every weather-marine condition.*

Sections	Weather-marine scenarios									
	a	**b**	**c**	**d**	**e**	**f**	**g**	**h**	**i**	**j**
S1	-1.4	-10.3	-32.6	10.6	-4.9	-7	-8.9	-24.5	1.4	-4.6
S2	-2.3	-8.4	-18.2	3.9	-0.4	-8.5	-13.3	-20	2.7	-3.3
S3	6.1	9.7	24.6	-6.2	0.7	14.4	18.7	26.7	8.8	13.1

V.3.4. Variability of the entrance attraction

To investigate the dynamics at the entrances, we proceeded to a particle-tracking method in La Rochelle bay. The objective was to characterise the level of attraction of each entrance for one flood tide in the function of the weather-marine conditions and the zonal releasing location. Drifting particles released from zone a (Figure V.2a) were not able to reach the entrances 1 and 3 (and thus, entrance 2) with only one flood tide, for every case. In consequence, we did not display the results for the zone a, which are equal to zero, in Figure V.6. Nevertheless, this result is very important as it shows that the water coming from the northern (and the shallowest) area of La Rochelle bay is not able to access the marina at the first tide, regardless of tidal and wind conditions.

Secondly, section 1 only catches particles coming from the channel access (zone c) while section 3 equally catch particles coming from both the central zone b and the access channel. At the scale of one flood tide, entrance 2 attracts only particles being passed through entrance 1. Spring and neap tides display some differences but the behaviour is similar. During neap tides, the percentage of particles entering via entrance 1 and 2 is higher for neap tides but the percentage of particles entering entrance 3 is higher for spring tides. South wind substantially hinders the passage of particles through each entrance which is directly related to its configuration, opposed to the arrival of flood currents in entrance 1 and 3. West wind increases the catchment of access channel particles in entrance 1 (at the expense of entrance 3) but decreases the exchanges with entrance 2. Exchange processes, at the level of section 3, are enhanced for particles coming from zone b and this effect intensifies with stronger winds.

Finally, north-east wind strongly and slightly enhanced the entry of particles via section 1 and section 2, respectively, while it strongly decreases the transport of particles in entrance 3. These results are coherent with previous observations concerning the influence of the wind and it enables to quantify the importance of the exchange processes occurring between the marina and its adjacent bay. Exchanges between the NE basin and the rest of the marina are very weak but they are enhanced during north-east winds and strong west winds. The presence of north-east and south wind globally decreases the transport of material until the entrance 3. Water parcels transported through the access channel mainly entry the marina via entrance 1 and this effect is enhanced by west wind and especially by the north-east wind. Finally, the westerly wind significantly improves the attractiveness of the marina for water parcels from the centre of the bay.

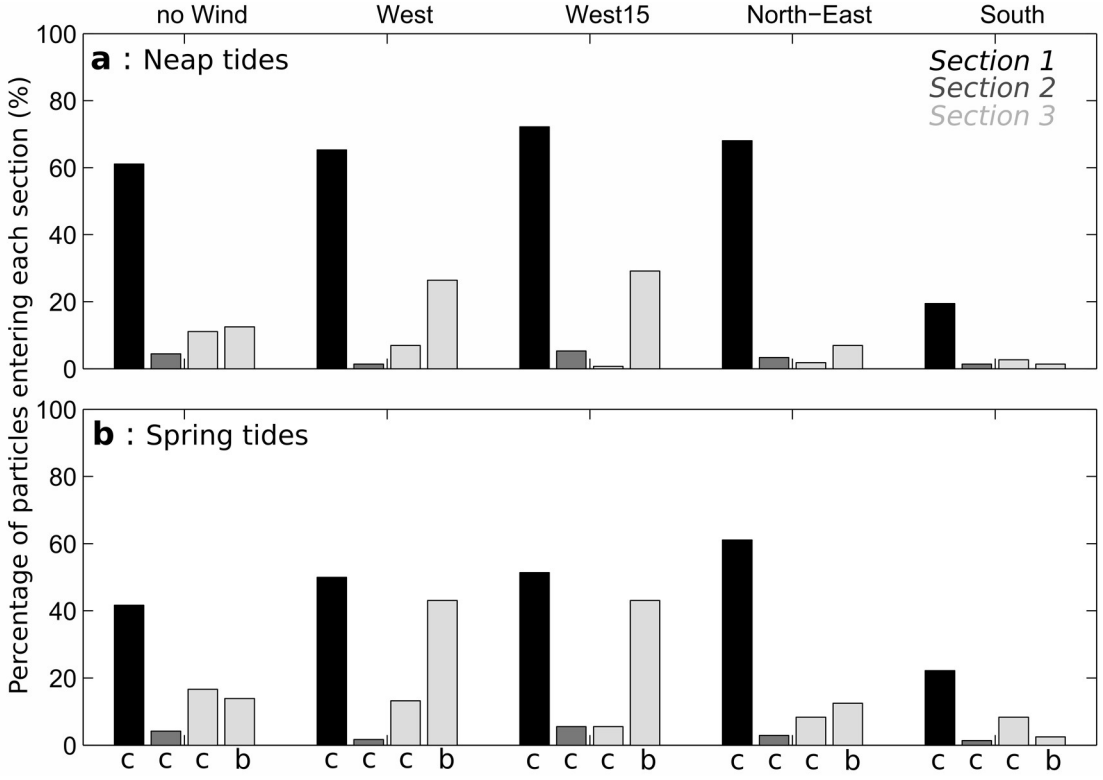

Figure V.6. *Percentage of particles (from each zone) entering each section in the function of weather-marine conditions. Each barplot corresponds to a specific tidal condition ((a) neap tides and (b) spring tides). Every wind condition are represented on the x-axis, (without wind, with a 7.5 ms^{-1} west wind, a 15 ms^{-1} west wind, a 7.5 ms^{-1} northeast wind and 7.5 ms^{-1} south wind). The y-axis represents the percentage of particles entering each section for the first flood tide after their release (%). Letters to the bottom represent the particles departure zone.*

V.4. Influence of the wind in the marina and its adjacent bay

V.4.1. Marina residual circulation

The characterisation of the section entrances activity has shown that the wind influence was anisotropic and not intuitive. The geometry of the marina as well as the configuration of the whole system bay-marina could explain the results obtained previously. Indeed, a previous study (*Huguet et al., 2019a*) has shown that the funnel configuration of the bay had a significant effect on water retention and an anisotropic response to different wind forcings. To understand more accurately the exchange processes between the marina and the bay, we thus computed the residual circulation over five tidal cycles. The spatial patterns of this circulation were displayed via streamlines superimposed to current intensity in Figure V.7.

Without winds, the residual circulation is very low (< 0.01 ms^{-1}) and concentrated along the access channel during neap tides. During spring tides, the circulation intensifies and develops nearby these locations (with maximum residual currents about 0.15 ms^{-1}). Regardless of the tidal range, the bay is dominated by complex recirculation cells and many residual eddies, induced by the tide-topography interaction, scatter the marina (*Huguet et al., 2019b*). The residual marina circulation globally fits with the pattern of currents established during flood while the residual circulation in the bay corresponds to an ebb situation even if it is less marked.

The wind generally stretches the residual marina eddies into its direction of propagation, but its effect is more pronounced in the bay and the NE basin (Figure V.7). Both the west and south winds trigger a longitudinal westward circulation in the NE basin even if the latter effect is lower. Strong west wind generates the largest residual currents during neap tides (0.2 ms^{-1}). It can force the residual circulation in the whole bay, even during spring tides, which is not the case with an average wind. During neap tides, west and north-east wind generate in la Rochelle bay, a clockwise and an anti-clockwise large-scale structure, respectively. These structures, drive a net residual inflow and outflow in the marina, respectively. They concern the northern part of the marina and the overlying bay. The NE basin, which includes two entrances (entrances 2 and 3) and is approaching the main entrance (entrance 1), is a key point of these structures. The very weak tidal eddy activity that normally occurs in this basin is rapidly reversed by the wind action that is able to generate a longitudinal residual current. This residual flux is carried out from entrance 3 to 2 for a west wind and from entrance 2 to 3 for a north-east wind. Entrance 1 is also extensively used and contributes to the development of the overlying large-scale structures. These different patterns explain the antagonist effects provoked by the west and north-east winds, and they highlight the role of the bay and its interaction with the NE basin in the residual and total volume transported through the marina. Results show that the response of the residual circulation to the wind is highly dependent on the topography, the configuration of the entrances and their connectivity.

V.4.2. Intra-basins exchanges

Exchange processes have been investigated within the marina to assess the influence of wind on the fate of water parcels entering the marina. This study was allowed by continuously emitting tracer from entrances 1 and 3 and to compute their residence time in each of the boxes defined in Figure V.2. The objective was to characterise the efficiency of the wind to transport water parcels through the marina. The results obtained are complementary to the observations made concerning the renewal of waters in the water (*Huguet et al., 2019b*). This study could also bring information about the fate of sediment particles entering the marina and thus on its associated siltation. Nevertheless, these results would necessarily need to be cross-correlated with spatial siltation maps to investigate mechanisms fostering the deposit. In Figure V.8, the cumulated tracer mass contained in each box was averaged by the total tracer mass contained in the whole marina to present relative percentages. Firstly, it is interesting to see that tracer released at entrance 1 experienced few excursions in the NE basin and similarly, tracer released at entrance 3 generally stayed in the NE basin. This effect increases during neap tides where the inner parts of the basins are rarely used, or even reached. The spring tides conditions foster the exchange processes and the excursions, but the passage of tracer through entrance 2 is not frequent. The three winds directions studied have very different influence on the exchange processes. South wind particular hinders the transport of tracer released both at entrances 1 and 3. North-east wind enhances the eastward exchange from entrance 1 to the NE basin via entrance 2 but decreases the reverse westward exchange. West wind has an opposite effect and mostly favours the exchanges from the NE basin to the rest of the marina, and it is particularly visible for a strong 15 ms^{-1} west wind. The larger transport of tracer to the SE and W basins is generated by the west and north-east winds, respectively.

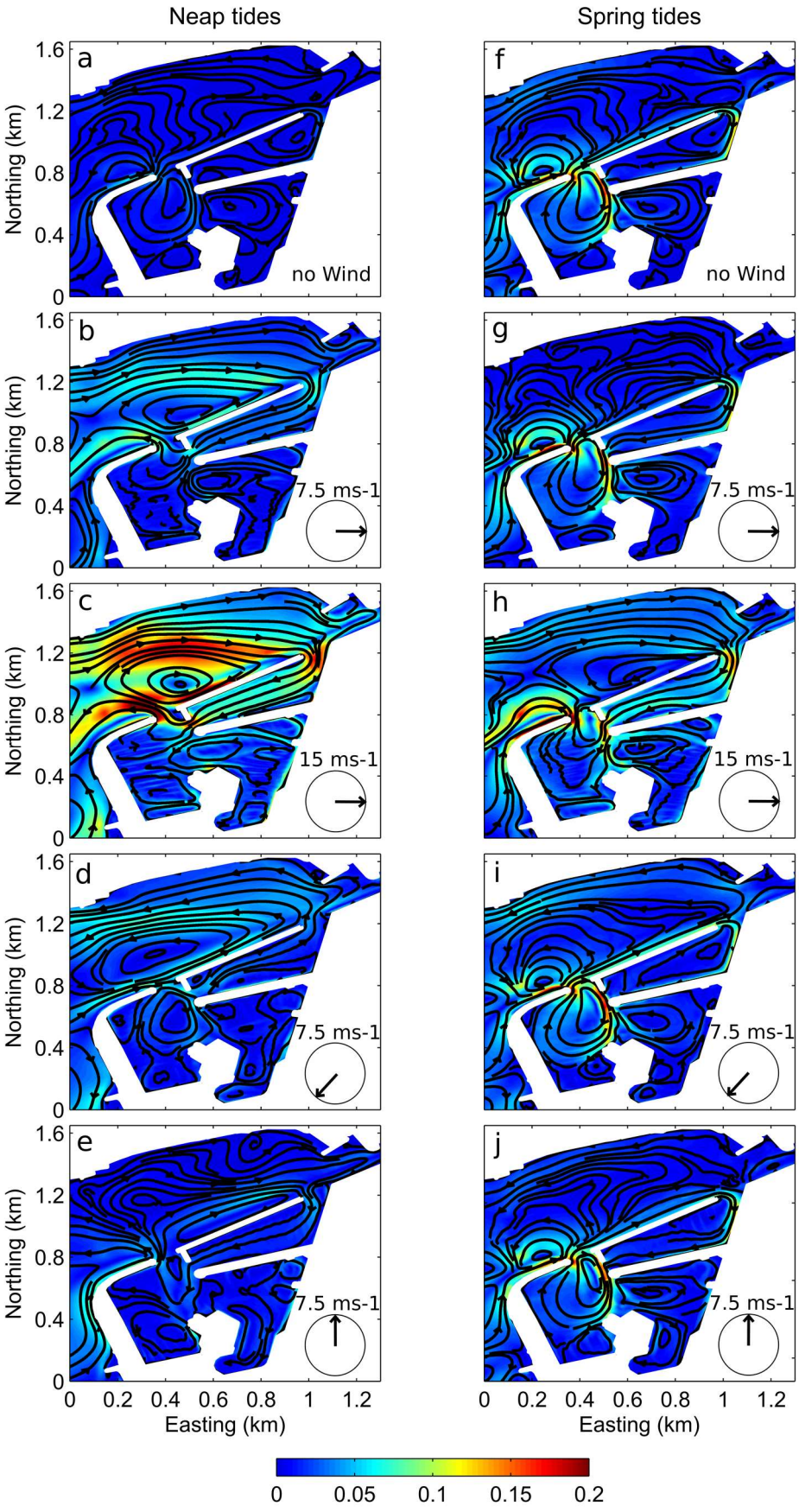

Figure V.7. *Maps of the residual circulation obtained by averaging currents over 6 tidal cycles for each scenario defined in Table V.1.*

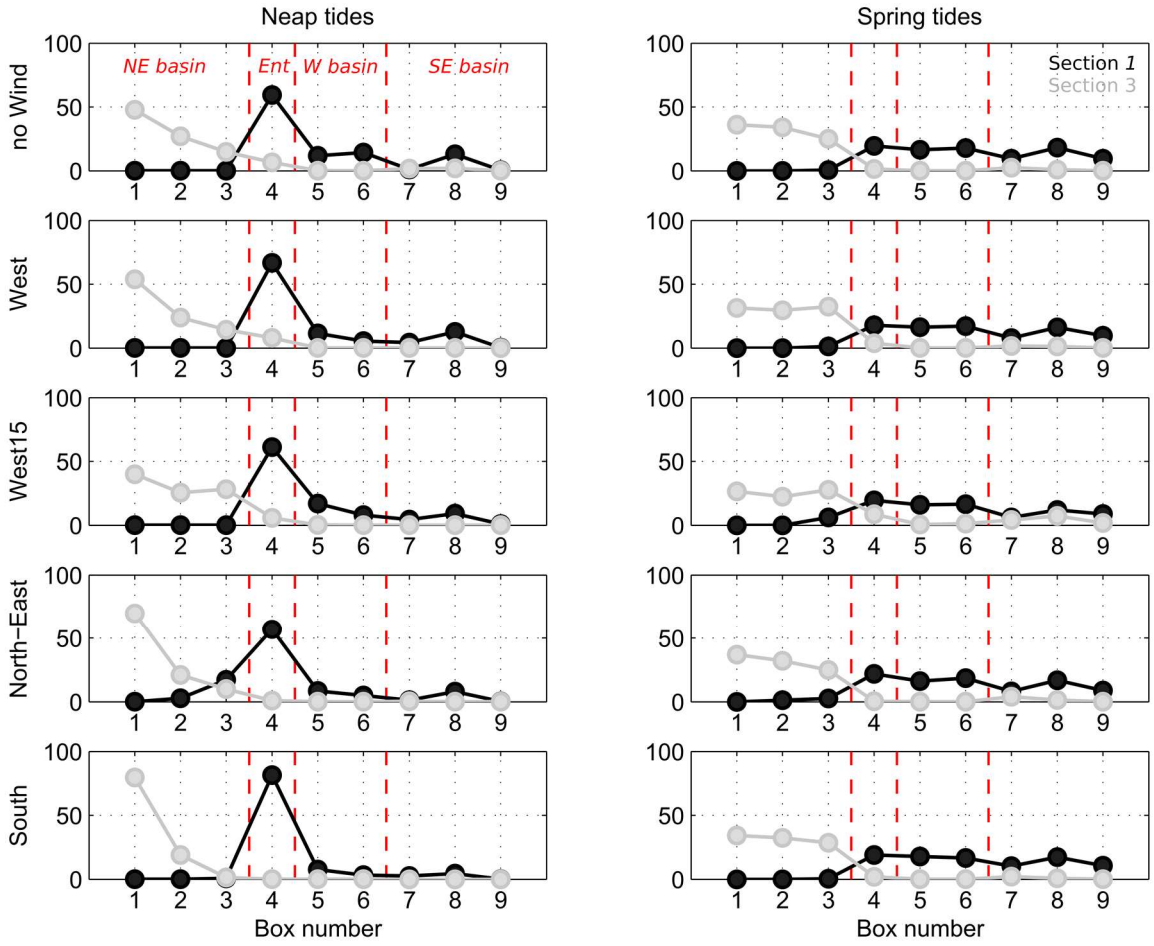

Figure V.8. *Basin/box attraction of tracer (%) computed over one tidal cycle after the release of particles through entrances 1 (black) and 3 (light grey). Rows correspond to the tidal conditions (neap to the left and spring to the right) and lines correspond to wind conditions.*

V.4.3. Influence of the wind in the set-up/down of the sea level

Here, the effect of wind on the sea surface level is analysed to understand the relationship between the wind and the volume transported. Figure V.9 displays the sea level difference (averaged over five tidal cycles) between a situation without wind and other situations with the studied wind forcing. There were very small differences obtained between each extreme tidal condition but as we ignored the dried tidal flats grid cell (coloured in white in Figure V.9), we preferred to display neap tides conditions. As expected, the effect of the wind was found to be anisotropic in the function of its direction. West winds favor set-up (~ + 6 cm for the 7.5 ms^{-1} and +12 to +13 cm for the 15 ms^{-1}), north-east winds favor set-downs (~ - 6 cm), and south wind favors minor step-up (~ +3 cm). Figure V.9 also indicates that the set-up/down is not restricted to the bay but originates from larger scales. These results are however minor compared to the Wadden sea (*Duran-Matute & Gerkema, 2015*), where specific wind conditions can generate 0.7 m set-down, for example. Here, west and north-east winds are more efficient in driving set-up and set-down, respectively, because they are aligned with the bay.

The results are in phase with the residual circulation previously obtained: the north-east wind tends to evacuate water from the bay while the west wind brings it more material. However, north-east wind-induced a residual inflow to the marina while residual outflow dominates under a west wind forcing. It reflects that the departure/arrival of water in the bay are more significant in term of volumes than the exchanges processes leading to the residual transport in the marina. In other words, during west wind activity, the marina tends to discharge excess of water while during north-easterly wind activity it tends to attract water.

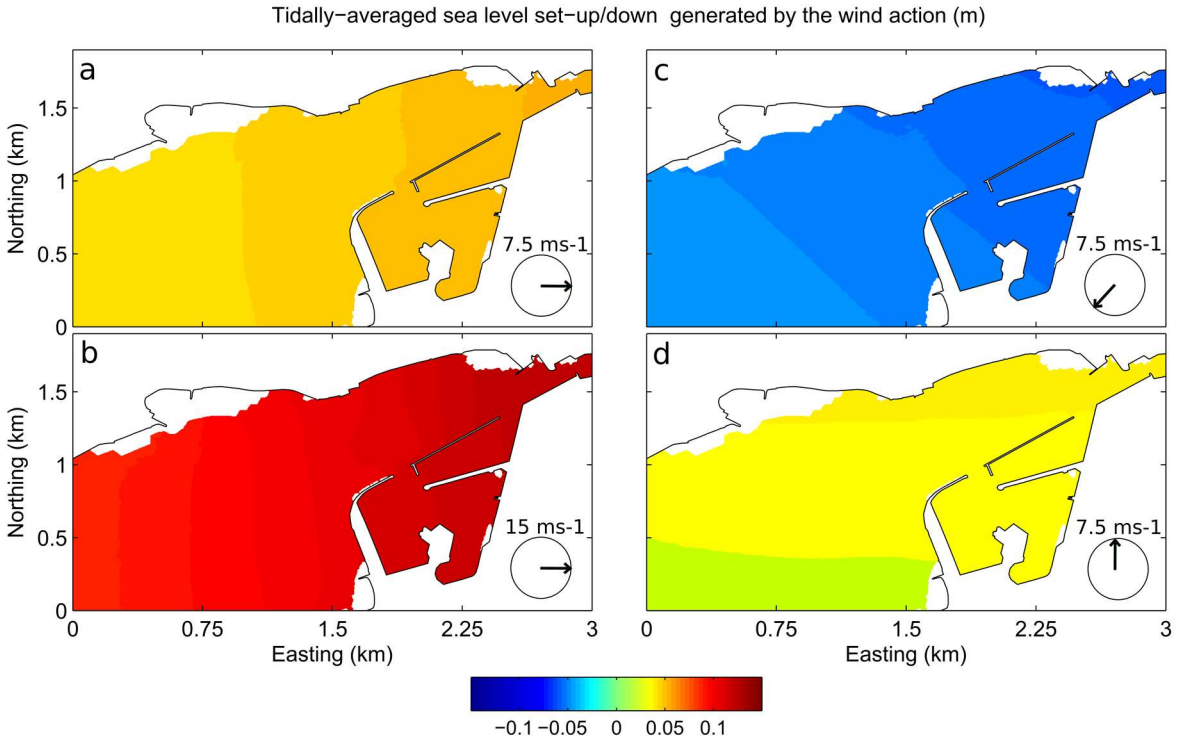

Figure V.9. *Maps of sea surface elevation difference (m) between a situation without wind and a situation: (a) with a 7.5 ms^{-1} west wind, (b) with a 15 ms^{-1} west wind, (c) with a 7.5 ms^{-1} north-east wind and (d) with a 7.5 ms^{-1} south wind. These maps were computed over 6 tidal cycles of neap tides in La Rochelle bay.*

V.6. Discussion and Conclusion

We carried out a thorough analysis of the joint-role of tide and wind on the exchange processes in a large marina with multiple entrances. Before this work, no major studies have investigated in details the exchanges mechanisms in such complex engineered coastal system. Three-dimensional numerical simulations were performed to predict the interactive response of the residual and total circulation of the system to local weather-marine forcing. We combined realistic extreme tidal ranges (neap and spring tides) and stationary winds (7.5 ms^{-1} west, north-east, south wind and 15 ms^{-1} west wind). The study focused as well on the hydrological activity of the different entrances as the spatial circulation in the marina and its adjacent sea. The objectives were twofold: characterising the tidal asymmetry in such a complex system; and studying the influence of the wind with respect to the tidally-driven

circulation. The direct and residual response of the system to these two forcings were analysed about the geometry of the bay-marina system.

Channel entrances of the marina are subjected to asymmetric tidal currents that are an inverse function of the tidal range. During neap tides, the flood currents are shorter but stronger than ebb currents, but these differences are reduced during spring tides. Regardless of the tidal range, the volume flowing through the marina is mainly concentrated in the main navigational entrance (entrance 1) which could be explained by its greater proximity to the sea and greater depth compared to the others entrances. The tidal asymmetry is also expressed through the tidal phase lag existing between the three entrances. The reverse of currents always comes first at the intermediary entrance (entrance 2) and always comes last in the north-eastern entrance (entrance 3) and these temporal variations can overpass 3H during neap tides. The short term and high-resolution study of the marina circulation has shown the role played by the configuration of the marina in the complexity of currents. In contrast to single opening systems, the connectivity between sub-basins increases the non-linearity of the hydrodynamics. The presence of the NE basin particularly complicates the circulation with the presence of two entrances. Its geometry induces an early arrival of the tide to the west (entrance 2) that hinders the intrusion of the tide to the east (entrance 3). Although the presence of two entrances significantly increases water renewal (*Huguet et al., 2019b*), the NE basin configuration restricts exchange processes with the rest of the marina. Tidal current asymmetry in intensity and duration generates an asymmetry of the time-integrated discharge at the entrances. It directly results in a marina-oriented residual transport, mainly focused in entrance 3, both at neap and spring tides.

At the scale of each sub-basins, residual flood-topographic eddies (*Huguet et al., 2019b*) are generated and their intensity varies linearly with the tidal range. Their presence could play a role in the deposition of particles in the inner parts of the marina. The transport and accumulation of sediments directly result from the tidal current asymmetry in tidal basins (*Postma, 1961; Ridderkinhof, 1988a; Ridderkinohf, 1988b; Dronkers, 1986*). Here, theses asymmetries are enhanced by the geometry of the marina, which could also impact the siltation. At a period of increasing maritime transport and leisure activity, it is necessary to study in detail the impact on currents and siltation before expanding, opening, or creating any port area in coastal systems. The tidal asymmetries can also be amplified by the flooding-drying process occurring over the intertidal flats in the bay. This mechanism, discussed in *Lopes & Dias (2007)*, could explain the differences obtained at the scale of a spring-neap cycle. Indeed, there is a significant variability in terms of tidal flats exposure during neap and spring tides. The latter exposes a significant part of the La Rochelle bay and thus, channel currents along the northern edges of the marina, which results in a strong residual activity at their level, in the flood direction (Figure V.7). Finally, while neap and spring tides display different patterns of current intensity and duration, they both generate a global residual inflow mainly focused in the NE basin. In this basin, where the currents are very variable but generally stronger than in the two others basins, the semi-diurnal spring-neap tidal cycle could particularly dictate the erosion-deposition patterns.

The importance of the wind on the total and residual circulation has been demonstrated by many authors in coastal environments (*Proctor & Greig, 1989; Souto et al., 2003; Sankaranarayanan, 2007*). Here, a complete analysis of the residual circulation was necessary to understand the variability of exchange processes through the marina. The computation of

several tidally-related parameters has shown that average winds were sufficient to impact significantly the tidal circulation. During neap tides, average and strong winds can easily improve or reverse the tidally induced residual transport (Figure V.4) and globally dominates the pathways of water in the bay at a subtidal time scale (Figure V.7). During spring tides, only strong west winds can reverse the residual circulation and thus, the residual transport. While the effect of the south wind is relatively weaker, north-east and west wind present strong antagonistic effects. West wind forces a flood-oriented residual flow in the bay that contributes to a global offshore residual transport. To the inverse, north-east wind generates an ebb-direction flow in the bay out that fosters a global marina-oriented residual transport. The geometry of the bay, parallel to these winds, and its connectivity to the marina entrances allowed wind to develop larger-scale circulation between the interconnected part of the marina and the overlying bay. Combined to the physical setup of the system, wind direction substantially alters the flood-ebb asymmetry at the entrances, determining the total and residual transport at the whole scale. In the inner parts of the marina, the wind effect is less visible, which can be explained by the presence of floating structures (*Huguet et al., 2019b*), that significantly reduces current velocities. In the inner parts of the marina, the residual circulation seems to be more driven by the basins topography.

Globally, exchange processes and volumes involved are increased by wind action. In such a shallow bay, the influence of average winds can create large-scale structures that are partly guided by the presence of several entrances in the marina. These large-scale structures can counteract the tidal reverse of currents. The west and north-east winds exert an opposite effect on the total and residual transport through the marina. The study area is subjected to inter-annual variability of the wind regime, which is partly controlled by the North Atlantic Oscillation (*Dodet et al., 2010*). The seasonal variability of the area is also particularly marked during winter where storms, associated with strong west winds, episodically occur while the summer season is marked by weak thermic breezes. Thus, considering the significant influence of average winds in the marina hydrodynamics, both an inter and intra-annual variability is expected in the long-term residual pattern of the system and thus on the transport and accumulation of sediments to the marina. The effect of the strong west wind, associated with storm surges, could lead to a surplus of water circulating within the marina. It is expected to carry more sediment in suspension and thus highly influence the siltation in the marina. The highly-variable residual circulation studied in the paper needs also more attention concerning the questions of sediment budgets and suspended sediment. To understand the mechanisms of siltation in the marina, cross-correlated sediment transport and residual circulation study should be performed. In the present study, wave effect was not investigated, and although it has a small influence on the residual circulation, many authors (*Geyer, 2004; Bolaños et al., 2013; Grifoll et al., 2018*) demonstrated its significant influence on sediment resuspension offshore. It adds another level of freedom in the transport of sediments during storms, and it should be further analysed.

Chapitre VI

Characterisation of the Water Renewal in a Macro-Tidal Marina Using Several Transport Timescales

Jean-Rémy Huguet[1], Isabelle Brenon[2] and Thibault Coulombier[3]

[1] PhD student at UMR 7266 LIENSs, CNRS-La Rochelle Université, 2 rue Olympe de Gouges, 17000 La Rochelle, France (corresponding author). E-mail: jean-remy.huguet@univ-lr.fr
[2] Associate professor at UMR 7266 LIENSs, CNRS- La Rochelle Université, 2 rue Olympe de Gouges, 17000 La Rochelle, France. E-mail: isabelle.brenon@univ-lr.fr
[3] Research engineer at UMR 7266 LIENSs, CNRS- La Rochelle Université, 2 rue Olympe de Gouges, 17000 La Rochelle, France. E-mail: thibault.coulombier@univ-lr.fr

Keywords: Marina; Water renewal; Transport timescales; Return-flow; Macro-tidal; Wind influence; Floating structures;

Ce Chapitre fait l'objet d'une publication dans la revue Water.

Résumé

Dans ce volet nous étudions le renouvellement des masses d'eaux portuaires. Pour décrire de manière synthétique et quantitative le renouvellement d'un système dynamique, il faut faire appel à des descripteurs temporels. Ici, nous avons choisi d'étudier et de comparer le temps de chasse, le temps de résidence mais aussi le temps d'exposition lié aux masses d'eaux portuaires des Minimes, à La Rochelle. Le temps de chasse correspond au ratio de la masse d'un scalaire et de son taux de renouvellement. Il a été calculé à partir de méthodes eulériennes nécessitant la libération puis le transport d'un traceur passif dans le modèle. Le temps de résidence correspond au temps mis par une particule pour sortir d'un système alors que le temps d'exposition tient aussi compte de leur retour dans le système. Nous avons pu les calculer à l'aide de méthodes lagrangiennes nécessitant la libération puis l'étude du déplacement de particules « dissoutes » au sein de la colonne d'eau. Un grand nombre de simulations a été effectué pour pouvoir caractériser ces descripteurs spatialement, et pour obtenir un panel étendu de conditions météorologiques et marines. L'étude comparée des vives-eaux et des mortes eaux mais aussi de l'effet de vents moyens de 7.5 ms^{-1}, de secteur ouest, nort-est et sud ainsi que des vents forts de 15 ms^{-1} a permis d'établir une vision quasi-exhaustive du renouvellement des eaux dans le port.

Le renouvellement des eaux du port présente une forte variabilité spatiale mais il reste relativement homogène sur la verticale, compte tenu des faibles profondeurs d'eau. Les eaux les plus confinées se situent au sud du bassin sud-est tandis que le bassin nord-est subit un renouvellement plus fort principalement dû à la présence de deux ouvertures. La marée et le vent contribuent significativement au renouvellement des eaux mais leurs modes d'action sont différents. La phase et le marnage de la marée sont des éléments importants à prendre en compte ainsi que l'intensité et la direction du vent. Les périodes de mortes-eaux sont des paramètres limitant du renouvellement tandis que la présence du vent l'accélère, en particulier pour les secteurs ouest et sud. L'influence du vent est cependant moins importante dans le port que dans la baie de la Rochelle. Sans vent, la configuration de cette dernière génère un piégeage important des eaux qui est amplifié en mortes-eaux. Les résultats ont montré l'importance de ce piégeage dans la dynamique de renouvellement des eaux du port. Ce piégeage peut rapidement disparaître à la faveur de vents moyens, qui permettent de disperser les eaux soit vers le Pertuis Breton soit au sud du Pertuis d'Antioche.

Enfin, l'impact des structures flottantes sur le renouvellement a été étudié et il a été montré que leur implémentation augmentait le confinement des eaux dans les parties les plus abritées alors que les parties les plus exposées, comme le bassin nord-est, voyait sa dynamique de renouvellement augmenter. Leur effet est toutefois minime à l'échelle de tout le port, en comparaison de la marée et du vent. Une comparaison des différents descripteurs physiques a aussi été entreprise afin de mettre en avant certains processus physiques mais aussi pour valider leur utilisation dans ce type d'environnement. Ce Chapitre constitue l'une des premières contributions en France dans le milieu portuaire. Le développement des outils méthodologiques développés dans ce Chapitre pourrait fournir des indications sur l'impact que pourrait avoir une restructuration du port sur le renouvellement (*e.g.* construction d'une digue, création d'une ouverture, excavation de souilles…). L'utilisation des descripteurs temporels obtenus dans cette étude peut aussi conduire à des diagnostics utiles pour les études interdisciplinaires dont le port des Minimes fait l'objet.

Abstract: In this paper, we investigate the water renewal of a highly populated marina, located in the south-west of France, and subjected to a macro-tidal regime. With the use of a 3D-numerical model (TELEMAC-3D), three water transport timescales were studied and compared to provide a fully detailed description of the physical processes occurring in the marina. Integrated Flushing times (IFT) were computed through a Eulerian way while a Lagrangian method allowed to estimate Residence Times (RT) and Exposure Times (ET). From these timescales, the return-flow (the fraction of water that re-enters the marina at flood after leaving the domain at ebb) was quantified via the Return-flow Factor (RFF) and the Return Coefficient (RC) parameters. The intrinsic information contained in these parameters is thoroughly analysed, and their relevance is discussed. A wide range of weather-marine conditions was tested to provide the most exhaustive information about the processes occurring in the marina. The results highlight the significant influence of the tide and the wind as well as the smaller influence of the Floating Structures (FS) on the renewal. Besides, this study provides the first investigation of the water exchange processes of La Rochelle marina. It offers some content that interest researchers and environmental managers in the monitoring of pollutants as well as biological/ecological applications.

VI.1. Introduction

Over the years, the increasing development of coastal areas has modified the quality of water and sediments as well as marine habitats. Ports, which are the main interfaces between cities and the sea, are primarily subjected to a multi-source of contamination due to intense anthropogenic activities. Their complex geometry and infrastructure (*e.g.* quays, channels, and docks) induce low circulation and stagnant waters which tend to enhance and to control the fate of contaminants. Given the tendency of pollutants to remain confined and settle on the bottom, the pollution generated within the ports is of grave concern. Then, improving water and sediment quality is of vital importance for the sustainable development of coastal waters.

In recent decades, managers have been under increasing pressure to demonstrate the environmental skills of the port they manage. Some studies focused on the effect of diffuse pollution originating from urban water runoffs and boat repair activities (*Ondiviela et al., 2013; Gómez et al., 2017*) as well as accidental oil spills (*Mestres et al., 2010; Grifoll et al., 2010*). Metal concentrations in water and sediments were also monitored and investigated (*Fatoki & Mathabatha, 2001; Bonamano et al., 2017)* but characterising the water quality of such areas is still a challenge as it requires many parameters.

Although ports are considered as low-energy systems, the hydrological pattern established within the port basin cannot be neglected in any study (*Mali et al., 2017*). The rate of renewal of a basin is useful information that provides a first-order description of its dynamics. Numerous transport timescales have been defined through the literature to quantify this renewal (*Bolin & Rodhe, 1973; Takeoka, 1984; Zimmerman, 1988; Monsen et al., 2002; Delhez et al., 2004*). With the growing use of numerical modelling, these water transport timescales are useful parameters to condense the considerable amount of data in intelligible and quantitative information (*Deleersnijder & Delhez, 2007*). The most commonly used, "flushing time", "residence time", "age", and "exposure time" have been applied in a wide range of studies all over the world (*Oliveira & Baptista, 1997; Abdelrhman, 2005; Cucco &*

Umgiesser, 2006; Sánchez-Arcilla et al., 2011). From the environmental port management point of view, these transport timescales offer an interesting indication of the spatial and temporal variability of the dynamic and of the susceptibility to pollution. However, such timescale descriptors need to be carefully employed because there is no real consensus on their application (*Monsen et al., 2002*).

After an expansion in 2014 (corresponding to the NE basin in Figure VI.1), La Rochelle Marina, located in the southwestern part of France, is currently considered as the biggest marina on the European Atlantic coast. Despite the environmental policy and ecological awareness of the marina, equipment and maritime activities may be a source of the pollution (*Breitwieser et al., 2018*). The main objective of this study is, therefore, to characterise the water renewal of La Rochelle Marina due to the horizontal and vertical variability of its currents. This contribution can be considered as a first scientific investigation because, even if the importance of such timescales is evident, no references or estimates were available in the literature for a similar marina.

To describe water renewal mechanisms accurately, we performed a large number of simulations with a 3D hydrodynamic model calibrated and validated in a previous study (*Huguet et al., 2019*b). The specificity of the model is to take into consideration the considerable number of structures floating in the marina (*e.g.* docks, boats). In this study, three timescales are compared (flushing time, residence time and exposure time) to find the most relevant parameter to describe water renewal of the domain. Besides, we estimated the return-flow in different ways, the fraction of water that leaves the marina at ebb tide before re-entering it at the next flood tide (*Sanford et al., 1992*), and its effect on the tidal flushing of the marina was analysed. The above-mentioned timescales and quantities were computed for different scenarios to characterise the influence of wind, tide and floating structures on the water renewal. In the next section, study site and numerical computations will be presented before introducing definitions and concepts of chosen timescales and quantities. In Section 3, a Lagrangian validation is carried out while timescale results are shown in Section 4 and discussed in Section 5.

VI.2. Materials and Methods

VI.2.1. Study Site

VI.2.1.1. La Rochelle Marina

The city of La Rochelle, the provincial administrative center of the department, has a land area of 28.43 km^2 and a population of 80 000 inhabitants. Its marina, created in 1972, has been the biggest marina (50 ha) along the Atlantic coast, since its expansion in 2014. This 900 m long and 820 m wide semi-enclosed area is divided in three basins totalling 4500 moorings, distributed along 15 km of floating docks. The southeastern (SE) basin is the more prominent, with 22 ha, while the western (W) and the northeastern (NE) basin, present respectively 17 and 15 ha. At sea, the marina is accessible by a 110 m wide main entrance, while the NE basin offers two openings: 150 m wide to the northeast and a 64 m wide to the southwest which connects the NE basin to the W basin (Figure VI.1). The marina is not spared by siltation and

has to spend 10 per cent of its total budget to dredge around 200 000 m^3 of cohesive sediment each year. The annual sediment deposition can overpass 50 *cm* in some of its basins, which requires recurring dredging of the basins, 8 months a year.

The environmental policy of the marina led to an ISO 14001 certification, an international reference in sustainable development. Despite their effort, water quality and marine biodiversity are still impacted by intensive anthropogenic inputs. Several potential sources of contamination have been identified in the marina (symbolised in Figure VI.1): the rainwater outlet, where runoff waters from streets and roadways can flow abundantly during storm events; the fairing area where boats are maintained (antifouled, painted and sanded); the fuel station where dripping fuel can be discharged. We can also consider diffuse pollution from boat activities.

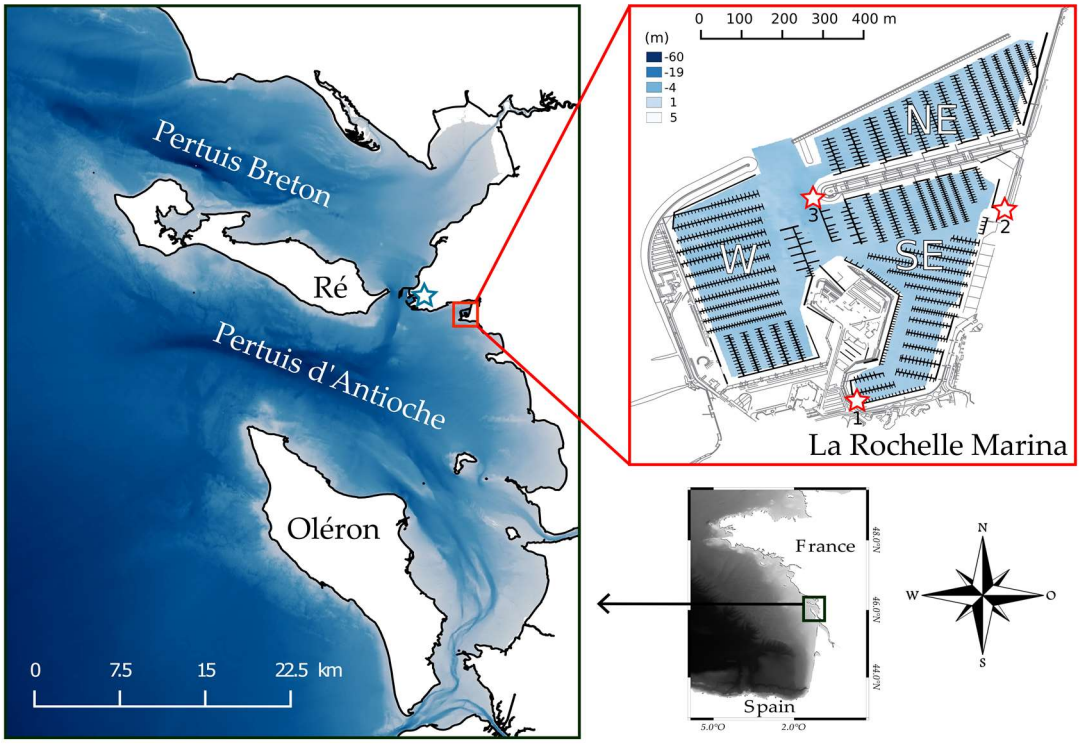

Figure VI.1. *Bathymetry/topography map of the modelling domain (left) and the La Rochelle marina (right). Depths are given with respect to mean-sea-level, and the straight, bold black line indicates the shoreline in the left figure while La Pallice weather station is symbolised by a blue-bordered white star. At right, the floating docks are signified by a black line, and the maritime infrastructures are indicated by a grey line. The red-bordered white stars numbered 1, 2, and 3, represent the location of the rainwater outlet, the fairing area, and the fuel station, respectively. Western, southeastern and northeastern basins are denoted by white characters W, SE and NE, respectively.*

VI.2.1.2. Geomorphology and Hydrodynamics of the Coastal Area

La Rochelle Marina is located in the northern landward part of the Pertuis d'Antioche embayment along the French Atlantic Coast, in the central part of the Bay of Biscay. This shallow water coastal area is protected from the Atlantic Ocean by Ré and Oléron islands and connected to the Pertuis Breton embayment through a narrow inlet. The bathymetry is characterised by silty to sandy-silty bottoms, with a 44 m deep trench and many tidal flats.

The coastal area is considered as a mixed, wave and tide-dominated estuary (*Chaumillon & Weber, 2006*). The tidal regime is semidiurnal and tidal range varies from 2 m during neap tides to more than 6 m during spring tides. This macro-tidal environment is dominated by M2, and its amplitude grows to more than 1.8 m in the inner part of the estuaries due to resonance and shoaling (*Bertin et al., 2012*). Because of resonance occurring on the Bay of Biscay shelf, the quarter-diurnal tidal constituents (M4, MS4 and MN4) are strongly amplified shoreward (*Le Cann, 1990).* In the embayments, average freshwater inflows are about 2 orders of magnitude less than tidal flows (*Bertin, 2005*).

VI.2.1.3. Meteorological Context

The study area is subjected to seasonal climate variations. Summer presents a weak low-pressure system activity resulting in weak northeasterly winds while northwest thermic breezes mainly dominate littoral. Low-pressure systems that cross the Atlantic Ocean from autumn are the most active during winter, generating extreme west and northwest winds. North Atlantic Oscillation (NAO) partly controls the inter-annual variability of the wind regime in the whole Bay of Biscay (*Dodet et al., 2010*). Weather-marine conditions were collected by La Pallice weather station (blue-bordered white star in Figure VI.1) over the temporal interval 2015–2018 (Figure VI.2). Data analysis reveals a predominance of four winds over the area of study: north-western (22 % mean yearly occurrence), western (21 % mean yearly occurrence), north-eastern (19 % mean yearly occurrence) and southern (14 % mean yearly occurrence).

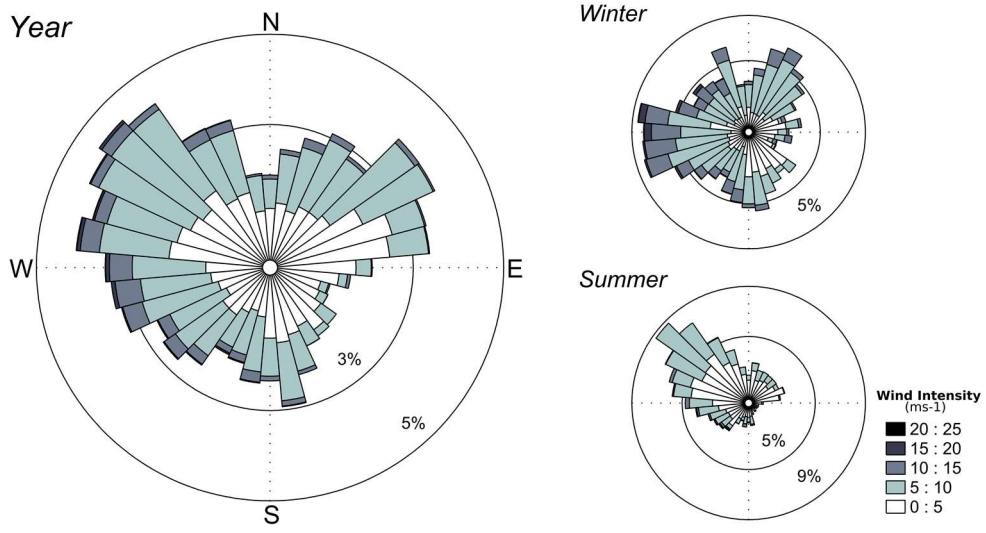

Figure VI.2. *The wind regime in La Pallice station over the period 2015–2018. Winter and summer periods are also distinguished to characterise their variability in terms of direction and intensity. The legend box at right indicates the intensity of wind velocity in* ms^{-1}.

VI.2.2. Numerical Model Implementation

To calculate water transport timescales, we used the TELEMAC-3D model (*Hervouet, 2007*), a three-dimensional hydrodynamic model adapted to free-surface flow. In this study, three-dimensional Navier-Stokes equations were solved in non-hydrostatic mode. Bottom stress was computed through a Chézy parametrisation over an unstructured grid. The semi-implicit Galerkin finite element method is used to solve continuity and momentum equations and a Lagrangian-Eulerian treatment of advective terms and a semi-implicit way ensure numerical stability. More insight and details about the equations are presented *in Huguet et al.*

(2019b). TELEMAC-3D provides the possibility of taking into account passive tracers in the model domain. The model solves the advection and diffusion equation of a conservative tracer.

The modelled area is 35 km wide and 100 km long and is discretised on a 41 000 nodes unstructured grid, with resolution from 2 km offshore to nearly 5 m in the marina (*Huguet et al., 2019b*). The size of the computational domain (4757.9 km^2) is considered sufficiently large so that the prescribed boundary conditions negligibly affect the tracer mass in the marina (0.5 km^2) as requested by (*Viero & Defina, 2016*). The model has eight vertical sigma levels, which are treated with the Arbitrary Lagrangian-Eulerian method (*Donea, 1982*) and lead to a total of 320,000 nodes. Our bathymetry originates from French Navy (*SHOM, 2015*) and single beam surveys acquired in the marina. Then, the topography of intertidal areas is determined using a LiDAR survey, acquired in 2010 (LITTO3D, French National Geographic Institute and SHOM). Along its open boundary, the model is forced by 34 astronomical tidal constituents obtained by linear interpolation from the global tide model FES2014 (*AVISO, 2014*). Atmospheric forcing is set over the whole domain with hourly sea-level atmospheric pressure and 10 m wind speed and direction originating from the Climate Forecast System Reanalysis (CFSR) provided by the National Center for Environmental Prediction (NCEP). All the simulations used a time step set to 5 s after sensitivity analysis. Wave effects are not simulated because the marina is considered sufficiently sheltered from ocean waves. Water fluxes across the sea surface (precipitation-evaporation) and rivers input are also neglected. Floating docks and moorings that occupy more than a third of the marina surface were implemented in the model by adding head losses at the surface. Their implementation and their effect on circulation are presented in *Huguet et al. (2019b)* as well as validation results in terms of currents and water levels.

VI.2.3. Water Transport Timescales

Flow exchanges between inner water and the open sea control the water quality of the domain. Numerous transport timescales have been tested to assess water renewal in semi-enclosed areas. This study focuses on three transport timescales: flushing, residence, and exposure time. They provide different space and time-dependent quantitative measures of the water renewal. They can help to determine water mass dynamics in aquatic systems and its influence on both geochemical and biological processes. Their definitions and numerical computation are explained in this section.

VI.2.3.1. Flushing Time

Flushing time characterises the general exchange characteristics of the waterbody and has been described as the ratio of the mass of a scalar in a semi-enclosed domain to the rate of renewal of the scalar (*Monsen et al., 2002*). It reflects the mean time spent by any pollutant discharged in the marina and measures the effectiveness of flushing to remove any pollutant from the water body of the marina. Here, FT calculation is based on the study of the evolution of a conservative tracer initially introduced at several locations in La Rochelle Marina. Flushing time was primarily defined as the time required to reduce the mass of the conservative tracer to 37 % (e^{-1}) of its initial value in the water body (*Choi & Lee, 2004; Plus et al., 2009; Grifoll et al., 2013*). This parameter was sometimes referred to as "e-folding flushing time" (*Monsen et al., 2002; Wang et al., 2004*). In this study, we used 37 % as a percentage reference, but it should be noted that it varies according to the authors (*e.g.* 2 % in *Andrejev et*

al., 2004 and 50 % in *Fugate et al., 2006*). Computation of flushing time is based on the assumption that the marina behaves as a continuously stirred tank reactor (CSTR). The main assumption for a CSTR is that any introduction of mass is wholly mixed throughout the domain, so the concentration of a constituent exiting the system is equal to the concentration everywhere inside the CSTR (*Thomann and Mueller, 1987; Monsen et al., 2002*). Assuming that a known quantity of conservative tracer has been introduced only at t = 0 and that the water entering the marina can mix totally with the existent water of the marina, the total mass of the tracer is:

$$M(t) = M_0 e^{-t/FT} \quad \text{(VI.1)}$$

$M(t)$ is the mass of conservative tracer that remains in the marina, M_0 the initial mass of conservative tracer introduced in the marina and t the time since the tracer has been discharged from a specific location. To spatially determine the flushing time of the marina, we computed the Integrated Flushing Time (hereafter *IFT*) at several locations of the marina. This timescale, defined by *Plus et al. (2009)* is the time for the mean mass of the tracer over the whole marina to fall below 37 % of the initial mass discharged at a specific location in the marina. *IM* and IM_0correspond to the spatial integration of the tracer mass over the entire domain, under stable conditions. By releasing tracer at a hundred source points evenly distributed in the marina domain, we obtained spatially-varying *IFT*. Building on Equation (VI.1), for the same previous assumptions, *IFT* was computed through the following equation:

$$IM(t) = IM_0 e^{-t/IFT} \quad \text{(VI.2)}$$

where *IM*(t) is the mass of conservative tracer over the whole marina for a release at a specific location, IM_0 the initial mass of conservative tracer released at a specific location. The use of a 3D-model has permitted to compute *IFT* at each layer of the water column.

VI.2.3.2. Residence and Exposure time

Residence time (hereafter RT) is a fundamental concept defined as the time until a water parcel, or particle at a specified location within the water body, leaves the system (*Bolin and Rodhe, 1973; Zimmerman, 1976; Dronkers & Zimmerman, 1982*). Similarly to the Lagrangian Water Transport Time (or Water Transit Time) defined by (*Cucco & Umgiesser, 2009*), RT is a property of the water parcel that is carried in and out of the marina by the hydrodynamic processes. A vast number of particles is necessary to capture the diffusive processes generated by the small-scale turbulence (*Spivakovskaya et al., 2007; Delhez et al., 2014*). For the computation of RT, 400 particles were released at arbitrary locations, and each particle was representative of a 1000 m^2 area. Then, the RT was computed for each particle, from their release to the first time they reached the boundaries (symbolised by the two main entrances of the marina). No random walk diffusion was implemented in the particle tracking method which will give us an interesting comparison axis with the IFT.

Previous residence time studies underestimated the total time that particles spend in the domain because of the possibility for the particles to re-enter the domain (*Monsen et al., 2002; Wolanski & Elliott, 2015*). This conceptual drawback of residence time timescale led to unrealistic timescales in tidal systems where water parcels can leave and re-enter the domain many times, especially close to the boundaries. *Monsen et al. (2002)* then introduced the concept of exposure time to take into account returning water parcels or particles. By computing the total time that a particle spends in the domain, exposure time offers an interesting alternative

to residence time and is particularly suited for macro-tidal seas. The two timescales are very similar in terms of region of interest and numerical computation, but exposure time requires additional assumptions and post-processing treatment. Indeed, the latter dwells on the hydrodynamic processes that occur not only within but also outside the marina. The computational domain must be much larger than the domain of interest, and the open boundaries need to be located far enough from the area of interest (*Brauwere et al., 2011; Delhez, 2013; Andutta et al., 2013*). For this study, we supposed that both open boundaries and model domain extension have a negligible influence on the computed exposure times. Then, we defined Exposure Time (hereafter ET) to get a spatial distribution of exposure time for each particle. While the RT was computed by detecting the first departure of the particles from the marina, we computed ET by considering the total time spent by the particles inside the marina before their last departure.

VI.2.3.3. Estimation of the Return-Flow

Comparing Residence Time (RT) and Exposure Time (ET) provides information about the contribution of returning water at each tidal cycle. For the same numerical computation, RT equal to ET indicates that the fraction of water flowing out of the domain during ebb tide is totally lost into the open sea, and does not return into the domain on the next flood tide. Conversely, ET much higher than RT indicates that a significant fraction of water that flowed out the area during ebb tide has returned into the area on the next flood tide. This fraction of effluent water that returns to the domain is called "Return-flow Factor (RFF)". It represents the fate of the water once it is outside the domain, and was introduced by *Sanford et al. (1992)* to figure the movements of water parcels in semi-enclosed areas where the tide is significant. The RFF depends on the phase and strength difference between the flow along the coast and the flow in the connecting channel, and the mixing that occurs between open seas and water masses flowing out of the domain (*Sanford et al., 1992*).

The timescales mentioned above can help us to compute RFF with different approaches. RFF was firstly introduced via the tidal prism method, which is a classical approach to easily estimate flushing time in tidal systems. This method is appropriate to small and well-mixed embayments with low river inputs compared to tidal flows, and sufficiently large enough receiving water to dilute water exiting the system (*Sanford et al., 1992; Oliveira & Baptista, 1997; Monsen et al., 2002*). The flushing time T_f is then given by:

$$T_f = \frac{TV}{(1-b)P} \tag{VI.3}$$

where T is the average tidal period, V the basin volume, P the intertidal volume and b, that lies in the interval [0, 1], represents the return-flow factor via the expression:

$$b = 1 - \frac{TV}{PT_f} \tag{VI.4}$$

If $b = 0$, no water, previously ejected, returns into the embayment and the situation $b = 1$ corresponds to a situation where all water returns to the embayment. Knowing the average flushing time of the marina (FT_{av}) thanks to the tracer simulations described in Section 2.3.1, the average return-flow factor b can be obtained with:

$$RFF = 1 - \frac{TV}{FT_{av}P} \quad \text{(VI.5)}$$

The return-flow can also be described through the concept of return coefficient developed by *Brauwere et al. (2011)*. It represents the relative difference between exposure time and residence time and is equal to:

$$r = \frac{E - R}{E} \quad \text{(VI.6)}$$

With E the exposure time and R the residence time. The coefficient r also lies in the interval [0, 1], and the first limit (r = 0) corresponds to a situation where the exposure time is equal to residence time, while r = 1 is reached when the exposure time is much higher than the residence time of the domain. The Lagrangian Particle Tracking methodology developed in Section 2.3.2 permits to compute average residence (RT_{av}) and exposure times (ET_{av}) of the marina which transforms Equation (VI.6) in:

$$RC = \frac{ET_{av} - RT_{av}}{ET_{av}} \quad \text{(VI.7)}$$

These two expressions of the return-flow factor were computed for each scenario described in the next section.

VI.2.4. General Simulation Set Up

Several simulations were carried out to calculate water transport timescales over La Rochelle marina, under meteorological and tidal forcing. Every scenario tested and analysed during this study are resumed in Table VI.1. The theoretical steady winds applied on the model domain correspond to the prevailing winds of the area: west, north-east, and south winds. Model results with north-west winds are not presented here because they are similar to model results with westerly winds. Five atmospheric conditions were tested: one without wind, three with an averaged 7.5 ms^{-1} wind from several directions and one 15 ms^{-1} west wind, typical of winter events (Table VI.1).

Table VI.1. *Summary of the scenarios tested and analysed in the study.*

Conditions		**Scenarios**											
		a	c	e	g	i	k	b	d	f	h	j	l
Tides	Neap	●	●	●	●	●	●						
	Spring							●	●	●	●	●	●
Wind	West 7.5 ms^{-1}			●						●			
	North-East 7.5 ms^{-1}				●						●		
	South 7.5 ms^{-1}					●						●	
	West 15 ms^{-1}						●						●
With floating structures (FS)			●	●	●	●	●		●	●	●	●	●

Every simulation was computed for both spring tides (tidal range about ±6 m) and neap tide conditions (tidal range about ± 2 m). The tidal conditions correspond to periods from 17th March 2017 to 3rd April 2017. Furthermore, to analyse the influence of floating structures (hereafter FS) on the marina hydrodynamics, simulations without FS were investigated with

the tide only. Considering that the tidal phase at the moment of release is considered as one of the main factors influencing water transport timescales (*Cucco et al., 2009*), four releases were implemented for each simulation: at low tide, rising tide, high tide and ebb tide. As TELEMAC-3D offers the possibility to release passive Eulerian tracer and Lagrangian particles in the same simulation, it led to a total of 48 simulations. The duration of each simulation was 10 days, with 1 spin-up day. The hypothesised scenarios tested do not reproduce the real situation, but they provide an overview of the typical hydrodynamic processes that affect the water renewal in La Rochelle Marina.

VI.3. Lagrangian Validation

In a previous study (*Huguet et al., 2019b*), the validation of the model was done in term of water levels and currents intensity, at numerous locations, inside and outside the marina. Here, the simulated velocities and trajectories of particles are compared with the observational data collected by the drifting buoys. The analysis offered in this section gives a spatially continuous distribution of model skill in the upper layer of La Rochelle bay and marina entrance. The Lagrangian time series of surface velocity allow evaluating the performance of the model to reproduce dispersion trends of surface waters, which differs from the Eulerian assessment commonly used in validation methodology.

In the framework of the study, several drifting buoys were released for a wide range of temporal and spatial scales. The drifters, manufactured by Pacific Gyres (Oceanside, CA, USA), are composed of a surface float with a diameter of 0.3 m and a drogue dimension of 1.2 m length. The buoy uses Iridium to send float positions with 5-min temporal resolution. First experiments involved their deployment at the marina entrance with less than 1-h transport while the following occurred more offshore for timescales reaching more than one day. The range of hydrodynamics and atmospheric conditions tested, and the settings of the experiments were resumed in Table VI.2 while the mean trajectories of each drifting buoy experiment were resumed in Figure VI.3a. Because of maritime infrastructure and boat navigation, more release of drifting buoys was needed to track sufficient currents patterns inside the marina.

Table VI.2. *The drifting buoys deployments and their corresponding settings.*

Deployment Date	Number of Drifters per Release	Number of Releases	Location	Duration	Weather-Marine Conditions
9 May 2017	3	5	46°08′54.1″ N 1°10′08.0″ W	Over one flood tide	Spring tides with strong south winds
17 May 2017	3	5	46°08′54.1″ N 1°10′08.0″ W	Over one flood tide	Neap tides with calm weather
14 June 2017	5	1	46°08′16.2″ N 1°10′46.4″ W	One ebb tide	Neap tides with calm weather
26 June 2017	5	1	46°08′15.8″ N 1°10′46.6″ W	One ebb tide	Spring tides with calm weather
15 January 2019	3	1	46°08′39.2″ N 1°10′52.7″ W	24 h	Neap tides with mixed winds

To facilitate the comparison, the real-time positions of the drifting buoys were averaged for each release while the positions of 10 simulated drifters were averaged for each corresponding release. Comparison is visible in Figure VI.3 and shows fair agreement between the observed and simulated circulation of the drifters. While the distance between simulated and observed drifters can reach 600 m after one day of release, the comparison indicates a good correlation in term of velocities and a 6 cms^{-1} Root-Mean-Squared-Discrepancy (hereafter *RMSE*). The meridional (V) and zonal (U) components of velocity also display a fair agreement but with less accuracy and consistency (Table VI.3). Globally, drifter buoy trajectories are better reproduced in the bay than in the marina, in particular during calm weather conditions where *RMSE* reaches 0.01 ms^{-1}. The tide in the bay rapidly and homogeneously advected drifter buoys while complex currents and micro-scale structures at the western marina entrance caused the buoys to diverge from each other. The model is less effective at reproducing the currents at the marina entrance, but the *RMSE* and R^2 results show a good reproducibility in particular concerning the meridional component of the velocity (Table VI.3). First and last deployments are characterised by stronger winds and the presence of waves in the bay. As the waves and their effects (Stokes drifts, interaction wave-currents) are not implemented in this modelling study, the quality of predictions of the model is slightly decreased (Table VI.3).

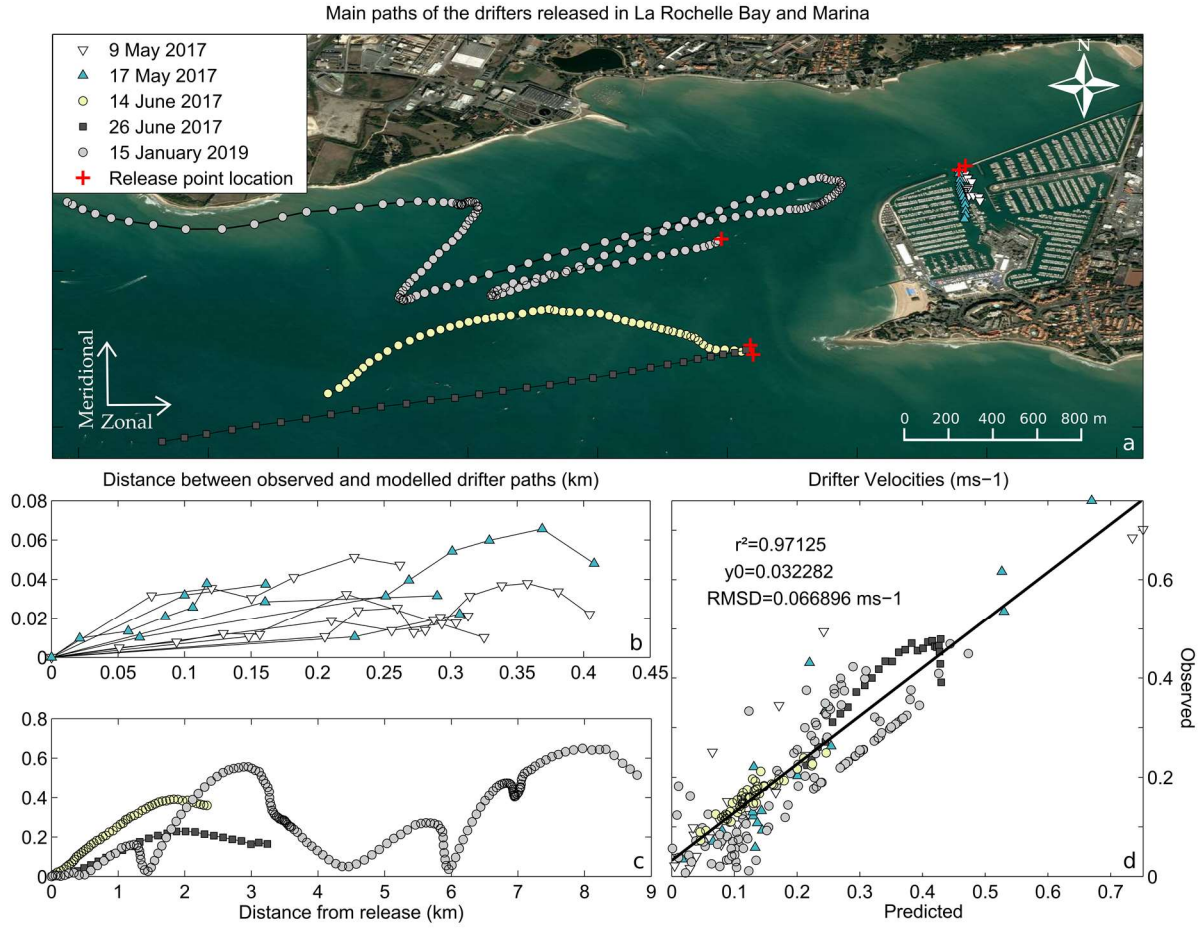

Figure VI.3. *(a) The mean paths of drifters released in La Rochelle bay and marina entrance; (b) and (c) The distance between observed and modelled drifter paths is displayed for every deployment; (d) Correlation of predicted-observed velocities (in* ms^{-1}*).*

Table VI.3. *Statistical analysis between the observed and predicted circulation of drifters. RMSE and linear regression analysis R^2 were computed for zonal (U) and meridional (V) components of the velocity.*

Deployment Date	$RMSE\ (ms^{-1})$		R^2	
	U	V	U	V
9 May 2017	0.19	0.15	0.69	0.75
17 May 2017	0.17	0.14	0.71	0.82
14 June 2017	0.01	0.04	0.91	0.80
26 June 2017	0.04	0.06	0.88	0.69
15 January 2019	0.11	0.17	0.76	0.72

VI.4. Results

VI.4.1. Integrated Flushing Time

Figure VI.4 shows the spatial distribution of vertically-averaged Integrated Flushing Time (IFT) within La Rochelle marina for two configurations (with and without Floating Structures (FS)) associated with several combinations of wind and tide. While the first scenario considers only the tide without FS, scenarios with the wind were computed with the FS. To quantify differences between each case, we also averaged IFT (spatially and across the tidal phases) and estimated the standard deviation of its spatial variability (Spatial Standard Deviation, hereafter SSD) over the marina. We computed the standard deviation of IFT between each release (corresponding to different phases of the tide) and named it Tidal Phase Standard Deviation (hereafter TPSD).

Figure VI.4 displays the spatial distribution of IFT while statistical results are visible in Table VI.4. Spatially, the NE basin generally presents the lower values while the SE basin generally displays the higher values and the higher variability of IFT. IFT generally increases from the entrances to the most sheltered areas and in particular the southern part of the SE basin. The neap tide conditions exhibit 2 to 4 times larger IFT and SSD than spring tides (Figure VI.4, Table VI.4). The presence of FS increases IFT in the southern part of the SE basin during spring tides (Figures VI.4b–4d), while it decreases IFT in the NE basin during neap tides (Figures VI.4a–4c). While their presence slightly increases the mean IFT (23.6/22.5 h at spring tides and 89.3/88.9 h at neap tides), it considerably increases SSD during spring tides (11.1/6.2 h) and neap tides (30.2/22.7 h) (Table VI.4).

The wind significantly reduces IFT and SSD (on average 2 to 3 times lower) compared with situations with tide only (Figures VI.4c-4d), in particular for the west and south directions. Although all wind cases decrease IFT in all basins relative to the tide-only case, the IFT patterns and directionality of IFT gradients vary with wind direction. For example, on neap tides the highest IFT tends to be in the southern part of the SE basin for north-east wind (Figure VI.4g); in the northern part of the SE basin for south wind (Figure VI.4i); and in the southern parts of the W and SE basins for west wind (Figure VI.4e). West wind is the most impacting on neap tides, and its effect increases with its magnitude. TPSD is significantly lower than SSD and is decreased by wind action and also by the presence of floating structures (Table VI.4). Here, we only present vertically-averaged results because the surface and bottom

layers were shown to be comparable in terms of IFT (data not shown), at the scale of the marina. The relative homogeneity of the water column was found to be slightly affected by the wind.

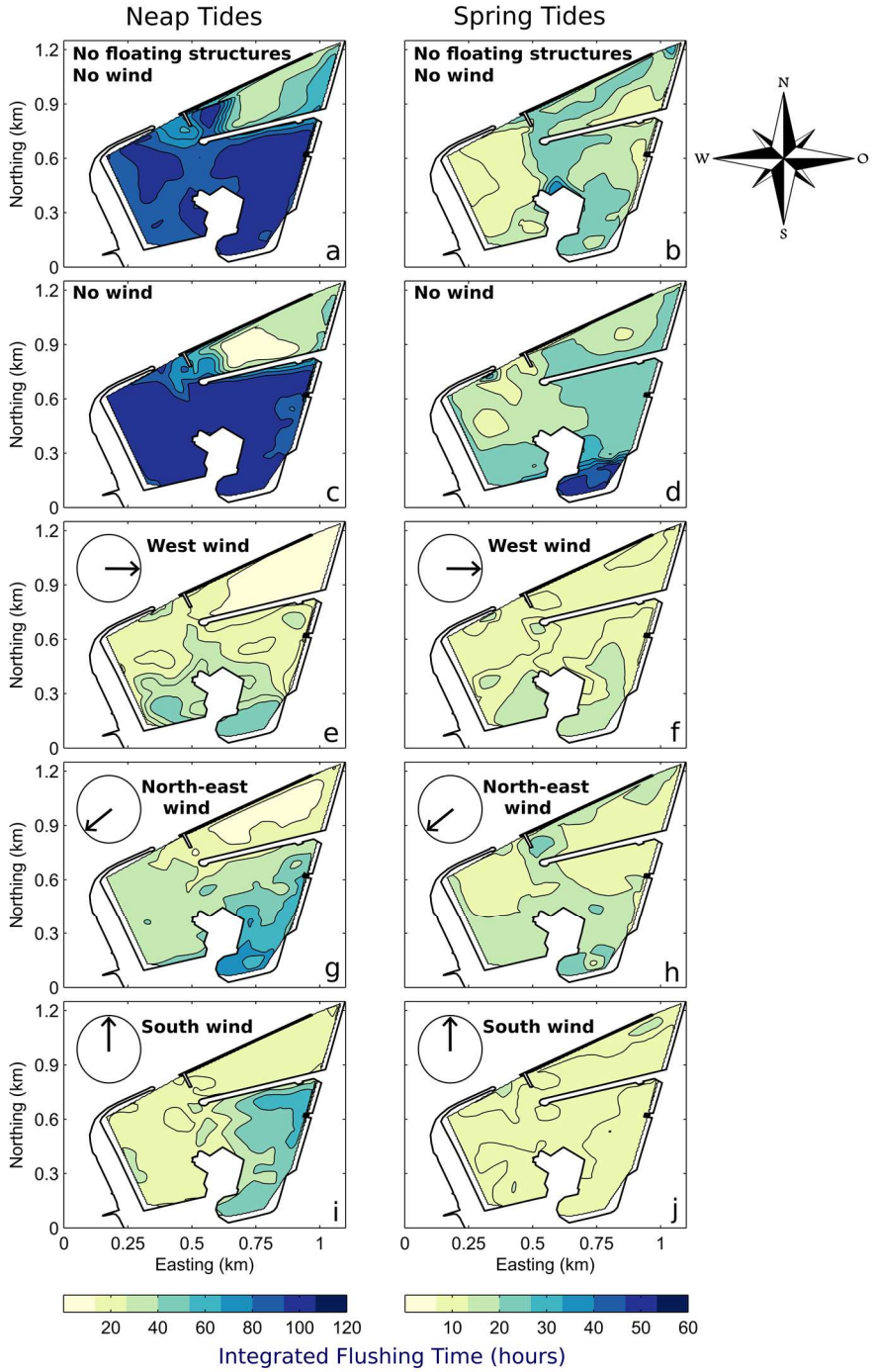

Figure VI.4. *Spatial distribution of vertically-averaged Integrated Flushing Time (expressed in hours) within the La Rochelle marina computed for the scenario (letters) defined in Table VI.1. Rows characterise the wind, and FS configurations and columns correspond to the tidal regime.*

VI.4.2. Residence Time

The vertically-averaged Residence Time (RT) of particles within La Rochelle marina is visible in Figure VI.5 for the same combinations of tide and wind than Figure VI.4. IFT and RT

share many similarities, but they are quantitatively different. Mean RT is up to 3 times lower than IFT, especially for neap tides, but its spatial variability (SSD) is significantly higher. According to Table VI.4, the presence of FS increases the RT (15.4/13.3 h at spring tides and 37/31.1 h at neap tides) and almost doubles SSD (20.6/12.7 h at spring tides and 42.9 h/28.3 h at neap tides). The wind has less influence on RT than on IFT and mainly reorganises RT spatially (Figure VI.5e–5j), without substantially affecting the mean RT (Table VI.4). West and south winds stay the most impacting winds during neap and spring tides, respectively (Table VI.4). On neap tides, the lowest residence times are reached with intense 15 ms^{-1} west wind while on spring tides this wind configuration slightly enhances residences times compared with a 7.5 ms^{-1} west wind.

Table VI.4. *Mean, Spatial Standard Deviation (SSD) and Tidal Phase Standard Deviation (TPSD) calculated for IFT, RT, ET, RFF and RC for the weather-marine scenarios (letters) defined in Table VI.1. Statistics results are in hours for IFT, RT and ET and without units for RFF and RC.*

Parameters		Weather–Marine Scenarios											
		Neap Tides						Spring Tides					
		a	c	e	g	i	k	b	d	f	h	j	l
IFT	Mean	88.9	89.3	27.3	43.6	35.4	25.6	22.5	23.6	13.5	19.4	12.5	10.1
	SSD	22.7	30.2	12.1	19.1	13.5	13	6.2	11.1	3.7	4.9	3.1	5.6
	TPSD	6.8	4.3	3.6	1.6	3.9	3.3	4.2	3.7	2.8	2.6	2	2.9
RT	Mean	31.1	37	24.9	33.9	26.4	23.9	13.3	15.4	9.3	10.3	8.1	9.6
	SSD	28.3	42.9	26.8	31.2	26.7	27.9	12.7	20.6	7.5	10.6	5.1	15.4
	TPSD	4.6	7.1	3.1	2.5	4.1	3.8	4.3	5.3	3.6	1.6	2.5	2.8
ET	Mean	124.1	129.3	35.5	69.9	41.3	27.5	34.5	34.8	19.3	19.5	14.2	11.8
	SSD	24.1	25.7	27.2	36.2	27.7	27.6	17.4	21.2	14.9	13.1	9.1	16.7
	TPSD	5	6.4	3.4	1.3	6.4	6	6.1	8	3.9	0.3	2.3	5.1
RFF	Mean	0.72	0.73	0.12	0.45	0.32	0.06	0.64	0.66	0.41	0.59	0.36	0.19
	SSD	0.02	0.01	0.11	0.02	0.08	0.10	0.07	0.05	0.11	0.10	0.10	0.11
	TPSD	0.05	0.03	0.03	0.01	0.01	0.01	0.04	0.03	0.01	0.01	0.02	0.02
RC	Mean	0.75	0.73	0.19	0.51	0.36	0.09	0.61	0.56	0.47	0.50	0.43	0.08
	SSD	0.03	0.04	0.05	0.04	0.05	0.11	0.09	0.06	0.13	0.06	0.08	0.1
	TPSD	0.06	0.07	0.04	0.03	0.01	0.01	0.06	0.05	0.02	0.01	0.03	0.03

VI.4.3. Exposure Time

The last timescale studied is ET and represents the total time that particles spend in the domain. Its computation was derived from the release of particles used to characterise RT. ET is necessarily equal to or greater than RT and is not only a function of hydrodynamic processes within the marina but also of the return-flow. Figure VI.6 presents the spatial distribution of the vertically-averaged exposure times computed and the statistics results related are visible in Table VI.4. Their behaviour share, though, some similarities with the pattern of RT and IFT but globally their magnitudes display larger values. Mean ET can significantly increase during neap tides, by doubling or almost quadrupling compared with spring tides (Table VI.4).

Similarly to IFT, the presence of FS does not increase significantly ET (34.8/34.5 h at spring tides and 129.3/124.1 h at neap tides). The wind has a more significant effect on exposure times than on residence times, and its impact is comparable for the behaviour of flushing times. It decreases ET by 2 to almost 5, particularly during neap tides with west winds (Table VI.4).

Northeast winds have less influence than the other winds and mainly increase the exposure time of particles coming from both the southern part of the NE basin (on neap tides) and the entire SE basin, relative to the other wind cases. TPSD is still lower than SSD but is generally decreased by the presence of wind. During this study, we also observed that the particles returned preferentially to the marina through the western entrance (Figure VI.1) regardless of weather-marine conditions.

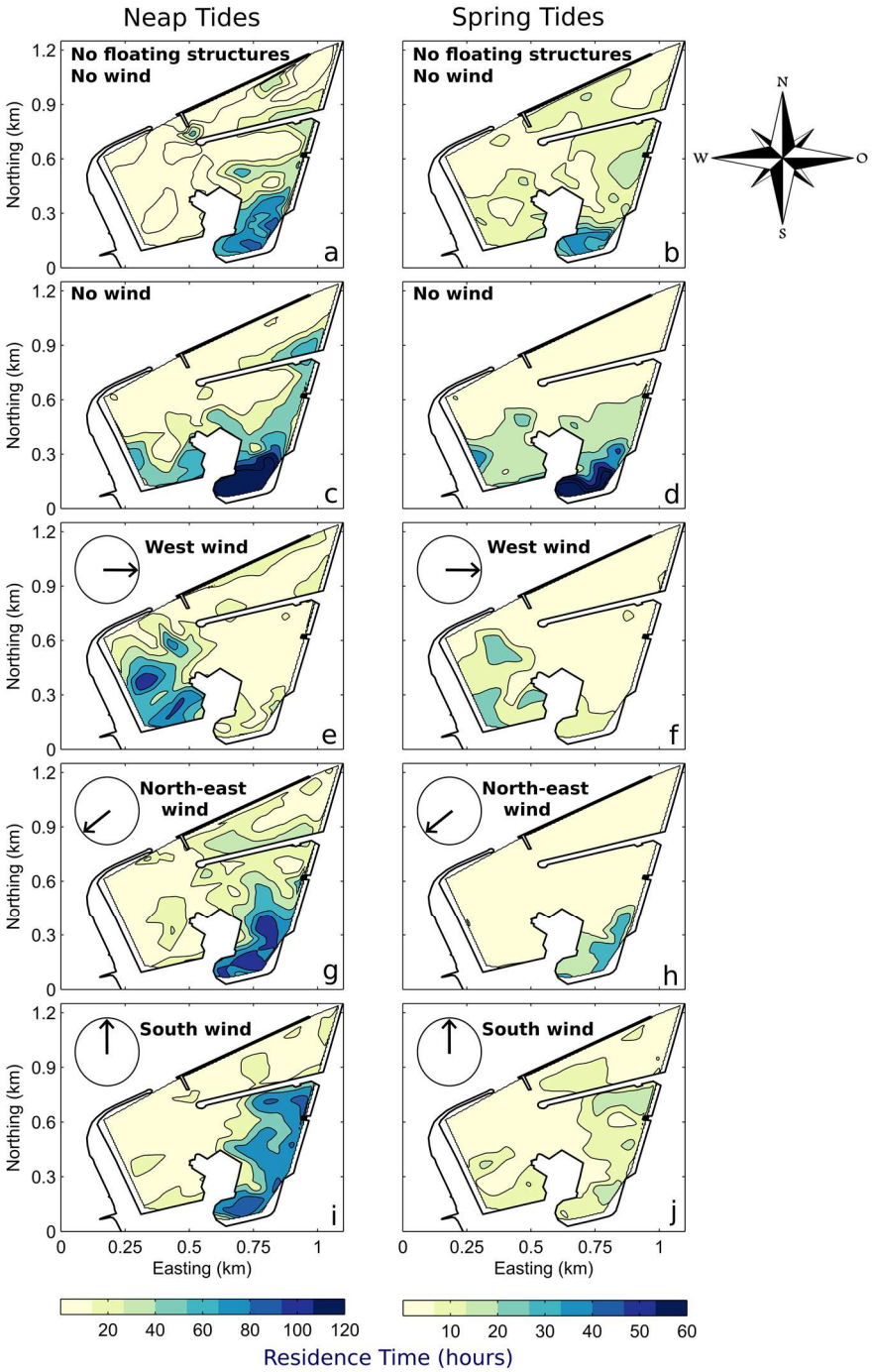

Figure VI.5. *Spatial distribution of vertically-averaged Residence Time (expressed in hours) within the La Rochelle marina computed for each scenario (letters) defined in Table VI.1. Rows characterise the wind and FS configurations and columns correspond to the tidal regime.*

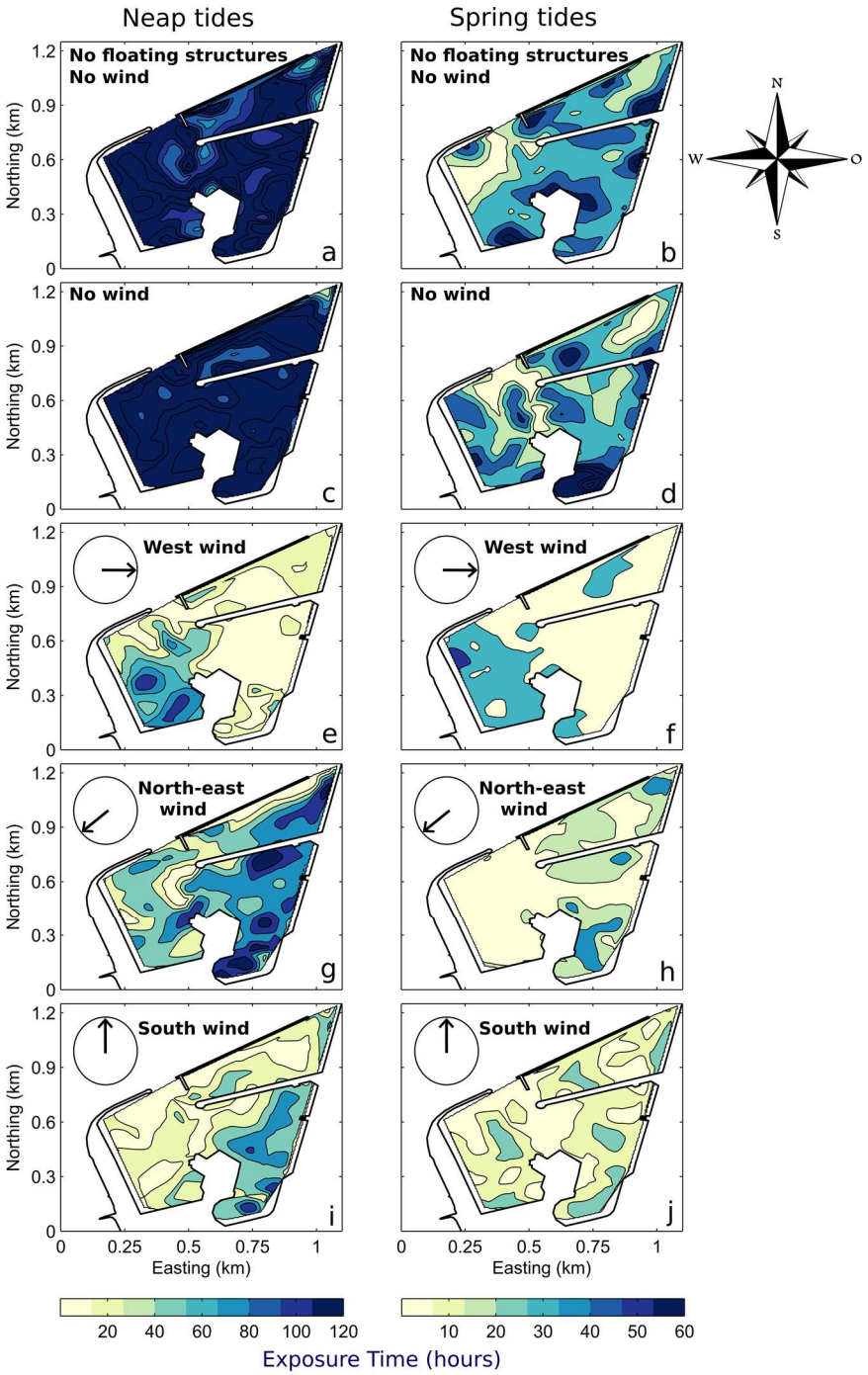

Figure VI.6. *Spatial distribution of vertically-averaged Exposure Time (expressed in hours) within the La Rochelle marina computed for each scenario (letters) defined in Table VI.1. Rows characterise the wind and FS configurations and columns correspond to the tidal regime.*

VI.4.4. Characterisation of the Return-Flow

From the previous timescales, we assessed the importance of the return-flow in the marina through the expressions established in Section 2.3.3. The Return-flow Factor (RFF) was obtained through Equation (VI.5) by using IFT values while the Return Coefficient (RC) was found via the Equation (VI.7) by using RT and ET values. RFF and RC are inherently different as they were estimated, respectively, in a Eulerian and a Lagrangian way. These factors can

provide relevant points of comparison that need to be analysed with caution. Results for each scenario were averaged and displayed in Table VI.4.

A large variety of return-flow values were found depending on the weather-marine conditions, but RFF globally displays the same behaviour than RC. The similarities mainly concern the influence of the wind and the tide. Neap tides show the higher variability of RC and RFF, with the lower and higher values respectively obtained with and without wind (Table VI.4). Without wind, the return-flow is always greater than 0.5, but its magnitude can drastically decrease during neap tides with the presence of wind, and particularly with the west wind (0.12 ± 0.11 and 0.19 ± 0.05 for RFF and RC, respectively). This decrease is also visible for spring tides but with less intensity (Table VI.4). These parameters can approach zero during intense 15 ms^{-1} western events. The maximum values are also obtained during neap tides without wind, with and without the presence of FS for RFF (0.73 ± 0.01) and for RC (0.75 ± 0.03), respectively. In general terms, the macro-tidal influence and the configuration of the area generate a high return-flow that is weakened under the action of the wind but not substantially affected by the presence of FS. The last result confirms the weak impact of floating structures on the circulation outside the marina.

VI.5. Discussion

VI.5.1. Assessment of the Main Drivers of the Water Renewal

Although the tide is a primary driver of the hydrodynamics, *Huguet et al. (2019a)* has shown that the wind, but also infrastructures, had a substantial impact on the physical processes in the marina. The results, visible in Section 4, provide a robust view of their influence in the macro-tidal marina of La Rochelle. Here, we gather the information collected through the study of the three transport timescales to discuss the importance of the tide, the wind and the Floating Structures (FS) in the marina renewal.

VI.5.1.1. Tidal Influence

Flushing, residence and exposure times (Figures VI.4–VI.6) reveal a strong spatial heterogeneity of the renewal. The NE and the SE basins generally present the lowest and largest timescale values in the marina, respectively, but the behaviour of the timescales significantly vary depending on the conditions. Close to the entrances, the water parcels are rapidly advected because of the continuous effect of the tidal currents, which decreases renewal times. On the opposite, the innermost parts of the marina are more sheltered from the flows and display the longest renewal times. This marked horizontal spatial variability has been found in estuaries and coastal embayments with macro-tidal influence (*Oliveira & Baptista, 1997; Plus et al., 2009; Barcena et al., 2012*) but also with micro-tidal influence (*Cucco & Umgiesser, 2006; Wijeratne & Rydberg, 2007; Ferrarin et al., 2014*).

The renewal time and its spatial variability increase as the tidal range decreases in our area: the neap tide is a very limiting factor in the renewing of waters. Indeed, tidal currents that are 3 to 4 times lower in intensity within the marina during neap tides increase the renewal time from a factor of 2–3 (for RT) to in some cases almost a factor of 4 (for IFT and ET). This result shows that the advective coastal tidal movement is a main driver of the water flow in

the marina is as it was demonstrated in previous studies (*Yuan et al., 2007; Cucco et al., 2009; Cavalcante et al., 2012*). Other European ports investigated the behaviour of their water masses, and the results displayed a broad range of renewal timescale values. *Schwartz & Imberger (1989)* and *Lisi et al. (2009)* found global flushing times of 288 and 120 *h*, for a Sicilian micro-tidal and an Australian macro-tidal port, respectively. In Spain, the local flushing times reached about 125 and 163 *h* for the meso-tidal port of Bilbao and the micro-tidal port of Barcelona, respectively (*Grifoll et al., 2013; Grifoll et al., 2006*). Thus, the renewal timescales are not strictly related to the tidal regime. The shape and dimension of ports also need to be considered.

VI.5.1.2. Wind Influence

Even if the marina is tidally dominated, the wind also has a substantial impact on the water renewal because of the presence of shallow depths. Its influence is exerted differently depending on its direction and its intensity, but the wind globally enhances the water exchange, up to a factor of almost 5 during neap tides. This significant effect on renewal timescales values has already been reported for several coastal environments (*Geyer, 1997; Wang et al., 2004; Orfila et al., 2005; Canu et al., 2012; Du & Shen, 2016*). The wind has a more significant influence on exposure and flushing times than on residence times, especially during neap tides (Table VI.4). Contrary to RT, ET and IFT take into account the return-flow into the marina. This suggests that, even if the wind has a significant influence on processes inside the marina, its impact is larger on outside processes and their interaction with processes inside the marina. It mainly pushes waters out from the marina influence and facilitates their renewal in the local environment. Among the moderate wind cases, South and west winds are the most impacting winds during spring tides and neap tides, respectively (Table VI.4). Water exchanges are indeed significantly enhanced by the west wind action, as reported in *Huguet et al. (2019b).* The effect of the south wind was less noticeable on marina flows, but we could explain its impact on renewal by the marina configuration. Its two main entrances (Figure VI.1) are almost perpendicular to the direction of propagation of southern winds which tends to evacuate water bodies more rapidly while hindering their return to the marina. The mechanisms involved during the west and south wind action are different and they are not strictly proportional to the tidal range. The funnel configuration of the bay linked to the complex architecture of the marina and the numerous tidal flats in the area could explain the non-linearity of the processes involved from neap tides to spring tides. Finally, as the variability depends mainly on the tidal forcing and the dominant wind regime, the winter which is characterised by tougher western winds, should display a faster renewal as found in *(Plus et al., 2009; Barcena et al., 2012; Umgiesser et al., 2016).*

The transport timescales were computed at the bottom layers, and a slight vertical variability was found in the water renewal (data not shown). With tide only, surface layers always experience the highest renewal even if the difference with bottom layers does not overpass 2 *h*. Even if it is less clear for north-east and south winds, west wind generally enhances the variability of the renewal between the surface and bottom layers. This result differs from the vertical heterogeneity found by some authors (*Warner et al., 2010; Grifoll et al., 2013*) that demonstrated a straight vertical variability of the renewal depending on the wind regime. In the marina, the presence of shallow depths associated with the macro-tidal forcing of the area ensure a quasi-homogeneity of the water column that is slightly affected by the action of winds.

VI.5.1.3. Influence of Floating Structures

Floating structures (FS) have a lower influence than the wind on the total water renewal of the marina. They increase the spatial variability of the renewal by reducing the water renewal in the most sheltered parts and slightly enhancing the hydrodynamics close to the entrances (*Huguet et al., 2019b*). With two entrances, the NE basin is particularly exposed to this enhancement. The presence of FS is also involved in the increase of the water renewal by channeling the circulation and reducing the flood-related micro-scale eddies (*Huguet et al., 2019b*). These eddies, generated by the tide-topography interaction, develop during the flood and affect the residual circulation within the marina. Their existence can interfere with the flushing processes and subsequently generate an increase in the residence time of the particles (*Babu et al., 2005*). The broad coverage of floating bodies in the marina reduces the eddy activity by decreasing velocities in the inner parts the marina and focusing it along the entrances. Although FS reduces eddies, the general decrease of currents induced is sufficient to lower the renewal of water bodies in a significant portion of the marina.

VI.5.1.4. Influence of the Tidal Phase

Given the macro-tidal regime of the area, the tidal phase release is considered as a possible factor influencing the water transport timescales. While many studies worked with only two opposite tidal phases (*Brauwere et al., 2011; Canu et al., 2012; Andutta et al., 2013*), we proposed to investigate the renewal properties of the mid-ebb, the mid-flood, the high tide and the low tide. Figure VI.7 enables us to investigate the influence of the tidal phase of release in the computation of the three timescale values in the marina (IFT, RT and ET).

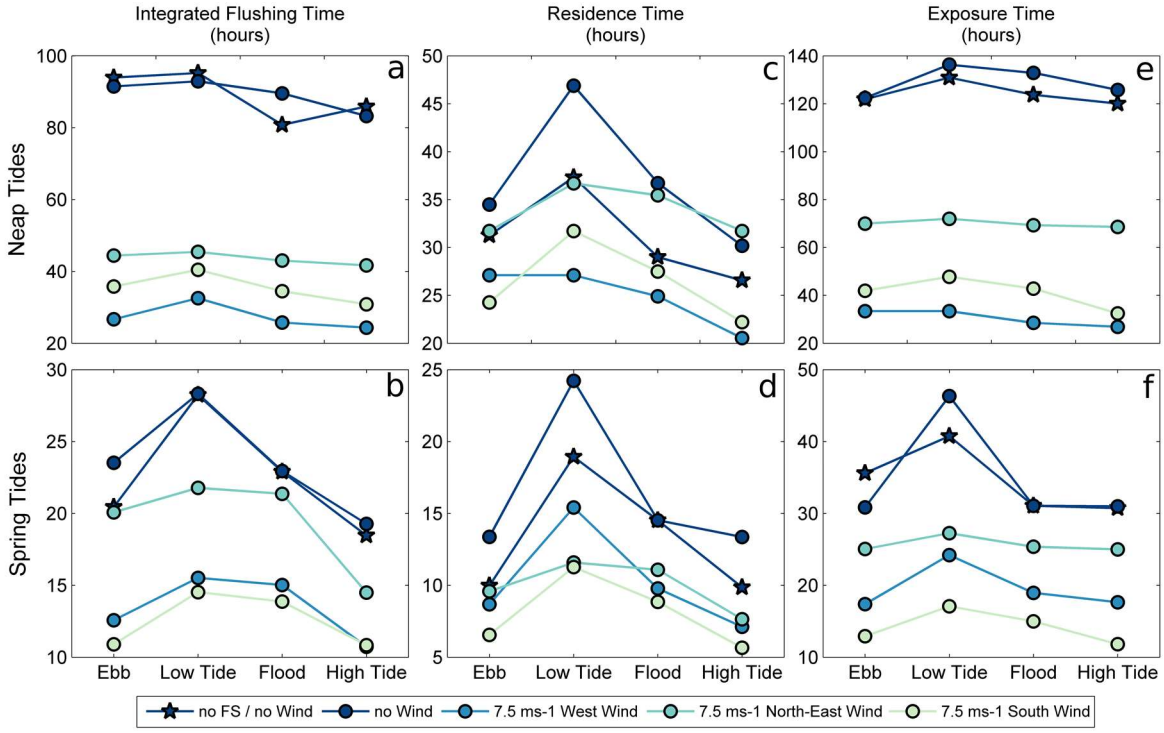

Figure VI.7. *Spatially-averaged timescales values obtained for each release (at Ebb, Low Tide, Flood and High Tide) for each scenario.*

Maximum timescale values are usually found when the release of tracer and particles occurs at low tide while the best moment to obtain lowest timescales is generally high tide (Figure VI.7). Generally, mid-ebb and mid-flood are quite similar in terms of renewal, even if spatial variabilities exist particularly close to the entrances. The Spatial Standard Deviation (SSD) was found to be always larger than the Tidal Phase Standard Deviation (TPSD) according to Table VI.4. It indicates that the variability of the renewing is more spatially than tidally dependent in the marina. Moreover, tidal phase variability of time scales generally decreased during spring tides and in the presence of wind (Table VI.4). This dependence on the tidal phase was already found and discussed in many studies (*Cucco et al., 2009; Arega & Badr, 2010; Brauwere et al., 2011*).

VI.5.2. Comparison of Water Transport Timescales

Based on the similarities shared by the several transport timescales, we highlighted general conclusions in the behaviour of the water renewal in the previous section. Here, we assess their differences to find the most relevant to describe the water transport processes occurring within the marina. The Eulerian (Integrated Flushing Time) and the Lagrangian transport timescales (Residence Time and Exposure Time) are inherently different as they follow advection-diffusion and only advection processes, respectively. The two approaches are complementary as their comparison provides exhaustive information about the motion features in the marina. As discussed in *Arega & Badr (2010)*, their good agreement could be explained in tide-dominated environments where advection is the main driver of the circulation. Conversely, their differences in their spatial distribution characterise diffusion dominated areas. The cross-correlation of these approaches indicates that the advection mostly dominates in the marina, even if diffusion processes occur in the most sheltered parts of the marina.

The spatial distribution of Lagrangian timescales (RT and ET) displays more chaotic variability and relatively less monotonic gradients than Eulerian timescale (IFT). These chaotic patterns are the result of turbulent Lagrangian flows that generate a chaotic and non-monotonic dispersion of particles. This concept of "Lagrangian chaos", demonstrated experimentally (*Aref, 1984*), and numerically (*Ridderkinhof et al., 1990*), has also been experienced in (*Arega & Badr, 2010*). It mainly contributes to greater spatial variability of Lagrangian timescales.

The Eulerian timescale IFT generally presents approximately average values between RT and ET. A sensitivity test of the « e-folding flushing time » parameter used to compute IFT (data not shown) demonstrated that the chosen percent reduction was a leading factor in the magnitude of IFT. As it was set to 63 % in this study, it could help explain why IFT presents approximately average values between RT and ET. Although IFT and ET are different in terms of magnitude, they globally follow the same trend. Without wind, the transition from spring to neap tides increases IFT and ET much more than RT. It means that the combination of processes outside and inside the marina is more sensitive to the tidal range than processes occurring only in the marina. Wind influences RT less than the two other timescales. It implies that hydrodynamics within the marina are less sensitive to the wind than in the system bay-marina. RT is more vulnerable to the presence of FS than the two other timescales, which

confirms that the presence of FS primarily modifies the circulation within the marina. The tidal phase release can significantly alter the time required for a water parcel to leave the marina, which noticeably affects the RT results. ET and IFT are less dependent on the tidal phase release (Table VI.4; compare TPSD/Mean). Considering only the tide, physical processes occurring in the marina are more sensitive to the tidal phase, while marina-bay exchanges are more tidal range dependent.

Some authors recommend to use Eulerian approaches or to take into consideration the return of particles in the system when using Lagrangian methods (*Cucco et al., 2009; Arega, 2013*). In such a macro-tidal environment, the importance of the return-flow on the water renewal requires that dynamic processes outside the area of study be considered. Taking into account the processes occurring outside the domain of study is of crucial importance to represent the water renewal of semi-enclosed tidal basins accurately. However, the computation of RT alone does not make it possible to fully characterise the behaviour of water bodies in a semi-enclosed domain with such tidal influence. In the framework of this study, the computation of IFT appears to be sufficient to represent the intra-marina exchanges as well as the exchanges between the bay and the marina. IFT and ET are also less sensitive to the initial moment of calculation, which ensures an easier solution for the calculation of currents and associated phenomena. Nevertheless, the information provided by RT was necessary to characterise the fate of waters leaving the marina via the Return Coefficient formulation. In that sense, the comparison of the three timescales allowed us to have a complete picture of the physical processes leading to the water renewal in the marina. As seen in the literature (*Monsen et al., 2002*), the relevance of each time scale depends on the initial question and the physical, biological, and geochemical characteristics of the study area. Thus, the question of the usefulness of each timescale depends on the characteristics of the scientific study proposed.

VI.5.3. Impact of the Return-Flow in the Water Renewal

The Return-flow Factor (RFF) and the Return Coefficient (RC) display the same behaviour while they are computed in two different ways. This consistency validates the several methods employed to characterise the water renewal in the marina. Although the three transport timescales (IFT, RT, and ET) show quantitative differences, their information allows computing the general return-flow occurring in the marina. The knowledge of the return-flow magnitude in a basin is also a straightforward way to represent the renewal by taking into account the dynamics outside the embayment. Its information and variability is a powerful indication of the water masses confinement in semi-enclosed tidal bays depending on the weather-marine conditions.

In the past, tidal prism flushing models have often set the return-flow to 0.5 or ignore it (*Dyer, 1973; Callaway, 1980*), but as suggested by *Sanford et al. (1992)*, it should be characterised in any study. Many authors described the return-flow in different embayments throughout the world. For example, reference *Arega et al. (2008)* found a maximum value of 0.15 for a micro-tidal creek in the US; *Gao et al. (2013)* computed 0.2 to 0.9 from the entrance to the inner parts of a meso-tidal lagoon in China; *Cucco & Umgiesser (2016)* estimated a mean return-flow of 0.66 for a micro-tidal lagoon in Italy ; an average return-flow of 0.32 was found by *Gilibrand (2001)* in a meso-tidal Scottish Fjord ; a maximum return-flow of 0.95 was reached in a meso to macro-tidal lagoon in France (*Plus et al., 2009*). As experienced in La Rochelle marina and

other embayments in the world, the return-flow is not correlated strictly to the tidal influence in the domain.

Here, the return flow is higher during neap tides than during spring tides in the absence of wind. The influence of the tide is particularly visible in the bay, and the back and forth movement generates significant trapping in the bay which extends to the marina. The funnel configuration of the bay and its sheltered position (Figure VI.1) combined with the tidal dominance of the area could explain the significant trapping of water masses, responsible for a high return-flow in the marina. This trapping is increased during neap tides when the excursions of water parcels are reduced. The study has shown that when water particles left the bay, they were rapidly ejected and their return to the system was hindered, especially in the marina. This mechanism is also described in *Arega et al. (2008)*, where the oscillatory flood and ebb processes caused the water masses to be trapped, particularly during neap tides. Conversely, *Brauwere et al. (2011)* computed the larger return coefficient during spring tides, but the estuarine environment studied was much more influenced by the freshwater inputs.

The comparison of the weather-marine scenarios highlights the leading role of the wind on the reduction of the return-flow (Table VI.4). Neap tide conditions are particularly concerned by this decrease, which is directly correlated to lower activity of the tidal currents. The influence of the wind can overpass the tide, especially during intense 15 ms^{-1} west events when the return-flow can approach zero (Table VI.4). When water parcels leave the marina during ebb, the wind can rapidly flush them out of the bay where they are exposed to the high renewal rates of the local embayments (*Kenov et al., 2015*).

VI.6. Conclusions and Perspectives

The purpose of the present study was to characterise the water renewal of La Rochelle marina under a complete range of weather-marine conditions. We mainly focused on the physical mechanisms allowing to describe the renewal, but the results obtained might provide sufficient material for future studies related to the monitoring of pollutants and biological/ecological applications. Pollution is one of the major threats to water quality in coastal areas and understanding the physical behaviour of such environments is the first step toward efficient management of the problem. The results provided in this paper enable us to identify the most vulnerable zones concerning accidental pollution, but they can also be useful for undertaking protection and management policies. Results emphasize the substantial variability of the water renewal depending on the weather-marine conditions and the location in the marina.

Two different approaches helped us determining the temporal and spatial renewal of waters in the marina. The computation of three water transport timescales (IFT, RT and ET) led to the estimation of the return-flow in the marina via the RFF and RC formulations. Based on their study and comparison, the main findings concerning the water renewal in the marina are:

- The marina displays a strong horizontal variability of the renewal. The most confined waters are located in the south of the SE basin, while the NE basin is generally the most renewed.
- Both the tide and wind substantially impact the water renewal of the marina. The transition from spring to neap tides significantly decreases the water renewal while the presence of the wind enhances it, in particular for west and south directions.

- In the marina, physical processes responsible for the water renewal are generally more affected by the tidal phase than in its surrounding bay.
- The influence of the wind is less significant in the marina than in the system bay-marina.
- The water renewal is relatively homogeneous over the water column even with the effect of the wind (data not shown).
- As shown by the study of RT, the Floating Structures (FS) particularly decreased the water renewal in the most sheltered parts (SE basin), but they also generally increase it in the most exposed parts of the marina (NE basin). The study of both ET and IFT showed that they do not alter the circulation significantly outside the marina and thus, slightly affect the return-flow in the marina.
- The return-flow has been consistently represented both in a Lagrangian and Eulerian way. Its information is a relevant indication of the circulation processes occurring outside the marina. Without wind, return-flow in the marina is amplified by neap tides that generate significant trapping of the water masses at the scale of the bay. Both ET and IFT results showed that return-flow was a key parameter in the dynamics of water renewal in the marina.
- The return-flow is very sensitive to the wind action and the trapping processes happening in the bay can be drastically reduced. Wind enhances the dispersion of water masses away from the bay and thus decreases the return-flow in the marina. Powerful west winds (15 ms^{-1}), typical of winter conditions, can generate a near-zero return-flow.
- Without wind, return-flow is amplified by neap tides that generate significant trapping.

Given the importance of the return-flow in the region of interest, we should point out that tracer mass and particles dispersion directly depend on the size of the computational domain (*Viero & Defina, 2016; Bialik & Karpiński, 2018*). We assumed the latter to be sufficiently large enough not to affect the tracer mass and the behaviour of the particles used in the definition of the water transport timescales. The use of only one transport timescale (IFT) enabled to thoroughly describe the renewal processes occurring in the marina but also between the marina and its local environment. This parameter is less sensitive to the tidal phase release moment than RT, displays less chaotic patterns than ET and RT and offers the possibility to compute the return-flow efficiently through the tidal prism method. However, the comparison with Lagrangian timescales allowed us to detail the physical processes responsible for the renewal and to assess the consistency of the results. It underlines the need to cross-reference complementary methods and also puts forward some methods employed to address questions in a wide range of scientific domains.

Future works should characterise the influence of freshwater inflow and waves. Indeed, many authors suggested the contribution of the freshwater to the enhancement of the renewal (*Asselin & Spaulding, 1993; Huang & Spaulding, 2002; Barcena et al., 2012; Canu et al., 2012; Umgiesser et al., 2016*). Even if river influence is negligible in our area, intense rainy events can significantly affect the renewal times (*Malhadas et al., 2010*). Waves that can be energetic offshore can also modify the exchange efficiency (*Sanford et al., 1992; Azevedo et al., 2009; Delpey et al., 2014; Guo et al., 2016*). In a next study, the influence of dredging maintenance of the marina on the water renewal will be investigated. Indeed, the water depth was found to increase the water exchange (*Malhadas et al., 2009*), and it could be interesting to identify the optimal depth to improve the water quality of the marina

Chapitre VII

Sediment Dynamics in La Rochelle Marina and Strategies to Reduce Siltation

Jean-Rémy Huguet[1], Isabelle Brenon[2] and Thibault Coulombier[3]

[1] PhD student at UMR 7266 LIENSs, CNRS-La Rochelle Université, 2 rue Olympe de Gouges, 17000 La Rochelle, France (corresponding author). E-mail: jean-remy.huguet@univ-lr.fr
[2] Associate professor at UMR 7266 LIENSs, CNRS - La Rochelle Université, 2 rue Olympe de Gouges, 17000 La Rochelle, France. E-mail: isabelle.brenon@univ-lr.fr
[3] Research engineer at UMR 7266 LIENSs, CNRS - La Rochelle Université, 2 rue Olympe de Gouges, 17000 La Rochelle, France. E-mail: thibault.coulombier@univ-lr.fr

Keywords: Marina; Sediment dynamics; Siltation reduction; Optimise dredging maintenance; Suspended sediment concentration; Macro-tidal influence; Wave regime; Wind regime

Ce Chapitre est soumis en tant qu'article dans la revue Ocean and Coastal Management.

Résumé

Dans ce Chapitre, nous étudions la dynamique d'envasement du port des Minimes à l'aide d'observations, et analysons numériquement l'effet de possibles mesures permettant de réduire l'envasement du portuaire dans notre zone. Le premier type d'observation correspond à des levés bathymétriques mono-faisceau effectuées deux fois par an, avant et après chaque période de dragage. Les différentiels bathymétriques, issus de la comparaison de ces levés, a permis d'analyser l'envasement à l'échelle saisonnière et annuelle. Une forte variabilité spatiale de l'envasement est visible mais la dynamique de dépôt moyen est de 50 cm par an. Des mesures de turbidité et d'altimétrie ont rendu possible la caractérisation de la dynamique sédimentaire à des échelles plus courtes mais plus résolues, en trois points du port. Ces deux paramètres sont fortement corrélés, à la fois au régime de vagues et de vent local, et à la marée. En raison des faibles courants, la re-suspension locale est assez limitée, en particulier à l'intérieur des bassins. Les particules sont donc principalement apportées par les courants de marée chargés en sédiment, venant du large. Les périodes de vives-eaux et les vagues sont les principaux contributeurs de la remise en suspension de sédiment cohésif au large.

Ces observations ont aussi servi à calibrer et valider l'utilisation du modèle hydro-sédimentaire TELEMAC-3D, validé en hydrodynamique dans les Chapitres IV et VI. L'objectif était de simuler l'effet que pourraient avoir les stratégies proposées pour réduire l'envasement du port de manière durable. La plupart des mesures visant à modifier la configuration du port ont eu un faible impact (avec le rétrécissement des entrées, création d'une ouverture au fond des bassins ouest et sud-est) voire un impact négatif (avec la fermeture de l'entrée secondaire). L'utilisation de panneaux déflecteurs (CDW) aux différentes entrées externes, semble efficace à partir d'un certain nombre mais nécessite un coût et un entretien considérable comparé au résultat obtenu, et leur construction pourrait en plus entraver la navigation et gêner les opérations de dragage. L'implémentation de souilles, c'est-à-dire des fosses creusées par dragage, à l'extérieur et à l'intérieur du domaine portuaire, a montré des résultats très contrastants. Ces souilles provoquent une diminution des vitesses de courants pour concentrer le dépôt à leur niveau et ainsi permettre de focaliser les opérations de dragage. Quelle que soit leur localisation dans le port, les souilles internes n'ont pas généré de résultats satisfaisants.

Les meilleurs résultats ont été obtenus en implémentant des souilles au niveau du coin nord-ouest du port, le long du chenal de navigation. Celles-ci profitent d'une position optimale pour intercepter les particules venant du large et peuvent réduire l'envasement dans le port, de manière assez significative. La longueur, la profondeur et la proximité de la souille au port sont des éléments déterminants à prendre en compte. Cette souille pourrait délocaliser une grande partie des activités de dragage à l'extérieur du port et donc, moins entraver la navigation et les usagers du port. Cependant les volumes dragués seraient équivalents aux volumes déjà engagés actuellement car il faudrait se défaire, chaque année, du dépôt accumulé dans la souille, afin qu'elle puisse continuer à piéger du sédiment. A moins d'une restructuration complète des infrastructures portuaires, l'apport de matériel cohésif dans le port semble difficile à endiguer. En plus d'une souille à l'extérieur du port, l'utilisation de systèmes de re-suspension capables de prendre avantage des courants du jusant pour évacuer du sédiment, serait peut-être à envisager ici.

Abstract: La Rochelle marina, located in the south-west of France, is one of the largest recreational port in Europe. As many ports through the world, the marina isn't spared by siltation and has to face serious dredging operations 8 months per year. Consequently, there is a big interest in determining sediment fluxes in the area and to implement possible measures to minimise siltation and/or to optimise dredging operations. In the present study, a three-dimensional hydro-sedimentary model (TELEMAC-3D) was calibrated with fields measurements taken from 2014 to 2019. It was shown analytically, from these *in situ* measurements, that the macro-tidal influence and local wind-wave regime significantly contribute to the siltation in the marina. In order to minimise the cost and time associated with maintenance dredging, several propositions have been tested. Numerous sediment traps configurations were defined to focus the deposition of sediment and constructional measures were also assessed in terms of siltation reduction (entrance closure, narrowing entrances, Current-Deflecting-Wall…). Numerical simulations showed that the best solution was to create a sediment trap at the downstream corner of the marina, along the main navigation channel, to intercept sediment particles arriving from the ocean. The constructional measures implemented were not efficient in reducing siltation as well as the use of sediment traps inside the marina. These results will allow the marina management to define a long-term and sustainable strategy to fight against siltation in a more efficient and less costly way.

VII.1. Introduction

Siltation of ports is an issue that exists as long as ports exist (*Nola and Franco, 2009; Marriner and Morhange 2007; Galili et al., 2010*) and is mainly related to the shelter function they provide. Ports are often designed or located on requirements imposed by safe and efficient navigation. They act as settling basins for cohesive sediments that are carried into the system by the flow and deposited when the flow is no longer able to transport the sediment. Main mechanisms responsible for sedimentation were extensively reported in the literature (*Langendoen, 1992; Winterwerp, 2005; PIANC, 1997*). They are governed by the tidal filling, the horizontal entrainment forming a turbulent mixing layer at the entrance; and sediment or cold/warm induced density currents (*Eysink, 1989; Lin & Metha, 1996; Van Rijn, 2016*). In coastal areas, waves, tides and density gradients are the main drivers of the resuspension of fine-grained sediment and of their transport into port basins (*Van Rijin, 1993; Van Maren et al., 2009*). Sediment-laden water masses approaching these systems also interact with the navigation channel and entrance area whose configurations play a role in the siltation of ports (*Van Rijn, 2016*).

Since siltation represents a risk to navigation safety and reduces accessibility to port infrastructure, many ports around the world have required frequent maintenance to maintain a sufficient water depth. The need to control siltation is a common feature shared by many ports since the earliest settlements along coasts and rivers (*Liu et al., 2017*). Although techniques have evolved, the most well-known, reliable and widespread method to deal with this issue remains dredging (*Montgomery, 1984; Batuca & Jordaan, 2000*). This ancient technique (*Herbich, 1975; Marriner & Morhange, 2006; Marriner et al., 2014*) consists of removing the bottoms where the excess silt has accumulated. Recurring dredging is often necessary a large part of the year to maintain the operativity of the port and sustain water-based activities such as fishing and boating. While the maritime traffic and recreational boats keep growing in the world, the siltation of ports and its management are issues of great importance. However, costs

associated with the removal, transport processing and storage of dredged sediment are often high (*Whitehouse et al., 2000; Winterwep, 2005; Bianchini et al., 2019*) and dredging operations can hinder nautical activities. Besides, dredging enables to reach a desired local depth, periodically, without guaranteeing the prevention of siltation over time. Moreover, the methods of extraction and disposal of dredging materials and their impact on water quality are becoming increasingly criticised from an environmental point of view (*Newell, 1998; Turekian et al., 2010; Becker et al., 2015*). Given the economic and ecological stakes, ports must adapt their dredging strategy to strike a balance between cost, environmental impact and efficiency.

At a time when sustainable management is required for the development of port infrastructure, minimisation of siltation and associated dredging maintenance should be one of the most relevant topics (*Acciaro et al., 2014; Kavakeb et al., 2015; Di Vaio & Varriale, 2018*). Recently, there has been a growing interest in developing medium to long-term strategies to fight against siltation. Such siltation-reduction strategies generally consist of a decrease in the water exchange volume between the port and its surrounding waters, and a decrease of sediment input carried by the exchange flow. In addition, the trapping efficiency of the basin should be reduced as much as possible. As recommended by *Kirby (2011),* the success of siltation-reduction strategies must be based on a thorough understanding of the physical processes of deposition. To minimise siltation, port managers must first consider the natural system and its interaction with the port geometry. The first and most important consideration is to avoid locating a port in an environment of intense sediment transport, and the configuration of the port needs to be adapted to the local geomorphology. Based on analysis results from siltation data and simulations models in many port basins, several design rules and entrance geometry described in *Van Rijn (2016)*, should be considered before any construction of port infrastructure.

Since the last decades, alternative solutions have emerged to diminish the amount of sediment to dredge in already existing ports and channel approaches. The first efficient research was initiated by the Port of Hamburg in the 1970s (*Christiansen, 1987*) and many studies on siltation regulation have followed, mostly in Germany, Netherlands and Belgium (*Hofland et al., 2001; Kirby, 2003; Winterwep, 2005; Stoschek & Zimmerman, 2006*). The first type of solution consists of the use of "anti-sedimentation structures", such as groins, mud traps, Current-Deflection-Walls (CDW) and bubble curtains located at the vicinity of the entrance section (*Winterwep, 1994; Decrop, 2013; Dugué, 2013*). These structures are supposed to keep a significant part of the sediment out of the port and thus, reduce the siltation maintenance. The second solution is represented by resuspension sediment systems that generally use water injection and/or mechanical devices to re-suspend and keep the sediment moving through the port, which reduces basin trap efficiency (*Weisman et al., 1996; Headland et al., 2007*). Sand-diversion installations are the third type of alternative solutions and allow the excess mud to be drained outside the port. These systems generally operate continuously without impact on navigation and drastically reduce dredging maintenance (*Williams & Visser, 1997; Wurpts & Greiser, 2007; Jones & Mehta, 1980; Kirby, 2013*). They are characterised by relatively high installation and operational costs (*Ware, 2016; Bianchini, 2019*). Other approaches, such as "passive nautical depth concept", take advantage of the ability of a vessel to sail through a low-density fluid mud, thereby preventing consolidation from taking place (*PIANC, 1997; Fontein & Byrd, 2007; Tubman et al., 2017*).

In La Rochelle marina, the dredging activities have recently increased since the port was expanded in 2014. As a consequence, dredging maintenance has become more frequent and intensive over the years, and the marina management requires more sustainable methods to minimise dredging maintenance. In this context, discussions with managers and stakeholders of the marina led us to test the effect of possible solutions to reduce the siltation in the marina. We then attempted to characterise the mechanisms of siltation occurring in the area, and we assessed the efficiency of constructional and dredging measures to control it. Their effect on both hydrodynamics and siltation will be discussed in this paper. Results will provide interesting information for the managers of the marina, that could help defining a new integrated approach to deal with the siltation issue. This work will also contribute to the planning of accurate dredging operations and the maintenance of dredging operativity levels cost-effectively. The material presented in this document is exploratory and preliminary. Therefore, future quantitative research should be conducted to provide more detailed information on the efficiency of the selected measures. In the next section, study site, *in situ* observations and numerical modelling will be presented before introducing local hydro-sedimentary patterns and the assessment of the several methods implemented to reduce siltation and maintenance dredging.

VII.2. Materials and Methods

VII.2.1. Study Site

La Rochelle marina is located in the landward part of the Pertuis d'Antioche embayment, along the French Atlantic coast, in the central part of the Bay of Biscay (Figure VII.1). The area is protected from the Atlantic Ocean by Ré and Oléron islands and connected to the Pertuis Breton embayment through a narrow inlet. The bottom is silty to sandy-silty, with the presence of many tidal flats and relatively shallow depths. The coastal area is considered as a mixed, wave and tide-dominated estuary (*Chaumillon & Weber, 2006*). The tidal regime is macro-tidal and dominated by the semi-diurnal component M2. Tide is also significantly affected by the quarter-diurnal band that is strongly amplified shoreward because of resonance occurring on the Bay of Biscay shelf (*Le Cann, 1990*). The tidal range varies from 2 m during neap tides to more than 6 m during spring tides. The wave energy is drastically reduced in the inner parts of the embayments because of refraction, diffraction and bottom friction. The marina is thus protected from the strong swells that can reach 8 m offshore during the winter period (*Bertin et al., 2015*). North Atlantic Oscillation (NAO) partly controls the inter-annual variability of the wind regime in the whole Bay of Biscay (*Dodet et al., 2010*). The winter period is generally characterised by a very active low-pressure activity generating strong west and northwest winds, which contrasts with the low activity and the domination of thermic breezes during the summer period.

The marina was constructed over an intertidal flat situated in the southern part of La Rochelle bay. The installation of the main infrastructures as well as the derocking and dredging operations have lasted more than 10 years (from 1969 to 1980). The total parking capacity was quickly reached and to respond to the increasing demand the marina was expanded in 2014. Since its expansion, La Rochelle marina has been considered as the biggest along the Atlantic coast and one of the largest in Europe. This 900 m long and 820 m wide

semi-enclosed area is divided in 3 basins totalling 4500 moorings, distributed along 15 km of floating docks. The south-eastern (SE) basin is the bigger, with 22 ha, while the western (W) and the north-eastern (NE) basin, present 17 and 15 ha, respectively (Figure VII.1c). The marina is accessible by a 110 m wide main entrance, while the expansion basin presents two entrances: an internal 64 m wide to the southeast and an external 150 m wide to the northeast which is not practicable (Figure VII.1c). Oscillating volumes in the marina are in the order of 1 million of m^3 to 3 million of m^3, from neap tides to spring tides. The bed sediment is cohesive with a mean size of 15 μm (*IDRA, 2015*). Sand (2 mm to 63 μm), silt (63 μm to 2 μm) and clay (< 2 μm) represent 7 %, 83 % and 10 % of the sediment, respectively, and this proportion is spatially homogeneous. The mean depth is about -0.87 m with a standard deviation of 1.1 m for the bathymetry displayed in Figure VII.1c.

As many ports throughout the world, La Rochelle marina suffers siltation and has to spend 10 per cent of its total budget to solve this issue. Each year, 200 000 m^3 of material are dredged each year, to keep depths in phase with navigation. Maintenance dredging lasts eight months from autumn to spring and is conducted over, approximately, one-third of the marina. Figure VII.1b displays the dredging strategy and the target depths required for each part of the marina. The navigation channel at the northern dike of the NE basin (Figure VII.1c) is dredged by a suction dredger pump each year to the target depth of -1 m CM. The NE basin is dredged between -2 and -3 m while the rest of the marina is dredged between -1 and -2 m in function of the siltation observed. A rotodredger is occasionally used to resuspend the most silted areas but most of the time a stationary suction dredger, connected with a suction pipe, dredges and releases mud at a southern location outside the marina. Due to the presence of strong currents, the navigation channel along the northern dike of the W basin is self-dredged until the main entrance between -2 and -3 m.

VII.2.2. *In situ* measurements

Spatial and temporal patterns of the siltation were characterised by using two kinds of data. Firstly, we have benefited from single-beam bathymetric surveys (transects visible in Figure VII.1c) performed by the marina before and after each dredging campaigns (2 per year, acquired by the management of the marina) from 2010 to 2017. We obtained Digital Terrain Model (DTM) from an Inverse Distance Weighted interpolation (IDW) and produced bathymetric differential allowing depth comparisons between months and years. The coverage of dredging operations had to be considered in the medium to long-term analysis of the medium-term evolution of the bed (Figure VII.1b). These results provided a very good basis for the calibration and the validation of the model, and they were supported by high-resolution bed altimetry observations acquired with an ALTUS altimeter. This autonomous device couples a 2-MHz acoustic transducer and a pressure sensor to measure the bed elevation at a resolution of 0.6/2 mm. From the 26th February to the 30th April 2019, two altimeters were positioned at two different locations. One was placed in the middle of the NE basin (circle 2 in Figure VII.1c) while the other was placed at the southern part of the SE basin (circle 3 in Figure VII.1c). The use of a tripod structure was necessary to secure the instrument at a fixed height of about 40 cm above the sediment surface. Turbidity probes *YSI 6600 V2* were also attached to the structures to measure suspension concentration at a constant depth (40 cm above sediment surface). Their 1000 NTU sensors displayed an accuracy of 0.3 NTU and were previously calibrated, which resulted in the regression $SSC = 976.92NTU$ for the sensor set in

the NE basin and $SSC = 1085NTU$ for the sensor set in the SE basin. R^2 value of 0.95 were found for both sensors. Turbidity data were also taken with the same sensor from the 19th April to 21th May 2014, at the entrance of the marina (circle 1 in Figure VII.1c). Time series of turbidity and seabed level were analysed in relation with weather-marine conditions to investigate siltation mechanisms and were also used to calibrate the hydro-sedimentary model developed for this study.

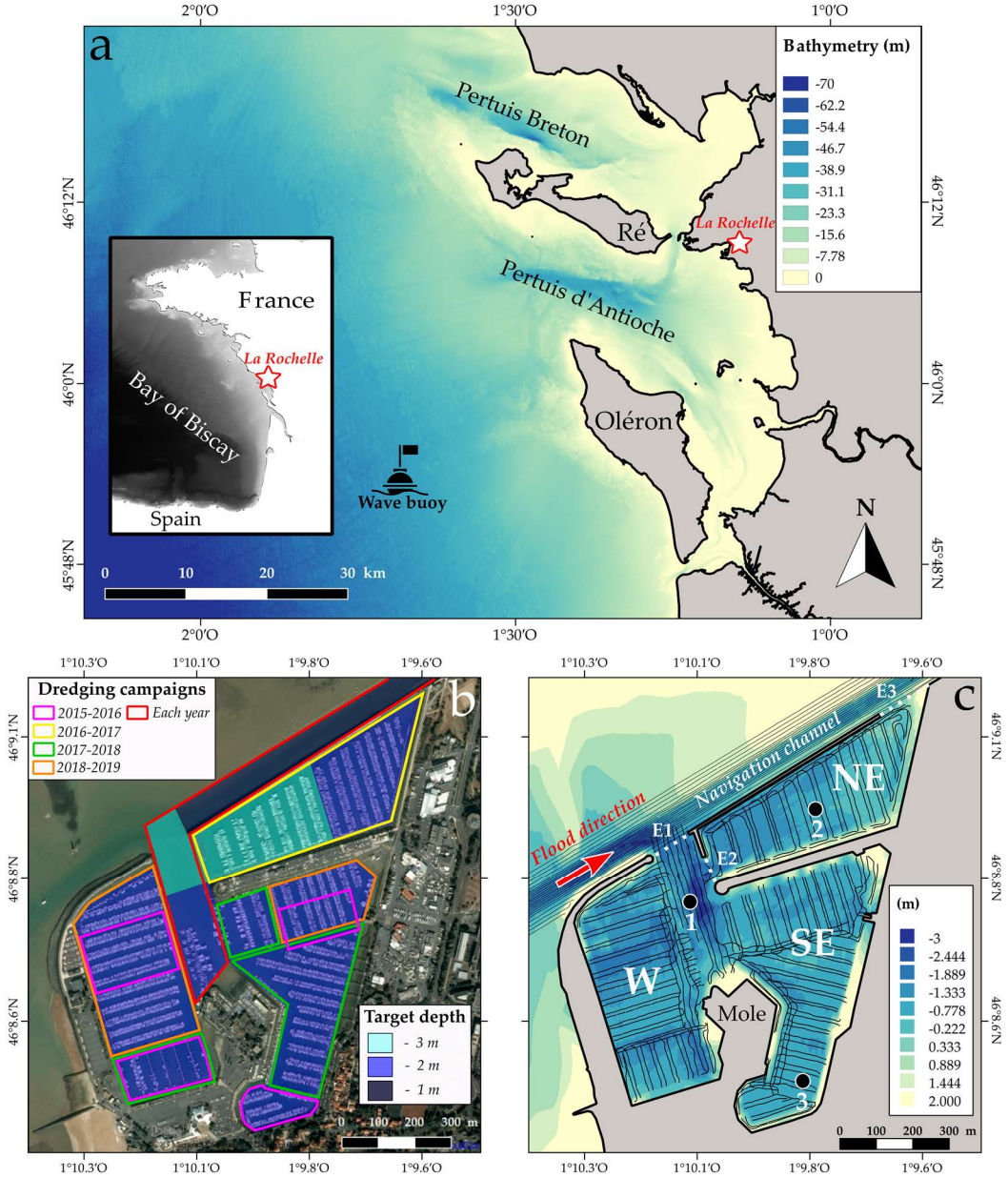

Figure VII.1. *(a) Bathymetry (SHOM, 2015) of the coastal area. The wave buoy (CANDHIS network) from where originate wave data is specified at a location offshore of the Oléron island. (b) Dredging area and target depth of the marina from 2015 to 2019. (c) Bathymetry of the La Rochelle marina and its navigation channel. The three entrances are specified in white dotted lines (E1, E2 and E3 for entrance 1,2 and 3, respectively) and the single-beam surveys taken in 2016 are represented by black lines. In situ data were taken at the level of the white-bordered black circles (circle 1 corresponds to a near-bottom turbidity measure taken in spring 2014 while circle 2 and 3 correspond to near-bottom turbidity and altimetry measures of the seabed taken in spring 2019).*

VII.2.3. Numerical modelling

To assess the efficiency of the siltation reduction methods tested in this study, we used the TELEMAC-3D model, part of the open-source hydrodynamic suite of TELEMAC MASCARET system (*Hervouet, 2000*), and adapted to free-surface flow modelling. This three-dimensional model, that solves the Reynolds-Averaged Navier-Stokes (RANS) equations, is able to compute 3D transport equation for the sediment concentration and to estimate the bed evolution. Turbulence was modelled with k-ε model, and the non-hydrostatic mode was used to perform simulations with a 5 s time step over a 35 km wide and 100 km long domain discretised on a 41 000 nodes unstructured grid. The resolution ranged from 2 km offshore to nearly 5 m in the marina and 8 vertical sigma layers were used, which led to a total of 320 000 nodes. Bathymetry originated from French Navy (hereafter SHOM) and single beam surveys acquired in the marina (Figure VII.1c). Bottom stress was computed through a Chézy parametrization. More details about the equations, the grid and the methods chosen are presented in *Huguet et al. (2019b)*. Along its open boundary, the model is forced by 34 astronomical tidal constituents obtained by linear interpolation from the global tide model FES2014. Atmospheric forcing was set over the whole domain with hourly sea-level atmospheric pressure and 10 $\boldsymbol{m}$ wind speed and direction (with a spatial resolution of 0.2°) originated from the Coupled Forecast System Model version 2 (CFSv2). The effect of floating docks and boats in the marina was also implemented in the model (*Huguet et al., 2019b*). Waves, water fluxes across the sea surface (precipitation-evaporation) and rivers input were neglected.

In the present study, we only work with cohesive sediment, thus we considered only the suspension load in the computation of the sediment transport. The vertical profile of the suspended sediment concentration is treated as passive scalar and is determined through a classical advection-diffusion equation with an additional advection term representing the settling velocity:

$$\frac{\partial c}{\partial t}+\frac{\partial uc}{\partial x}+\frac{\partial vc}{\partial y}+\frac{\partial wc}{\partial z}=\frac{\partial \nu_t \frac{c}{x}}{\partial x}+\frac{\partial \nu_t \frac{c}{y}}{\partial y}+\frac{\partial \nu_t \frac{c}{z}}{\partial z}+\frac{\partial w_s c}{\partial z} \quad \text{(VII.1)}$$

Where c represents the sediment concentration (gl^{-1}), w_s the settling velocity of the sediment (ms^{-1}), and ν_t the turbulent diffusivity coefficient (m^2s^{-1}), t the time (s), $[x, y, z]$ the components of the coordinate vector (m), and $[u, v, w]$ the mean flow velocities (ms^{-1}).

The variation of bed elevation is derived from the Exner equation:

$$(1-p)\frac{\partial Z_f}{\partial t}=D-E \quad \text{(VII.2)}$$

With p the bed porosity, Z_f the bed elevation (m), D and E the deposition and erosion fluxes of the sediment ($\mathrm{kg}\,m^{-2}s^{-1}$) that followed *Krone (1962)* and *Partheniades (1965)* formulae:

$$D=w_s C_0\left(\frac{\tau_{cd}-\tau_0}{\tau_{cd}}\right) \; if \; \tau_0<\tau_{cd}$$
$$E=M\left(\frac{\tau_0-\tau_{ce}}{\tau_{ce}}\right) \; if \; \tau_0>\tau_{ce} \quad \text{(VII.3)}$$

Where τ_0 is the bed shear stress (Nm^{-2}), C_0 the near bed concentration (gl^{-1}), M the empirical erosion rate Partheniades coefficient (kg $m^{-2}s^{-1}$), τ_{ce} and τ_{cd} the critical bed shear stress for erosion and deposition (Nm^{-2}), respectively.

As previous analysis (*IDRA, 2015*) showed that the sediment was very homogeneous in the marina, we used only one fraction of cohesive sediment and we set it to 15 μm, which represents the mean grain size of the marina (*IDRA, 2015*). One bed layer was chosen and was set at 0.1 m at the beginning of the simulation. Non-erodible areas were implemented at the level of rocky bottoms (*SHOM, 2015*). The mud layer density and the sediment density were set to 500 kg m^{-3} and 2650 kg m^{-3}, respectively. Flocculation was considered via the Soulsby formulation that is derived from Manning floc database (*Soulsby et al., 2013*). In this formulation, which is based on two-class floc populations (micro and macro flocs), the settling velocity is a function of the particle diameter, whose size is controlled by the turbulent shear stress and the sediment concentration. No consolidation model was solved for this study considering the small period simulated. A constant sediment concentration of 0.007 gl^{-1} was given to the liquid boundary and was representative of the suspended sediment concentration collected by SOMLIT network the 26th March 2019. Everywhere else, the initial concentration of sediment in the water column was set to 0 gl^{-1}.

VII.2.4. Methods to reduce siltation and to optimise dredging maintenance

To diminish the cost associated with dredging in La Rochelle marina, different approaches were adopted in the framework of this study. These approaches can be divided into two categories: the first aimed at reducing the siltation itself in the system with the help of constructional measures, while the second approach aimed at optimizing the dredging maintenance by excavating sediment traps inside and outside the marina.

VII.2.4.1. Constructional measures

The constructional measures implemented mostly consist of keeping the sediment out (KSO) and keeping the sediment moving (KSM) which are concepts developed in *Kirby (2011)* and *Headland et al. (2007)*. The strategies adopted are represented in Figure VII.2. In this section we develop their objective and their possible impact on siltation and hydrodynamics in the marina.

Narrowing entrance:

The entrance needs to be wide enough to allow the passage of vessels and thus optimize the nautical navigation. Entrance of a basin is one of the main factors controlling the water and sediment exchange (*Van Rijn, 2016*), and it is recommended to reduce as possible the width and depth of the entrance (*Krone, 1987*) and to optimise its shape and orientation. (*Jenkins, 1981a; Langedoen et al., 1994*). La Rochelle marina already presents specific features preventing from sediment trapping: its main entrance 1 is small and is placed parallel to the navigation channel. The entrance geometry can generate strong currents (> 1 ms^{-1}) during spring tides which promotes self-cleaning of the bottom. Consequently, this part of the marina does not

require dredging maintenance. The entrance 3, at the north-east, is larger, but the presence of complex and chaotic currents does not guarantee the safe passage of vessels. This, plus the presence of a pedestrian bridge overlooking the entrance, and the high siltation rates observed in the area, forced recreational boaters to use the entrance 1 to access the extension basin. In the framework of this study, we implemented the narrowing of the two external entrances to reduce sediment input into the marina (Figure VII.2). Considering the nautical requirements for navigation., three scenarios were investigated: entrance 1 and 2 sections were reduced by 15 - 20 %; entrance 3 section was reduced up to 80 %; a combination of the two scenarios.

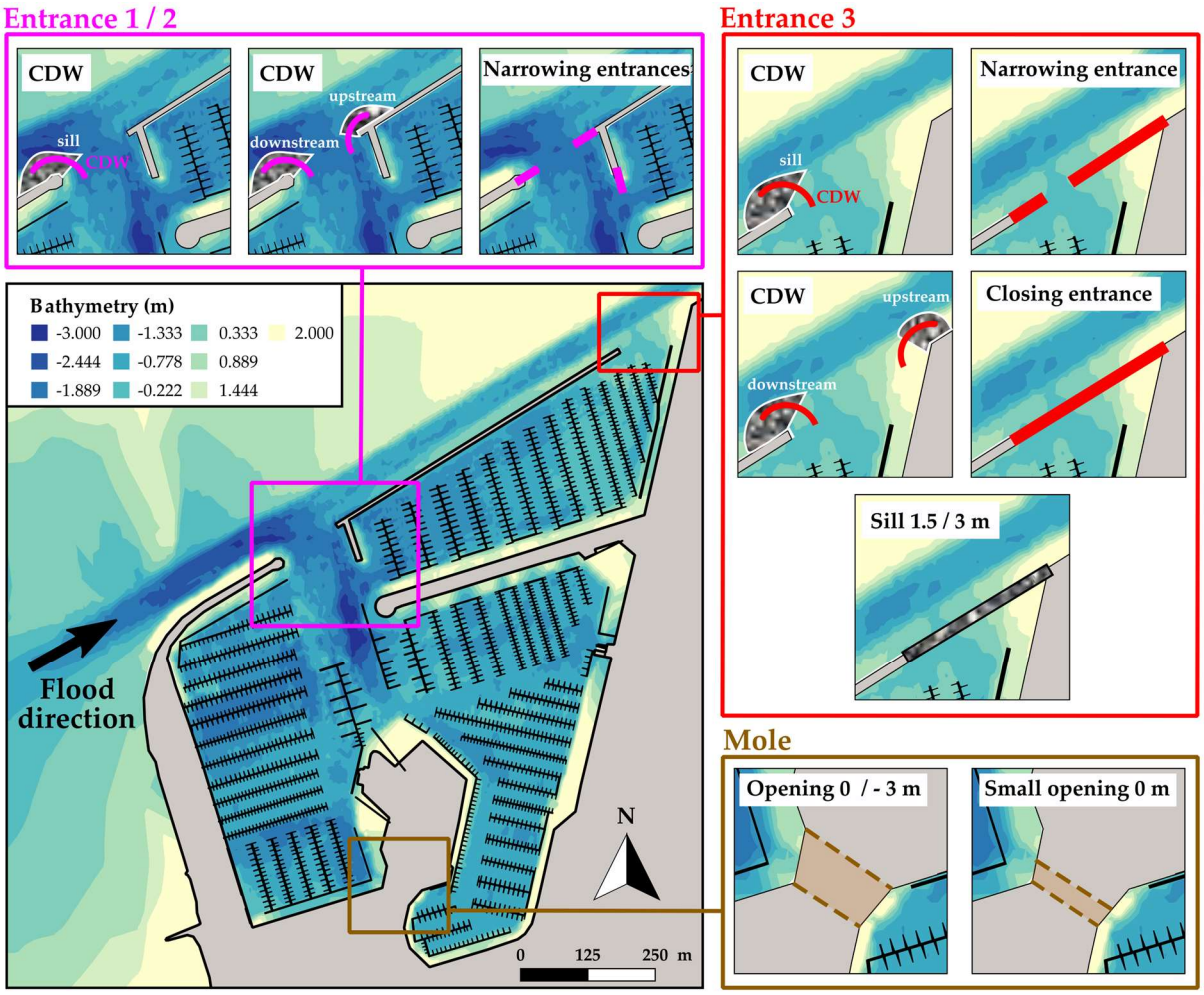

Figure VII.2. *Constructional measures implemented in the numerical study.*

Closing entrance 3:

Port basins with two or more entrances are opposed to single entry basins in terms of water renewal but also siltation. If the presence of several inlets can keep the sediment in suspension longer and can avoid constant and regular silting, it is nevertheless necessary to ensure that the flow velocities are sufficiently large. Otherwise, the additional inlets may contribute to an increase in siltation. La Rochelle marina is currently connected with the open sea via two external entrances (Figure VII.1). While entrance 1 is essential for the passage of ships, entrance 3 offers no navigational advantage. We have defined a situation where entrance 3 would be completely closed. The close of this entrance is expected to significantly alter the tidal prism

exchange of the marina and thus the sediment exchange mechanisms. Basin siltation was reduced at the Port of Bremen (Germany) by closing a side entrance in 1992 (*Nasner, 1997*). The closure diminished the maintenance dredging by 36 %. The construction of a lock for the main entrance 1, which is relatively present in small-scale basins with high tidal ranges, has not been considered here because the port must always be practicable.

Sill:

Underwater sills consisted of raising the bottom locally to reduce the effective water depth for horizontal and vertical circulation. The effect of underwater sill structures on siltation was studied in laboratory (*Van Schijndel & Kranenburg, 1998*) and also numerically (*Azizah et al., 2017*) but was extensively investigated in a wide range of application in the field of river dynamics (*Thompson, 2002; Saleh et al., 2003; Galia et al., 2016*). Even if it restricts navigation, a sill positioned at the level of an entrance can be used to reduce exchange volume but also sediment input from sediment-laden density currents in tidal semi-enclosed basins (*Van Rijn, 2016*). In this view, the construction of a sill at the level of the entrance 3 was tested. The building of such structure would not have been possible at the level of entrance 1 and entrance 2 because of the necessity to keep depths in phase with vessels draughts. Two different heights of sills were tested with a length and width equivalent to the entrance 3 dimensions. The rectangular shape of the underwater sill was naturally based on the dimensions of the entrance 3 (Figure VII.2) and two different heights were tested (1.5 m and 3 m above chart datum, corresponding to 3/8 and 6/8 of the mean water depth, respectively).

Current-Deflecting-Wall:

The Current Deflection Wall (CDW) is a curved vertical wall that extends from the bottom to the surface, and that is positioned at the seaward flood corner of a port entrance, as close as possible to the navigation channel (Figure VII.2). This passive structure is designed to control the flow within the system to divert sediment path by reducing the flow entrainment and the strength of the mixing layer. It also prevents from eddy flow formation and its associated siltation and reduces the retention time of the sediments in the basin (*Christiansen and Kirby 1991; Schwarz et al., 1995; Winterwep, 2005; Barneveld & Hugtenburg, 2008; Van Rijn, 2016*). The device can be combined with a low bed-mounted sill linking CDW to the shore and used to control the vertical exchange at the entrance and to trap the sediment-laden near-bed transport before entering the port (*Kirby, 2011*). Finally, the CDW is supposed to promote the tidal filling of the basin through the channel between the curved wall and the entrance corner (around 10 to 15 % of the total entrance width for *Van Leeuwen & Hofland, 1999*), rather than through the rest of the entrance.

The first CDW was constructed in 1991 at the entrance corner of the Köhlfleet basin of the Port of Hamburg located in the Elbe river. The 150 m long curved wall reduced the dredged quantities by approximately 40 % (*Winterwerp, 2005*). In the same port, a new CDW was designed for the Parkhafen basin, and numerical simulations have shown a possible reduction of siltation of about 50 % (*Winterwerp et al., 1994; Delft Hydraulics, 2001*). Over several years it was found that the yearly siltation rate was reduced by up to 45 % (*PIANC, 2008*). Another study from the Port of Antwerp showed a reduction of 10 - 20 % after the implementation of a CDW (*Decrop et al., 2013; Roose & Meersschaut, 2013*). The efficiency of CDW significantly

depends on the hydrodynamic conditions and the geometry of entrance, but the result is also quite sensitive to the detailed design of the device. Incorrect design can deteriorate flow patterns by generating new eddies and provokes additional siltation. Laboratory experiments (*Crowder et al., 2001; Van Leeuwen & Hofland, 1999*) showed that the optimal height for the sill ranges is around 25 – 35 % of the mean water depth. The width of the channel between the CDW and the port has to be comprised between 10 % to 15 % of entrance width and the total length of the wall is about 30 % to 40 % of entrance width. The orientation of the wall, as well as the shape of the nose and leading edge of the wall, has to be streamlined to be the most efficient possible in reducing siltation, without affecting navigation. (*Van Leussen & Winterwerp 1990; Kujiper & Winterwep, 2003; Van Rijn, 2003).*

For this study, we implemented a 90 m long and 4 m wide CDW at the corners of entrance 1 and 3, following the recommendations provided through the literature mentioned above. The crest level of the associated sill was set to 25 % of the mean water depth (1.5 m above chart datum) and the external nose of the CDW is rounded. One of the main limitations is the narrowness of the already existing navigation channel and entrance 1 that did not enable to place the device further away from the infrastructures, especially at the level of entrance 1. The device is about 20 m from the corners of entrance 1 and about 30 m from the corner of entrance 3 (Figure VII.2). Both a downstream (towards the sea) and an upstream (towards the land) were implemented. The aim is to operate on the sediment transport of both flow and ebb. The upstream CDW could allow preventing from the massive return of sediment particles during ebb that has been deflected initially by the downstream CDW during flood.

Creation of an opening:

While in the previous scenarios, the approach was to minimise the sediment-laden flows into the system, the strategy here is to maximise flow velocity within the system to prevent sediment from settling (*Headland et al., 2007*). We concentrated our efforts on improving the structural elements of the marina to enhance the training of natural flows and suspended sediment. An opening between the W and SE basins was proposed at the southern (and most sheltered) part of the marina (Figure VII.2). The original opening is 90 m long and 40 m width and follows the layout of the central mole. If the idea is selected, the mole would be accessible by a gateway. This measure could create a circulation between the most sheltered areas of the marina, especially at the southern part of the SE basin where the renewal is low compared with the rest of the marina (*Huguet et al., 2019a*). It would result in a decrease in the retention time of the water in the marina via recirculation. The main objective is to generate sufficiently large velocities to keep sediment in suspension and reduced the siltation in the system. The effect of a smaller opening (90 m long, 12 m width) was also investigated. Several depth levels were defined at the level of the opening (-3 m and 0 m below chart datum).

VII.2.4.2. Dredging Measures

Dredging measures involved the creation of sediment traps. In high-silted harbours and fairways, sediment traps represent a conventional form of sedimentation control that allows to keep water depths compatible with navigation and to reduce the maintenance dredging (*Claassens, 2002; Duràn et al., 2009; Hamburg Port Authority, 2012*). The concept is to

dredge a trench by excavation that reduces flow velocities in the above water column and then decreases the capacity to transport sediment and generates the settling of sediment. The sediment trap represents storage space for the deposited sediment that will be dredged. This method does not generally decrease the volume of dredged material required, but it can reduce the unit cost of dredging by avoiding interference with navigation during dredging operations if the trap is outside the port (*Sharp, 2010*). It can also place the dredging closer to the disposal area and allows to focus dredging operations in specific locations rather than everywhere in the port. To restore a sediment trap depth, an ordinary maintenance dredging is required, but sand by-passing systems can be integrated into the trap if the mud has not been consolidated (*Clausner, 1999*). Location of the trap must be defined considering the convenience for dredging operations, the maintenance cost, but also and especially its efficiency to minimise siltation in the desired area. *Gardner (1980)* has shown that the sediment trap is particularly effective when the sediment transport has a dominant direction, and when the particle size is less than 63 μm (which is our case). However, finer particles as clay and silt, take time to settle and practical limitations of trap storage space and settling time available do not allow sediment trap to capture every particle flowing over (*Van Rijn, 2016*).

For this study, we defined thirteen sediments traps inside and four outside La Rochelle marina (Figure VII.3) to test their efficiency in order to optimise maintenance dredging. Each trap has a surface area ranging from 2.5 to 5 ha and a constant depth of 3 m below chart datum. Inside the marina, sediment traps were defined in function of the geographical and siltation dynamics pattern characteristics. Outside, the four sediment traps were positioned along with the navigation channel. One (front) was placed just in front of the entrance 1, on the other side of the channel and the three others were located further west, on the sides of the channel. Every sediment trap is supposed to be situated on the muddy seabed (*SHOM, 2015*) to avoid derocking operations. The external traps are supposed to reduce the supply of sediment directly arriving into the port, while the internal traps should focus the siltation without having a significant influence on the supply, upstream.

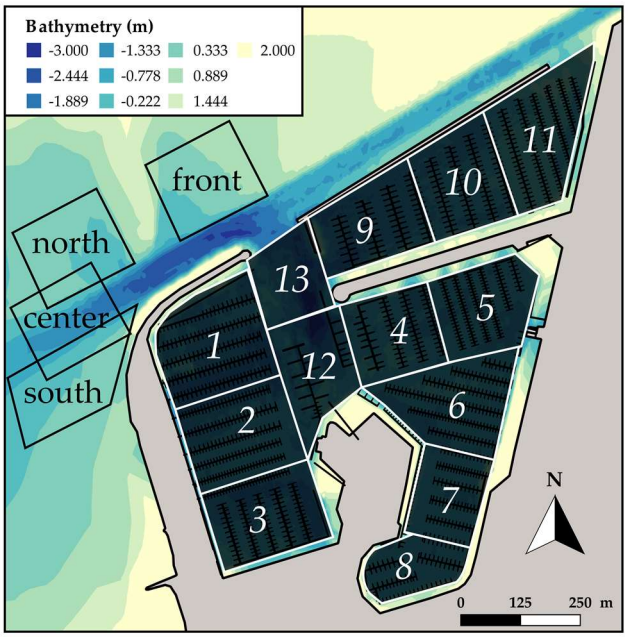

Figure VII.3. *Localization of the sediment traps implemented as dredging measures.*

VII.3. Results

VII.3.1. Seasonal to annual siltation dynamics

By computing the bathymetric differences over the period 2010 to 2017, we compiled information about the annual and seasonal sedimentation in the marina. As the area is extensively dredged, we had to consider the areas, target depths and volumes involved at each dredging operations since 2010. Some operations, as roto-dredging, were not referenced and the comparison of single-beam bathymetric surveys also led to uncertainties, and the absence of data under floating docks and moored boats also create a gap in measurements. Thus, it has been challenging to compute the siltation rate accurately, but we managed to determine typical siltation patterns in the temporal and spatial context (Figure VII.4).

The siltation rate is lower during summer with average monthly sedimentation about 2-4 cm depending on the location while during winter it can increase over 7 *cm* per month. We did not detect annual trends in the dynamics of siltation in the period 2010-2017 and the regularity of dredged volumes (200 000 m^3 per year) can support this finding. It is worth noting that the marina is not entirely dominated by siltation and in particular at the main entrance of the marina where there is no siltation. An area from entrance 1 to the central mole, which corresponds to the access channel leading to the SE basin, is self-dredged all year long because of the high velocities occurring during the flood (Figure VII.4). To the east of this area, at the level of the access channel leading to the W basin, the largest siltation rates occur with 50 to 70 *cm* per year depending on the location (Figure VII.4). The W basin presents higher annual siltation rates (40 to 50 *cm*) than the SE basin (20 to 30 *cm*). The most sheltered areas from deposition are the northern parts of the W and SE basins and the southern part of the SE basin. Finally, the NE basin displays high rates (40 to 60 *cm* per year) and comparison between 2010 - 2014 and 2014 - 2017 periods has shown that the expansion has not substantially affected the siltation rates in the initial marina.

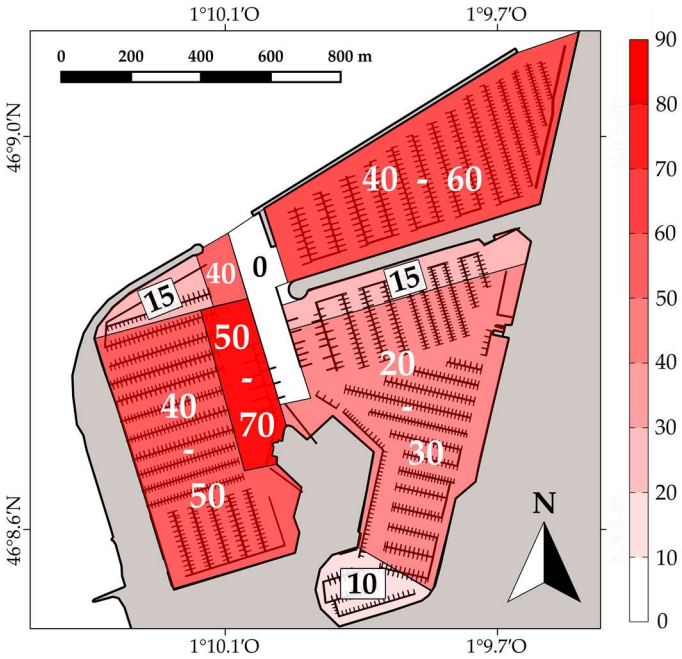

Figure VII.4. *Approximative annual siltation rate (cm) determined by the comparison of bi-annual single-beam bathymetric surveys from 2014 to 2018.*

VII.3.2. Daily to monthly siltation dynamics

In Figure VII.5, results obtained from the acquisition of sediment-related data (turbidity, bed elevation) were analysed about the weather-marine conditions (tide, wave and wind regime). The objective here is to characterise the relationship between the siltation, the suspended sediment concentration (SSC), and the main environment forcings. Only data taken from 18th March to 27th April 2019 are shown because of the presence of artefacts in the bed-elevation data acquired in the SE basin at the beginning of the measurement. For this period, total siltation of about 3.5 cm and 2 cm was measured in the NE and SE basins, respectively. In the NE basin, siltation dynamics is stronger (a 2 cm increase was observed in 5 days at the beginning and the end of April) but more contrasting, while in the SE basin it is more linear (Figure VII.5d). The two locations present a very high variability of near-bed SSC (less than 0.005 to more than 0.35 gl^{-1}). SSC signals generally display the same behaviour at both locations, but the values are more than two times lower in the SE basin. (0.021 gl^{-1} against 0.045 gl^{-1} on average). Near-bed SSC signals are highly variable at both short-term (daily) and medium-term (weekly and monthly) timescales, and they are well correlated spatially (R^2=0.56). Deposition patterns also present a good correlation (R^2=0.54). Finally, SSC and deposition are slightly less correlated between them (R^2=0.36 in the NE basin and R^2=0.44 in the SE basin) but Figure VII.5 shows the relative good phasis between the most turbid measurements and the largest deposition rates. Comparatively, the lowest turbidities coincide with stable to (slight) erosive periods. Spring tides generally display more than five times higher SSC than neap tides depending on the wind-wave conditions.

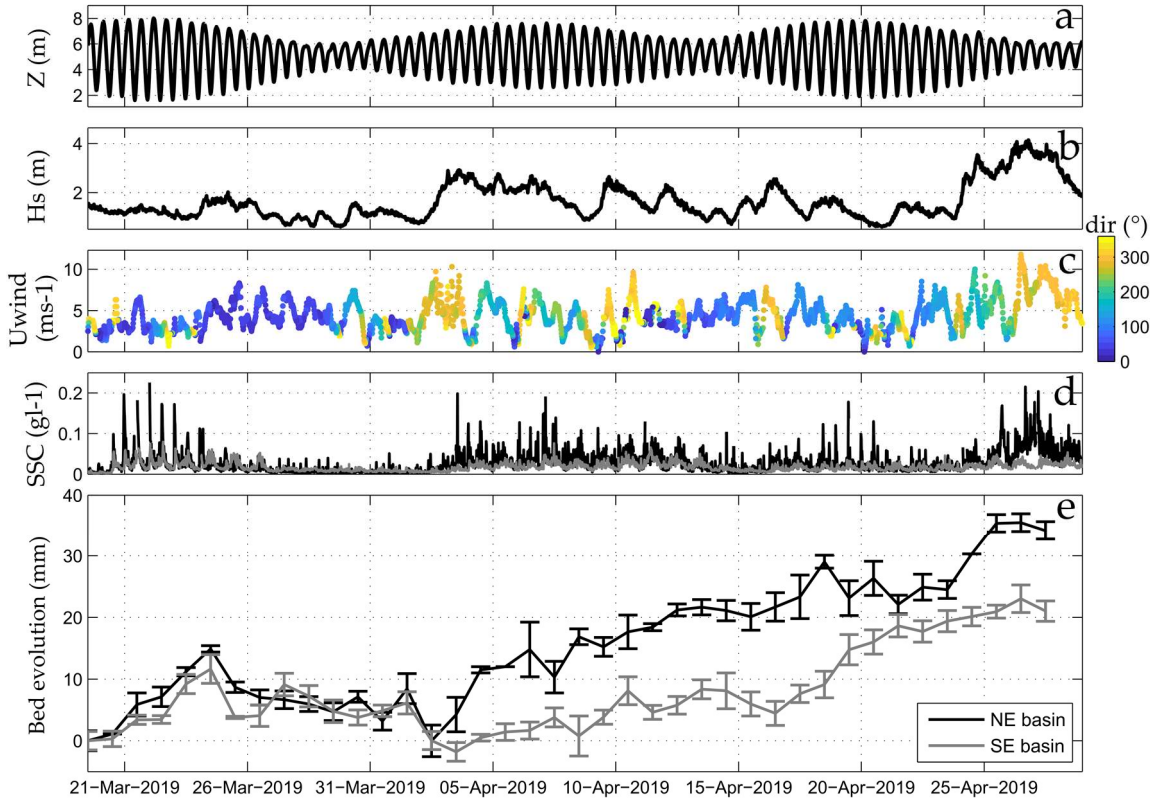

Figure VII.5. *Time series of water level (a), significant wave height provided by CANDHIS network (b), wind velocity provided by Météo-France (c), near-bed suspended sediment concentration (d), and daily-average evolution of the seabed (e) acquired in spring 2019.*

Over time, near-bed SSC, siltation and environmental data varied strongly at daily to monthly scales. To investigate the different mechanisms involved in the dynamic of siltation, we assessed the relative importance of the different environmental drivers via the computation of Pearson correlation coefficients (Table VII.1). Results were obtained by daily-averaging data to detrend the tidal signal.

SSC was primarily correlated with the wind and offshore wave regime at the three locations. The correlation for SSC is lower in the SE basin than in the NE basin (Table VII.1). Deposition patterns are more correlated to the environmental data in the SE basin than in the NE basin. No correlation was found with wave period and wave direction was not considered as a determining factor in the SSC and bed elevations patterns (waves mainly originate from north-west to south-west directions). A high correlation exists between the wind and the wave regime ($R^2 = 0.75$ between wave height and wind intensity and $R^2 = 0.61$ between wave direction and wind direction). The wind effects are anisotropic depending on its direction. Western winds are relatively in phase with strong wave energy and large SSC that led to strong deposition rates for both spring and neap tides. In phase with 6 m wave height and 15 ms^{-1} west to south-west winds, SSC displayed maximum values of 0.35 gl^{-1} and 0.22 gl^{-1} in the NE and SE basin, respectively (data not shown). Eastern winds, that correspond to offshore winds, are in phase with low wave energy (Figures VII.5b-5c), and also low SSC during neap tides.

The general trend of siltation and turbidity is also correlated to the tidal range (Table VII.1). The semi-diurnal rhythmicity of the currents is in phase with the SSC signals. SSC is way more correlated at the entrance and the SE basin compared to the NE basin where the complexity of the currents can alter the SSC signal. The distinction between spring and neap tides is significant in particular when the wave and wind contribution is small. Spring tides alone can generate 0.17 $gl^{-1}$and 0.05 gl^{-1} peak turbidities at the level of the NE and SE basins while neap tides generally display constant 0.01 gl^{-1} turbidities. The deposit variations can be linked to the sediment availability variations displayed by SSC signals. Spring tides promote the accretion in the two basins while during neap tides there is a quasi-no modification of the seabed except in the NE basin where slight erosive patterns are visible. This behaviour could be the result of the width reduction of the bottom fluid mud layer because of self-weighted consolidation, which is more visible when a smaller amount of sediments is brought into the marina.

Table VII.1. *Pearson correlation obtained between environmental forcings and in situ measurements. Shaded boxes correspond to coefficients with p-value < 0.005.*

	Wave Height	**Wave direction**	**Wind intensity**	**Wind direction**	**Tidal range**
SSC 1 (2014)	0.73	0.16	0.80	0.52	0.47
SSC 2	0.79	0.21	0.57	0.45	0.15
SSC 3	0.30	0.25	0.18	0.12	0.43
Bed elevation 2	0.21	0.06	0.08	0.16	0.13
Bed elevation 3	0.44	0.23	0.26	0.33	0.16

Even if wave energy is able to significantly increase SSC and the related siltation, the tidal signal is the main driver of SSC variability, at the three locations. From the analysis of the

2019 (Figure VII.5) and 2014 (Pers. Comm.) SSC time series, we depicted four typical hydro-sedimentary periods in the marina: neap tides with small waves offshore, neap tides with large waves offshore, spring tides with small waves offshore and spring tides with large waves offshore. For the sake of clarity, we showed SSC signals obtained in 2014 (at the entrance) and 2019 (in the NE and SE basins) separately in Figures VII.6-VII.7, respectively. We tried as much as possible to select similar weather-marine conditions. The resolution of the bed elevation data did not enable us to observe the fluctuations of the seabed at the scale of one tidal cycle. However, the characterisation of SSC obtained during these specific periods will help us to understand the temporal and spatial mechanisms of siltation in the marina.

As mentioned above, with small wave energy, neap tides display very low SSC values (between 0.05 and 0.1 gl^{-1}) but with 4 m wave regime, SSC can be the same order of magnitude or even larger than during spring tides (Figures VII.6b-7b). With and without waves, spring tides generate larger variability of SSC values which is reflected by the presence of peak SSC up to 10 times larger than the rest of the time (Figures VII.6c-6d-7c-7d). Maximum near-bed SSC occurs at mid-flood at the entrance. In the NE basin, SSC peak is in phase with the high tide while it occurs 1 - 2 h after high tide, in the sheltered part of the SE basin (the latter result is also observed during neap tides in Figure VII.7a). SSC peaks are generally, more quickly attenuated at the level of the main entrance. This attenuation is the slowest in the SE basin (Figures VII.7c-7d). SSC patterns observed during neap tides are more complex, in particular with the presence of strong waves (Figures VII.6b-7b). With small waves, we can notice the presence of quasi-systematic SSC peaks. At the entrance and NE basin, SSC peaks occurred approximatively at mid-flood, mid-ebb and high tide while SE basin displayed only one peak right after high tide (similarly to spring tides situation). Neap tides with large waves situation generate numerous SSC peaks. SSC is generally larger during ebb in the NE and SE basin (Figure VII.7b).

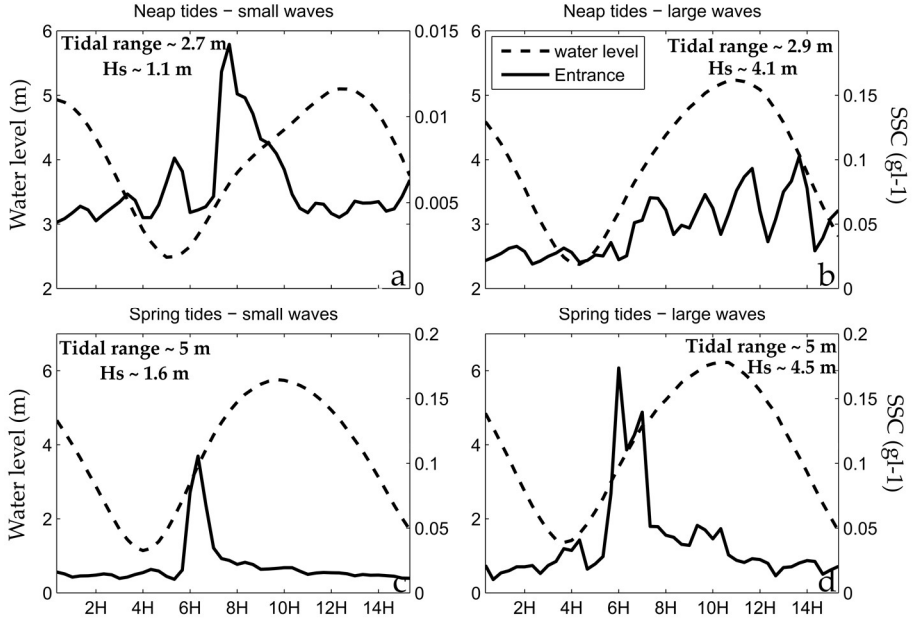

Figure VII.6. *Four typical periods occurring at the entrance of the marina in terms of near-bed SSC (black line): (a) neap tides situation with small waves (b) neap tides situation with large waves (c) spring tides situation with small waves (d) spring tides situation with large waves. The tidal range and wave regime conditions are displayed on the figures and the dashed line specifies the water level.*

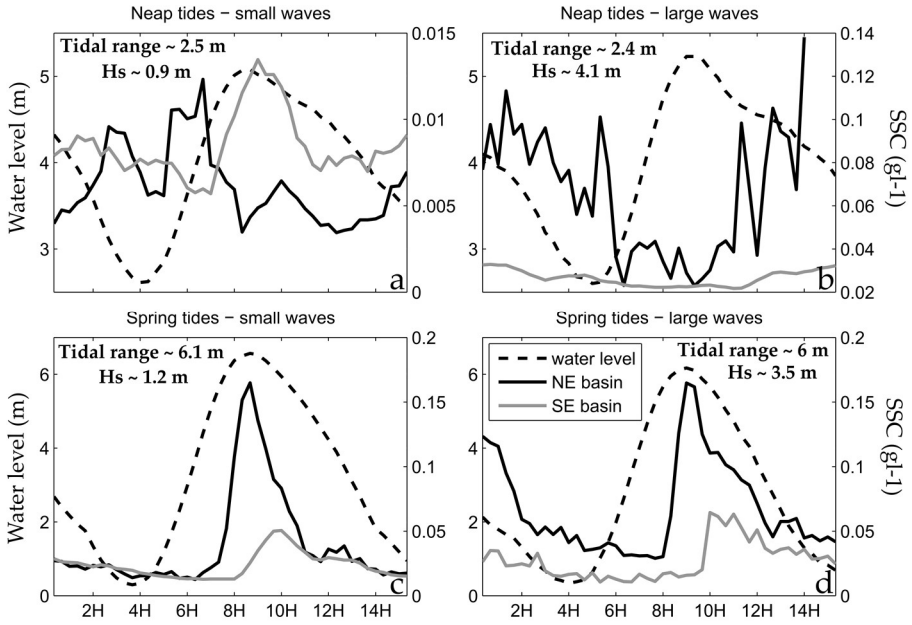

Figure VII.7. *Four typical periods occurring at the entrance of the marina in terms of near-bed SSC at the NE basin (black) and the SE basin (grey). (a) neap tides situation with small waves (b) neap tides situation with large waves (c) spring tides situation with small waves (d) spring tides situation with large waves. The tidal range and wave regime conditions are displayed on the figures and the dashed line specifies the water level.*

VII.3.3. Reduction siltation measures

VII.3.3.1. Validation and general simulation set up of the model

To investigate the efficiency of constructional and dredging measures in reducing marina siltation, we performed a 15-days simulation beginning from 19th March to 3rd April 2019. This period was characterised by the presence of small waves (< 2 m) and eastern winds, and was subjected to spring tides and neap tides. As our model only simulate tide and wind effect, we selected a low wave energy interval of time to calibrate and validate its performance. Calibration process involved the calibration of specific parameters whose the chosen values for this study are displayed in Table VII.2. The value of the Partheniades erosion coefficient used ($1 \times 10^{-4}\ kg\ m^{-2}\ s^{-1}$) is within the range generally found in the literature (*Whitehouse, 2000; Benson et al., 2014*). The main challenge was to reproduce the same patterns of SSC and siltation at two locations at the same time. Comparison with near-bed SSC and bottom elevations observations taken during this period shows an accurate correlation between calculation and measurements (Figure VII.8). *RMSE* of 3.3 mm and 2.5 mm were reached for near-bed SSC acquired in the NE and SE basin, respectively. Modelled SSC peaks were relatively in phase with observations but amplitudes were better reproduced during spring tides than neap tides. Predicted SSC was effectively lower than expected during neap tides, in particular in the NE basin. A strange SSC behaviour is observed in Figure VII.8b, just before the 26th March 2019. This pattern, which is not in phase with the tidal signal, and decorrelated from the rest of the time-series, could be the result of anthropic local re-suspension. Raw observed bottom elevations displayed a large variance in the two basins. Figures VII.8c-8d clearly show that the modelled bottom elevation follows the same trend and minimise the

RMSE. The erosive pattern slightly visible in the NE basin (Figure VII.8c) is not reproduced by the model but can be the result of the consolidation effect which is not implemented in our model parametrization for this study.

Table VII.2. *Calibration parameters used for this study.*

Calibration parameters	Partheniades coefficient	Critical erosion shear stress	Critical deposition shear stress
Value chosen after calibration	1×10^{-4} kg m^{-2} s^{-1}	0.18 Nm^{-2}	2.5 Nm^{-2}

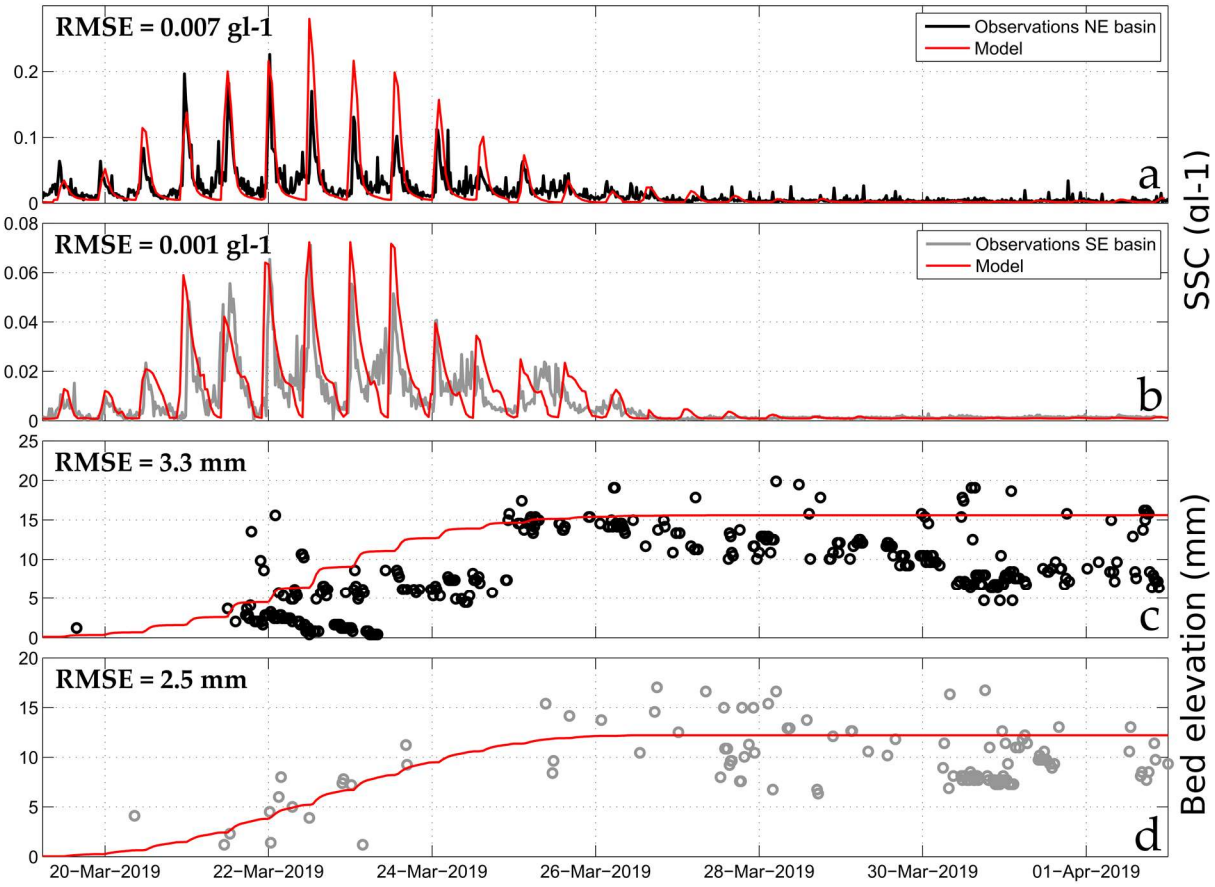

Figure VII.8. *Comparison of SSC and bed evolutions observed (in black and grey, for NE and SE basins, respectively) and modelled (in red) for a 15-days simulation (from the 18th March to 2nd April 2019). RMSE between modelled and measured data are also presented for each variable.*

VII.3.3.2. Constructional measures effect

The proposed scenarios were investigated considering siltation induced both in the marina and its navigation channel. For the sake of clarity, we did not analysed the effect of each and we retained the most representative scenario. Table VII.3 gathers siltation results obtained for scenario involving constructional measures. Siltation volumes, mean siltation and the reduction (or increase) induced by the implementation of constructional measures were

computed for each scenario after a 15-day simulation with spring and neap tides. Reference scenario corresponds to the current situation with the actual marina configuration.

Table VII.3. *Simulation results obtained with the implementation of constructional measures, after a 15-day simulation.*

Constructional measures		Marina		Navigation channel		Total Evolution
		Siltation volume [m^3]	**Siltation evolution [%]**	**Siltation volume [m^3]**	**Siltation evolution [%]**	
Reference		*12 725*	/	*980*	/	/
Closing Entrance 3		12 920	+ 1.6	1 874	+ 91.2	**+ 7.9 %**
Shallowing entrance 3	Sill 4 m	12 734	+ 0.1	1 882	+ 92	**+ 6.7 %**
	Sill 2 m	12 674	- 0.6	1 419	+ 44.8	**+ 2.8 %**
Narrowing	Entrance 1/2	12 630	- 0.7	741	-24.4	**- 2.4 %**
	Entrance 3	12 290	- 3.4	1 668	+ 70.2	**+ 1.9 %**
	Entrance	11 930	- 6.2	1 048	+ 6.9	**- 5.3 %**
Opening	0 m depth	12 466	- 1.9	1 077	+ 9.	**- 1.2 %**
	- 3 m depth	12 592	- 1	997	+ 1.8	**- 0.9 %**
	Small 0 m	12 568	- 1.2	989	+ 1.1	**- 1.1%**
CDW Entrance 1	Down	12 610	- 0.9	926	- 5.5	**- 1.2 %**
	Up-down	12 230	- 3.8	254	- 84	**- 8.9 %**
CDW Entrance	Down	12 310	- 3.2	1 099	+ 12.1	**- 2.1 %**
	Up-down	10 430	- 16	959	- 2.2	**- 16.9 %**

The most efficient constructional measures involved the implementation of CDW at the corner entrances of the marina. Figure VII.9 allows comparing the effect induced by the presence of CDW compared to the reference situation (Figure VII.9a). The installation of CDW only at entrance 1 mainly generates supplementary siltation in the NE basin (Figure VII.9b), without decreasing the total volume of siltation in the marina (Table VII.3). The presence of both upstream and downstream CDW at the corners of entrance 1 more than slightly reduces siltation (Figure VII.9c, Table VII.3) by significantly reducing the deposition in the navigation channel but at the same time, focusing it in the NE basin. The presence of downstream CDW at each corner of entrances 1 and 3 is not able to really improve the situation but the combination of both upstream and downstream CDW enables a global siltation reduction of 16.9 % in the marina, while it slightly increases siltation in the western part of the navigation channel (between entrance 1 and 3). The latter result is the most significant, even by combining it to other constructional measures (opening, narrowing...) we did not improve this ratio of siltation reduction.

Generally, Figures VII.9f-9g-9h-9i-9j-9k and Table VII.3 confirm the lack of efficiency induced by the modifications applied to the entrances. The shallowing, narrowing and closing of entrance 3 even increased siltation, in particular in the navigation channel. The worst result appeared when closing entrance 3 with a global increase in siltation of 7.9 % even if the siltation is reduced up to 18 % in the NE basin. These measures reduce the amount of siltation

in the NE basin but increase it in the W and SE basins. Only the narrowing of entrances 1 and 2 and the combination of the narrowing of entrances 1, 2 and 3 reduced siltation, but in a very moderate way, in the NE basin (a maximum of 5.3 % siltation reduction compared to reference situation). This latter scenario is also the most efficient (among all the scenario involving constructional measures) to reduce siltation in the NE basin (Figure VII.8h).

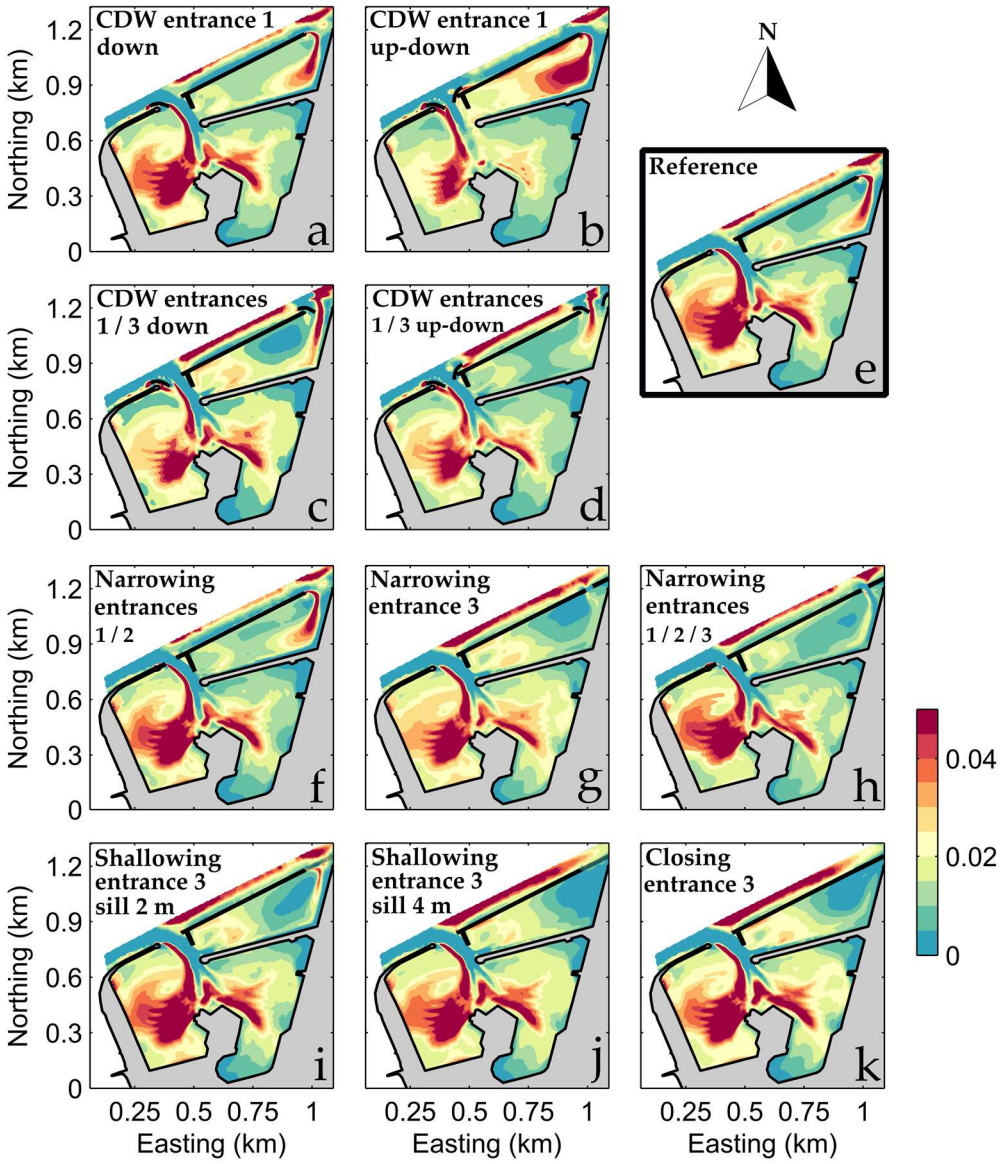

Figure VII.9. *Final evolution of the bed elevation in the marina, for the reference situation (e), the scenarios with CDW (a), (b), (c), (d), and the scenarios with entrances modifications (f), (g), (h), (i), (j), (k).*

The influence of an opening between SE and W basins is displayed by bed elevation differences (compared to the non-constructional situation) in Figure VII.10. We observe a slight reduction of the siltation in the inner parts of the marina while the siltation in the eastern part of the navigation channel is slightly increased. When comparing it with Table VII.3, this measure is non-efficient in terms of siltation (around 1 %) and the modulation of the depth and the width of the opening do not improve its effect.

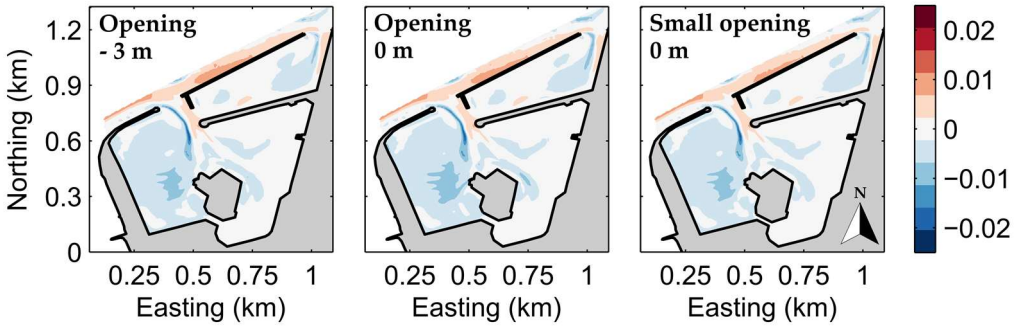

Figure VII.10. *The bathymetric differences obtained between the scenarios with opening and the reference situation.*

VII.3.3.2. Dredging measures

Table VII.4 provided results obtained with the implementation of internal and external sediment traps. Internal sediment traps slightly affected the siltation in the marina. Here, we present cases where the sediment trap configurations generate a decrease of the siltation in the marina (other cases very slightly decrease or increase it). These cases correspond to internal sediment traps 3, 6 and 13 (Figure VII.3). Similarly to Figure VII.9, Figure VII.11 displays the final evolution of the bed elevation obtained at the end of each simulation. Compared to reference situation (Figure VII.4a), additional siltation is visible at the level of each sediment trap (symbolised by dashed lines), but it does not attenuate drastically the rate of siltation in the rest of the marina. Table VII.4 results confirm the very moderate impact of the implemented sediment traps, and for every other configuration (data not shown) the impact is relatively minimised at the scale of the entire marina. Internal sediment traps can capture a maximum of 8% more sediment compared to a situation without trap. It highlights their small trapping efficiency. They do not, therefore, focus deposition and do not permit to optimise dredging maintenance.

Sediment trap configurations		Marina		Navigation channel		Total Evolution
		Siltation volume [m^3]	Siltation evolution [%]	Siltation volume [m^3]	Siltation evolution [%]	
Reference		*12 725*	/	*980*	/	/
Internal	2	12 581	- 1.2	977	- 0.4	**- 1.3 %**
	6	12 591	- 1.1	974	- 0.6	**-1.2 %**
	12	12 527	- 1.6	975	- 0.5	**- 1.7 %**
External	Front 3 *m*	12 645	- 0.7	1 159	+ 18.3	**+ 0.7 %**
	Center 3 *m*	11 065	- 14	1 256	+ 28.2	**- 11.1 %**
	North 3 *m*	9 328	- 26.7	564	- 43.5	**- 27.8 %**
	South 3 *m*	9 041	- 29	524	- 46.5	**- 30.2 %**
	North + South 3 *m*	6 839	- 46.3	244	- 75.1	**- 48.3 %**
	North + South 6 *m*	5 002	-60.7	188	- 80.1	**- 62.8 %**
	South 6 *m*	7 129	- 44	463	- 52.8	**- 44.6 %**

Table VII.4. *Simulation results obtained with the implementation of dredging measures, after a 15-day simulation.*

The influence of external sediment traps is more pronounced. Four configurations were tested. The front main entrance trap was not able to reduce siltation (Table VII.4) even if its

influence is visible in the NE basin (Figure VII.11e). North, and especially south trap, significantly reduced siltation in every basin of the marina (Figures VII.11f-11g). Their combination is even more effective and allows to minimise sediment deposition up to 48.3 % (Table VII.4). Finally, to test the depth sensitivity of the trap, we performed simulations with 6 m south and the combination of 6 m north and south traps (which are extreme cases). These traps were found to be 30 % more effective in reducing siltation in the marina and we obtained a 62.8 % reduction with the combination of north and south 6 m below chart datum traps. The deposition is also drastically reduced in the navigation channel in particular when the two traps are combined (Table VII.4). Even if the deposition was reduced by keeping the sediment out of the marina, the spatial patterns of the siltation are the same than in the reference situation. Consequently, external sediment traps located along with the main channel navigation, before the main entrance, are the most effective solutions modelled among both constructional and dredging measures.

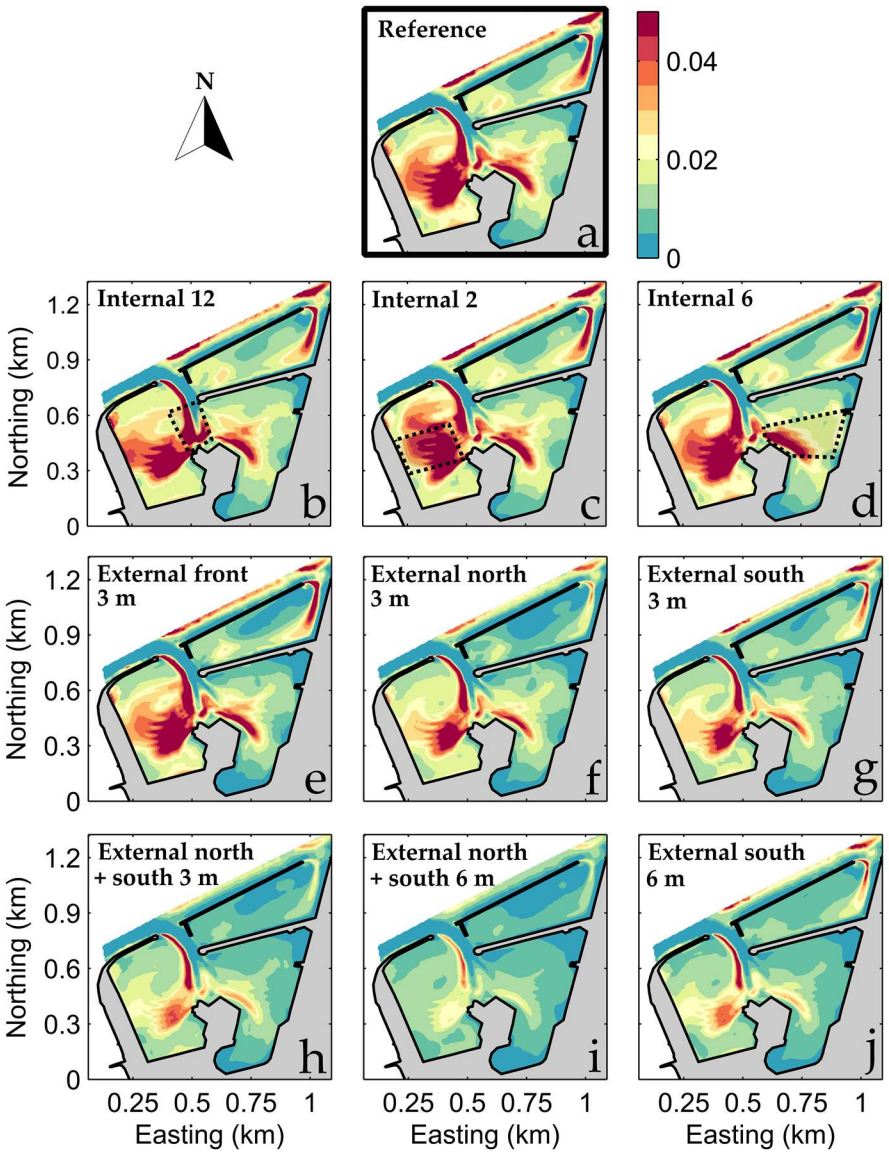

Figure VII.11. *Final bed evolution obtained for each simulation with dredging measures. (b), (c) and (d) represents situations with internal sediment traps while (e), (f), (g), (h), (i), (j) represents the situations with external traps.*

VII.5. Discussion

VII.5.1. Sediment dynamics and siltation mechanisms in the marina.

Contrary to many ports in the world (*Vanlede and Dujardin, 2014; Shanehsazzareh & Ardalan, 2019; Lee, 2019; Ramakrishnan, 2019*), La Rochelle marina does not suffer from siltation at the level of its entrance. It is important to consider this feature because an excess of sediment at the entrance and access channels can significantly reduce the accessibility of a port, which is thus, not the case here. While the amount of sediment dredged every year in the marina infers an average sedimentation rate of 50 cm/year, significant spatial variability of the siltation is, however, observed in the marina (Figure VII.5). The highest variability is seen at the entrance where the highest levels of siltation and also the lowest, are located side by side in the continuity of the entrance. When comparing siltation patterns to the circulation (*Huguet et al., 2019b*), we observe that the most dynamic part of the marina is also the less silted. This area can even suffer from episodic erosive periods (< 5 cm/year) which suppose that bed shear stress at this level is sufficient to re-suspend the muddy bottom. From the main entrance to the SE basin, the access channel is subjected to strong flood and ebb currents, particularly during spring tides where it can overpass 1.5 ms^{-1}, while currents intensity drastically attenuate when entering the several basins of the marina (*Huguet et al., 2019b*). On the opposite, the western part of the entrance, situated along with the W basin, is subjected to weaker currents, especially in the direct vicinity of the entrance. This contrasting behaviour of the velocities during the flood could explain the siltation patterns expressed in Figure VII.4. When considering the hydrodynamics within the marina, the dominance of semi-diurnal rhythmicity of the circulation shows that the tidal filling represents the main mechanism involved in the sediment transport into the marina. It could explain why siltation patterns, in particular at the entrance, differs from high siltations levels encountered in the ports mentioned above. In these ports, exchange flow at the port entrance is dominated by horizontal entrainment by mixing layers, often expressed by the presence of an eddy, and generating maximum siltation at the entrance (*Winterwep, 2005*).

As mentioned by several authors (*De Nijs et al. 2009; Van Maren et al., 2009*), the siltation of a port will also depend on the relationship between water exchange and SSC. Large fluctuations were presented in the SSC time series, and a significant relationship was observed between SSCs and the phase of tidal currents, particularly during spring tides. In the marina, tidal cycles are an important source of variability in turbidity, as seen in other harbours (*Ruhl et al., 2001; Schoellhamer, 2002; Xiong et al., 2017*). The presence of near-bed SSC peak in phase with the high tide in the two basins (Figure VII.6) is the reflection of sediment deposition under the influence of weak current activity. The mid-flood SSC peak experienced at the entrance could be generated by both the presence of sediment suspended outside but also more locally in the marina. The homogeneity of the water column in terms of SSC could, however, be explained by the predominance of external sediment input arriving into the marina during the flood peak currents. Neap tides display more complex SSC patterns, and even if the fluctuations are less pronounced, the presence of mid-ebb SSC peaks both at the entrance and the NE basin (Figures VII.6a-7a) could be the reflection of local re-suspension. This behaviour is not visible in the SE basin, where the maximum SSC is only reached at slack tides, which could be explained by the relative weaker intensity of the currents at this level, compared to the two other locations. More generally, during spring tides, the marina is dominated by semi-

diurnal suspended concentrations which indicate that the sediment transport is mainly driven by advection. The Spring/neap tide variation in sediment import and deposition also supports this hypothesis of sediment import through advection.

Contrary to the port of Zeebrugge (*Vanlede & Dujardin, 2019)*, this spring/neap tide variation is also visible in the landward part of the port, which implies that circulation and deposition patterns occurring in the most sheltered part of the marina is still governed by tidal processes. However, the discrepancies displayed between the two locations NE and SE basin locations could be explained by boat re-suspension, dredging activities or even gravitational flow of mud layers inside the marina (*Vanlede & Dujardin, 2019*). Conversely, neap tides display quarter-diurnal signal of the concentration in the entrance and NE basin, which could be the result of localised resuspension (*Weeks et al., 1993*). Concentrations involved demonstrate the main dominance of sediment transport from the ocean to the marina and the weak contribution of currents to the re-suspension in the marina itself. The amount of sediment brought into the marina is significant during spring tides which infers the prominent role of the tide in the re-suspension, offshore, and its main contribution to the advection of this re-suspended material into the marina. SSC signals also revealed that a significant part of the material brought is deposited at high tide in the basins. Maximum deposit then occurred during spring tides when more sediment particles are transported into the marina. Finally, the data support the hypothesis that most of the sediment input occurs from mid-flood to high tide, as experienced in the Port of Zeebrugge (*Vanlede & Dujardin, 2019*).

As seen in Figure VII.5 and Table VII.1, local wind and wave regimes also contribute significantly to the global increase in SSC and the related deposition in the marina. The significant correlation with wave energy suggests that wave resuspension, offshore, is an important driver of turbidity, as seen in other coastal areas (*Jing & Ridd, 1996; Geyer, 2004; Green, 2011; Seers, 2015; Grifoll et al., 2018; Tang, 2019*). This result confirms the simulation results obtained by *Le Hir et al. (2010)* which stated that swells had a dominant effect, particularly during storms, on the resuspension and transport of cohesive sediments (up to 4 times greater than the action of spring tides). Strong westerly winds (from SW to NW) are the main vectors for the transport of re-suspended sediment in the marina. They drastically increase wave energy (Figures VII.5b-5c) and thus, resuspension, which generates high levels of turbidity (Figures VII.5d-5e). The duration of the wind action is also a limiting factor in the generation of waves, even if the wave-turbidity environment is highly sensitive to short-term wind events. Once disturbed, fine sediments remain in suspension for longer periods depending on the tidal influence. The wave effect is the main driver of turbidity (and thus of deposition) during neap tides, while during spring tides, it is added to the tidal effect to generate large deposition rates in the marina. To the opposite, offshore easterly winds do not generate sufficient wave energy to resuspend bed sediments and thus, do not impact the spring/neap tidal process of deposition occurring in the marina. As the study area is subjected to strong seasonal climate variations, we could expect a significant seasonal variation of the sediment concentration and related-deposition in the marina. In the area, summer presents minimal low-pressure system activity resulting in a weak wind regime while winter is characterised by extreme western wind activity (*Huguet et al., 2019a*). Consequently, turbidity and related siltation in the marina could be increased during winter, as measured in *Vanlede & Dujardin (2019)*. The comparison of bathymetric surveys and the measurements of higher levels of turbidity offshore in winter (*Luna-Costa et al., 2015*) also support this assertion. As

waves are significant contributors to the turbidity and related siltation experienced in the marina, future changes to the global wind-wave climate (*Young et al., 2019; Morim et al., 2019*) could also influence marina siltation and thus port operations.

VII.5.2. The efficiency of the constructional measures in reducing siltation

Results show the relative inefficiency of the constructional measures to prevent siltation in the marina. The modifications of the entrances are not able to reduce significantly the amount of sediment entering the marina. This result could signify that the current configuration of the entrances is already effective in controlling the water exchange with the local environment and associated sediment input. Entrance 1, which is the only practicable external entrance, is already narrow, compared to the size of the marina. The presence of a constant self-dredging at this level also reflects the efficiency of the entrance to increase circulation and minimise sediment input.

The closure of entrance 3 is worse than expected and more than slightly increased the siltation in the W and SE basins. This result demonstrates that, even if the NE basin appears structurally separated from the rest of the marina, exchange processes taking place there substantially affect hydro-sedimentary dynamics in the rest of the marina. The recirculation generated by the presence of two entrances in the NE basin is, thus, able to minimise siltation in the W and SE basins. However, the through-flow of water and sediment in the NE basin does not generate sufficiently large velocities to prevent from the settling of particles which could explain the significant siltation experienced by this basin (Figure VII.4), and the significant reduction of deposition obtained when limiting the external exchanges. Finally, reducing the width entrance of every entrance is the most efficient constructional scenario to reduce siltation in the NE basin. Width reduction increased the capacity of the currents to transport sediments in the water column and thus reducing the deposition, but this effect is mostly restricted to the NE basin where velocities are increased about 10 %. Even if interesting results were obtained in the NE basin, the limited margin-left to modify the marina structure and layout did not allow us to find an ideal scenario to reduce significantly the siltation.

Simulation results with different configurations of CDW showed that the construction of only one CDW structure isn't efficient enough to reduce subtantially the siltation in the marina. This could be mainly due to the dominance of the tidal filling in the exchanges processes of the marina. CDW structures act mainly on the near-bed density currents and the turbulent mixing layer generated by the horizontal entrainment and thus, do not substantially alter tidal filling. Even if we obtained interesting results implementing CDW at each entrance and both at the upstream and downstream positions, it is still significantly lower than the results obtained in the literature (*e.g.* 40 % and 50 % of siltation reduction in *Winterwerp (2005) and Winterwerp et al. (1994)*). Considering the high costs involved in the construction of such structures and the possible inconvenience for the navigation, it does not seem applicable to the marina of La Rochelle. The attempt to generate recirculation flow patterns between the most sheltered parts of the marina appears not sufficient to keep sediment moving through the marina and reduced overall siltation. Even if currents can reach 0.09 ms^{-1} at the level of the opening, hydrodynamics at the back of the SE and W basins are very slightly enhanced (+ 0.5 % of the velocities on average in each basin). The resulting circulation appears not sufficient to significantly re-suspend sediments or to keep sediments moving through the marina (Figure VII.8). The deposition patterns and associated siltation are thus not really impacted, which

proves that the recirculation obtained in the landward part of the marina is finally not a good solution.

All these results demonstrate that minor constructional measures are not able to significantly alter the sediment input at the scale of the entire marina. As seen above, tide and waves are the two key processes driving the coastal sediment transport in the coastal area and thus the inexorable accumulation of particles in the La Rochelle marina. According to an extensive literature (*Straaten & Kuenen, 1958; Postma, 1961; Postma, 1967; Groen, 1967; Dronkers, 1986; Ridderkinhof, 1997; Cheng & Wilson, 2008*), tidal asymmetry and settling lag effect are the main mechanisms involved in the particle entrapment of tidal embayments. As explained in *Friedrichs et al. (1998)*, the settling lag effect could be enhanced by along-channel width convergence resulting from the funnel-shaped configuration of La Rochelle bay. The almost dead-end position of the marina in the bay could add to this deposition trend, even if the entrances configurations are oriented along with the main cross-shore sediment transport. To effectively control siltation in the long term, a more significant restructuring of the marina should be undertaken. It highlights the importance of considering hydro-sedimentary dynamics in the selection of site location when a new port basin is projected.

VII.5.3. The efficiency of the dredging measures in reducing siltation

Results showed that 3 m below chart datum internal sediment trap are not effective in focusing siltation in specific areas and thus, in optimizing dredging maintenance. We did not test deeper levels because it the bedrock outcrops at this level and derocking operations are costly operations. Conversely, the implementation of external sediment traps located downstream to the port, along the navigation channel, reduced very significantly the siltation rate inside the marina. The north and south trap benefit from the fact that the circulation is mostly focused onto the navigation channel during flood when most of the particles are brought to the system. In Figure VII.1c it is visible that the navigation channel, in the bay, is guided to the south by the port infrastructure and to the north by a local shallowing in the cross-shore axis. It corresponds to the remains of an old dike built during the Grand Siege of La Rochelle in 1627 (*De Beauce & Thurninger, 1885*). This effect is enhanced during spring tides when, from low tide to almost mid-flood, a major part of the bay has emerged, which forces the water masses entering the marina through the navigation channel. The downstream traps, locating at the western side of the navigation channel take advantage of this nautical constraint and provide space for the particles, resuspended offshore, to settle just before pursuing their travel along with the navigation channel. It should also be noted that the implementation of a centered trap located between the north and south traps was less effective in reducing siltation in the marina (-11.1 % in Table VII.4) which signifies that the most effective solution is to place the trap along and not transversely to the main sediment transport.

Considering the effective results obtained with the south trap and the potential presence of rocky outcrops at the level of the north trap, the most feasible option resulting from this study, is the dredging of a trap at the level of the South trap described in Figure VII.3. Figure VII.12 allows investigating the siltation of the south trap obtained from a simulation with a 3 m depth below chart datum. The bed evolution differential (Figure VII.12a) clearly shows the trapping efficiency of the measure and the net filling of the trap. The deposition generated by the trap is not restricted to its level but also extends further north. Significant deposition occurs at the northern part of the trap (and also the nearest from the navigation

channel) and also in the center, according to the cross-shore transect made in Figure VII.12b. The longshore transect (Figure VII.12c) demonstrates the relative homogeneity in the deposition, even if it increases eastward. Finally, the south trap suffered a 0.08 *m* of deposition, on average. If we approximate this value to a year (without considering the climate and wave effect, and the diminishing of the trapping efficiency related to the filling), we obtained a 2 m deposition. This value is theoretical but can provide a good approximate of the amount of material that can be deposited at this level, and the necessity to dredge this trap frequently (each year), to keep its trapping efficiency and avoid adverse effects. It should also be noted that this value is obtained via simulations based on large spring tides (tidal range > 6 *m*) that induced one of the most significant deposition rates measured in the NE and SE basins during the entire acquisition period (Figure VII.7e).

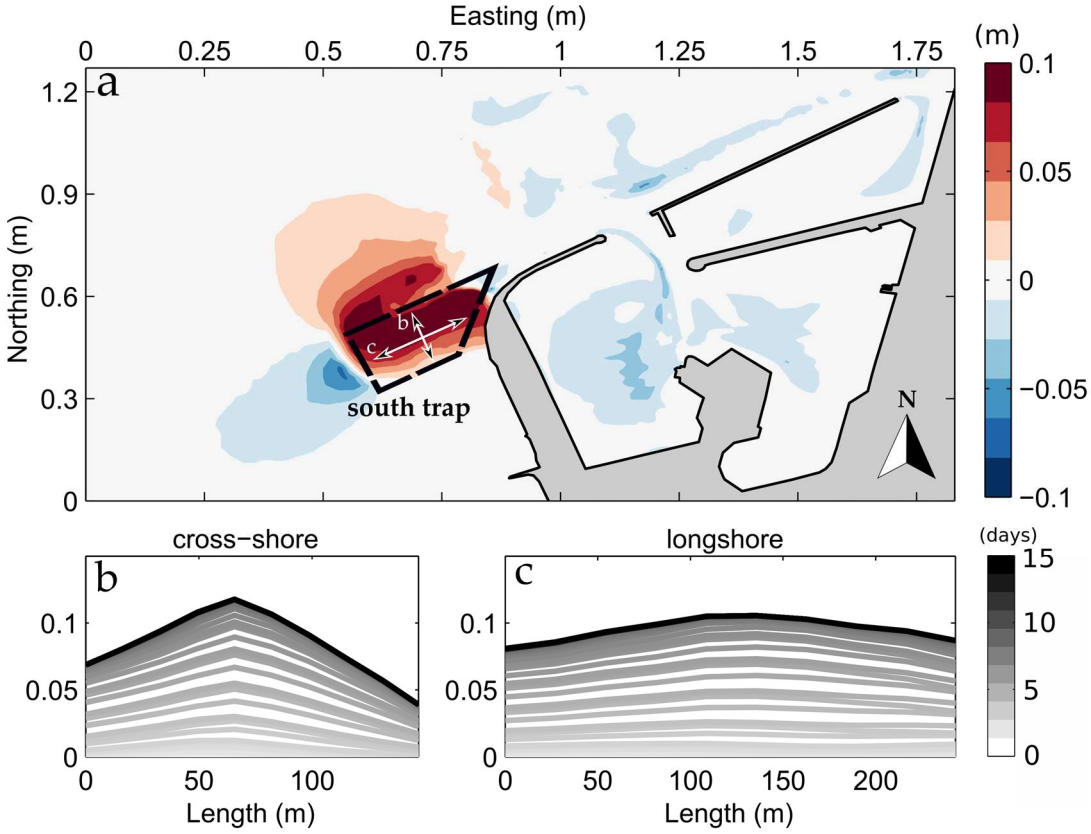

Figure VII.2. *(a) Differential bed evolution between the simulation with a 3 m south trap and the reference situation. South trap location and cross-shore/longshore axis are specified. (b) South trap cross-shore transect of the bed evolution difference obtained between the simulation with a 3 m south trap and the reference situation. (c) South trap longshore transect of the bed evolution difference obtained between the simulation with a 3 m south trap and the reference situation.*

The trapping efficiency of the south trap was then investigated by setting different depths levels in the trap (Figure VII.13). The maximum of siltation reduction that was obtained in the marina involved the use of a 12 *m* below chart datum the south trap and reached 53.2 %. This case is very extreme and not realistic but highlights the maximum possible capacity to capture sediment particles for the south trap. Results show that depth was a key parameter in the control of siltation until a certain depth (approximately 8 *m* below chart datum). The location and the size of the trap were also tested to find the optimal configuration. Table VII.5 resumes the setting parameters and the results obtained in terms of siltation for

different south traps with a depth set to 3 m below chart datum. A trap located more offshore (300 m further west, still in the navigation channel axis) was less effective in trapping cohesive sediment. The trapping efficiency of the trap was not really improved by increasing its width southward, but is, on the contrary, highly sensitive to its length (Table VII.5). As indicated by the results, the depth, length, and location of the trap significantly control the trapping efficiency of such features. In our case, it would be recommended to use a trap at the north-west corner of the marina, at the south and the nearest possible of the navigation channel. This trap should be longer than wider, and its depth should be ideally overpassed 3 m below chart datum in the function of the rocky outcrops presence. Future bottom surveys will be carried out to determine the hard rock bottom depth. In function of the results obtained, a more thorough modelling study will be undertaken to determine the most optimal sediment trap configuration possible. A full-scale test could be carried out in 2020 during the next dredging maintenance season. In the long-term, it will allow us to assess not only the effectiveness of this method but also sediment dynamics via the measurement of deposition levels inside the traps.

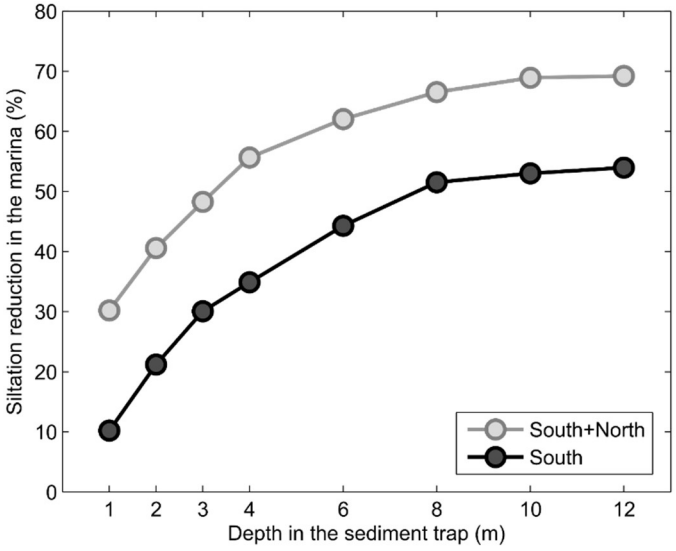

Figure VII.3. *Siltation reduction obtained by setting different depth levels to the South and North sediment traps in the 15-day simulations.*

Table VII.5. *Characteristics of the several south traps configurations and their effect on siltation reduction in the marina.*

Trap configurations	Area	Dimensions	Initial volumes to dredge the trap	Siltation reduction observed in the marina
1: South	4.5 ha	250 x 150 m	75 500 m^3	30.2 %
2: South more offshore	4.5 ha	250 x 150 m	55 000 m^3	24.2 %
3: South longer	8 ha	400 x 150 m	120 000 m^3	44.3 %
4: South smaller	2.5 ha	150 x 150 m	40 000 m^3	19.5 %
5: South larger	7 ha	250 x 250 m	100 000 m^3	31.1 %

VII.6. Conclusion & Perspectives

In high-silted ports environments, reducing siltation should be an essential component of port management strategies. In La Rochelle marina, a more integrated and long-term approach was initiated to fight against siltation and reduce the cost associated with dredging maintenance. Many mechanisms, described in *Winterwep (2005)*, are involved in port siltation and their complex interaction is not easy to understand when considering only the geometric component (*Vanlede & Dujardin, 2014*). The variety of port configurations and site location requires a detailed study of the sediment dynamics before designing siltation-reducing measures. We used measurements acquired from 2010 to 2019 to characterise sediment dynamics and siltation rates within the marina but also to set up, calibrate and validate the use of numerical modelling with TELEMAC-3D.

Measurements have shown the large variability displayed by the turbidity and deposition patterns in the marina. Particles entering the marina are mainly brought by tidal advection and the contribution of local re-suspension was found to be very weak in terms of suspended sediment concentration. Turbidity and siltation are highly correlated to the wind-wave regime and to the tide. Tidal currents are the main driver of the resuspension offshore and the transport of fine sediment into the marina. Waves, particularly during large events, significantly contribute to the offshore resuspension. The combined action of tide and wave regime in the area produces an average of 50 *cm* annual siltation in the marina, with strong spatial variations. The funnel-shaped morphology of the surrounding bay, the tidal asymmetry and settling lag effect are supposed to mainly contribute to this deposition rate. The configuration of the marina also promotes siltation by drastically decreasing the velocities in its inner parts and thus preventing from local re-suspension.

The hydro-sedimentary model implemented for this study aimed at investigating the efficiency of possible remedial actions to minimise siltation and its associated dredging maintenance in the marina. Most of the constructional measures implemented herein exerted very slight influence on the total deposition in the La Rochelle marina. The shallowing and closing of a side entrance increased the siltation in the rest of the marina while the narrowing of entrances slightly decreased it. The creation of an opening in the landward part of the marina did not improve sufficiently the circulation and more than slightly decreased the siltation. Finally, the use of CDW structures did not appear feasible, considering the expensive costs involved and the lack of efficiency. The implementation of dredged sediment traps inside the marina did not really permit to focus sediment deposition and thus, could not optimise the associated dredging maintenance. The best strategy consisted of dredging external traps at the north-west corner of the marina, along with the main navigation channel. Thanks to the particular configuration of the La Rochelle bay and marina, these traps intercept the main source of sediment from the ocean. Our results indicate that siltation, in the marina, can be reduced by more than 50 % with the use of a single trap (south). Optimum trap dimensions were also determined in terms of location, width, length and depth. Even if a significant reduction was computed when implementing an external trap, it remains clear that the amount of dredged material will be approximately the same in the current situation if we want to keep the trapping efficiency of the trap. However, dredging operations will be less frequent inside the marina and will less hinder the navigation and boating activities. Beyond the siltation management aspect, the creation of a trap and its regular monitoring could allow us to study more accurately sediment dynamics by avoiding measurements artefacts generated

by dredging (*Henriksen et al., 2012; Van Maren et al., 2015; Stark et al., 2017),* and boating activities (*Hamill et al., 1999; Rapaglia et al., 2011; Gelinas et al., 2012*) on local resuspension. Future research will allow us to identify the depth of the rocky bottom at the level of trap location. Following the results obtained, an optimum trap will be planned, considering the results obtained in this study. Other possible solutions will also be investigated as the use of re-suspension systems (*Weisman et al., 1996; Headland et al., 2007*) to take advantage of ebb currents to evacuate sediment particles from the system.

This study has contributed significantly to the understanding of sediment dynamics in the marina and provided several development paths concerning siltation management. Despite all the solutions proposed, the volume to dredge in the local environment remains the same, which clearly shows the difficulty to reduce or to divert the sediment input arriving in the bay and in the marina. It highlights the importance of the site selection and the necessity to study beforehand the trapping efficiency of such maritime infrastructure. Further developments are needed to consider wave effect, several grain size fractions and consolidation processes. Sediment dynamics but also the trap effect will be modelled over longer periods (monthly to annually) for a wider range of weather-marine conditions. River inputs were not discussed here because of their distance from the marina. However, even if they do not seem to have a direct influence on the sediment processes they provide a source of fine sediments in the long-term and the use of numerical modelling, supported by *in situ* data could help us assessing their contribution into the marina siltation. The use of multi-beam echo-sounder will enable to characterise more accurately the deposition patterns, in particular below the floating docks. Finally, to monitor the abundance, size and properties of flocs we will also benefit from UVP measurements (*Gorsky et al., 2000; Picheral et al., 2010*) inside the marina.

Chapitre VIII

Conclusion & Perspectives

VIII.1. Conclusion Générale

Ce travail est né d'une volonté commune, entre la régie du port de plaisance de La Rochelle et La Rochelle Université, de mieux comprendre la dynamique sédimentaire au sein du port des Minimes. Les mécanismes d'envasement et les processus de renouvellement des eaux ont été caractérisés au travers d'approches mêlant les observations *in situ* à une modélisation numérique opérationnelle. Les résultats obtenus viennent étoffer la connaissance de la dynamique des littoraux artificialisés, un sujet qui représente un enjeu sur le plan sociétal, économique et environnemental. Ils permettent aussi de répondre des problématiques concernant la gestion du dragage et plus généralement de l'envasement. Dans ce travail, la caractérisation de l'hydrodynamique portuaire fut un enjeu important et nécessaire pour pouvoir appréhender de manière holistique la dynamique sédimentaire. En se basant sur une approche couplée modèle-observations, les principales thématiques abordées ont concerné:

- L'impact des structures flottantes (pontons et bateaux) sur l'hydrodynamique.
- L'influence du vent et de la marée sur la circulation et le renouvellement des masses d'eaux.
- La connaissance des rythmes de sédimentation et des flux associés en lien avec le vent, les vagues et la marée.
- La mise en place et l'évaluation de stratégies de lutte contre l'envasement et d'optimisation des activités de dragage.

L'originalité de ce travail réside principalement dans la prise en compte des structures flottantes. La forte couverture spatiale des bateaux et des pontons auxquels ils sont amarrés freine de manière drastique les vitesses de courants dans les bassins, en particulier pendant le flot. Leur présence force la courantologie principalement dans les chenaux d'accès principaux et secondaires. Leur impact est très localisé et impacte peu la dynamique extérieure au port. Nous avons intégré ces structures dans le système de modélisation et corroboré leur influence à l'aide d'observations *in situ*. Les résultats obtenus ont montré la nécessité de prendre en

compte ces structures flottantes dans ce type d'étude, pour des environnements similaires (bassin semi-fermé, faible profondeur d'eau, forte densité d'aménagements flottants).

L'étude, par modélisation, des flux totaux et résiduels a permis de quantifier l'influence conjuguée de la marée et du vent sur la dynamique spatiale et temporelle du port. La présence de trois entrées complexifie la direction et l'intensité des courants observés au cours d'un cycle de marée, ce qui génère de fortes asymétries en fonction du marnage. L'effet du vent peut s'avérer déterminant dans les processus d'échanges se déroulant entre la baie de La Rochelle et son port. L'utilisation d'outils permettant de tracer les masses d'eaux de manière lagrangienne et eulérienne a permis de quantifier le renouvellement des eaux portuaires au travers de différents descripteurs. Celui-ci est très variable en fonction de la position dans le port, mais aussi en fonction des conditions climatiques et océanographiques. La marée et la configuration fuselée de la baie de La Rochelle tendent à freiner le renouvellement alors que le vent peut l'augmenter drastiquement, en particulier les vents d'ouest.

L'analyse des données observées a permis de mettre en avant la forte corrélation entre la turbidité, l'évolution du fond et le régime de vent et de vagues et le rôle prépondérant que joue la marée dans le transport de sédiment cohésif à l'intérieur du port. Le sédiment apporté se dépose alors rapidement et génère un envasement annuel moyen de 50 cm, avec de fortes variations spatiales. De nombreuses stratégies ont été implémentées dans le modèle afin de diminuer l'envasement du port. Les mesures dites « constructionnelles », consistant à modifier les configurations d'entrée voire à créer des ouvertures au fond du bassin, ont peu affecté la sédimentation locale. D'après nos résultats, la solution la plus envisageable et la plus efficace consiste à creuser une souille le long du chenal de navigation afin de piéger une partie de l'apport sédimentaire en amont. Cette stratégie permettrait de diminuer de moitié les activités de dragage dans le port et de les concentrer plutôt au niveau du chenal.

Pour conclure, l'impact observé et modélisé des structures flottantes a montré l'importance de les prendre en compte dans ce type d'étude. La caractérisation de la dynamique du port, notamment exprimée par l'étude du renouvellement des eaux, pourra aussi bénéficier à d'autres observateurs scientifiques du port, travaillant sur des champs d'études variés (toxicité, biologie des organismes, corrosion des ouvrages…). De ce travail de recherche ont aussi émané plusieurs solutions concrètes dont la faisabilité sera discutée par la suite. Même si la diversité des ports et de leur environnement local ne permet pas de généraliser nos résultats, toutes les études et méthodes exposées dans ce manuscrit peuvent être transposables à d'autres ports dans le monde.

VIII.2. Perspectives

Comme tout projet de recherche, une thèse amène des questions et permet d'envisager des perspectives pour la suite. Les perspectives envisageables concernent principalement la compréhension de la dynamique hydro-sédimentaire et peuvent se classer en trois catégories: l'amélioration de la compréhension de la dynamique sédimentaire, l'enrichissement du modèle hydro-sédimentaire, et la mise en place et l'analyse de stratégies de lutte contre l'envasement.

Amélioration de la compréhension de la dynamique sédimentaire

Une des principales limitations techniques provient de l'utilisation de données bathymétriques obtenues par sondeur mono-faisceau. La faible résolution mais aussi l'absence d'informations sous les pontons ont limité l'analyse et l'interprétation des MNT et différentiels bathymétriques générés. L'utilisation d'un sonar multi-faisceaux est donc recommandée, notamment si la démarche du port est d'intégrer la compréhension des processus hydro-sédimentaires dans la gestion à long-terme des opérations de dragage. Sur le court terme, il est aussi envisagé de déployer de nouveau, des capteurs de turbidité à la fois en surface et au fond, et des ALTUS à d'autres endroits du port, et pour des périodes plus longues, afin de caractériser la dynamique sédimentaire plus finement. Pour étudier les flux sédimentaires de manière plus précise, le déploiement d'un ADCP à l'entrée du port et le traitement des données par backscattering pourrait être une éventualité. L'éventail de données pourra aussi permettre de valider de manière plus précise le système de modélisation. L'étude de la taille, de la forme et de la vitesse de chute des flocs pourrait aussi nous permettre d'investiguer de manière plus précise des comportements sédimentaires, en fonction des moments de la marée. Cette étape sera réalisable dans un futur proche avec l'utilisation d'un UVP (« Underwater Video Profiler »), dans le cadre de la thèse de Vincent Hamani initiée en 2018 à La Rochelle Université. Cet instrument de mesure nous permettra à la fois de caractériser les flocs mais aussi les produits issus de la bioflocculation tels que les fèces. Dans le port des Minimes, la partie immergée des pontons est marquée par une forte présence d'organismes colonisateurs: les ascidies. Les fèces de ces organismes marins, sont supposés avoir un impact non négligeable sur l'envasement dans le port, et notamment sous les pontons. Les informations récoltées, combinées aux données multi-faisceaux de l'évolution du fond sous les pontons, pourraient permettre d'évaluer l'influence de la biologie sur la sédimentation portuaire en général. La convergence de ces études biologiques, physiques et sédimentaires rappelle l'importance d'intégrer une approche interdisciplinaire dans la gestion de ce type d'espace littoral et anthropisé.

Enrichissement du modèle hydro-sédimentaire

Le développement du modèle hydro-sédimentaire est aussi à considérer. L'implémentation des vagues, par le biais du module TOMAWAC, serait une étape nécessaire pour caractériser et reproduire de manière le plus réaliste possible les processus hydro-sédimentaires à la fois dans les Pertuis et aussi dans le port. Il serait possible de quantifier et de comparer l'effet des vagues et de la marée sur l'envasement dans le port et dans la baie de La Rochelle. Cela permettrait de calibrer le modèle pour des périodes plus longues, pour pouvoir ainsi valider son utilisation sur le long-terme. Dans le cas où des simulations long-terme seraient mises en place, il faudrait prendre en considération les phénomènes de consolidation (physiques, mais aussi en lien avec l'activité biologique). L'intégration de plusieurs classes de sédiment est aussi à envisager comme axe d'amélioration même si on constate une grande homogénéité des sédiments dans la zone portuaire. Enfin, une calibration des paramètres des différentes méthodes prenant en compte la floculation pourrait être effectuée grâce aux observations que fournira l'UVP. A terme, si l'influence des fèces dans la sédimentation globale du port est avérée, le développement d'outils de modélisation prenant en compte la bioflocculation pourrait être entrepris.

Mise en place et analyse de stratégies de lutte contre l'envasement

Comme indiqué dans le Chapitre VII, de futures prospections géophysiques permettront de restituer la profondeur du socle rocheux dans le port et à proximité immédiate. Les résultats obtenus détermineront l'approche à adopter concernant l'implémentation de la souille à l'extérieur du port, le long du chenal de navigation. Cette solution, même si elle reste la plus envisageable, ne permettra pas de diminuer drastiquement les activités de dragage déjà mises en place. De nombreuses autres stratégies ont été développées et analysées pendant la thèse pour diminuer l'envasement et très peu ont semblé altérer le cycle d'envasement du port. Cependant, d'autres solutions techniques existent, tels que les systèmes de by-pass ou les systèmes de re-suspension. Ces derniers permettraient de maintenir en suspension les sédiments apportés par le flot jusqu'à ce qu'ils soient expulsés du port par les courants de jusant (*Weisman et al., 1996; Headland et al., 2007*). Les techniques engagées sont diverses et peuvent être de type hydraulique ou mécanique et le côut élevé d'installation et d'entretien pourrait rapidement être rentabilisé si elles sont efficaces. Cette stratégie aurait de plus un faible impact environnemental comparé aux opérations de dragage. Le recours à la modélisation devra être nécessaire pour étudier le comportement et le devenir des vases en suspension qui seraient évacuées du port au jusant. Un intérêt sera tout particulièrement porté à la part de retour des vases draguées et clapées à l'extérieur du port. Les résultats permettront d'établir les meilleures heures en fonction de la marée, propices au clapage et à l'évacuation des vases pour limiter la part de retour induite. Enfin, des simulations (Figure VIII.1) ont montré l'influence de la profondeur du port dans sa capacité de piégeage des sédiments. Les résultats indiquent que des profondeurs plus faibles, notamment lorsqu'elles sont supérieures à -1 *m* sous le zéro hydrographique, génèrent un apport sédimentaire moins important. Il serait donc nécessaire de réfléchir à l'amélioration des techniques de dragage actuelles qui imposent de creuser de -1.5 jusqu'à – 3 *m* dans les bassins du port.

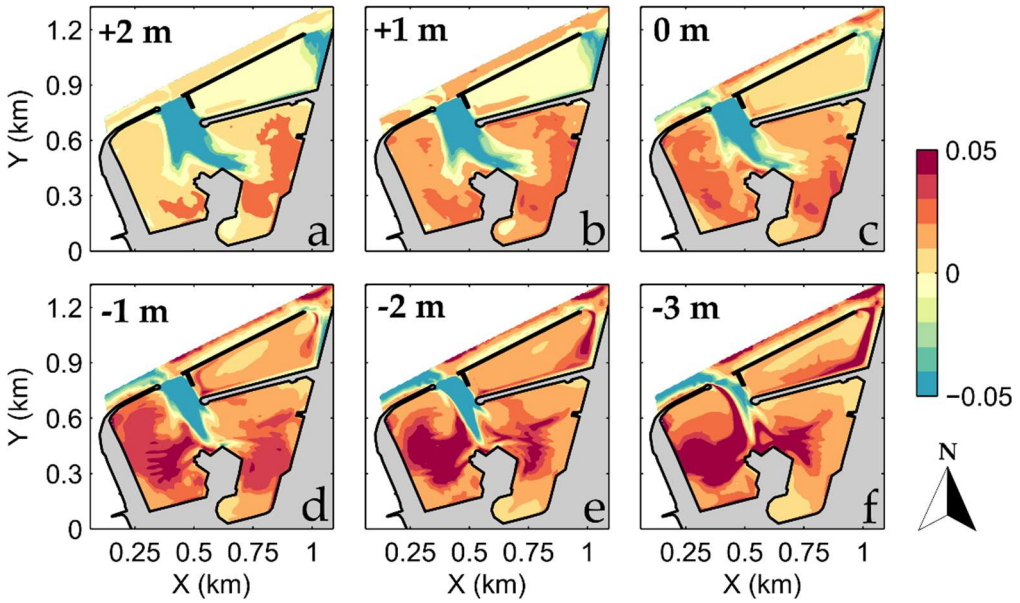

Figure VIII.1. *Evolution du fond simulée dans le port des Minimes et son chenal de navigation pour des profondeurs initiales de (a) +2 m, (b) +1 m, (c) 0 m, (d) -1 m, (e) -2 m et (f) -3 m par rapport au zéro hydrographique. La simulation dure quinze jours et les paramétrisations sont les mêmes que celles énoncées dans le Chapitre VII. (les évolutions affichées sont en m).*

Bibliographie

Abdelrhman, M. A. (2005). Simplified modeling of flushing and residence times in 42 embayments in New England, USA, with special attention to Greenwich Bay, Rhode Island. *Estuarine, Coastal and Shelf Science*, *62*(1-2), 339-351.

Abessolo Elouma, C. (2013). *Moyens permettant de limiter l'envasement dans un port à flot: Etude d'un bassin de configuration annulaire* (Doctoral dissertation, Nantes).

Acciaro, M., Ghiara, H., & Cusano, M. I. (2014). Energy management in seaports: A new role for port authorities. *Energy Policy*, *71*, 4-12.

Airoldi, L., & Beck, M. W. (2007). Loss, status and trends for coastal marine habitats of Europe. In *Oceanography and Marine Biology* (pp. 357-417). CRC Press.

Allard, J., Bertin, X., Chaumillon, E., & Pouget, F. (2008). Sand spit rhythmic development: A potential record of wave climate variations? Arçay Spit, western coast of France. *Marine Geology*, *253*(3-4), 107-131.

André, X. (1986). *Elaboration et analyse de cartes bathymétriques détaillées du proche plateau vendéo-charentais(Golfe de Gasgogne): reconstitution des paléorivages de la transgression holocène* (Doctoral dissertation).

Andrejev, O., Myrberg, K., Alenius, P., & Lundberg, P. A. (2004). Mean circulation and water exchange in the Gulf of Finland-a study based on three-dimensional modelling. *Boreal Environment Research*, *9*(1), 1-16.

Andutta, F. P., Helfer, F., de Miranda, L. B., Deleersnijder, E., Thomas, C., & Lemckert, C. (2016). An assessment of transport timescales and return coefficient in adjacent tropical estuaries. *Continental Shelf Research*, *124*, 49-62.

Arcère, L. E. (1756). *Histoire de la ville de La Rochelle et du pays d'Aulnis* (Vol. 1). R.-J. Desbordes.

Aref, H. (1984). Stirring by chaotic advection. *Journal of fluid mechanics*, *143*, 1-21.

Arega, F., Armstrong, S., & Badr, A. W. (2008). Modeling of residence time in the East Scott Creek Estuary, South Carolina, USA. *Journal of Hydro-environment Research*, *2*(2), 99-108.

Arega, F., & Badr, A. W. (2010). Numerical age and residence-time mapping for a small tidal creek: case study. *Journal of Waterway, Port, Coastal, and Ocean Engineering*, *136*(4), 226-237.

Arega, F. (2013). Hydrodynamic modeling and characterising of Lagrangian flows in the West Scott Creek wetlands system, South Carolina. *Journal of hydro-environment research*, *7*(1), 50-60.

Asselin, S., & Spaulding, M. L. (1993). Flushing times for the Providence River based on tracer experiments. *Estuaries*, *16*(4), 830.

Athar, M., Ardalan, A. A., & Karimi, R. (2019). Hydrodynamic Tidal Model of the Persian Gulf Based on Spatially Variable Bed Friction Coefficient. *Marine Geodesy*, *42*(1), 25-45.

Aubrey, D. G., & Speer, P. E. (1985). A study of non-linear tidal propagation in shallow inlet/estuarine systems Part I: Observations. *Estuarine, Coastal and Shelf Science*, *21*(2), 185-205.

AVISO+ Satellite Altimetry Data. Available online: https://www.aviso.altimetry.fr/en/data/products/auxiliary-products/global-tide-fes.html (acceessed on 2th July 2019)

Azevedo, A., Oliveira, A., Fortunato, A. B., & Bertin, X. (2009). Application of an Eulerian-Lagrangian oil spill modeling system to the Prestige accident: trajectory analysis. *Journal of Coastal Research*, 777-781.

Azizah, N., Triatmadja, R., & Kironoto, B. A. (2017). Numerical Simulation of Sediment Transport along a Channel with Underwater Sill. *Procedia Engineering*, 170, 202-209.

Babu, M. T., Vethamony, P., & Desa, E. (2005). Modelling tide-driven currents and residual eddies in the Gulf of Kachchh and their seasonal variability: A marine environmental planning perspective. *Ecological Modelling*, 184(2-4), 299-312.

Baker, C. J. (1980). The turbulent horseshoe vortex. *Journal of Wind Engineering and Industrial Aerodynamics*, 6(1-2), 9-23.

Bárcena, J. F., García, A., Gómez, A. G., Álvarez, C., Juanes, J. A., & Revilla, J. A. (2012). Spatial and temporal flushing time approach in estuaries influenced by river and tide. An application in Suances Estuary (Northern Spain). *Estuarine, Coastal and Shelf Science*, 112, 40-51.

Barneveld, H. J., & Hugtenburg, J. (2008). *Feasibility study for implementation of sedimentation reduction measures in river harbours*. In River, Coastal and Estuarine Morphodynamics: RCEM 2007 (pp. 1187-1192). Taylor Francis Group London.

Barusseau, J. P. (1973). *Evolution du plateau continental rochelais (Golfe de Gascogne) au cours du pleistocene terminal et de l'holocene: les processus actuels de la sedimentation.(*Doctoral dissertation, Bordeaux).

Bassoullet, P., Verney, R., Kervella, Y., Kervella, S., Jestin, H., & Voineson, G. (2010). Utilisation d'un altimètre (ALTUS) destiné à la quantification des dépôt/érosion en

domaine littoral pour l'étude des corrélations avec les caractéristiques de vagues et les interfaces de dépôt. *La Houille Blanche*, (5), 81-86.

Batuca, D. G., & Jordaan, J. M. (2000). *Silting and desilting of reservoirs*. CRC Press.

Becker, J., van Eekelen, E., van Wiechen, J., de Lange, W., Damsma, T., Smolders, T., & van Koningsveld, M. (2015). Estimating source terms for far field dredge plume modelling. *Journal of Environmental Management*, *149*, 282-293.

Bedri, Z., Bruen, M., Dowley, A., & Masterson, B. (2011). A three-dimensional hydro-environmental model of Dublin Bay. *Environmental Modeling & Assessment*, *16*(4), 369-384.

Berling, E. (2015). *Le Grand Port Maritime de La Rochelle.* Editeur Lulu, 320 pp.

Bernard, N. (1999). Du port-parking au produit touristique: l'évolution des ports de plaisance en France. *Norois*, *182*(2), 275-285.

Bernard, N. (2000). *Les ports de plaisance: équipements structurants de l'espace littoral*. Editions L'Harmattan.

Bertin, X. (2005). *Morphodynamique séculaire, architecture interne et modélisation d'un système baie/embouchure tidale: le Pertuis de Maumusson et la baie de Marennes-Oléron. (*Doctoral dissertation, La Rochelle).

Bertin, X., Chaumillon, E., Sottolichio, A., & Pedreros, R. (2005). Tidal inlet response to sediment infilling of the associated bay and possible implications of human activities: the Marennes-Oléron Bay and the Maumusson Inlet, France. *Continental Shelf Research*, *25*(9), 1115-1131.

Bertin, X., Castelle, B., Chaumillon, E., Butel, R., & Quique, R. (2008). Estimation and inter-annual variability of the longshore transport at a high-energy dissipative beach: the St Trojan beach, SW Oléron Island, France. *Continental Shelf Research*, *28*, 1316-1332.

Bertin, X., Bruneau, N., Breilh, J. F., Fortunato, A. B., Karpytchev, M. (2012). Importance of wave age and resonance in storm surges: the case Xynthia, Bay of Biscay. *Ocean Modelling.* 42, 16–30.

Bertin, X., Li, K., Roland, A., Bidlot, J.-R. (2015). The contribution of short-waves in storm surges: Two case studies in the Bay of Biscay. *Continental Shelf Research.* 96, 1-15.

Bétourné, N., & Valcke, S. (2015). *Les ports de plaisance en France: une approche dynamique et multidimensionnelle*. Editions L'Harmattan.

Bialik, R. J., & Karpiński, M. (2018). On the effect of the window size on the assessment of particle diffusion. *Journal of Hydraulic Research*, *56*(4), 560-566.

Bianchini, A., Cento, F., Guzzini, A., Pellegrini, M., & Saccani, C. (2019). Sediment management in coastal infrastructures: Techno-economic and environmental impact assessment of alternative technologies to dredging. *Journal of Environmental Management*, *248*.

Bizzarri, C., & La Foresta, D. (2011). Yachting and pleasure crafts in relation to local development and expansion: Marina di Stabia case study. *WIT Transactions on Ecology and the Environment*, *149*, 53-61.

Blanton, J. O., Lin, G., & Elston, S. A. (2002). Tidal current asymmetry in shallow estuaries and tidal creeks. *Continental Shelf Research*, *22*(11-13), 1731-1743.

Bohlin, C., Ligier, P. L., Söderström, A., & Lier, Ø. (2016). Modelling complex vertical structures with TELEMAC-3D. *Proceedings of the XXIIIrd TELEMAC-MASCARET User Conference 2016, 11 to 13 October 2016, Paris, France* (pp. 259-265).

Bolaños, R., Brown, J. M., & Souza, A. J. (2014). Wave–current interactions in a tide dominated estuary. *Continental Shelf Research*, *87*, 109-123.

Bolin, B., & Rodhe, H. (1973). A note on the concepts of age distribution and transit time in natural reservoirs. *Tellus*, *25*(1), 58-62.

Bonamano, S., Madonia, A., Piazzolla, D., Paladini de Mendoza, F., Piermattei, V., Scanu, S., & Marcelli, M. (2017). Development of a Predictive Tool to Support Environmentally Sustainable Management in Port Basins. *Water*, *9*(11), 898.

Bouquet de la Grye, J-J.A. & Hatt, P.E. (1876). *Baie de La Rochelle - Etude hydrographique*. Archives du SHOM.

Boutier, B., Chiffoleau, J.-F., Gonzalez J.-L., Lazure, P., Auger, D., Truquet, I. (2000). Influence of the Gironde estuary outputs on cadmium concentrations in the coastal waters: consequences on the Marennes-Oleron bay (France) . Oceanologica Acta , 23, 745-757.

Brauwere, A., De Brye, B., Blaise, S., & Deleersnijder, E. (2011). Residence time, exposure time and connectivity in the Scheldt Estuary. *Journal of Marine Systems*, *84*(3-4), 85-95.

Breitwieser, M., Dubillot, E., Barbarin, M., Churlaud, C., Huet, V., Muttin, F., & Thomas, H. (2018). Assessment of the biological quality of port areas: A case study on the three harbours of La Rochelle: The marina, the fishing harbour and the seaport. *PloS one*, *13*(6), e0198255.

Brown, S., Nicholls, R. J., Woodroffe, C. D., Hanson, S., Hinkel, J., Kebede, A. S., ... & Vafeidis, A. T. (2013). Sea-level rise impacts and responses: a global perspective. In *Coastal Hazards* (pp. 117-149). Springer, Dordrecht.

Brown, S., Hanson, S., & Nicholls, R. J. (2014). Implications of sea-level rise and extreme events around Europe: a review of coastal energy infrastructure. *Climatic Change*, *122*(1-2), 81-95.

Canu, D. M., Solidoro, C., Umgiesser, G., Cucco, A., & Ferrarin, C. (2012). Assessing confinement in coastal lagoons. *Marine Pollution Bulletin*, *64*(11), 2391-2398.

Cavalcante, G. H., Kjerfve, B., & Feary, D. A. (2012). Examination of residence time and its relevance to water quality within a coastal mega-structure: The Palm Jumeirah Lagoon. *Journal of Hydrology*, *468*, 111-119.

Cearreta, A., Irabien, M. J., & Pascual, A. (2004). Human activities along the Basque coast during the last two centuries: geological perspective of recent anthropogenic impact on the coast and its environmental consequences. *Oceanography and marine environment of the Basque Country. Elsevier oceanography series*, *70*, 27-50.

Cerema. (2018). *Dynamiques et évolution du littoral: Fascicules 1-10*. Editeur Cerema, 498 pp.

Charles, D. (1980). *Le yachting: une histoire d'hommes et de techniques*. Éditions maritimes et d'outre-mer.

Chasse-Marée. (1991). *Quand La Rochelle s'envasait.* Editions Chasse-Marée.

Chaumillon, E., & Weber, N. (2006). Spatial variability of modern incised valleys on the French Atlantic coast: comparison between the Charente and the Lay-Sèvre incised valleys. Incised Valleys in Time and Space. 85. Society for Sedimentary Geology. In *Incised Valleys in Time and Space*. SEPM Special Publication 85.

Chaumillon, E., Proust, J. N., Menier, D., & Weber, N. (2008). Incised-valley morphologies and sedimentary-fills within the inner shelf of the Bay of Biscay (France): a synthesis. *Journal of Marine systems*, *72*(1-4), 383-396.

Chaumillon, E., Gaudefroy, J., Merle, T., Bertin, X., Pignon, C., 2019. Controls on shoreline changes at pluri-annual to secular timescale in mixed-energy rocky and sedimentary estuarine systems. In: Castelle, B. and Chaumillon, E. (eds.), Coastal Evolution under Climate Change along the Tropical Overseas and Temperate Metropolitan France. *Journal of Coastal Research*, Special Issue 88.

Cheng, P., & Wilson, R. E. (2008). Modeling sediment suspensions in an idealized tidal embayment: importance of tidal asymmetry and settling lag. *Estuaries and Coasts*, 31(5), 828-842.

Choi, K. W., & Lee, J. H. W. (2004). Numerical determination of flushing time for stratified water bodies. *Journal of Marine Systems*, *50*(3-4), 263-281.

Christiansen H. (1987) New insights on mud formation and sedimentation processes in tidal harbours, *International Conference on Coastal and Port Engineering in Developing Countries*, China, 2, 775-816.

Christiansen, H., & Kirby, R. (1991). Fluid mud intrusion and evaluation of a passive device to reduce mud deposition. In *Proceedings of CEDA-PIANC Conference on Accessible Harbours* (pp. 1-14). International Navigation Association.

Claassens, H., Theron, A. K., & Schoonees, J. S. (2002). Port of East London: design and optimisation of the sand traps. *Journal of the South African Institution of Civil Engineering*, 44(4), 8-15.

Clausner, J. E. (1999). *Sand bypassing cost and performance database*. US Army Engineer Research and Development Center Vicksburg United States.

Cornett, A., Durand, N., & Serrer, M. (2010). 3-D Modelling and assessment of tidal current resources in the Bay of Fundy, Canada. In *Proc. 3rd Int. Conf. on Ocean Energy*.

Couneau, É. (2012). *La Rochelle disparue*. Edition des régionalismes.

CREOCEAN. (2004). *Etude des conditions naturelles en vue de l'extension du port des Minimes. Phase 1: Synthèse bibliographique.* 43 pp.

CREOCEAN. (2005). *Etude des conditions naturelles en vue de l'extension du port des Minimes. Phase 2: Analyse des campagnes de mesure.* 45 pp.

CREOCEAN. (2008). *Extension du port de plaisance des Minimes: Modélisations hydro-sédimentaires de plusieurs sites d'immersion.* 89 pp.

CREOCEAN. (2010). *Extension du port des Minimes: Modélisations complémentaires, d'agitation et niveau de surcôte, pour la prise en compte de l'évènement Xynthia.* 38 pp.

CREOCEAN. (2012). *Etude de dispersion des sédiments.* 116 pp.

CREOCEAN. (2014). *Mesures de courants le port des Minimes.* 59 pp.

Crowder, R., Hofrand, B., & Kirby, R. (2001). Particle Tracking Velocimetry Measurement To Assess The Performance Of Flow Control Structures. *WIT Transactions on The Built Environment*, *58*.

Cucco, A., & Umgiesser, G. (2006). Modeling the Venice Lagoon residence time. *Ecological modelling*, *193*(1-2), 34-51.

Cucco, A., Umgiesser, G., Ferrarin, C., Perilli, A., Canu, D. M., & Solidoro, C. (2009). Eulerian and lagrangian transport time scales of a tidal active coastal basin. *Ecological Modelling*, *220*(7), 913-922.

Cutroneo, L., Ferretti, G., Scafidi, D., Ardizzone, G. D., Vagge, G., & Capello, M. (2017). Current observations from a looking down vertical V-ADCP: interaction with winds and tide? The case of Giglio Island (Tyrrhenian Sea, Italy). *Oceanologia*, *59*(2), 139-152.

Dabrin, A., Schäfer, J., Bertrand, O., Masson, M., & Blanc, G. (2014). Origin of suspended matter and sediment inferred from the residual metal fraction: application to the Marennes Oleron Bay, France. *Continental Shelf Research*, *72*, 119-130.

Daryl, P. (1890). *Le yacht; histoire de la navigation maritime de plaisance.* Librairies-imprimeries réunies, Paris.

De Beauce & Thurninger (1885). *Ports maritimes de la France. Tome sixième (1ère partie): de La Rochelle à Maubert - Notice du port de La Rochelle*. Archives du SHOM, 61p.

Deleersnijder, E., & Delhez, E. (2007). Timescale-and tracer-based methods for understanding the results of complex marine models. *Estuarine Coastal and Shelf Science*, 74(4).

Decrop, B., Sas, M., Zimmermann, N., & Roose, F. (2013). Monitoring the siltation rate at Deurganckdock, Port of Antwerp, and its reduction by a current deflecting wall. In *CEDA (2013). 20th World Dredging Congress and Exhibition* (pp. 622-634).

Delft Hydraulics. (2001). *Design of a current deflection wall for the Parkhafen in Hamburg.* (in Dutch).

Delhez, É. J., Heemink, A. W., & Deleersnijder, É. (2004). Residence time in a semi-enclosed domain from the solution of an adjoint problem. *Estuarine, Coastal and Shelf Science*, *61*(4), 691-702.

Delhez, É. J. (2013). On the concept of exposure time. *Continental Shelf Research*, *71*, 27-36.

Delhez, É. J., de Brye, B., de Brauwere, A., & Deleersnijder, É. (2014). Residence time vs influence time. *Journal of Marine Systems*, *132*, 185-195.

Deloffre, J., Verney, R., Lafite, R., Lesueur, P., Lesourd, S., & Cundy, A. B. (2007). Sedimentation on intertidal mudflats in the lower part of macrotidal estuaries: sedimentation rhythms and their preservation. *Marine Geology*, *241*(1-4), 19-32.

Delpey, M. T., Ardhuin, F., Otheguy, P., & Jouon, A. (2014). Effects of waves on coastal water dispersion in a small estuarine bay. *Journal of Geophysical Research: Oceans*, *119*(1), 70-86.

Deng, Z. Q., Bengtsson, L., Singh, V. P., & Adrian, D. D. (2002). Longitudinal dispersion coefficient in single-channel streams. *Journal of Hydraulic Engineering*, *128*(10), 901-916.

De Nijs, M. A., Winterwerp, J. C., & Pietrzak, J. D. (2009). On harbour siltation in the fresh-salt water mixing region. *Continental Shelf Research*, 29(1), 175-193.

Di Franco, A., Graziano, M., Franzitta, G., Felline, S., Chemello, R., & Milazzo, M. (2011). Do small marinas drive habitat specific impacts? A case study from Mediterranean Sea. *Marine Pollution Bulletin*, *62*(5), 926-933.

Dion, R. (1956). Les origines de la Rochelle et l'essor du commerce atlantique aux XIIe et XIIIe siècles. *Norois*, *9*(1), 35-50.

Direction des Affaires Maritimes (DAM). (2015). *Observatoire des ports de plaisance.* (in French).

Direction Générale des Infrastructures, des Transports et de la Mer (DGITM). (2018). *La plaisance en chiffres, du 1er septembre 2017 au 31 août 2018.* (in French).

Di Vaio, A., & Varriale, L. (2018). Management innovation for environmental sustainability in seaports: Managerial accounting instruments and training for competitive green ports beyond the regulations. *Sustainability*, *10*(3), 783.

Dodet, G., Bertin, X., & Taborda, R. (2010). Wave climate variability in the North-East Atlantic Ocean over the last six decades. *Ocean modelling*, *31*(3-4), 120-131.

Donea, J. (1983). Arbitary Lagrangian-Eulerian Finite Elements Methods. *Computational Methods in Transient Analysis*.

Drobyshevski, Y. (2004). Hydrodynamic coefficients of a two-dimensional, truncated rectangular floating structure in shallow water. *Ocean Engineering*, *31*(3-4), 305-341.

Dronkers, J., & Zimmerman, J. T. F. (1982). Some principles of mixing in tidal lagoons. *Oceanologica Acta*, *4*(Suppl.), 107-118.

Dronkers, J. (1986). Tidal asymmetry and estuarine morphology. *Netherlands Journal of Sea Research*, *20*(2-3), 117-131.

Dronkers, J. (1998). Morphodynamics of the Dutch delta. *Physics of Estuaries and Coastal Seas*, 297-304.

Du, J., & Shen, J. (2016). Water residence time in Chesapeake Bay for 1980–2012. *Journal of Marine Systems*, *164*, 101-111.

Dugué, V., Blanckaert, K., Qiuwen, C. H. E. N., & Schleiss, A. J. (2013). Reduction of bend scour with an air-bubble screen–morphology and flow patterns. *International Journal of Sediment Research*, *28*(1), 15-23.

Durán, R., Nuez, M., Alonso, B., Ercilla, G., Estrada, F., Casas, D., & Farran, M. L. (2009). Assessment of sand trapped by coastal structures towards better management. El Masnou (Maresme, Catalunya). *Geotemas*, *10*, 511-514.

Duran-Matute, M., & Gerkema, T. (2015). Calculating residual flows through a multiple-inlet system: the conundrum of the tidal period. *Ocean Dynamics*, *65*(11), 1461-1475.

Dussier, M. (2011). *La Rochelle-Les Minimes: un port, une histoire*. Croît Vif.

Dussier, M. (2015). *La Rochelle, capitale de la plaisance en Charente-Maritime (1945-2005): étude sur l'évolution d'un loisir nautique et de ses aménagements urbano-portuaires* (Doctoral dissertation, La Rochelle).

Dyer, K. R. (1973). *Estuaries: a physical introduction*.

Callaway, R. J. (1980). Flushing study of South Beach Marina, Oregon. *Journal of the Waterway, Port, Coastal, and Ocean Division*, 207, 42-58.

European Environment Agency (EEA). (2006). *Changing Faces of Europe's Coastal Areas.* Available at:http://reports.eea.eu/eea_report_2006_6/en

El Fadili, M., & Messager, M. (2015). *Enquête dragage 2011. Synthèse des données.* Cerema-Cetmef, 39 p.

EL-Hattab, A. I. (2014). Single beam bathymetric data modelling techniques for accurate maintenance dredging. *The Egyptian Journal of Remote Sensing and Space Science*, *17*(2), 189-195.

Environmental Protection Agency (EPA). (1989). *Characteristics and Effects of Dredged Material Disposal in the Marine Environment*.

Eysink, W. D. (1989). Sedimentation in harbour basins. Small density differences may cause serious effects. In *International Harbour Congress, 9th*.

Falconer, R. A., Guoping, Y., & YU, G. (1991). Effects of depth, bed slope and scaling on tidal currents and exchange in a laboratory scale model. *Proceedings of the Institution of Civil Engineers*, *91*(3), 561-576.

Falconer, R. A. (1992). Flow and water quality modelling in coastal and inland water. *Journal of Hydraulic Research*, *30*(4), 437-452.

Fan, L., Wilson, W. W., & Dahl, B. (2012). Congestion, port expansion and spatial competition for US container imports. *Transportation Research Part E: Logistics and Transportation Review*, *48*(6), 1121-1136.

Fatoki, O. S., & Mathabatha, S. (2001). An assessment of heavy metal pollution in the East London and Port Elizabeth harbours. *Water Sa*, *27*(2), 233-240.

Faucherre, N., Prost, P., Chazette, A. & Le Blanc, F-Y. (1996). Les fortifications du littoral: la Charente-Maritime, Patrimoines et Médias, 222p.

Ferrarin, C., Zaggia, L., Paschini, E., Scirocco, T., Lorenzetti, G., Bajo, M., ... & Guerzoni, S. (2014). Hydrological regime and renewal capacity of the micro-tidal Lesina Lagoon, Italy. *Estuaries and Coasts*, *37*(1), 79-93.

Flather, R. A. (1976). *Results from a storm surge prediction model of the north-west European continental shelf for April, November and December, 1973.* Wormley, UK, Institute of Oceanographic Sciences, 37pp. (Institute of Oceanographic Sciences Report 24).

Fontein, W. F., & Byrd, R. W. (2007). The nautical depth approach, a review for implementation. In *Proc., WODCON XVIII Annual Dredging Seminar* (pp. 767-772). Western Dredging Association, Vancouver, WA.

Frémont, A. (2019). Le transport maritime depuis 1945: facteur clé de la mondialisation. *Entreprises et histoire*, (1), 16-29.

Friedrichs, C. T., Armbrust, B. D., & De Swart, H. E. (1998). Hydrodynamics and equilibrium sediment dynamics of shallow, funnel-shaped tidal estuaries. *Physics of Estuaries and Coastal Seas*, 315-327.

Fugate, D. C., Friedrichs, C. T., & Bilgili, A. (2006). Estimation of residence time in a shallow back barrier lagoon, Hog Island Bay, Virginia, USA. In *Estuarine and Coastal Modeling (2005)* (pp. 319-337).

Galia, T., Škarpich, V., Hradecký, J., & Přibyla, Z. (2016). Effect of grade-control structures at various stages of their destruction on bed sediments and local channel parameters. *Geomorphology*, *253*, 305-317.

Galili, E., Rosen, B., Zviely, D., Silberstein, N. A., & Finkielsztejn, G. (2010). The evolution of Akko harbour and its Mediterranean maritime trade links. *Journal of Island & Coastal Archaeology*, *5*(2), 191-211.

Ganthy, F., Sottolichio, A., & Verney, R. (2013). Seasonal modification of tidal flat sediment dynamics by seagrass meadows of Zostera noltii (Bassin d'Arcachon, France). *Journal of Marine Systems*, *109*, 233-240.

Gardner, W. D. (1980). Field assessment of sediment traps. *Journal of marine Research*, *38*(1), 41-52.

Gelinas, M., Bokuniewicz, H., Rapaglia, J., & Lwiza, K. M. (2012). Sediment resuspension by ship wakes in the Venice Lagoon. *Journal of Coastal Research*, *29*(1), 8-17.

Geyer, W. R. (1997). Influence of wind on dynamics and flushing of shallow estuaries. *Estuarine, Coastal and Shelf Science*, *44*(6), 713-722.

Geyer, W. R., Hill, P. S., & Kineke, G. C. (2004). The transport, transformation and dispersal of sediment by buoyant coastal flows. *Continental Shelf Research*, 24(7-8), 927-949.

Ghadimi, P., Maleki, F. S., & Chekab, M. A. F. (2014). Hydrodynamic Study of a Fixed Pontoon Structure under Wave Loads with Different Reynolds Numbers. *Journal of Marine Science and Technology*, *22*(2), 186-195.

Gillibrand, P. A. (2001). Calculating exchange times in a Scottish fjord using a two-dimensional, laterally-integrated numerical model. *Estuarine, Coastal and Shelf Science*, *53*(4), 437-449.

Goiran, J. P., Tronchère, H., Salomon, F., Carbonel, P., Djerbi, H., & Ognard, C. (2010). Palaeoenvironmental reconstruction of the ancient harbours of Rome: Claudius and Trajan's marine harbours on the Tiber delta. *Quaternary International*, *216*(1-2), 3-13.

Gómez, A. G., Ondiviela, B., Fernández, M., & Juanes, J. A. (2017). Atlas of susceptibility to pollution in marinas. Application to the Spanish coast. *Marine Pollution Bulletin*, *114*(1), 239-246.

Gorsky, G., Picheral, M., & Stemmann, L. (2000). Use of the Underwater Video Profiler for the study of aggregate dynamics in the North Mediterranean. *Estuarine, Coastal and Shelf Science*, *50*(1), 121-128.

Gould, R. A. (2011). *Archaeology and the social history of ships*. Cambridge University Press.

Gouriou, T. (2012). *Evolution des composantes du niveau marin à partir d'observations de marégraphie effectuées depuis la fin du 18ème siècle en Charente-Maritime* (Doctoral dissertation).

Green, M. O. (2011). Very small waves and associated sediment resuspension on an estuarine intertidal flat. *Estuarine, Coastal and Shelf Ccience*, 93(4), 449-459.

Grifoll, M., Espino, M., González, M., Ferrer, L., & Sánchez-Arcilla, A. (2006). Spatial residence time description for water discharges in harbours. In *Proceedings of the 4th International Conferences on Marine Waste Water Discharges and Coastal* (pp. 6-10).

Grifoll, M., Fontán A., Ferrer, L., Mader J., González, M., Espino, M. (2009). 3D hydrodynamic characterisation of a meso-tidal harbour: The case of Bilbao harbour (northern Spain). *Coastal Engineering*. 56, 907-918.

Grifoll, M., Jordà, G., Borja, Á., & Espino, M. (2010). A new risk assessment method for water quality degradation in harbour domains, using hydrodynamic models. *Marine Pollution Bulletin*, *60*(1), 69-78.

Grifoll, M., Del Campo, A., Espino, M., Mader, J., González, M., & Borja, Á. (2013). Water renewal and risk assessment of water pollution in semi-enclosed domains: Application to Bilbao Harbour (Bay of Biscay). *Journal of Marine Systems*, *109*, S241-S251.

Grifoll Colls, M., Cerralbo Peñarroya, P., Guillén Aranda, J., Espino Infantes, M., Boye Hansen, L., & Sánchez-Arcilla Conejo, A. (2018). Characterisation of bottom sediment resuspension events observed in a micro-tidal bay. *Ocean Science*, 15(2), 307-319.

Groen, P. I. E. R. (1967). On the residual transport of suspended matter by an alternating tidal current. *Netherlands Journal of Sea Research*, 3(4), 564-574.

Gulbin, V. V., Arzamastsev, I. S., & Shulkin, V. M. (2003). Ecological monitoring of the water area of Port Vostochnyi (Wrangel Bay) in the Sea of Japan (1995–2002). *Russian Journal of Marine Biology*, *29*(5), 284-295.

Guo, W., Wu, G., Liang, B., Xu, T., Chen, X., Yang, Z., ... & Jiang, M. (2016). The influence of surface wave on water exchange in the Bohai Sea. *Continental Shelf Research*, *118*, 128-142.

Hamburg Port Authority. (2012). *Work package 5 "Measures": Dredging and Disposal Strategies. Tidal River Development.* Available at: https://www.tide-toolbox.eu/pdf/reports/Dredging_strategies_Elbe_estuary.pdf

Hamill, G. A., Johnston, H. T., & Stewart, D. P. (1999). Propeller wash scour near quay walls. *Journal of Waterway, Port, Coastal, and Ocean Engineering*, *125*(4), 170-175.

Headland, J. R., Kirby, R., Winterwerp, H., Nasner, H., Vested, J., Sas, M., ... & Paul, J. (2007). Minimizing Harbour Siltation (MHS). In *Ports 2007: 30 Years of Sharing Ideas: 1977-2007* (pp. 1-10).

Heaps, N. S., & Jones, J. E. (1977). Density currents in the Irish Sea. *Geophysical Journal International*, *51*(2), 393-429.

Heaver, T. (2006). The evolution and challenges of port economics. *Research in Transportation Economics*, *16*, 11-41.

Henriksen, J., Randall, R., & Socolofsky, S. (2011). Near-field resuspension model for a cutter suction dredge. *Journal of Waterway, Port, Coastal, and Ocean Engineering*, *138*(3), 181-191.

Herbich, J. B. (1975). *Coastal & Deep Ocean Dredging*. Gulf Publishing Company.

Hervouet, J. M. (2000). TELEMAC modelling system: an overview. *Hydrological Processes*, *14*(13), 2209-2210.

Hervouet, J. M. (2007). *Hydrodynamics of free surface flows: modelling with the finite element method* (Vol. 360). New York: Wiley.

Hervouet, J. M., Razafindrakoto, E., & Villaret, C. (2011). Dealing with dry zones in free surface flows: a new class of advection schemes. In *Proceedings of the 34th World Congress of the International Association for Hydro-Environment Research and Engineering: 33rd Hydrology and Water Resources Symposium and 10th Conference on Hydraulics in Water Engineering* (p. 4103). Engineers Australia.

Hervouet, J., Pavan, S., & Ata, R. (2015). Distributive advection schemes and dry zones, new solutions. *Proceedings of the 22nd Telemac User Club, STFC Daresbury, UK*, 13-16.

Hofland, B., Christiansen, H., Crowder, R. A., Kirby, R., Van Leeuwen, C. W., & Winterwerp, J. C. (2001). The Current Deflecting Wall in an estuarine harbour. In *Proceedings of the Congress-International Association for Hydraulic Research* (pp. 613-621).

Huang, W., & Spaulding, M. (2002). Modelling residence-time response to freshwater input in Apalachicola Bay, Florida, USA. *Hydrological Processes*, *16*(15), 3051-3064.

Huguet, J. R., Brenon, I., & Coulombier, T. (2019a). Characterisation of the Water Renewal in a Macro-Tidal Marina Using Several Transport Timescales. *Water*, 11(10), 2050.

Huguet, J.-R.; Brenon, I.; Coulombier, T. (2019b). Influence of floating structures on the tide and wind-driven hydrodynamics of a highly populated marina. *Journal of Waterway, Port, Coastal and Ocean Engineering.* In press

ICOMIA (International Council of Marine Industry Associations). (2018). *Recreational Boating Industry Statistics 2017.* Available at: https://www.icomia.org/

IDRA. (2015). *Autosurveillance de la qualité des sédiments du port de plaisance de La Rochelle.*

Imasato, N. (1983). What is tide-induced residual current?. *Journal of Physical Oceanography*, *13*(7), 1307-1317.

Jenkins, B. S. (1981a). Effects of channel geometry on exchange processes in river side-bays. In *Conference on Hydraulics in Civil Engineering 1981: Preprints of Papers* (p. 156). Institution of Engineers, Australia.

Jenkins, S. A. (1981b). *The Evaluation of Sediment Management Procedures: Phase IV-VI Final Report, 1978-1980*. University of California, Scripps Institution of Oceanography, 81(22).

Jestin, H., Bassoullet, P., Le Hir, P., L'Yavanc, J., & Degres, Y. (1998). Development of ALTUS, a high frequency acoustic submersible recording altimeter to accurately monitor bed elevation and quantify deposition or erosion of sediments. In *IEEE Oceanic Engineering Society. OCEANS'98. Conference Proceedings.* (Vol. 1, pp. 189-194).

Jing, L., & Ridd, P. V. (1996). Wave-current bottom shear stresses and sediment resuspension in Cleveland Bay, Australia. *Coastal Engineering*, 29(1-2), 169-186.

Jones, C. P., & Mehta, A. J. (1980). *Inlet sand bypassing systems in Florida*. American Shore and Beach Preservation Association.

Kavakeb, S., Nguyen, T. T., McGinley, K., Yang, Z., Jenkinson, I., & Murray, R. (2015). Green vehicle technology to enhance the performance of a European port: a simulation model with a cost-benefit approach. *Transportation Research Part C: Emerging Technologies*, *60*, 169-188.

Kenov, I. A., Muttin, F., Campbell, R., Fernandes, R., Campuzano, F., Machado, F., ... & Neves, R. (2015). Water fluxes and renewal rates at Pertuis d'Antioche/Marennes-Oléron Bay, France. *Estuarine, Coastal and Shelf Science*, *167*, 32-44.

Kervella, S. (2009). *Dynamique des sédiments fins et mixtes des zones intertidales de la baie de Marennes-Oléron: caractérisation des sédiments, processus hydro-sédimentaires et modélisation appliquée* (Doctoral dissertation, La Rochelle).

Kirby, R. (2003). Optimized harbour basins. In *Dredging'02: Key Technologies for Global Prosperity* (pp. 1-15).

Kirby, R. (2011). Minimising harbour siltation—findings of PIANC Working Group 43. *Ocean Dynamics*, *61*(2-3), 233-244.

Kirby, R. (2013). Managing industrialised coastal fine sediment systems. *Ocean & Coastal Management*, *79*, 2-9.

Kopmann, R., & Markofsky, M. (2000). Three-dimensional water quality modelling with TELEMAC-3D. *Hydrological Processes*, *14*(13), 2279-2292.

Krone, R. B. (1962). *Flume studies of the transport of sediment in estuarial shoaling processes*, Final report, Hydraul. Eng. Lab. and Sanit. Eng. Res. Lab., Univ. of Calif., Berkeley.

Krone, R. B. (1987). Reducing sedimentation rates in harbour facilities. *Sedimentation control to reduce maintenance dredging of navigation facilities in estuaries. Report and symposium proceedings, Marine Board, Commission on Engineering and Technical Systems, National Research Council. National Academy, Washington, DC* (pp. 128-140).

Kuijper, C., & Winterwerp, J. C. (2003). *The Current Deflecting Wall: mitigating harbour siltation; Set-up and integration of physical and numerical modelling techniques.* Delft Cluster. Institutional Repository.

Langedoen, E. J. (1992). *Flow patterns and transport of dissolved matter in tidal harbours.* (Doctoral dissertation, Delft).

Langendoen, E. J. (1994). Flow patterns and transport of dissolved matter in tidal harbours. *Journal of Hydraulic Research*, 32(2).

LCHF. (1987). *Catalogue sédimentologique des côtes francaises: Côtes de la Manche et de l'Atlantique.* Collection de la Direction des Etudes et Recherches d'Electricité de France.

Le Cann, B. (1990). Barotropic tidal dynamics of the Bay of Biscay shelf: observations, numerical modelling and physical interpretation. *Continental Shelf Research*, *10*(8), 723-758.

Le Carrer, O. (2003). *Un siècle de voile*. Calmann-Lévy.

Lee, G. H., Shin, H. J., Kim, Y. T., Dellapenna, T. M., Kim, K. J., Williams, J., ... & Figueroa, S. M. (2019). Field investigation of siltation at a tidal harbour: North Port of Incheon, Korea. *Ocean Dynamics*, *69*(9), 1101-1120.

Le Hir, P., Kervella, S., Walker, P., & Brenon, I. (2010). Erosions, dépots et transits sédimentaires associés dans le bassin de Marennes-Oléron. *La Houille Blanche*, (5), 65-71.

Le Moine, O. (2013). *Bassins versants et débits des principaux fleuves des pertuis charentais.* Available at: http://archimer.ifremer.fr/doc/00120/23094/

Lesueur, P. (1992). *Les vasières de la plate-forme Ouest-Gironde (France): modèle faciologique et archive sédimentaire des flux côtiers* (Doctoral dissertation, Bordeaux 1).

Lesueur, P., Tastet, J. P., & Weber, O. (2002). Origin and morphosedimentary evolution of fine-grained modern continental shelf deposits: the Gironde mud fields (Bay of Biscay, France). *Sedimentology*, *49*(6), 1299-1320.

Li, D., Panchang, V., Tang, Z., Demirbilek, Z., & Ramsden, J. (2005). Evaluation of an approximate method for incorporating floating docks in harbour wave prediction models. *Canadian Journal of Civil Engineering*, *32*(6), 1082-1092.

Li, C. (2013). Subtidal water flux through a multiple-inlet system: Observations before and during a cold front event and numerical experiments. *Journal of Geophysical Research: Oceans*, *118*(4), 1877-1892.

Lin, P. P., & Mehta, A. J. (1997). A study of fine sedimentation in an elongated laboratory basin. *Journal of Coastal Research*, 19-30.

Liria, J., Coelho, H., Sproson, D., Martinho, P., Webb, C., Oropeza, F., ... & Peng, Z. (2018). A Novel Approach to Generating a Hurricane Database for the Gulf of Mexico Based on Numerical Weather Prediction Models. In *Offshore Technology Conference*. Offshore Technology Conference.

Lisi, I., Taramelli, A., Di Risio, M., Cappucci, S., & Gabellini, M. (2009). Flushing efficiency of Augusta harbour (Italy). *Journal of Coastal Research*, 841-845.

Liu, J. T., & Aubrey, D. G. (1993). Tidal residual currents and sediment transport through multiple tidal inlets. *Coastal and Estuarine Studies*, 113-113.

Liu, B., Wang, N., Chen, M., Wu, X., Mo, D., Liu, J., ... & Zhuang, Y. (2017). Earliest hydraulic enterprise in China, 5,100 years ago. *Proceedings of the National Academy of Sciences*, *114*(52), 13637-13642.

Lopes, J. F., & Dias, J. M. (2007). Residual circulation and sediment distribution in the Ria de Aveiro lagoon, Portugal. *Journal of Marine Systems*, *68*(3-4), 507-528.

Luna-Acosta, A., Bustamante, P., Budzinski, H., Huet, V., & Thomas-Guyon, H. (2015). Persistent organic pollutants in a marine bivalve on the Marennes–Oléron Bay and the Gironde Estuary (French Atlantic Coast)—Part 2: Potential biological effects. *Science of The Total Environment*, 514, 511-522.

Malhadas, M. S., Silva, A., Leitão, P. C., & Neves, R. (2009). Effect of the bathymetric changes on the hydrodynamic and residence time in Óbidos Lagoon (Portugal). *Journal of Coastal Research*, 549-553.

Malhadas, M. S., Neves, R. J., Leitão, P. C., & Silva, A. (2010). Influence of tide and waves on water renewal in Óbidos Lagoon, Portugal. *Ocean Dynamics*, *60*(1), 41-55.

Mali, M., De Serio, F., Dell'Anna, M. M., Mastrorilli, P., Damiani, L., & Mossa, M. (2017). Enhancing the performance of hazard indexes in assessing hot spots of harbour areas by considering hydrodynamic parameters. *Ecological Indicators*, *73*, 38-45.

Marriner, N., & Morhange, C. (2006). Geoarchaeological evidence for dredging in Tyre's ancient harbour, Levant. *Quaternary Research*, *65*(1), 164-171.

Marriner, N., & Morhange, C. (2007). Geoscience of ancient Mediterranean harbours. *Earth-Science Reviews*, *80*(3-4), 137-194.

Marriner, N., Morhange, C., Kaniewski, D., & Carayon, N. (2014). Ancient harbour infrastructure in the Levant: tracking the birth and rise of new forms of anthropogenic pressure. *Scientific Reports*, *4*, 5554.

Martinuzzi, R., & Tropea, C. (1993). The flow around surface-mounted, prismatic obstacles placed in a fully developed channel flow (data bank contribution). *Journal of Fluids Engineering*, *115*(1), 85-92.

McKinley, E. (2012). Drivers for Marina 2020 in the Channel Region: A draft report.

Melet, A., Almar, R., & Meyssignac, B. (2016). What dominates sea level at the coast: a case study for the Gulf of Guinea. *Ocean Dynamics*, *66*(5), 623-636.

Mestres, M., Sierra, J. P., Mösso, C., & Sánchez-Arcilla, A. (2010). Sources of contamination and modelled pollutant trajectories in a Mediterranean harbour (Tarragona, Spain). *Marine Pollution Bulletin*, *60*(6), 898-907.

Monsen, N. E., Cloern, J. E., Lucas, L. V., & Monismith, S. G. (2002). A comment on the use of flushing time, residence time, and age as transport time scales. *Limnology and Oceanography*, *47*(5), 1545-1553.

Montgomery, R. L. (1984). Dredging and dredged material disposal techniques for contaminated sediments. *Lake and Reservoir Management*, *1*(1), 586-591.

Morim, J., Hemer, M., Wang, X. L., Cartwright, N., Trenham, C., Semedo, A., ... & Erikson, L. (2019). Robustness and uncertainties in global multivariate wind-wave climate projections. *Nature Climate Change*, *9*(9), 711-718.

Murphy, E., Deiber, M., & Perrin, S. (2012). Shear-driven flushing of micro-tidal marinas. *Coastal Engineering Proceedings*, *1*(33), 59.

Nasner, H. (1992). *Siltation in tidal harbours, part I.* Die Küste, 127-170.

Nasner, H. (1997). *Siltation in tidal harbours, part II.* Die Küste, 63-114.

Nece, R. E., & Richey, E. P. (1973). Flushing characteristics of small-boat marinas. In *Coastal Engineering 1972* (pp. 2499-2512).

Nece, R. E. (1984). Planform effects on tidal flushing of marinas. *Journal of Waterway, Port, Coastal, and Ocean Engineering*, *110*(2), 251-269.

Newell, R. C., Seiderer, L. J., & Hitchcock, D. R. (1998). The impact of dredging works in coastal waters: a review of the sensitivity to disturbance and subsequent recovery of biological resources on the sea bed. *Oceanography and Marine Biology: an annual review*, *36*(1), 127-178.

Nicolle, A. (2006). *Modélisation des marées et des surcotes dans les Pertuis Charentais* (Doctoral dissertation, La Rochelle).

Nicolle, A., & Karpytchev, M. (2007). Evidence for spatially variable friction from tidal amplification and asymmetry in the Pertuis Breton (France). *Continental Shelf Research*, *27*(18), 2346-2356.

Noli, A., & Franco, L. (2009). The ancient ports of Rome: new insights from engineers. *Archaeologia Maritima Mediterranea*, *6*, 189-207.

Oleson, J. P., Brandon, C., Cramer, S. M., Cucitore, R., Gotti, E., & Hohlfelder, R. L. (2004). The ROMACONS Project: A contribution to the historical and engineering analysis of hydraulic concrete in Roman maritime structures. *International Journal of Nautical Archaeology*, *33*(2), 199-229.

Oliveira, A., & Baptista, A. M. (1997). Diagnostic modeling of residence times in estuaries. *Water Resources Research*, *33*(8), 1935-1946.

Ommen, H. C., & Schaap, G. (1995). *Nautical dredging problems in marinas: Final report.* (in Dutch)

Ondiviela, B., Gómez, A. G., Puente, A., & Juanes, J. A. (2013). A pragmatic approach to define the ecological potential of water bodies heavily modified by the presence of ports. *Environmental Science & Policy*, *33*, 320-331.

Onuf, C. P. (1994). Seagrasses, dredging and light in Laguna Madre, Texas, USA. *Estuarine, Coastal and Shelf Science*, *39*(1), 75-91.

Orfila, A., Jordi, A., Basterretxea, G., Vizoso, G., Marbà, N., Duarte, C. M., ... & Tintoré, J. (2005). Residence time and Posidonia oceanica in Cabrera Archipelago National Park, Spain. *Continental Shelf Research*, *25*(11), 1339-1352.

Oricchio, F. T., Marques, A. C., Hajdu, E., Pitombo, F. B., Azevedo, F., Passos, F. D., ... & Dias, G. M. (2019). Exotic species dominate marinas between the two most populated regions in the southwestern Atlantic Ocean. *Marine Pollution Bulletin*, *146*, 884-892.

Pallis, A. A., Vitsounis, T. K., & De Langen, P. W. (2010). Port economics, policy and management: review of an emerging research field. *Transport Reviews*, *30*(1), 115-161.

Parola, F., & Musso, E. (2007). Market structures and competitive strategies: the carrier–stevedore arm-wrestling in northern European ports. *Maritime Policy & Management*, *34*(3), 259-278.

Parchure, T. M., & Teeter, A. M. (2003). *Potential Methods for Reducing Shoaling in Harboursand Navigation Channels. Coastaland Hydraulics Engineering Technical Note ERDC*. CHL CHETN-XIV-6, Vicksburg, MS: US Army Engineer Researchand Development Center, Coastaland Hydraulics Laboratory.

Parra, M., Trouky, H., Jouanneau, J. M., Grousset, F., Latouche, C., & Castaing, P. (1998). Étude isotopique (Sr⊙ Nd) de l'origine des dépôts fins holocènes du littoral atlantique (SO France). *Oceanologica Acta*, *21*(5), 631-644.

Partheniades, E. (1965). Erosion and deposition of cohesive soils. *Journal of the Hydraulics Division*, *91*(1), 105-139.

Paskoff, R. (2010). *Les littoraux: impact des aménagements sur leur évolution*. Armand Colin.

Patterson, M., & Hardy, D. (2008). Economic drivers of change and their oceanic-coastal ecological impacts. *Ecological economics of the oceans and coasts. Edward Elgar Publishing*, 187-209.

PIANC, P. (1997). Approach Channels A Guide for Design. *Report of Working Group II-30.*, *95*, 14-28.

Picheral, M., Guidi, L., Stemmann, L., Karl, D. M., Iddaoud, G., & Gorsky, G. (2010). The Underwater Vision Profiler 5: An advanced instrument for high spatial resolution studies of particle size spectra and zooplankton. *Limnology and Oceanography: Methods*, *8*(9), 462-473.

Pingree, R. D. & L. Maddock. (1977). Tidal residuals in the English Channel. *Journal of the marine Biological Association United Kingdom.* 57, 339–354.

Plus, M., Dumas, F., Stanisière, J. Y., & Maurer, D. (2009). Hydrodynamic characterisation of the Arcachon Bay, using model-derived descriptors. *Continental Shelf Research*, *29*(8), 1008-1013.

Poincaré, H., & Fichot, E. (1910). *Leçons de mécanique céleste: Théorie des marées, rédigée par E. Fichot* (Vol. 3). Gauthier-Villars.

Prandle, D. (2004). How tides and river flows determine estuarine bathymetries. *Progress in Oceanography*, *61*(1), 1-26.

Postma, H. (1961). Transport and accumulation of suspended matter in the Dutch Wadden Sea. *Netherlands Journal of Sea Research*, 1(1-2), 148-190.

Postma, H. (1967). Sediment transport and sedimentation in the estuarine environment. *American Association of Advanced Sciences*, 83, 158-179.

Proctor, R., & Greig, M. J. (1989). A numerical model investigation of the residual circulation in Hauraki Gulf, New Zealand. *New Zealand Journal of Marine and Freshwater Research*, *23*(3), 421-442.

Raban, A. (1995). The heritage of ancient harbour engineering in Cyprus and the Levant. In *Proceedings of the International Symposium 'Cyprus and the Sea* (pp. 139-189).

Ramakrishnan, B., Singh, N. P., & Jeyaraj, S. (2019). Input reduction and acceleration techniques in a morphodynamic modeling: A case study of Mumbai harbour. *Regional Studies in Marine Science*, 31.

Ranasinghe, R., & Pattiaratchi, C. (2000). Tidal inlet velocity asymmetry in diurnal regimes. *Continental Shelf Research*, *20*(17), 2347-2366.

Rapaglia, J., Zaggia, L., Ricklefs, K., Gelinas, M., & Bokuniewicz, H. (2011). Characteristics of ships' depression waves and associated sediment resuspension in Venice Lagoon, Italy. *Journal of Marine Systems*, *85*(1-2), 45-56.

Rehitha, T. V., Ullas, N., Vineetha, G., Benny, P. Y.; Madhu, N. V., Revichandran, C. (2017) Impact of Maintenance Dredging on Macrobenthic Community Structure of a Tropical Estuary. *Ocean & Coastal Management*,144,71-82.

Retière, D. (2003). *Les bassins de plaisance: structuration et dynamiques d'un territoire: étude comparative Mor Bras (France)-Solent (Grande-Bretagne)* (Doctoral dissertation, Brest).

Ridderinkhof, H. (1988a). Tidal and residual flows in the Western Dutch Wadden Sea I: numerical model results. *Netherlands Journal of Sea Research*, *22*(1), 1-21.

Ridderinkhof, H. (1988b). Tidal and residual flows in the Western Dutch Wadden Sea II: an analytical model to study the constant flow between connected tidal basins. *Netherlands Journal of Sea Research*, *22*(3), 185-198.

Ridderinkhof, H., Zimmerman, J. T. F., & Philippart, M. E. (1990). Tidal exchange between the North Sea and Dutch Wadden Sea and mixing time scales of the tidal basins. *Netherlands Journal of Sea Research*, *25*(3), 331-350.

Ridderinkhof, H. (1997). The effect of tidal asymmetries on the net transport of sediments in the Ems Dollard estuary. *Journal of Coastal Research*, 41-48.

Rivero, N. K., Dafforn, K. A., Coleman, M. A., & Johnston, E. L. (2013). Environmental and ecological changes associated with a marina. *Biofouling*, *29*(7), 803-815.

Rodriguez, R. R. (2014). *Integration of Topographic and Bathymetric Digital Elevation Model using ArcGIS Interpolation Methods: A Case Study of the Klamath River Estuary* (Doctoral dissertation, University of Southern California).

Roose, F., Sas, M., & Meersschaut, Y. (2013). The development of a current deflecting wall in estuarine conditions (salinity gradients) to reduce siltation in the tidal Deurganckdok, port of Antwerp. *In: CEDA (2013). 20th World Dredging Congress and Exhibition 2013 (WODCON XX). The Art of Dredging. Brussels, Belgium*, pp. 613-621.

Ruhl, C. A., Schoellhamer, D. H., Stumpf, R. P., & Lindsay, C. L. (2001). Combined use of remote sensing and continuous monitoring to analyse the variability of suspended-sediment concentrations in San Francisco Bay, California. *Estuarine, Coastal and Shelf Science*, *53*(6), 801-812.

Sabol, B. M., & Shafer, D. J. (2005). Dredging effects on seagrasses: case studies from New England and Florida. *Proceedings of the Western Dredging Association*, 336-346.

Saha, S., Moorthi, S., Pan, H. L., Wu, X., Wang, J., Nadiga, S., ... & Liu, H. (2010). The NCEP climate forecast system reanalysis. *Bulletin of the American Meteorological Society*, *91*(8), 1015-1058.

Saha, S., Moorthi, S., Wu, X., Wang, J., Nadiga, S., Tripp, P., ... & Ek, M. (2014). The NCEP climate forecast system version 2. *Journal of Climate*, *27*(6), 2185-2208.

Saleh, O. K., Negm, A. M., Waheed-Eldin, O. S., & Ahmad, N. G. (2003). Effect of end sill on scour characteristics downstream of sudden expanding stilling basins. In *Proc. of 6th Int. Conf. On River Eng., Ahvaz, Iran* (pp. 28-30).

Salman, A., Lombardo, S., & Doody, P. (2004). *Living with coastal erosion in Europe: Sediment and Space for Sustainability.* Eurosion project reports. 500 pp.

Salles, P., Voulgaris, G., & Aubrey, D. G. (2005). Contribution of nonlinear mechanisms in the persistence of multiple tidal inlet systems. *Estuarine, Coastal and Shelf Science*, *65*(3), 475-491.

Samir, K. C., & Lutz, W. (2017). The human core of the shared socioeconomic pathways: Population scenarios by age, sex and level of education for all countries to 2100. *Global Environmental Change*, *42*, 181-192.

Sanchez-Arcilla, A., Caceres, I., Gonzalez, D., Sierra, J. P., Escutia, R. (2002). Water renovation in harbour domains. The role of wave and wind conditions. *Coastal Engineering*. 1267-1278.

Sankaranarayanan, R., Esmy, P. O., Rajkumar, R., Muwonge, R., Swaminathan, R., Shanthakumari, S., ... & Cherian, J. (2007). Effect of visual screening on cervical cancer incidence and mortality in Tamil Nadu, India: a cluster-randomised trial. *The Lancet*, *370*(9585), 398-406.

Sánchez-Arcilla, A., Espino, M., Grifoll, M., Mösso, C., Sierra, J. P., Mestres, M., ... & Alvarez-Fanjul, E. (2011). Quay Design and Operational Oceanography. The Case of Bilbao Harbour. *Coastal Engineering Proceedings*, *1*(32), 51.

Sanford, L. P., Boicourt, W. C., & Rives, S. R. (1992). Model for estimating tidal flushing of small embayments. *Journal of Waterway, Port, Coastal, and Ocean Engineering*, *118*(6), 635-654.

Saz-Salazar, S., García-Menéndez, L., & Feo-Valero, M. (2012). Meeting the environmental challenge of port growth: A critical appraisal of the contingent valuation method and an application to Valencia Port, Spain. *Ocean & coastal management*, *59*, 31-39.

Schoellhamer, D. H. (2002). Variability of suspended-sediment concentration at tidal to annual time scales in San Francisco Bay, USA. *Continental Shelf Research*, 22(11-13), 1857-1866.

Schwarz, H., Streich, G., & Zimmermann, C. (1995). Reduction of sedimentation in harbour entrances on tidal rivers by modifications of the entrance geometry and installation of stream guiding structures. In *Proc. of the 4th Int. Conf. on Coastal & Port Engineering in Developing Countries, Rio de Janeiro, Brasil* (pp. 1652-1662).

Schwartz, R. A., & Imberger, J. (1989). Flushing behaviour of a coastal marina. In *Coastal Engineering 1988* (pp. 2626-2640).

Seers, B. M., & Shears, N. T. (2015). Spatio-temporal patterns in coastal turbidity–long-term trends and drivers of variation across an estuarine-open coast gradient. *Estuarine, Coastal and Shelf Science*, 154, 137-151.

Seifi, F., Deng, X., & Baltazar Andersen, O. (2019). Assessment of the Accuracy of Recent Empirical and Assimilated Tidal Models for the Great Barrier Reef, Australia, Using Satellite and Coastal Data. *Remote Sensing*, *11*(10), 1211.

Shanehsazzadeh, A., & Ardalan, H. (2019). Regional-Scale Study on Sediment Processes of Khuran Strait at Persian Gulf with Implications for Engineering Design. *China Ocean Engineering*, *33*(3), 356-364.

Sharp, J. A., Johnson, H. N., Pevey, K. C., & McAnally, W. H. (2010). *Sediment management alternatives for the Port of Bienville* (No. FHWA/MS-DOT-RD-10-199). Mississippi. Dept. of Transportation.

SHOM. (2010). Carte de Natures de Fond au format Shape. (Partie sédimentologie).

SHOM. (2015). MNT Topo-Bathymétrique Côtier des Pertuis Charentais (Projet Homonim).

SHOM. (2015). MNT Bathymétrique de façade Atlantique (Projet Homonim).

Short, F., & Wyllie-Echeverria, S. (1996) Natural and human-induced disturbance of seagrasses. *Environmental Conservation*, 23, 17-27.

Silva, G. A. M., & Mendes, D. (2013). Comparison results for the CFSv2 hindcasts and statistical downscaling over the northeast of Brazil. *Advances in Geosciences*, *35*, 79-88.

Silva, G. A., Dutra, L. M., da Rocha, R. P., Ambrizzi, T., & Leiva, É. (2014). Preliminary analysis on the global features of the NCEP CFSv2 seasonal hindcasts. *Advances in Meteorology*, *2014*.

Silvestrova, K., Myslenkov, S., & Zatsepin, A. (2019). Variability of Wind-Driven Coastal Upwelling in the North-Eastern Black Sea in 1979–2016 According to NCEP/CFSR Data. In *Meteorology and Climatology of the Mediterranean and Black Seas* (pp. 287-295).

Signell, R.P., & Geyer, W.R. (1991). Transient eddy formation around headlands. *Journal of Geophysical Research.* 96, 2561-2575.

Sigwald R., Ledoux S., Spencer K. (2012) *Guide méthodologique sur le dragage par injection d'eau.* Rapport GEODE (Groupe d'Etudes et d'Observation sur les Dragages et l'Environnement). 68p (in French).

Soletchnik, P., Polsenaere, P., Le Moine, O., Guesdon, S., Bechemin, C. (2014). *Relations entre apports terrigènes et conchyliculture dans les Pertuis Charentais.* Available at: https://archimer.ifremer.fr/doc/00248/35964/

Sonnic, E. (2005). *la navigation de plaisance: territoires de pratiques et territoires de gestion en Bretagne entre dualité et nécessité de fusion pour une évolution progressiste de l'activité* (Doctoral dissertation).

Sonnic, E. (2010). La navigation de plaisance en Bretagne. Espaces de pratiques et territoires de gestion.

Soulsby, R. L., Manning, A. J., Spearman, J., & Whitehouse, R. J. S. (2013). Settling velocity and mass settling flux of flocculated estuarine sediments. *Marine Geology*, *339*, 1-12.

Souto, C., Gilcoto, M., Fariña-Busto, L., & Pérez, F. F. (2003). Modeling the residual circulation of a coastal embayment affected by wind-driven upwelling: Circulation of the Ría de Vigo (NW Spain). *Journal of Geophysical Research: Oceans*, *108*(C11).

Speer, P. E., & Aubrey, D. G. (1985). A study of non-linear tidal propagation in shallow inlet/estuarine systems Part II: Theory. *Estuarine, Coastal and Shelf Science*, *21*(2), 207-224.

Spivakovskaya, D., Heemink, A. W., & Deleersnijder, E. (2007). Lagrangian modelling of multi-dimensional advection-diffusion with space-varying diffusivities: theory and idealized test cases. *Ocean Dynamics*, *57*(3), 189-203.

Sullivan, N. (2000). The use of agitation dredging, water injection dredging and side casting: Result of a survey of ports in England and Wales. *Terra et Aqua*, *78*, 11-20.

Stanisière, J. Y., Dumas, F., & Plus, M. (2006). *Caractérisation des composantes hydrodynamiques d'un système côtier semi-fermé: Le Bassin de Marennes-Oléron*. Available at: https://archimer.ifremer.fr/doc/00000/2353/

Stanisière, J.-Y., Le Moine, O., Soletchnik, P. (2008). *Morphologie et hydrodynamique comparées des pertuis charentais: résultats de modélisation par Mars 2D*. Available at: https://archimer.ifremer.fr/doc/00000/4036/

Stanisière, J.-Y., Le Moine, O., Soletchnik, P. (2009). *Influence des fleuves : Lay, Sèvre et Charente, dans les pertuis charentais, selon la direction du vent.* Available at: https://archimer.ifremer.fr/doc/00442/55358/

Stommel, H., & Farmer, H. G. (1952). Abrupt change in width in two-layer open channel flow. *J. Mar. Res*, *11*(2), 205-214.

Stopa, J. E., Ardhuin, F., Babanin, A., & Zieger, S. (2016). Comparison and validation of physical wave parameterizations in spectral wave models. *Ocean Modelling*, *103*, 2-17.

Stoschek, O., & Zimmermann, C. (2006). Water exchange and sedimentation in an estuarine tidal harbour using three-dimensional simulation. *Journal of Waterway, Port, Coastal, and Ocean Engineering*, *132*(5), 410-414.

Straaten, L. V., & Kuenen, P. H. (1958). Tidal action as a cause of clay accumulation. *Journal of Sedimentary Research*, *28*(4), 406-413.

Strady, E., Blanc, G., Baudrimont, M., Schäfer, J., Robert, S., & Lafon, V. (2011). Roles of regional hydrodynamic and trophic contamination in cadmium bioaccumulation by Pacific oysters in the Marennes-Oléron Bay (France). *Chemosphere*, *84*(1), 80-90.

Stark, C., Whinney, J., Ridd, P., & Jones, R. (2017). *Estimating sediment deposition fields around dredging activities.* Final report of Theme 4 – Project 4.3 prepared the Western Australian Marine Science Institution.

Strasser, T. F., Runnels, C., Wegmann, K., Panagopoulou, E., Mccoy, F., Digregorio, C., ... & Thompson, N. (2011). Dating Palaeolithic sites in southwestern Crete, Greece. *Journal of Quaternary Science*, *26*(5), 553-560.

Sztano, O., & de Boer, P. L. (1995). Basin dimensions and morphology as controls on amplification of tidal motions (the Early Miocene North Hungarian Bay). *Sedimentology*, *42*(4), 665-682.

Tajali, Z., & Shafieefar, M. (2011). Hydrodynamic analysis of multi-body floating piers under wave action. *Ocean Engineering*, *38*(17-18), 1925-1933.

Tang, J., Wang, Y. P., Zhu, Q., Jia, J., Xiong, J., Cheng, P., ... & Wu, H. (2019). Winter storms induced high suspended sediment concentration along the north offshore seabed of the Changjiang estuary. *Estuarine, Coastal and Shelf Science*, 228, 106351.

Takeoka, H. (1984). Fundamental concepts of exchange and transport time scales in a coastal sea. *Continental Shelf Research*, *3*(3), 311-326.

Tesson, M. (1973). *Aspects dynamiques de la sedimentation dans la baie de Marennes-Oleron (Charente-Maritime).* (Doctoral dissertation, Bordeaux).

Thomann, R. V., & Mueller, J. A. (1987). *Principles of surface water quality modeling and control*. Harper & Row Publishers.

Thompson, D. M. (2002). Long-term effect of instream habitat-improvement structures on channel morphology along the Blackledge and Salmon rivers, Connecticut, USA. *Environmental Management*, *29*(2), 250-265.

Timmerman, P. & White, R. (1997) Megahydropolis:coastal cities in the context of global environmental change. *Global Environmental Change*, 7, 205–234.

Toublanc, F., Brenon, I., Coulombier, T., Le Moine, O. (2015). Fortnightly tidal asymmetry inversions and perspectives on sediment dynamics in a macrotidal estuary (Charente, France). *Continental Shelf Research.* 94, 42–54.

Tranchant, M. (2005). *Ports maritimes et ports fluviaux au moyen âge: XXXVe congrès de la SHMES, la Rochelle, 5 et 6 juin 2004* (Vol. 35). Publications de la Sorbonne.

Tranchant, M. (2010). Au risque de l'étranger: un sujet majeur de gouvernance à La Rochelle à la fin du Moyen Âge. *Annales de Bretagne et des Pays de l'Ouest. Anjou. Maine. Poitou-Charente. Touraine*, 117(1), 91-108.

Tsay, T.-K., Liu, P. L.-F. (1983). A finite element model for wave refraction and diffraction. *Applied Ocean Research.* 5, 30-37.

Tubman, M., Welp, T., Sullivan, M., & Colombo, C. (2017). *Evaluation of the Use of a Bedleveler to Improve Navigability of Atchafalaya River Bar Channel Fluid Mud*. Vicksburg United States.

Turekian, K. K., Steele, J. H., & Thorpe, S. A. (2010). *A derivative of the Encyclopedia of Ocean Sciences: Marine Chemistry & Geochemistry.* Academic Press, London.

Umgiesser, G., Zemlys, P., Erturk, A., Razinkova-Baziukas, A., Mežine, J., & Ferrarin, C. (2016). Seasonal renewal time variability in the Curonian Lagoon caused by atmospheric and hydrographical forcing. *Ocean Science*, *12*, 391-402.

UNWTO Wolrd Tourism Organization. (2017). *Tourism Highlights.* Available at: https://www.e-unwto.org/doi/pdf/10.18111/9789284419029

U.S. Census Bureau. (2009). *World Population: 1950-2050.* Available at: http://www.census.gov/ipc/www/idb/worldpopgraph.php

Valadez-Rocha, V., & Ortiz-Lozano, L. (2013). Spatial and temporal effects of port facilities expansion on the surface area of shallow coral reefs. *Environmental management*, *52*(1), 250-260.

Vanlede, J., & Dujardin, A. (2014). A geometric method to study water and sediment exchange in tidal harbours. *Ocean Dynamics*, 64(11), 1631-1641.

Vanlede, J., Dujardin, A., Fettweis, M., Van Hoestenberghe, T., & Martens, C. (2019). Mud dynamics in the Port of Zeebrugge. *Ocean Dynamics*, 69(9), 1085-1099.

Van Leeuwen, S., & Hofland, B. (1999). *The current deflecting wall in a tidal harbour with density influences.* Final Report in the Framework of the European Community's Large Scale Installations and Facilities Programme II, Delft, The Netherlands.

Van Leussen, W., & Winterwerp, J. C. (1990). Laboratory experiments on sedimentation of fine-grained sediments: a state-of-the-art review in the light of experiments with the Delft tidal flume. In *Residual currents and long-term transport* (pp. 241-259). Springer, New York, NY.

Van Maren, D. S., Winterwerp, J. C., Sas, M., & Vanlede, J. (2009). The effect of dock length on harbour siltation. *Continental Shelf Research*, *29*(11-12), 1410-1425.

Van Maren, D. S., Van Kessel, T., Cronin, K., & Sittoni, L. (2015). The impact of channel deepening and dredging on estuarine sediment concentration. *Continental Shelf Research*, *95*, 1-14.

Van Rijn, L. C. (1984). Sediment transport, part III: bed forms and alluvial roughness. *Journal of hydraulic engineering*, *110*(12), 1733-1754.

Van Rijn, L. C. (1993). *Principles of sediment transport in rivers, estuaries and coastal seas* (Vol. 1006). Amsterdam: Aqua publications.

Van Rijn, L. C. (2016). Harbour siltation and control measures. Available at: http://www.leovanrijn-sediment.com/papers/Harboursiltation2016.pdf

Van Schijndel, S. A., & Kranenburg, C. (1998). Reducing the siltation of a river harbour. *Journal of Hydraulic Research*, *36*(5), 803-814.

Verney, R., Deloffre, J., Brun-Cottan, J. C., & Lafite, R. (2007). The effect of wave-induced turbulence on intertidal mudflats: Impact of boat traffic and wind. *Continental Shelf Research*, *27*(5), 594-612.

Vethamony, P., Reddy, G.S., Babu, M.T., Desa, E., Sudheesh, K. (2005). Tidal eddies in a semi-enclosed basin: a model study. *Marine Environmental Research.* 59, 519–532.

Viero, D. P., & Defina, A. (2016). Renewal time scales in tidal basins: Climbing the Tower of Babel. *Sustainable Hydraulics in the Era of Global Change*, 338-345.

Villaret, C., Hervouet, J. M., Kopmann, R., Merkel, U., & Davies, A. G. (2013). Morphodynamic modeling using the Telemac finite-element system. *Computers & Geosciences*, *53*, 105-113.

Von Glasow, R., Jickells, T. D., Baklanov, A., Carmichael, G. R., Church, T. M., Gallardo, L., ... & Raine, R. (2013). Megacities and large urban agglomerations in the coastal zone: interactions between atmosphere, land, and marine ecosystems. *Ambio*, *42*(1), 13-28.

Warner, J. C., Geyer, W. R., & Arango, H. G. (2010). Using a composite grid approach in a complex coastal domain to estimate estuarine residence time. *Computers & Geosciences*, *36*(7), 921-935.

Wang, C. F., Hsu, M. H., & Kuo, A. Y. (2004). Residence time of the Danshuei River estuary, Taiwan. *Estuarine, Coastal and Shelf Science*, *60*(3), 381-393.

Wang, B., Fringer, O. B., Giddings, S. N., & Fong, D. A. (2009). High-resolution simulations of a macrotidal estuary using SUNTANS. *Ocean Modelling*, *26*(1-2), 60-85.

Ward, S. L., Robins, P. E., Lewis, M. J., Iglesias, G., Hashemi, M. R., & Neill, S. P. (2018). Tidal stream resource characterisation in progressive versus standing wave systems. *Applied energy*, *220*, 274-285.

Ware, D. (2016). Tweed River entrance sand bypass project. *Case Study for CoastAdapt, National Climate Change Adaptation Research Facility, Gold Coast*.

Weber, N. (2004). *Morphologie, architecture des dépôts, évolution séculaire et millénaire du littoral charentais: apports de la sismique réflexion combinée à des suivis bathymétriques et validée par des vibrocarottages* (Doctoral dissertation, La Rochelle).

Weber, N., Chaumillon, E., Tesson, M., & Garlan, T. (2004). Architecture and morphology of the outer segment of a mixed tide and wave-dominated-incised valley, revealed by HR seismic reflection profiling: the paleo-Charente River, France. *Marine Geology*, *207*(1-4), 17-38.

Weeks, A. R., Simpson, J. H., & Bowers, D. (1993). The relationship between concentrations of suspended particulate material and tidal processes in the Irish Sea. *Continental Shelf Research*, 13(12), 1325-1334.

Weisman, R. N., Lennon, G. P., & Clausner, J. E. (1996). *A Guide to the Planning and Hydraulic Design of Fluidizer Systems for Sand Management in the Coastal Environment*. Army engineer waterways experiment station vicksburg ms.

Weltz, M. A., Arslan, A. B., & Lane, L. J. (1992). Hydraulic roughness coefficients for native rangelands. *Journal of Irrigation and Drainage Engineering*, *118*(5), 776-790.

Whitehouse, R. J. S., Soulsby, R. L., Roberts, W., & Mitchener, H. J. (2000). Dynamics of estuarine muds.

Wijeratne, E. M. S., & Rydberg, L. (2007). Modelling and observations of tidal wave propagation, circulation and residence times in Puttalam Lagoon, Sri Lanka. *Estuarine, Coastal and Shelf Science*, *74*(4), 697-708.

Williams, G. L., & Visser, K. G. (1997). The Punaise: a remotely operated submerged dredging system. *Terra et Aqua*, 20-28.

Winterwep, J.C., Christiansen H., Eysink W.D., Kirby R., Smith T.J. (1994) The Current Deflecting Wall: a device to minimize harbour siltation. *Dock and Harbour Authority*, 74, 243-246.

Winterwerp, J. C. (2005). Reducing harbour siltation. I: Methodology. *Journal of Waterway, Port, Coastal, and Ocean Engineering*, *131*(6), 258-266.

Wolanski, E., and King, B. (1990). Flushing of Bowden Reef Lagoon, Great Barrier Reef. *Estuarine Coastal and Shelf Science*. 31(6), 789-804.

Wolanski, E., & Elliott, M. (2015). *Estuarine ecohydrology: an introduction*. Elsevier.

Woo, S. H., & Pettit, S. J. (2010). Trends and themes in port research since 1980-a decadal approach. In *International Association of Maritime Economists (IAME) 2010 Annual Conference, Lisbon, Portugal, 7-9 July 2010.*

Woo, S. H., Pettit, S. J., Kwak, D. W., & Beresford, A. K. (2011). Seaport research: A structured literature review on methodological issues since the 1980s. *Transportation Research Part A: Policy and Practice*, *45*(7), 667-685.

Wurpts, D. I. R. W., & Greiser, N. (2007). Monitoring and dredging technology in muddy layers. In *Proceedings of World Dredging Congress (WODCON) XVIII, Lake Buena Vista Florida*.

Xiong, J., Wang, X. H., Wang, Y. P., Chen, J., Shi, B., Gao, J., ... & Gong, X. (2017). Mechanisms of maintaining high suspended sediment concentration over tide-dominated offshore shoals in the southern Yellow Sea. *Estuarine, Coastal and Shelf Science*, 191, 221-233.

Yanagi, T. (1974). Dispersion due to the residual flow in the hydraulic model. *Contributions of Geophysics Institute Kyoto University*, 14, 1–10.

Young, I. R., & Ribal, A. (2019). Multiplatform evaluation of global trends in wind speed and wave height. *Science*, 364(6440), 548-552.

Yuan, D., Lin, B., & Falconer, R. A. (2007). A modelling study of residence time in a macro-tidal estuary. *Estuarine, Coastal and Shelf Science*, *71*(3-4), 401-411.

Zawadzki, L., Ablain, M., Carrere, L., Ray, R. D., Zelensky, N. P., Lyard, F., ... & Picot, N. (2017). Reduction of the 59-day error signal in the Mean Sea Level derived from TOPEX/Poseidon, Jason-1 and Jason-2 data with the latest FES and GOT ocean tide models. *IEEE Transactions on Geoscience Remote Sensing.*

Gao, X., Chen, Y., & Zhang, C. (2013). Water renewal timescales in an ecological reconstructed lagoon in China. *Journal of Hydroinformatics*, *15*(3), 991-1001.

Zimmerman, J. T. F. (1976). Mixing and flushing of tidal embayments in the western Dutch Wadden Sea part I: Distribution of salinity and calculation of mixing time scales. *Netherlands Journal of Sea Research*, *10*(2), 149-191.

Zimmerman, J., & Kjerfve, B. (1988). Estuarine residence times. *Hydrodynamics of Estuaries,* pp 171.

Appendix

Appendix A

Velocity intensity in the marina during flood, with varying friction coefficients to represent floating structures effect

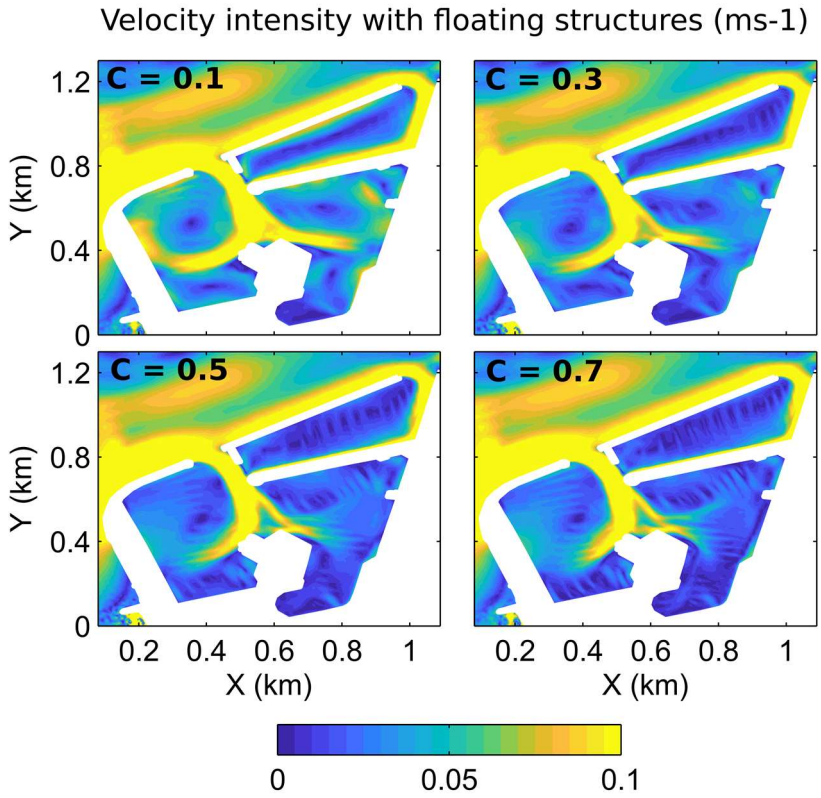

Figure A. *Depth-averaged velocities modelled for a mid-flood situation, with varying C friction coefficient (m^{-1}).*

Appendix B

Sensitivity of the critical erosion shear stress in the numerical model

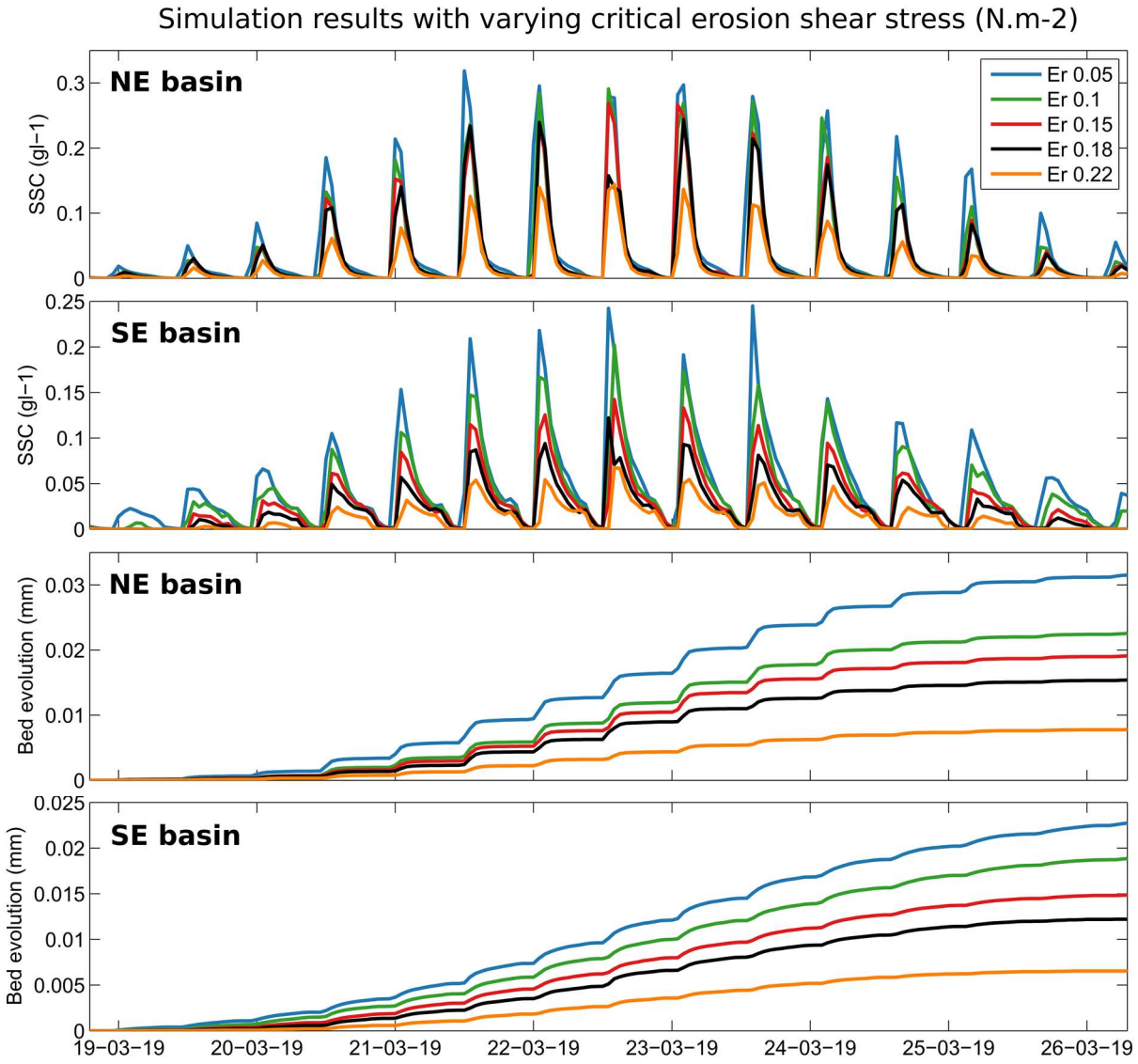

Figure B. *Comparison of SSC and bed evolution signals obtained in the NE and SE basins with varying critical erosion shear stress (legend). Simulations were performed over a spring tide situations with the same parametrisations than in the Chapter VII.*

Appendix C

Sensitivity of the critical deposition shear stress in the numerical model

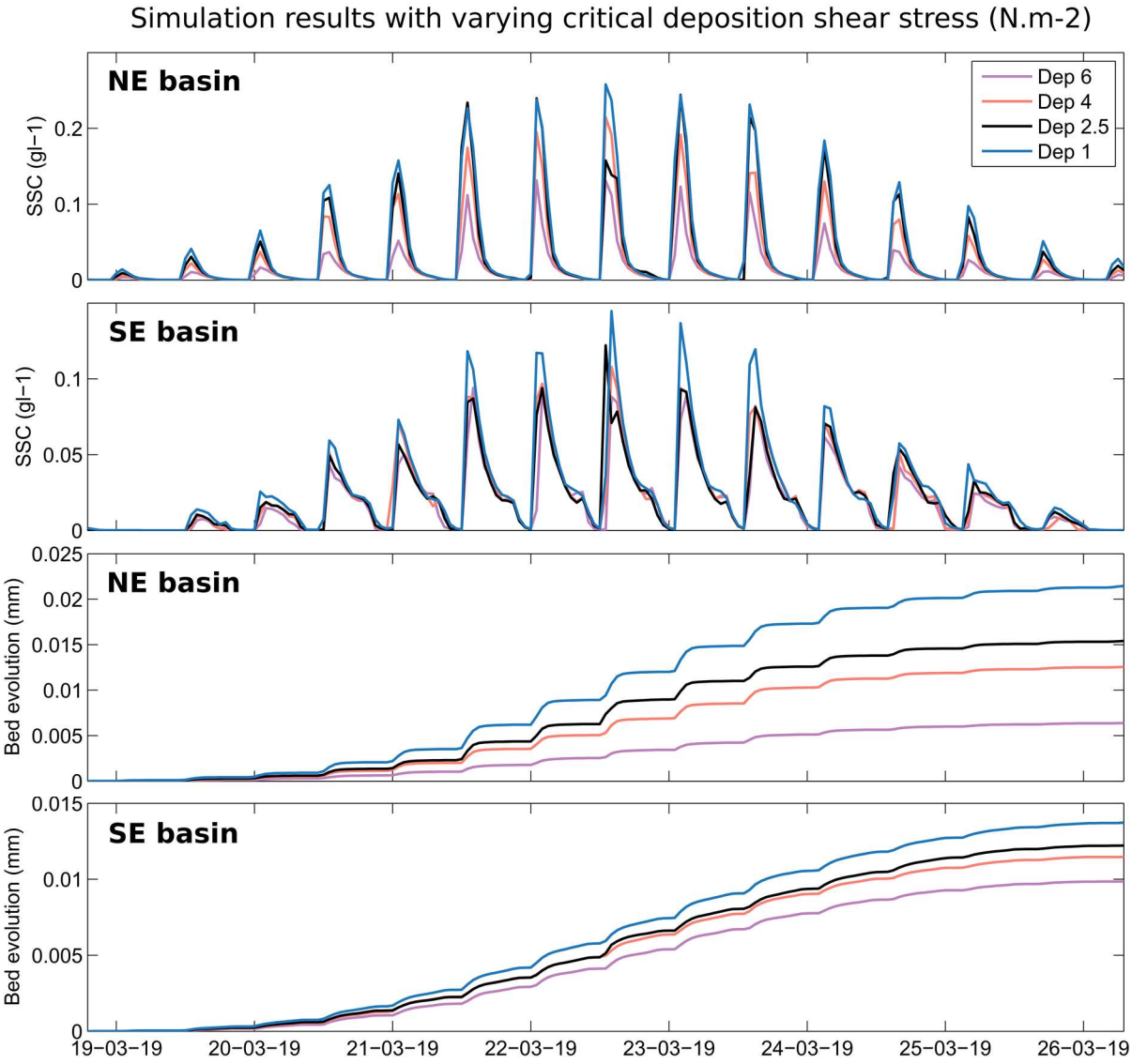

Figure C. *Comparison of SSC and bed evolution signals obtained in the NE and SE basins with varying critical deposition shear stress (legend). Simulations were performed over a spring tide situation with the same parametrisation than in the Chapter VII.*

Appendix D

Bed evolution simulations with and without floating structures

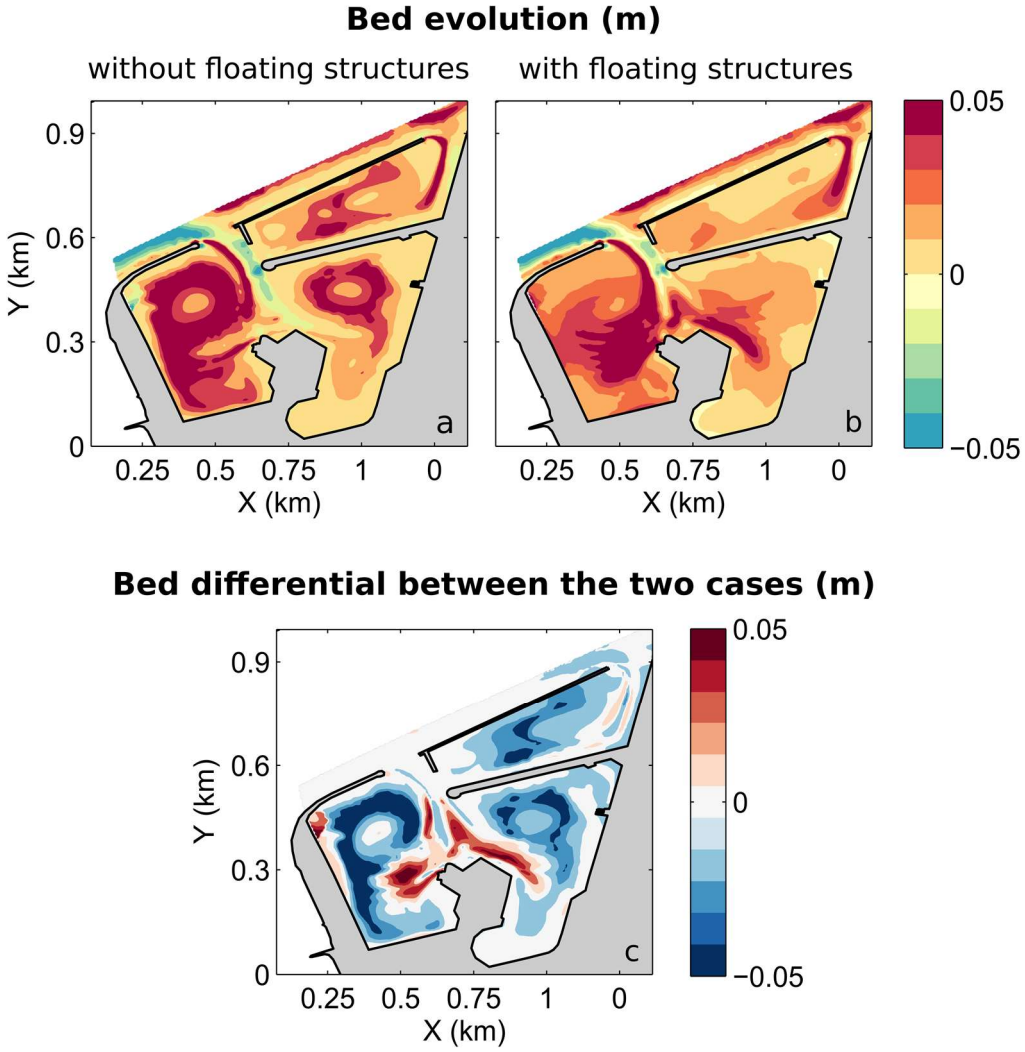

Figure D. *Bed evolution comparison between a case without (a) and with (b) floating structures. (c) presents the bed differential between the two cases. The 15-days simulations were computed with the same parametrisation than in the Chapter VII.*

Dynamique hydro-sédimentaire en milieu portuaire: application au port de plaisance de La Rochelle

Résumé:
Présents sur toutes les façades maritimes et fluviales du monde, les ports sont aujourd'hui des interfaces majeures du développement des territoires. L'envasement naturel de ces zones calmes peut obstruer les voies navigables et empêcher ces infrastructures de jouer leur fonction primaire d'abri pour les bateaux. Cela implique souvent la mise en œuvre de travaux de dragages onéreux et chronophages, afin de retrouver des profondeurs compatibles avec la navigation. Le port des Minimes (La Rochelle, France), qui est un des plus gros ports de plaisance de la façade Atlantique, n'est pas épargné par ce phénomène et requiert des activités de dragage huit mois par an. Face à cette problématique, le port de plaisance et La Rochelle Université ont eu la volonté de mieux comprendre la dynamique du milieu et les processus menant à l'accumulation de sédiments sur le site des Minimes. En combinant une approche instrumentale *in situ* à une modélisation numérique opérationnelle, l'objectif de ce travail de thèse a donc consisté à caractériser la dynamique hydro-sédimentaire de cet espace littoral anthropisé. Une quantification de l'impact des structures flottantes (bateaux, pontons) sur l'hydrodynamique portuaire, a tout d'abord été menée. Le second champ d'étude a visé à décrire la circulation des masses d'eaux et leur renouvellement sous l'action du vent et de la marée. Les observations récoltées ont permis d'étudier la dynamique sédimentaire spatiale et temporelle, en lien avec l'action du vent, de la marée et des vagues. Plusieurs scénarios de lutte contre l'envasement ont été mis en place et analysés dans le but de fournir des éléments de réponse et pistes de recherche sur la gestion de l'envasement et du dragage associé.
Mots-clés : *port de plaisance, structures flottantes, hydrodynamique, renouvellement des eaux, marée, vent, vagues, flux sédimentaires, envasement, mesures anti-sédimentation, modélisation numérique, instrumentation*

Hydro-sedimentary dynamics in port environments: application to the marina of La Rochelle

Summary:
Ports are presents on all maritime and river fronts of the world, and represent major interfaces in the development of territories. The natural siltation of these calm areas can obstruct waterways and prevent these infrastructures from fulfilling their primary function as a shelter for boats. This often involves the implementation of expensive and time-consuming dredging operations to restore depths compatible with navigation. Les Minimes marina (La Rochelle, France), which is one of the largest marinas on the Atlantic coast, is not spared by this phenomenon and requires dredging activities for a large part of the year. In response to this problem, the marina and La Rochelle University, has wanted to understand better the natural environment and the processes leading to the accumulation of sediments in the marina. By combining an instrumental *in situ* approach with operational numerical modelling, the objective of this thesis was, therefore, to characterise the hydro-sedimentary dynamics of the area. Quantification of the impact of floating structures (boats, pontoons) on marina hydrodynamics was firstly carried out. The second field of study aimed to study the circulation of water masses and their renewal about the effect of wind and tide. The observations collected made it possible to study spatial and temporal sediment dynamics, under the action of wind, tide and waves. Thus, numerous siltation control measures have been implemented and analysed to provide solutions and research perspectives in view with siltation and dredging management.
Keywords: *marina, floating structures, hydrodynamics, water renewal, tide, wind, wave, sedimentary fluxes, siltation, anti-sedimentation measures, numerical modelling, instrumentation*

LIENSs, 2 rue Olympe de Gouges
17000 LA ROCHELLE CEDEX